

The University of Nottingham

Department of Mineral Resources Engineering



**A STUDY OF OPTIMISATION METHODS APPLIED TO METHANE
RECOVERY AND MINE VENTILATION SYSTEMS**

BY

A.T.J. MOLL, B.Sc.

Thesis submitted to the University of Nottingham for the degree of

Doctor of Philosophy

October 1993

The great theoretical physicist P.A.M. Dirac wrote that it is more important to have beauty in one's equations than to have them fit the experiment.

Contents

| | Page |
|--|-------------|
| LIST OF TABLES | viii |
| LIST OF FIGURES | xi |
| SYNOPSIS | xvi |
| INTRODUCTION | 1 |
| PART ONE : THE OPTIMISATION OF METHANE RECOVERY | 5 |
| Chapter 1 The Mechanisms of Gas Retention and Release | 6 |
| 1.1 Introduction. | 6 |
| 1.2 Properties of Methane. | 6 |
| 1.3 Methane Retention. | 8 |
| 1.4 Estimation of Gas Content. | 11 |
| 1.5 Gas Release. | 12 |
| 1.5.1 Empirical Gas Emission Prediction. | 13 |
| 1.5.2 Numerical Gas Emission Prediction. | 15 |
| 1.5.2.1 D'Arcy's Law. | 16 |
| 1.5.2.2 The Dependence on Permeability. | 17 |
| 1.5.2.3 The Development of Numerical Models. | 20 |
| 1.6 Summary and Conclusions. | 22 |
| Chapter 2 Methane Drainage | 23 |
| 2.1 Introduction | 23 |
| 2.2 Drainage From Surface Boreholes | 24 |
| 2.3 Drainage During Underground Development | 26 |
| 2.4 Drainage During Extraction | 30 |
| 2.4.1 Background | 30 |
| 2.4.2 Advancing Longwall Mining | 32 |
| 2.4.3 Retreat Longwall Mining | 33 |
| 2.4.4 Drainage of Stoppings and Wastes | 33 |

| | Page |
|--|---------------|
| 2.5 Factors Affecting Methane Drainage Efficiency | 35 |
| 2.5.1 Borehole Configuration | 36 |
| 2.5.2 Standpipe Configuration | 38 |
| 2.5.3 Pipe Network Configuration | 39 |
| 2.5.4 Pressure, Flow and Purity Measurement | 40 |
| 2.6 Pipe Network Modelling | 41 |
| 2.6.1 Previous Modelling Programs | 42 |
| 2.6.2 Analysis of Previous Methods | 43 |
| 2.7 Summary and Conclusions | 43 |
| Chapter 3 The Pipe Network Model | 45 |
| 3.1 Introduction | 45 |
| 3.2 Principles of Fluid Flow | 45 |
| 3.2.1 Conservation of Mass | 45 |
| 3.2.2 Conservation of Momentum | 46 |
| 3.2.3 Conservation of Energy | 47 |
| 3.2.4 Measurement of Pressure and Flow | 48 |
| 3.2.5 The Orifice Plate | 50 |
| 3.3 Flow in Methane Drainage Ranges | 51 |
| 3.4 The Single Pipe Model | 53 |
| 3.5 Combinations of Pipes in Series and Parallel | 55 |
| 3.5.1 Pipes in Series | 56 |
| 3.5.2 Pipes in Parallel | 56 |
| 3.6 Generalisation to Pipe Networks | 57 |
| 3.6.1 The Linear Theory Method | 58 |
| 3.6.2 Specification of the Problem | 59 |
| 3.6.3 Calculation of Purity | 60 |
| 3.6.4 Solution Method | 62 |
| 3.6.5 Calculation of the Gas Constant, R | 64 |
| 3.6.6 Inclusion of Valves and Pipe Fittings | 66 |
| 3.6.7 Calculation of the Friction Factor | 67 |
| 3.7 Sensitivity Analysis Applied to Governing Equations | 70 |
| 3.7.1 Dependence on Diameter | 70 |
| 3.7.2 Dependence on Absolute Pressure | 70 |
| 3.7.3 The Effect of Pressure Loss Changes on Pipes in Series | 71 |
| 3.7.4 Larger Diameter vs. Pipes in Parallel | 72 |

| | | |
|------------------|--|-------------------|
| 3.8 | Summary and Conclusions | Page 74 |
| Chapter 4 | Correlation Exercises and the Development of an Optimisation Strategy | 75 |
| 4.1 | Introduction | 75 |
| 4.2 | Case Study 1 - Harworth Colliery | 76 |
| 4.2.1 | Background | 76 |
| 4.2.2 | Application of the Model to Harworth's Network | 81 |
| 4.3 | Use of The Program as an Optimisation Tool | 83 |
| 4.3.1 | Network Monitoring | 83 |
| 4.3.2 | Analysis of Measured and Predicted Data | 84 |
| 4.3.2.1 | Air Inleakage | 87 |
| 4.3.2.1.1 | Flow Rate Measured | 88 |
| 4.3.2.1.2 | Purity Measured | 88 |
| 4.3.2.2 | Condition of the Pipeline | 89 |
| 4.3.3 | Network Reconfiguration | 92 |
| 4.4 | Case Study 2 - Thoresby Colliery | 93 |
| 4.4.1 | Background | 93 |
| 4.4.2 | Thoresby's Current Drainage Range | 95 |
| 4.4.3 | Application of the Model to Thoresby's Network | 95 |
| 4.4.3.1 | Initial Model | 96 |
| 4.4.3.2 | Correlated Model | 99 |
| 4.4.3.3 | Reconfigured Model | 101 |
| 4.5 | Summary and Conclusions | 103 |
| Chapter 5 | General Conclusions and Suggestions for Further Work | 104 |
| 5.1 | General Conclusions | 104 |
| 5.2 | Suggestions for Further Work | 106 |
| 5.2.1 | Further Correlation Studies | 106 |
| 5.2.2 | The Development of a Decision Support System | 106 |
| 5.2.3 | The Incorporation of a CAD Package | 107 |

| | |
|---|------------|
| PART TWO : THE OPTIMISATION OF MINE VENTILATION | 108 |
| Chapter 6 Mine Ventilation Systems | 109 |
| 6.1 Introduction | 109 |
| 6.2 Optimisation Strategies | 109 |
| 6.2.1 Air Leakage | 111 |
| 6.2.2 Reduction in Effective Resistance | 112 |
| 6.2.3 Airflow Control | 112 |
| 6.3 The Use of Underground Booster Fans | 112 |
| 6.4 Mine Ventilation Calculations | 114 |
| 6.4.1 Assumptions | 114 |
| 6.4.1.1 Natural Ventilation | 114 |
| 6.4.2 Atkinson's Equation | 116 |
| 6.4.3 Shape Factors | 117 |
| 6.4.4 Airways in Series and Parallel | 119 |
| 6.4.5 Fans and Fan Selection | 120 |
| 6.4.6 Fans in Parallel and Series | 122 |
| 6.5 Summary and Conclusions | 123 |
| Chapter 7 The Mathematical Analysis and Optimisation of Mine Ventilation Networks | 125 |
| 7.1 Introduction | 125 |
| 7.2 Kirchhoff's Laws | 126 |
| 7.2.1 Kirchhoff's First Law | 126 |
| 7.2.2 Kirchhoff's Second Law | 126 |
| 7.3 Application of Graph Theory | 127 |
| 7.3.1 The Junction-Branch Incidence Matrix | 127 |
| 7.3.2 The Spanning Tree | 128 |
| 7.3.3 The Mesh-Branch Incidence Matrix | 130 |
| 7.4 Solutions to the Network Equations | 131 |
| 7.4.1 The Relationship Between Mesh and Branch Flows | 132 |
| 7.4.2 The Hardy Cross Method | 133 |
| 7.4.3 The Newton-Raphson Method | 135 |
| 7.4.4 The Linear Theory Method | 136 |

| | Page |
|---|-------------|
| 7.4.5 Fan Characteristics and Fixed Flow Branches | 138 |
| 7.5 The Categorisation of the Controlled Flow Problem | 139 |
| 7.5.1 Pure Controlled Flow | 140 |
| 7.5.1.1 Linear Programming Models | 141 |
| 7.5.1.2 Critical Path Methods | 142 |
| 7.5.2 Semi Controlled Flow | 147 |
| 7.5.2.1 The Single Fan System | 149 |
| 7.5.2.2 The Two Fan System | 150 |
| 7.5.2.3 Analysis of Booster Fan Locations | 154 |
| 7.5.2.4 Analysis of Intersection Points | 156 |
| 7.5.2.5 Analysis of Total Leakage | 156 |
| 7.5.2.6 A General Strategy for Network Analysis | 156 |
| 7.6 Summary and Conclusions | 159 |
| Chapter 8 Program Results and Correlation Exercises | 160 |
| 8.1 Case Study 1 - Bilsthorpe Colliery | 160 |
| 8.1.1 The One Fan System | 161 |
| 8.1.2 The Two Fan System | 166 |
| 8.1.3 Leakage and Volumetric Efficiency | 174 |
| 8.2 Case Study 2 - Clipstone Colliery | 176 |
| 8.2.1 The One Fan System | 178 |
| 8.2.2 The Two Fan System - Booster in High Resistance Split | 181 |
| 8.2.3 The Two Fan System - Booster in Low Resistance Split | 186 |
| 8.2.4 The Three Fan System - Booster Fan in Each Split | 189 |
| 8.3 Summary and Conclusions | 192 |
| Chapter 9 General Conclusions and Suggestions for Further Work | 194 |
| 9.1 General Conclusions | 194 |
| 9.2 Suggestions for Further Work | 196 |
| 9.2.1 Further Correlation Studies | 196 |
| 9.2.2 Automation of Analysis Procedure | 196 |
| ACKNOWLEDGEMENTS | 197 |
| REFERENCES | 198 |

| | Page |
|--|-------------|
| APPENDICES | 209 |
| Appendix 1 The Pipe Network Simulation Program | 210 |
| A1.1 Introduction | 210 |
| A1.2 Coding Specifications | 210 |
| A1.2.1 Parameter Statements and Common Blocks | 210 |
| A1.2.2 Subroutine Format | 211 |
| A1.2.3 Function Tests | 211 |
| A1.2.4 Status on Exit Flag | 213 |
| A1.3 Structure of the Program | 213 |
| A1.3.1 Data Input | 217 |
| A1.3.1.1 'DATAXXXX' | 217 |
| A1.3.1.2 'BOUNXXXX' | 218 |
| A1.3.2 Data Validation | 219 |
| A1.3.3 Calculation of Suction and Mass Flow | 219 |
| A1.3.4 Calculation of Flow Rate, Velocity and Purity | 219 |
| A1.3.5 Results Output | 220 |
| A1.4 Program Execution | 220 |
| A1.4.1 Single Pipe Calculations | 221 |
| A1.4.2 Network Calculations | 222 |
| A1.4.2.1 Create Nodes | 222 |
| A1.4.2.2 Create Pipes | 222 |
| A1.4.2.3 Create Data File | 223 |
| A1.4.2.4 Boundary Conditions | 223 |
| A1.4.2.5 View Network | 223 |
| A1.4.2.6 Execute Job | 223 |
| A1.4.2.7 View Results | 223 |
| A1.4.2.8 Edit File | 223 |
| A1.5 List of Program Subroutines | 224 |
| Appendix 2 The Mine Ventilation Simulation Programs | 226 |
| A2.1 Introduction | 226 |
| A2.2 Coding Specifications | 226 |
| A2.3 Directory Structure | 227 |
| A2.4 Compiling and Linking Executables | 228 |

| | Page |
|---|-------------|
| A2.5 Program Execution | 228 |
| A2.5.1 Problem Type | 229 |
| A2.5.1.1 Data File Structure | 229 |
| A2.5.2 Natural Splitting | 230 |
| A2.5.2.1 Data Input | 230 |
| A2.5.2.2 Program Structure | 231 |
| A2.5.2.3 Results Output | 231 |
| A2.5.3 Controlled Flow | 234 |
| A2.5.3.1 Data Input | 234 |
| A2.5.3.2 Program Structure | 234 |
| A2.5.3.3 Results Output | 235 |
| A2.5.4 Inclusion of Additional Booster Fans | 238 |
| A2.5.4.1 Results Output | 240 |
| A2.5.5 Semi Controlled Flow | 241 |
| A2.5.5.1 Data Input | 241 |
| A2.5.5.2 Program Structure | 242 |
| A2.5.5.3 Results Output | 243 |
| A2.5.6 Fan Characteristics | 250 |
| A2.6 List of Program Subroutines | 251 |

LIST OF TABLES

| | | Page |
|------|---|-------------|
| 2.1 | Comparative coal seam characteristics. | 24 |
| 2.2 | Firedamp drainage data for the European Community in 1974. | 31 |
| 3.1 | Properties of methane and air at standard atmospheric pressure. | 52 |
| 3.2 | Friction coefficients for a selection of valves located in pipe networks. | 67 |
| 3.3 | Typical values of surface roughness, k. | 69 |
| 4.1 | Borehole parameters and configuration on 11's face, Harworth colliery. | 78 |
| 4.2 | Comparison of measured and predicted pressure distributions | 82 |
| 4.3 | Thoresby colliery manager's rules for borehole patterns on both retreat and advance faces. | 94 |
| 4.4 | Predicted pressure drops for the initial model of Thoresby colliery. | 96 |
| 4.5 | Pipe flows, velocities and purities for the initial model of Thoresby colliery. | 97 |
| 4.6 | Air inleakage determined from the initial model and measured data. | 99 |
| 4.7 | Increase in resistance values in comparison with a normal rough steel pipe. | 99 |
| 4.8 | Pressure drops for the correlated model of Thoresby colliery. | 100 |
| 4.9 | Pipe flows, velocities and purities for the correlated model of Thoresby colliery. | 100 |
| 4.10 | Predicted pressure drops for the network with a surface exhauster and 14 inch pipes in parallel. | 102 |
| 4.11 | Predicted flows, velocities and purities for the network with a surface exhauster and 14 inch pipes in parallel. | 102 |
| 6.1 | Coefficients of friction, k, of typical mine airways. | 118 |
| 6.2 | Relative shape factors. | 119 |
| 7.1 | Branch resistances and flows for the controlled flow test network. | 143 |
| 7.2 | Cumulative pressure losses for the controlled flow test network. | 144 |
| 7.3 | Regulation required from the forward pass procedure. | 144 |
| 7.4 | Added resistance of the fixed flow branches, to maintain the specified airflows, for the single fan system. | 149 |
| 7.5 | Calculated linear regression coefficients for the single fan system. | 150 |

| | Page |
|--|-------------|
| 7.6 Added resistance of the fixed flow branches for the two fan system. | 151 |
| 7.7 Calculated linear regression coefficients for the two fan system. | 151 |
| 7.8 Optimum combination of main and booster fan pressures for varying booster fan locations. | 157 |
| 8.1 The airflow quantities specified for the Bilsthorpe network. | 160 |
| 8.2 Added resistance required, to maintain specified airflows, for each fixed flow branch with increasing fan pressure. | 162 |
| 8.3 Coefficients from linear regression analysis of data presented in Table 8.2. | 162 |
| 8.4 Duty points for the Bilsthorpe colliery main fan. | 166 |
| 8.5 Duty points for Davidson booster fans - 4Banks , 2 Stages. | 166 |
| 8.6 Added resistance required to maintain the specified airflows for varying main and booster fan pressure combinations. | 168 |
| 8.7 Coefficients from linear regression analysis of data presented in Table 8.6. | 169 |
| 8.8 Main and booster fan pressures required to maintain the specified airflows. | 172 |
| 8.9 The airflow quantities specified in the Clipstone network. | 176 |
| 8.10 Added resistance required, to maintain specified airflows, for each fixed flow branch with increasing fan pressure. | 178 |
| 8.11 Coefficients from linear regression analysis of data presented in Table 8.10. | 179 |
| 8.12 Regulation for each fixed flow branch with varying main and booster fan pressure combinations. | 181 |
| 8.13 Coefficients from linear regression analysis of data presented in Table 8.12. | 182 |
| 8.14 Intersection points of the lines of zero added resistance. | 184 |
| 8.15 Regulation required to maintain pre-assigned airflows. | 185 |
| 8.16 Added resistance of each fixed flow branch for varying main and booster fan pressure combinations. | 186 |
| 8.17 Coefficients from linear regression analysis of results presented in Table 8.16. | 186 |
| 8.18 Intersection point for 202's and 204's face. | 189 |
| 8.19 Added resistance on each fixed flow face for varying booster fan combinations. | 189 |

| | <u>Page</u> |
|---|--------------------|
| 8.20 Results calculated from linear regression of data presented in Table 8.19. | 190 |
| 8.21 Suggested fan pressures for the 3 fan system. | 191 |
| 8.22 Regulation required for the 3 fan system results presented in Table 8.21. | 191 |

LIST OF FIGURES

| | | Page |
|------|--|-------------|
| 1.1 | Explosibility diagram for a methane/air mixture. | 7 |
| 1.2 | Physical representation of molecules in a coal pore. | 8 |
| 1.3 | Gas storage graph for a typical British coal. | 9 |
| 1.4 | Variation of coal adsorption capacity with temperature and rank | 10 |
| 1.5 | Gas emission zones considered by German researchers. | 14 |
| 1.6 | Permeability of core sample to hydrogen, nitrogen and carbon dioxide at different pressures. | 18 |
| 1.7 | The variations of stress and permeability in strata above and below an advancing longwall coal face. | 19 |
| 1.8 | Different permeability zones and suggested flow paths of methane around a working longwall face. | 21 |
| 2.1 | Methane drainage above an active goaf using surface boreholes. | 26 |
| 2.2 | Typical arrangement for the pre-drainage of a development heading. | 27 |
| 2.3 | A development heading Point of Ayr colliery. | 28 |
| 2.4a | Methane drainage from the working seam. | 28 |
| 2.4b | Methane drainage from the working seam. | 29 |
| 2.5 | Longhole drainage of an adjacent seam. | 30 |
| 2.6 | 'Retreat longwall' methane drainage using cross measure boreholes. | 32 |
| 2.7 | Methane drainage in advancing longwall mining. | 32 |
| 2.8 | Retreat mining methane drainage using the <i>Back Return</i> system. | 33 |
| 2.9 | Methane drainage from stopped off areas. | 34 |
| 2.10 | Methane drainage using the pack cavity system. | 35 |
| 2.11 | Selection of an optimum borehole spacing. | 37 |
| 3.1 | Flow through a fixed control volume. | 46 |
| 3.2 | Measurement of dynamic, total and static pressures. | 49 |
| 3.3 | Relationship between gauge, absolute and atmospheric pressures. | 50 |
| 3.4 | An orifice plate measurement station. | 50 |
| 3.5 | A typical methane drainage range. | 59 |
| 3.6 | Roughness elements. | 68 |
| 3.7 | Variation of pressure losses with diameter and inlet pressure. | 71 |
| 3.8 | The effect of pressure loss changes on pipes in series. | 71 |
| 3.9 | A comparison of pressure losses for pipes in parallel and an inlet pressure of 100 kPa. | 73 |

| | Page |
|--|-------------|
| 4.1 Stratigraphic section of Harworth colliery from the Low Farm borehole. | 77 |
| 4.2 Harworth colliery face layout of the Deep Soft seam. | 77 |
| 4.3 Harworth colliery methane drainage pipe layout. | 79 |
| 4.4 Performance curves for 8 CL3002 methane vacuum pumps. | 80 |
| 4.5 A simple network for comparison of measured and predicted data. | 85 |
| 4.6 Using the measured data to effectively simulate the drainage range. | 86 |
| 4.7 Factors affecting the flow parameters. | 87 |
| 4.8 Determination of air inleakage and the condition of the pipeline. | 88 |
| 4.9 Factors affecting the friction factor. | 90 |
| 4.10 Variation of 'effective' resistance over the extraction period. | 90 |
| 4.11 Routine maintenance of the pipe network. | 91 |
| 4.12 Examination of alternative network configurations. | 92 |
| 4.13 Thoresby colliery face layout of the Parkgate seam. | 93 |
| 4.14 Schematic of Thoresby colliery methane drainage range. | 98 |
| 4.15 Paralleled section of the Thoresby colliery methane drainage network. | 101 |
| 6.1 The effect of booster fan location on ventilating pressure. | 114 |
| 6.2 Resistance curve of the complete mine ventilation circuit. | 120 |
| 6.3 A typical p - Q fan characteristic. | 120 |
| 6.4 Intersection of fan characteristic and mine resistance curve to find the operating point. | 121 |
| 6.5 Changing fan operating points with varying mine resistance. | 122 |
| 6.6 Combinations of fans in series and parallel. | 123 |
| 7.1 A simple mine ventilation network with alternative spanning trees. | 129 |
| 7.2 A controlled flow test network. | 143 |
| 7.3 Algorithm for the positioning of fans and regulators in a controlled flow network. | 146 |
| 7.4 A semi-controlled flow test network. | 149 |
| 7.5 Added resistance required, on each fixed flow branch, to maintain the specified airflows, for increasing fan pressure. | 150 |
| 7.6 Added resistance required to maintain the specified airflows for a varying main fan pressure and a booster fan pressure of 200 Pa. | 152 |
| 7.7 Added resistance required to maintain the specified airflows for a varying main fan pressure and a booster fan pressure of 600 Pa. | 152 |

| | Page |
|--|-------------|
| 7.8 Main and booster fan pressures required for zero added resistance on each fixed flow face. | 153 |
| 7.9 Network for the example of optimum booster fan location. | 155 |
| 7.10 Analysis strategy for a general mine ventilation network. | 158 |
| 8.1 Schematic of the Bilsthorpe colliery pit bottom area. | 163 |
| 8.2 Schematic of the Bilsthorpe colliery face layout. | 164 |
| 8.3 Actual added resistance required to maintain specified airflows with increasing fan pressure. | 165 |
| 8.4 Actual added resistance required to maintain specified airflows with increasing fan pressure. | 165 |
| 8.5 Performance characteristic for the Bilsthorpe colliery main fan. | 167 |
| 8.6 Performance characteristic for the Davidson booster fans - 4 Banks , 2 Stages. | 167 |
| 8.7a Added resistance required to maintain specified airflows with increasing main fan pressure and a booster fan pressure of 3000 Pa. | 169 |
| 8.7b Added resistance required to maintain specified airflows with increasing main fan pressure and a booster fan pressure of 3500 Pa. | 170 |
| 8.7c Added resistance required to maintain specified airflows with increasing main fan pressure and a booster fan pressure of 4000 Pa. | 170 |
| 8.8 Main and booster fan pressure combinations for zero added resistance on each fixed flow branch. | 171 |
| 8.9 Air power consumed for main and booster fan combinations shown in Table 8.8 | 173 |
| 8.10 Total leakage in the two fan system for increasing main fan pressure. | 175 |
| 8.11 Volumetric efficiency in the two fan system for increasing main fan pressure. | 175 |
| 8.12 Diagrammatic layout of Clipstone colliery. | 177 |
| 8.13 Actual added resistance required to maintain specified airflows with increasing fan pressure. | 178 |
| 8.14 Calculated added resistance required to maintain specified airflows with increasing fan pressure. | 179 |
| 8.15 Total Leakage with increasing main fan pressure. | 180 |
| 8.16 Volumetric efficiency with increasing main fan pressure. | 181 |
| 8.17 Added resistance required to maintain specified airflows with increasing main fan pressure and a booster fan pressure of 3500 Pa. | 182 |

| | | |
|-------|---|-----|
| 8.18 | Added resistance required to maintain specified airflows with increasing booster fan pressure and a main fan pressure of 3500 Pa. | 183 |
| 8.19 | Main and booster fan pressure combinations for zero regulation on each fixed flow face. | 183 |
| 8.20 | Added resistance required to maintain specified airflows for increasing main fan pressure and a booster fan pressure of 3500 Pa. | 187 |
| 8.21 | Added resistance required to maintain specified airflows for increasing booster fan pressure and a main fan pressure of 3500 Pa. | 187 |
| 8.22 | Main and booster fan pressure combinations for zero regulation on each fixed flow face. | 188 |
| 8.23 | Booster fan in 200's split set at 2145 Pa. | 190 |
| 8.24 | Booster fan in 100's split set at 4250 Pa. | 191 |
| A1.1 | Parameter statement file 'NUMBERS'. | 211 |
| A1.2 | Common block file 'GEOM.CMN'. | 211 |
| A1.3 | Subroutine structure. | 212 |
| A1.4a | Flowchart for the validation of data. | 214 |
| A1.4b | Subroutine structure for the validation of data. | 214 |
| A1.5a | Flowchart for the iterative solution program loop. | 215 |
| A1.5b | Subroutine structure of the main program loop. | 216 |
| A1.6 | Structure of the network data file. | 217 |
| A1.7 | The axis set of the methane drainage network. | 218 |
| A1.8 | Structure of the boundary condition data file. | 218 |
| A1.9 | Example of results output. | 220 |
| A1.10 | The top level menu. | 221 |
| A1.11 | The single pipe calculations menu. | 221 |
| A1.12 | The network calculations menu. | 222 |
| A2.1 | Parameter statements included in the mine ventilation simulation models. | 227 |
| A2.2 | Common block included in the mine ventilation simulation models. | 227 |
| A2.3 | Menu for the mine ventilation network analysis programs. | 228 |
| A2.4 | Directory structure for the ventilation optimisation programs. | 228 |
| A2.5 | Structure of a typical data file. | 229 |
| A2.6 | The natural splitting menu options. | 230 |
| A2.7 | Results output for the natural splitting problem. | 231 |
| A2.8a | Flowchart for the natural splitting program. | 232 |
| A2.8b | Subroutine flowchart for the natural splitting problem. | 233 |

| | Page |
|---|-------------|
| A2.9 The controlled flow menu options. | 234 |
| A2.10a Flow chart for the controlled flow program. | 235 |
| A2.10b Subroutine flowchart for the controlled flow problem. | 236 |
| A2.11 Results output for the controlled flow program. | 237 |
| A2.12 Algorithm for installing additional booster fans in the controlled flow network. | 239 |
| A2.13 Results output for the inclusion of additional booster fans. | 240 |
| A2.14 The semi-controlled flow menu options. | 241 |
| A2.15 Structure of data held in file required for linear regression analysis. | 242 |
| A2.16a Flowchart of the semi controlled flow program. | 244 |
| A2.16b Flowchart of the semi controlled flow program. | 245 |
| A2.17 Subroutine flowchart for the semi-controlled flow program. | 246 |
| A2.18 Results output for the one fan system. | 247 |
| A2.19a Results output for the two fan system. | 248 |
| A2.19b Results output for the two fan system. | 249 |
| A2.20 Data input for the fan characteristics option. | 250 |
| A2.21 Results output for the fan characteristics option. | 250 |

SYNOPSIS

The current trends towards increased coal production from seams at greater depth has led to increased demands being placed on the methane drainage and mine ventilation systems.

This study has been directed towards the development of computer models to simulate and analyse the gas flows in methane drainage ranges and the airflow and pressure distribution in mine ventilation networks.

The first part of this thesis describes the conventional techniques of methane drainage currently employed and the mathematical approach used to model gas flow in the methane drainage range. It also discusses how, when combined with measured underground data, predicted results can be used to assess the performance of the range. Subsequent analysis techniques will suggest measures that can be undertaken to optimise this performance and assess the effect of selective network reconfiguration.

The second part of the thesis includes a discussion of the increasing application of booster fans in U.K. underground coal mines and a critical analysis of the mathematical methods used to model airflow and pressure distribution in mine ventilation networks. One particular method was adopted in a simulation model used to analyse networks with booster fans and specified face airflows.

Both simulation models developed have been used to analyse representative underground methane drainage ranges and mine ventilation networks.

The thesis concludes that the accuracy of the methane drainage models can only be guaranteed when developed in conjunction with suitable measured data. The mine ventilation model requires user guidance through the solution and analysis procedure. results are presented in a simple graphical manner and this approach, rather than the 'black box' non interactive approach, is to be favoured in the analysis of mine ventilation networks.

INTRODUCTION

The current trends towards increased mining of gassier coal beds, at greater depth, in areas more remote from surface connections has been followed by a corresponding increase of pollutant emission into a mine ventilation circuit. These pollutants are principally methane and other flammable and noxious gases, respirable dusts and unacceptable levels of heat and humidity. The problem has been exacerbated by increased mechanisation resulting in improved production output from longer coal faces.

The concentration of these pollutants, particularly methane, in the ventilation airstream must be maintained below limits specified in legislation. Methane is explosive if a concentration between 5% and 15% when mixed with air is maintained. Legislation states that if the concentration exceeds 1.25% then production must stop until the methane concentration is diluted below this level by the ventilating airstream.

The primary tool available to a ventilation engineer, to maintain concentrations below the Threshold Limiting Values (TLV's), is a sufficient quantity of fresh air, at the correct velocity, to allow rapid dispersal and removal. Increasing pollutant emissions could be overcome, therefore, by simply increasing the air quantities around the mine ventilation circuit. This , however, has limitations which include ;

- (i) Increasing air quantities i.e. velocities could exacerbate the problem of coarse dust pick-up.
- (ii) The power requirements of fans providing ventilation is proportional to the cube of the airflow passing through them.

The ventilation engineer must seek alternative ways of capturing methane gas before it enters the working areas and becomes a hazard to the mining operation. The drainage of methane, using boreholes drilled into the strata, has many advantages ;

- (i) The safety of the working environment is improved.
- (ii) Coal production can be increased further.
- (iii) The methane gas collected can be used commercially.

The majority of gas collected will be from the fractured strata above and below the working areas. During the lifetime of a mine the working area will become more remote from the surface connection and the costs associated with operating a methane

drainage system will substantially increase. Greater vacuums will be created on the surface to overcome losses through the pipe network and generate the low pressure zones around each borehole to stimulate the gas capture. Increased operating costs will be matched by the increased capital costs involved with procuring the equipment needed for the construction of a longer and more complex drainage system.

The ventilation engineer must ensure the integrity of the system is maintained and that the purity and quantity of gas captured are maximised. He will need to ensure the drainage system is large enough to cope with the estimated volume of gas capture, obtained from gas emission predictions, for production levels to be maintained unhindered by any restrictions. The rate of gas drainage will depend on many factors including the capacity of the exhauster, the degree of fracturing, the in-situ characteristics of the strata and the design of the drainage network.

Effective modelling and assessment of the pipe network will indicate to a ventilation engineer where modifications could be made to provide the optimum performance of the system. Because of the large pressure drops experienced in drainage ranges the assumption of incompressibility of flow cannot be made. Equations describing compressible flow need to be derived. Research carried out has centred on the development of a computer simulation model capable of predicting compressible flow pressure losses in a pipe network thus aiding a ventilation engineer in his assessment of the system performance.

Prior to the pipe network program being utilised to assess the optimal performance the user must be confident it is accurately simulating the existing drainage range. Only when supplied with carefully monitored data can the simulation model be used to assess the actual performance of an existing range and predict the effect of any changes. Monitored data is essential for the good maintenance and simulation of the drainage operation, and necessary if capture efficiencies are to be maintained. Efficiencies of the order of 70% are considered excellent with 50-60% being normal and acceptable.

Obviously fresh air is still necessary to ventilate the mine and dilute the remaining methane liberated into the mine atmosphere. Adequate quantities will still be needed to dilute what methane cannot be captured to levels below the TLV. The ventilating airstream will also provide a comfortable working environment by the dispersal of other mine air pollutants. Too small an airflow will not alleviate these problems and place restrictions on the mining operation. Too great an airflow will exacerbate other

problems such as coarse dust pick-up and the nuisance factor caused by high air velocities. The airflow to the working areas of a mine must therefore be carefully controlled and distributed to provide a safe and acceptable working environment.

In the case of the UK mining industry many collieries are faced with having to increase the quantities of air flowing through high resistance airways, not originally designed to cope with such airflows, thus incurring larger pressure drops and leakages. This will substantially increase the load on the main fan. There are a number of formal strategies the ventilation engineer may employ in order to maintain the efficiency and reduce the operating costs of the ventilation system. These include the sealing of leakage paths, the sinking of additional surface connections, and the installation of booster fans and regulating doors.

The additional fan power required in many collieries has been supplied by underground booster installations. Not only will these installations supply the extra energy required by the current airflow demands, but will be able to deliver and control the airflow in the required locations of the ventilation circuit. Today 25% of all power supplied to ventilating systems in U.K. collieries comes from booster fans [1].

Ventilation engineers are increasingly turning to analysis tools to assist them in the design and operation of mine ventilation systems. The objective of any analysis would be to determine the steady-state airflow and pressure distribution, given the airway characteristics and network topology. The analysis would also indicate the operating points of surface and booster fans placed in the network.

If no airflow constraints are placed on branches within the network then the airflow will distribute itself according to the resistance characteristics of the airways i.e. it would be allowed to split naturally. However, if there exists specified airflow levels (as is commonly the case e.g. on working districts) then booster fans and regulators can be used to control the splitting of the airflow. If all the airflows can be specified the network will be a 'pure controlled' mine ventilation system ; the objective of this type of system would be to find suitable locations for booster fans and regulators in order to maintain the desired fresh air flows. However, if some of the airflows in the network are allowed to vary with others being specified, then the introduction of fans and regulators will alter the flow distribution and the problem becomes one of maintaining the specified flows as well as optimising the power consumed by fans in the network. This network is termed a 'generalised controlled' mine ventilation system.

The objective of the research work undertaken, was the development of two simulation models ;

- (i) To assess the operational performance and pipe network design for a methane drainage system.
- (ii) To analyse the optimum combination of surface and booster fan installations for the 'generalised controlled' mine ventilation problem.

This thesis describes the development of the research project, summarises the results and outlines the general conclusions. The thesis concludes by making suggestions for further research studies in this field.

PART 1

THE OPTIMISATION OF METHANE RECOVERY

Chapter 1

The Mechanisms of Gas Retention and Release

1.1 Introduction

The evolution of coal seams have been brought about by the initial deposition and subsequent decomposition of vegetal matter exposed to air and water. The subsequent covering of this matter leaves bands of the decomposed material in the strata now known as coal seams.

The principal gas produced in the early part of the decomposition process is carbon dioxide (CO_2). However little of this will be retained due to the presence of only a thin permeable cover allowing easy migration of the gas to the surface and of water having the ability to absorb CO_2 .

The later stages of the decomposition process, with increased depth of cover and temperature, produced methane gas (CH_4) which largely flushed away the remaining CO_2 and water. With an increased depth of cover the majority of this gas subsequently became trapped in the coal measures with a small amount diffusing into the surrounding rock.

Methane is therefore the predominant gas stored in coal measure strata with smaller amounts of CO_2 , carbon monoxide (CO), hydrogen sulphide (H_2S), and nitrogen (N_2). This mixture of gases is commonly known as *firedamp*. Hargraves [2] has suggested that cases where CO_2 is the dominant gas have been caused by igneous material intruding the coal measure strata in recent geological time and with this gas displacing the CH_4 . These occurrences however are small and attention has been focused on the problems created by methane gas release.

1.2 Properties of Methane

Methane is an inert, odourless and colourless gas with a density of 0.716 kg/m^3 or specific density (relative to air) of 0.55. It has a specific diffusion coefficient of 0.726 and so will flow more easily than air through porous material. It is a gas which, unfortunately, will burn when mixed with air and becomes explosive with a methane content between 5 and 15% by volume. At a content of 9.6% the mixture will be at its

most explosive. This range could be even lower if coal dust is also present in the atmosphere.

The explosibility of a methane/air mixture can be determined through the use of the Coward Diagram (Figure 1.1). This will determine if the mine atmosphere is explosive, whether or not it is likely to become explosive and if so, when it will become explosive.

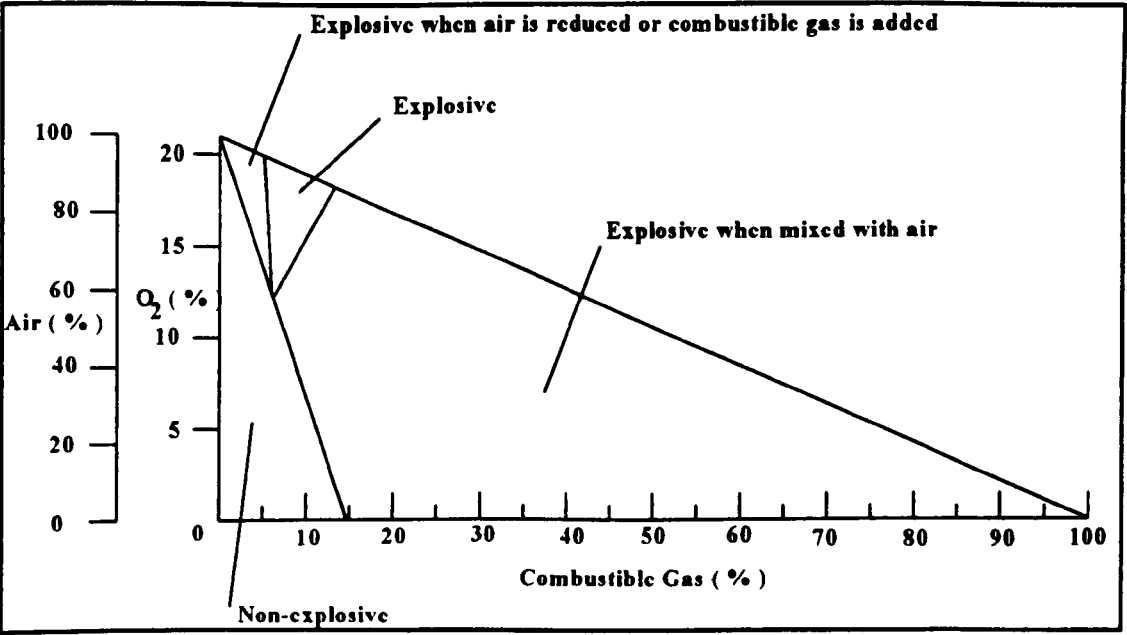


Figure 1.1. Explosibility diagram of a methane/air mixture. (after Coward [3])

Being lighter than air means that the gas will gather in the roof of mine workings. Ventilation air quantities must be sufficient to ensure adequate mixing of the gas to avoid this problem of gas 'layering'. Legislation [4] states that the volume of methane in the mine atmosphere must be less than 0.25% in an intake and less than 1.25% in a powered return. If the levels rise above this then all machinery will be disabled until there has been a drop to a satisfactory level for operations to re-start. Should levels exceed 2% then all men will have to leave the working areas. It is of great importance, therefore, that as much as possible is known about the methane content of coal seams and the mechanisms which affect its retention and release.

1.3. Methane Retention.

The volume of methane released from coal measure strata is far greater than that which would be expected if all methane were stored as 'free' gas in the pores of the coal structure. Zhao [5] suggests that the typical porosity, or ratio of void area to total bulk volume, of coal is between 5 and 6%. Hargraves [6] states this figure is as low as 1 to 3% for Australian coals. For British coals the pore space typically occupies between 3 and 8% of the volume. These figures suggest that there must be other ways in which gas is stored within the coal matrix.

Although the total porosity is small, the void volume is made up of 'an immense number of small pores making the surface area absolutely enormous' [7]. The total surface area can be as high as 20 to 200 square metres per gram of coal. Gas is stored on this internal surface through a process known as adsorption. Adsorption is a surface effect whereby one substance is physically held onto the surface of another. Figure 1.2 demonstrates this with methane and coal.

Only when the 'pressure equilibrium' is disturbed by mining operations will this adsorbed gas be released through a process, the opposite of adsorption, called desorption.

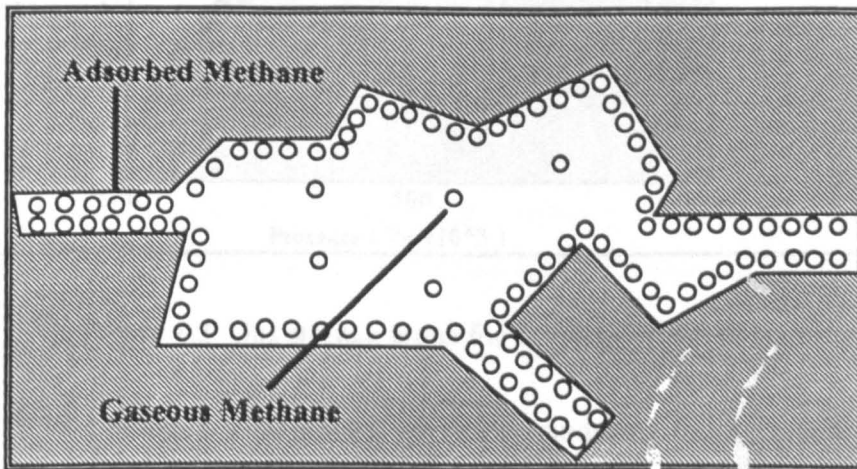


Figure 1.2. Physical representation of molecules in a coal pore
(after McPherson [7])

The volume of gas stored on the free surface, and hence a large proportion of the gas content of the seam is dependent on many factors. These include;

- (i) Gas Pressure.
- (ii) Depth and Rank of Coal Measure.
- (iii) Temperature.
- (iv) Moisture Content.
- (v) Porosity
- (vi) Percentage of Volatile Matter

The deeper the coal seam, the greater the cover load and the greater the gas trapped in the pore structure. Ettinger [8], and later confirmed by Jolly [9], carried out experiments to show how the gas storage or sorptive capacity of tested coal samples increases with pressure. A typical result of these experiments for a British coal is shown in Figure 1.3. The sorptive capacity will increase until a limiting gas pressure is reached. After this any gas content increase will be due to the free gas being compressed in the pore spaces.

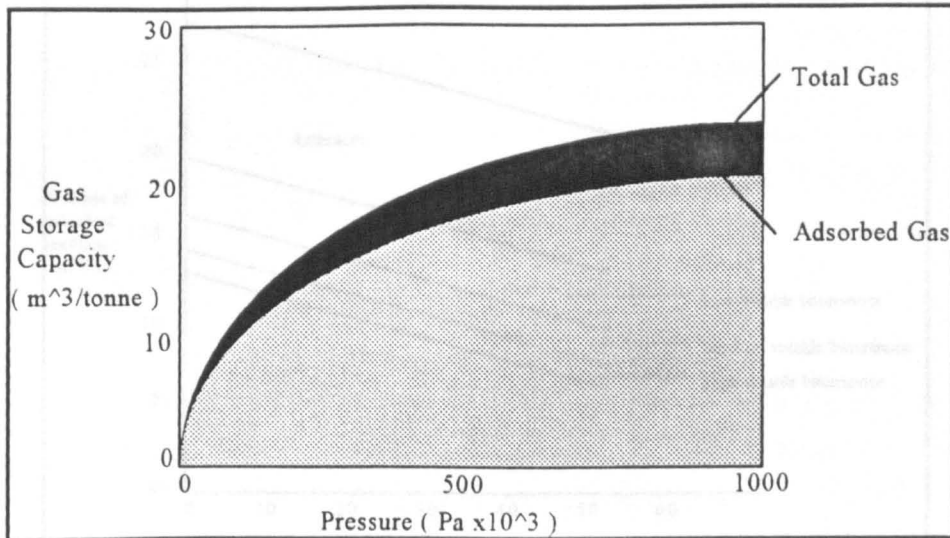


Figure 1.3 Gas storage graph for a typical British coal.

Langmuir [10] adopted a theoretical approach, modelling the adsorbed gas as an idealised monolayer of methane on the coal surface. The dependence on pressure can be stated as ;

$$V = V_t \frac{k_c p}{1 + k_c p} \quad (1.1)$$

where V is the volume of gas adsorbed, V_t the volume required to cover the surface completely,

p the partial pressure of the methane in the coal seam,
and k_c a characteristic constant of the coal seam.

For low gas pressures ($< 100 \text{ kPa}$) V will be proportional to p but for high gas pressures ($> 5000 \text{ kPa}$) V will show no increase with increasing pressure.

The depth of cover, as well as providing an estimate of the gas pressure, will also dictate the temperature of a virgin coal seam. A typical figure for the geothermal gradient (Hargraves [6]) is about 1°C increase in temperature per 30-40 metres increase in depth. Ettinger [8] and others have demonstrated that the sorptive capacity of coal will fall as temperature rises. Graphs of gas storage capacity against pressure are always plotted at a constant temperature and are known as sorption isotherms.

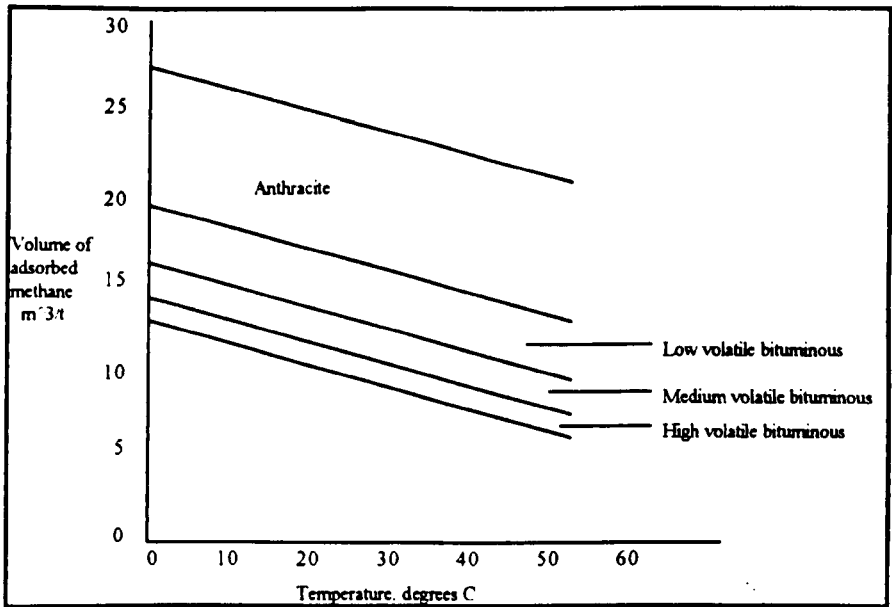


Figure 1.4. Variation of coal adsorption capacity with temperature and rank.
(after Curl [11])

Gunther [12] confirmed the falling sorption capacity with temperature and also concluded that increased moisture content will diminish the sorption capacity. Graham [13] observed that a 10 per cent moisture content was found to reduce to one-third the quantity of CH_4 which was adsorbed by the dried coal. Moisture is a normal constituent of coal and the moisture content is directly related to the porosity. Normal procedure when calculating gas adsorption isotherms is to evacuate the coal prior to the experiment and then make corrections for the moisture content once results are known. Ettinger [8] suggested this could be written as ;

$$\frac{V_{\text{moist}}}{V_{\text{dry}}} = \frac{1}{1 + 0.31h} \quad (1.2)$$

where h is the moisture content in %

V_{moist} is the gas content of moist coal in m^3/tonne ,

V_{dry} is the gas content of dry coal in m^3/tonne

Adsorption isotherms, calculated under laboratory conditions for particular coal samples, will be one of the aids to a mining engineer when assessing the gas content of coal measure strata. Only when the gas content is known can postulates as to the rate of gas emission into mine working areas be made.

1.4 Estimation of Gas Content

The varied methods of estimating the gas content of coal seams can be split into two basic categories ;

(i) Direct Methods.

(ii) Indirect Methods.

Direct methods involve the extracting of a coal sample, immediately placing it in a sealed container and directly measuring the gas emitted over a length of time. This method will therefore require knowledge of the gas emission laws which will ultimately be affected by the degree of fracturing of the sample on removal. Care must be taken to remove the sample from areas as consistent with virgin conditions as possible.

Indirect methods involve the calculation, or measurement, of the in-situ gas pressure and hence calculating gas content from laboratory determined adsorption isotherms.

Care must be taken to make corrections for temperature, moisture and the % of volatile matter in the coal. Ettinger [8] and Kim [14] have used the indirect method. Ettinger used direct pressure readings from boreholes whereas Kim estimated the gas pressure from knowledge of the coal depth and rank. Kissell [15] suggested that water in the coal strata would give misleading pressure readings and so affect the reliability of results. Subsequent research by King [16] on American coals has derived empirical relationships for the gas content of coal with knowledge of just the

% of volatile matter, one of the factors directly affecting adsorption. Generally speaking the % of volatile matter will decrease with coal rank and depth.

Creedy [17] has described a statistical analysis over a series of sample gas content measurements. If a sufficient number of samples are collected some will have degassed very little from the prevailing seam gas content. These samples could be fitted to a suitable distribution and a particular probability point chosen as the best estimate.

1.5 Gas Release

The gas adsorbed in coal pores will remain in equilibrium until this equilibrium is disturbed by mining operations. Breaks in the strata caused by stress changes around the point of mining activity will release gas. The drop in gas pressure will mean the coal measure is less able to hold methane in the adsorbed state and the process of desorption will be initiated. A gas pressure gradient, ranging from virgin gas pressure some way into the strata to near atmospheric at the point of mining activity, will be created in the strata. This gas pressure gradient will cause the gas to migrate to the pressure sink. The lower the gas pressure the less able the strata will be to retain methane in the adsorbed state and so the greater will be the rate of methane release.

The rate of gas emission into the mine workings will depend on this rate of methane release and the ability of the coal to allow gas to flow. This is known as the fluid conductance or permeability of the strata.

Airey [18] [19] derived an empirical relationship to describe the amount of methane, $V(t)$, released during the desorption process ;

$$V(t) = A(1 - \exp\left(\frac{-t}{t_0}\right)^n) \quad (1.3)$$

For small values of $\left(\frac{t}{t_0}\right)^n$ this can be written as ;

$$V(t) = A\left(\frac{t}{t_0}\right)^n \quad (1.4)$$

where A is the initial methane content of the coal in m^3/tonne ,
 t is the time in seconds,
 $V(t)$ is the volume of gas released at time t in m^3/tonne ,
and t_0 and n are empirically derived constants.

Typically n ranged from 0.25 to 0.35 depending on coal rank and t_0 varied quite substantially depending on the coal size (600 seconds for coal below 200 mesh to 7.2×10^5 seconds for 1/4 - 1/2 inch coal). A series of experiments carried out by Lama [20] confirmed this relationship for Australian coals, with n varying between 0.2 and 0.33.

The prediction of gas emission into mine workings depends not only on the volume of gas released during the desorption process but also the nature of this gas flow through the strata. Research into the prediction of emission into mine airways and drainage systems has fallen into two broad categories ;

- (i) Empirical predictions
- (ii) Numerical modelling of gas emission

1.5.1 Empirical Gas Emission Prediction

Empirical methods will be simple, requiring few input parameters, and easy to use. Their derivation will primarily stem from statistical data or readily available data such as adsorption isotherms. They will however lack the theoretical base for a more rigorous analysis.

The development of empirical models has been carried out in a number of European Countries [11]. Varying assumptions have been made as to the zone of gas emission and the degree of gas emission from these zones. All methods will require details of the proximity of other gas sources and their gas content. All have been found to be a useful predictive tool in the mining situation for which they were derived but would require extensive modification if applied elsewhere.

The methods developed by Cerchar in France and in Belgium are very similar, considering total gas emission from the roof and a linear degree of gas emission from the floor. Cerchar fixed the limit of the relaxed zone in the roof and floor at 100

metres whereas the Belgian methods varied this according to the mining situation and also considered sources of gas other than coal.

A number of methods have been developed in Germany, applicable to the analysis of gas emission from sloping seams. The methods differ primarily in the consideration of the gas emission zones and the degree of gas emission functions.

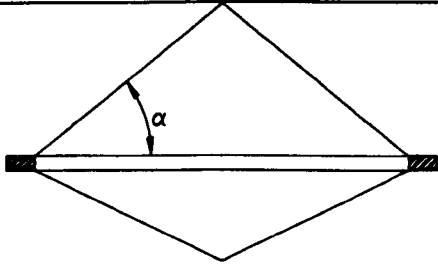
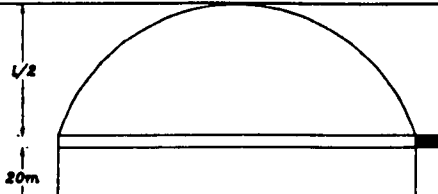
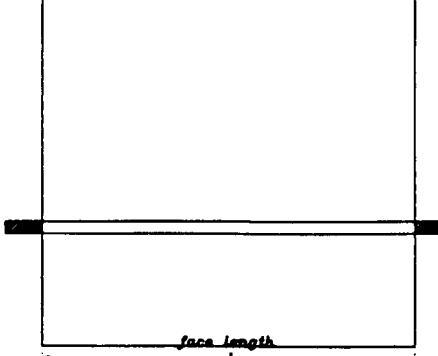
| Author | Zone of Gas Emission | Degree of Gas Emission |
|---|--|--|
| Flugge (after Curl ^[11]) |  | $100 - \frac{200h}{l} \cot \alpha$ where l is the face length and h is the height in roof |
| Schulz (after Curl ^[11]) |  | $\frac{100}{l} \sqrt{l^2 - 4h^2}$ |
| Winter (after Curl ^[11]) |  | $\begin{aligned} \text{roof} &= 100 \exp(-\mu(h - 20)) \\ \text{floor} &= 100 \exp(\mu(h + 8)) \end{aligned}$ where μ is the weakness number indicating the strength of roof and floor. |

Figure 1.5. Gas emission zones considered by German researchers.

The methods developed in Eastern European Countries such as Poland and USSR [11] have a far greater theoretical base. Gas emission estimation involve: the measuring of residual gas pressures and estimating the amount of methane desorbed from the appropriate adsorption isotherm. Both suffer due to the need for an accurate measure of seam gas pressure.

Dunmore [21] in the U.K. used Airey's theory as the basis for the development of a gas emission model. The model was the first to include mining parameters in its

derivation. Face advance and coal production rates are added to the other variables as factors influencing the degree of emission function.

It was also assumed the total gas emission comes from three separate sources ;

- (i) The worked seam
- (ii) Any over and underlying seams.
- (iii) Broken coal on the conveyors.

Gas from behind the face is assumed to flow into the methane drainage system, whereas gas ahead of the face line from adjacent seams flows into the return airway without polluting the face airstream. Gas emitted from the worked seam is assumed to flow into the face airstream.

The zone of gas emission is assumed to be 200 metres above the worked seam and 100 metres below. The degree of gas emission is calculated from the weekly advance rate, the depth of working and the age of the district.

The U.K. method stands alone in being based on physical theory and including mining parameters in the model. This method has subsequently been programmed into a firedamp prediction program, FPPROG.

Although these methods are simple and easy to use, with the greater understanding of the mechanics of methane flow through coal measure strata much work has been done into the numerical modelling for the prediction of gas emission. Numerical methods are based on principles of gas flow in porous permeable media and the flow equations are mainly derived from D'Arcy's Law.

1.5.2 Numerical Gas Emission Prediction

Of all the parameters included in derivations of equations, permeability is the one most crucial in affecting the reliability of results. Disturbances created by mining operations affect the permeability of the strata and hence determine the pattern of methane emission. It is therefore essential that when studying gas flow the components of stress and stress-permeability behaviour are included. This will allow analysis of permeability changes occurring under conditions which simulate actual mining operations.

1.5.2.1 D'Arcy's Law

With mining operations the pressure equilibrium of a virgin coal seam and the surrounding strata is disturbed. The pressure gradient will force gas into the mine workings. With the falling in-situ gas pressure more methane will desorb and diffuse into the cleats and fractures before flowing towards the low pressure sink.

The rate at which gas will flow is governed by the ability of the strata to transmit gas with the pressure gradient existing across it. This is known as permeability. Permeability can be broken down into two components ;

- (i) micro-permeability giving an indication of the desorption process and subsequent diffusion into fissures.
- (ii) macro-permeability giving an indication of the flow through these fissures.

Flow through fissures obviously constitutes the greater component of emission into mine workings and is frequently modelled using D'arcy's viscous laminar flow model ;

$$Q = \frac{kA}{\mu} \frac{dp}{dl} \quad (1.5)$$

where Q is the flow rate in m^3/s ,

k the permeability in millidarcys (mD)

A the cross-sectional area of the sample in m^2 ,

μ the dynamic viscosity in kg/ms and,

$\frac{dp}{dl}$ the pressure gradient across the sample.

For compressible flow this is sometimes written as ;

$$Q = \frac{kA}{\mu} \frac{\bar{p}}{p} \frac{dp}{dl} \quad (1.6)$$

where \bar{p} is the mean pressure across the sample.

1.5.2.2 The Dependence on Permeability

Permeability obviously plays an important role in dictating gas flow into mine workings. Knowledge and assessment of the factors governing permeability is therefore essential. These factors include ;

- (i) coal rank and depth.
- (ii) gas pressure.
- (iii) cleat and fracture systems.
- (iv) stress disturbances.

Depth and rank has the greatest influence on the gassiness of coal measure strata. With increase in depth there is an associated increase in confining pressure and hydrostatic stress which will dramatically reduce permeability. The approach of mining operations will change this simple stress and pressure pattern.

Gas pressure, as well as affecting the adsorption of gas in coal, will also alter the permeability of the strata.

Klinkenberg [22] observed a decrease in permeability with an increase in the mean gas pressure towards a value identical with the liquid permeability of the sample. This is written as ;

$$k_d = k_l \left(1 + \frac{b}{\bar{p}} \right) \quad (1.7)$$

where k_d is the apparent permeability,

k_l the liquid permeability,

\bar{p} the mean pressure and,

b the Klinkenberg constant. different for each material.

This apparent change in permeability was ascribed to the decrease in slip flow at the solid gas boundaries with increasing pressure.

Several researchers have investigated the Klinkenberg effect with coal samples [23] [24]. McPherson reported a reverse Klinkenberg effect at high pressures. He postulated this could be due to a re-structuring of the flow paths and also reported that coal permeability is strongly dependent on pressure history.

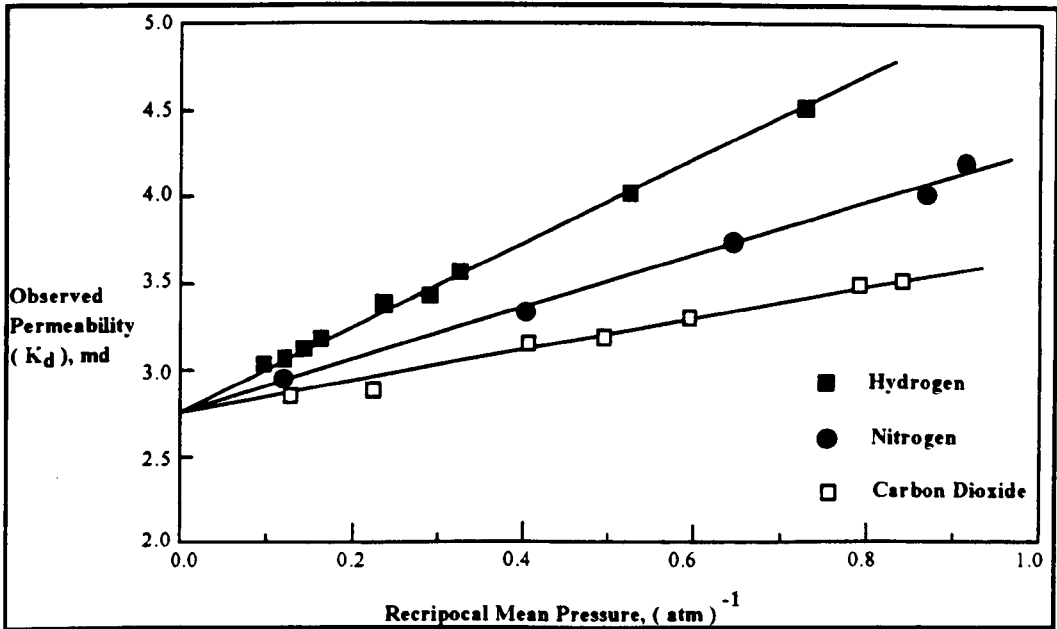


Figure 1.6. Permeability of core sample to hydrogen, nitrogen and carbon dioxide at different pressures (after Klinkenberg [22]).

There will also be a significant stress redistribution around mine workings. Early research into the effect of stress on the gas flow characteristics of coal measure strata dealt with the simple laboratory analyses of stressed samples. More recent work has focused on the global mining situation and particularly the stress profiles around longwall faces.

Fatt and Davies [25] demonstrated the reduction in permeability with overburden pressure (hydrostatic stress) on a range of sandstone samples.

Mordecai [26] and Somerton [27] continued this work by stressing samples of coal, both hydrostatically and triaxially, to failure. Both confirmed the dramatic drop in permeability with applied stress until a minimum is reached. Mordecai then observed, upon increasing the stress further, an increase in permeability until the specimen failed. After failure permeability values were found to be 2 or 3 orders of magnitude greater. Both authors recognised the more impermeable the sample the greater was its sensitivity to stress.

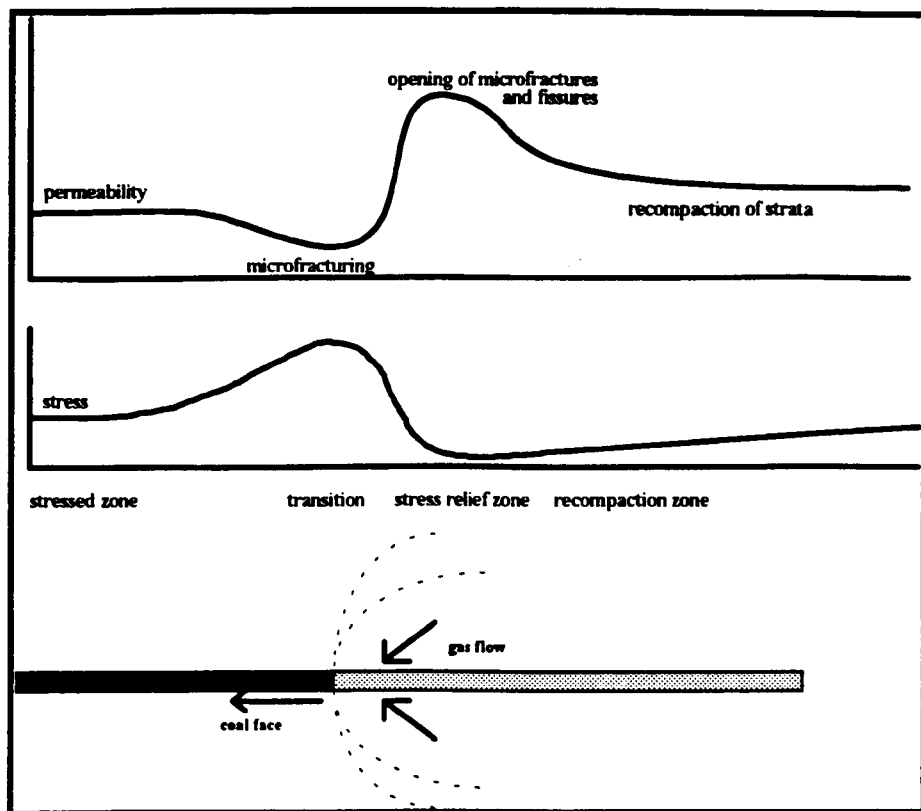


Figure 1.7. The variations of stress and permeability in strata above and below an advancing longwall coal face (After McPherson [7]).

McPherson took these results, along with results indicating the stress distribution around mine openings, to suggest possible permeability profile around a longwall coal face.

He indicated a decrease in permeability ahead of the face with an increase in the applied stress even though minute fractures were appearing in the strata. Behind the face there is a dramatic increase in the permeability as these fractures open up in the stress relaxation zone before the strata recompacts and the permeability settles down to a constant value but higher than that experienced in the virgin conditions.

Durucan [28] categorised the stress profile into zones and analysed the nature of the stresses in each zone as an aid to predicting permeability. Ahead of the face in the zone of increased stress is known as the 'front abutment zone' and principal stresses are assumed to be compressive. However 3 to 5 metres before the face one of the principal stresses becomes tensile, causing fracturing of the rock and a dramatic increase in permeability, in the area known as the 'crushing zone'. The state of stresses in the stress relief zone is very complex before a cover load is re-established in the 'recompaction zone' where the stresses become triaxially compressive in nature.

The stress characteristics of the surrounding strata could then be used to predict permeability changes and methane migration paths around the longwall opening. This is shown in Figure 1.8.

1.5.2.3 The Development of Numerical Models

Keen [29] , O'Shaughnessy [30] and Ediz [31] have all developed numerical models to analyse gas emission into mine workings which include the essential components of stress and stress permeability analysis. Keen used a finite difference modelling approach whereas O'Shaughnessy and Ediz favoured the more versatile finite element approach.

The Finite Element method allows a structural domain to be broken down into simpler parts or elements. The behaviour of these elements can be defined by a simple relational equation in terms of load, stiffness and displacement. All element equations can then be combined into a system of simultaneous equations which allows the solution for the whole structure. Material properties giving indications of mechanical strength and elastic behaviour can be assigned to each element. This allows variations in stress-permeability behaviour occurring in different strata sections to be included in the model. Vertical and horizontal stresses in the program are generated using routines which calculate stress as a function of depth and material type. Once this stress behaviour of the strata has been determined an assessment of the induced permeability patterns can be made from measured behaviour of rocks and coal seams.

In order to make better use of the stress analysis results more information is needed about post-failure stress-permeability relationships for coal measure strata. Gas flow in these areas is quite different from the virgin or pre-failure values and more knowledge is needed to improve understanding and the reliability of the current model.

This stress data can then be supplied to the finite element routine to calculate the gas pressure distribution.

As well as material properties the required inputs include parameters to define model size, and initial and time dependant pressure boundary conditions. The programs terminate when the flow equation has been solved and the output gives the predicted gas pressure distribution and the methane flow rates into roadways and boreholes.

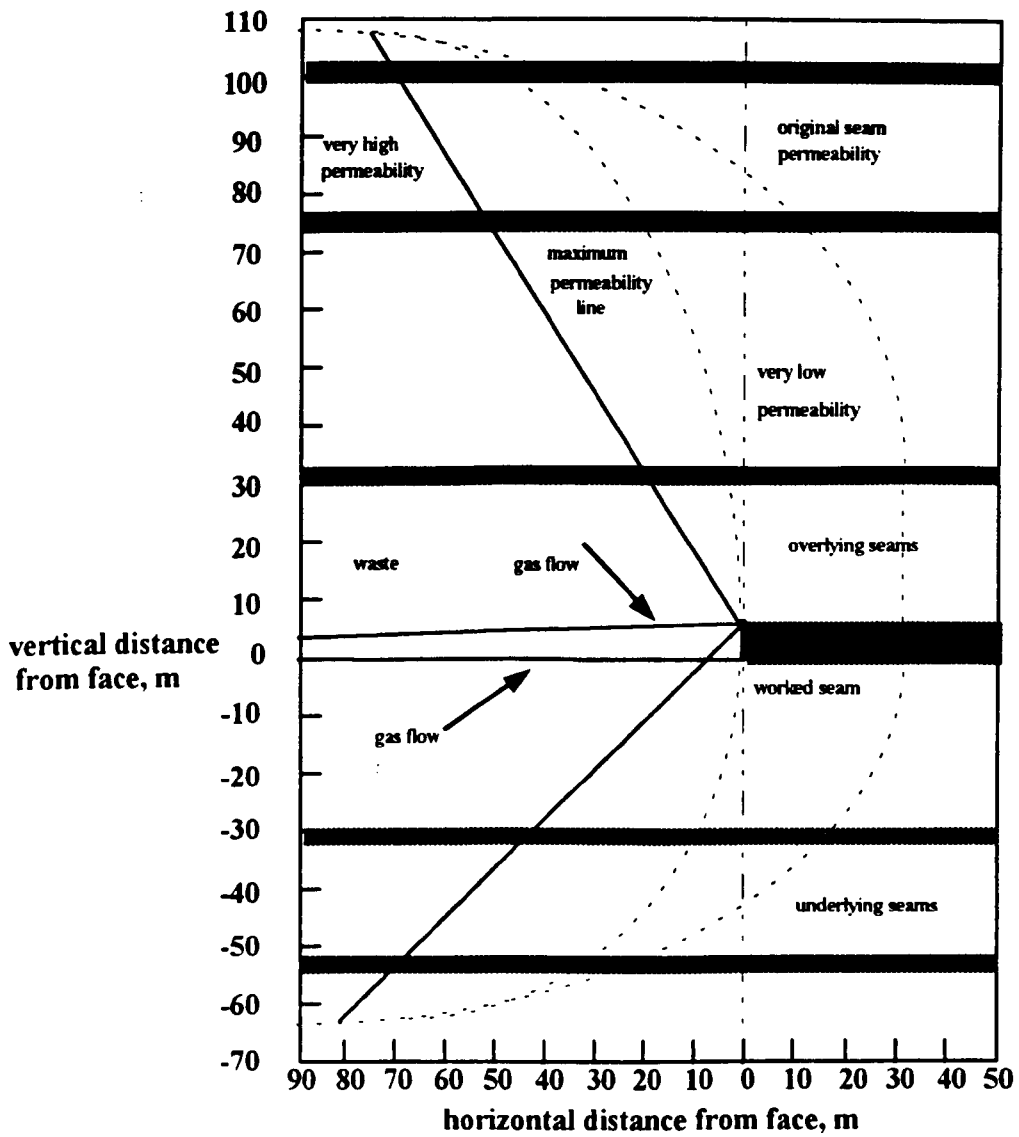


Figure 1.8. Different permeability zones and suggested flow paths of methane around a working longwall face. (after Durucan [28])

1.6 Summary and Conclusions

This chapter has discussed the retention of methane gas as a monomolecular layer on the internal surfaces of coal measure strata. The volume of gas retention has shown to be influenced by a number of physical parameters such as pressure, temperature, moisture content and porosity. Methods of measuring the volume of gas retention have also been discussed.

The gas will remain adsorbed to the interior surfaces of the coal until mining operations disturb the equilibrium and the gas is released. The rate of gas release is primarily dependent on the permeability of the coal measure strata which in turn is influenced by the stress disturbances created around mine workings.

Only once the characteristics of the strata have been determined and an assessment made of the expected methane flows can an effective drainage system be designed to remove the in-situ strata gases. The practices developed in the various mining locations throughout the world have varied depending on the situations prevalent in the area. Chapter 2 will discuss these practices and the factors which have influenced the development of the particular drainage methods.

Chapter 2.

Methane Drainage

2.1 Introduction

The current trends towards deeper coal seams and higher production rates has aggravated the problem of methane emissions into working areas of a mine. This problem has had to be alleviated, not only through increased ventilation air quantities, but by the selective application of methane drainage.

Methane drainage is a method of removing the gas contained in the coal seam and surrounding strata by the application of suction through pipelines and thus preventing the gas entering the ventilating airstream. This, along with prediction of gas emissions, today forms an integral part of the overall ventilation planning strategy.

Methane drainage was first introduced in the Ruhr coalfields of Germany some 40 years ago as a means of controlling excessive methane emissions from longwall coal faces. Since then the development of gas drainage technology has taken a number of complementary paths.

Apart from providing a safer working environment and allowing greater production rates, methane drainage can provide gas for commercial utilisation. The objectives of gas extraction for commercial and safety reasons may not directly coincide. In the first case there may be no intention of mining coal after the extraction of the gas. This forms part of an operation to extract gas at a maximum concentration for end use. The latter has the overriding objective to remove the maximum amount of gas from the surrounding strata so that the residual gas entering the mine workings can be effectively diluted by the designed fresh air quantities.

The differing methods of drainage, employed today throughout the world, are dependent primarily on the end use of the gas and the characteristics of the gas bearing strata. The development of a suitable drainage system requires the determination of a number of physical parameters dependent on the strata characteristics and the production methods employed. Once these strata parameters, and their interdependence, have been identified then an effective drainage system can be designed to remove the in-situ strata gases.

Shallow seams with high permeabilities, such as those experienced in the U.S.A. and Canada, offer good conditions for access and gas extraction from surface operations hence also allowing access prior to any mining activity.

Deeper seams with a greater depth of cover and reduced permeability, but higher in-situ gas contents, will only release large amounts of gas when disturbed by mining operations. In this case access for methane drainage operations will principally be from the mine openings and roadways with the use of cross measure boreholes. If necessary gas can be captured during the development or driving of roadways and particular gas sources, such as seams above or below the one being developed, can be isolated with in seam boreholes.

| Seam | Depth (m) | Permeability (mD) | Gas Pressure (MPa) | Gas Content (m ³ /t) |
|--------------------|----------------|------------------------|-------------------------|--------------------------------------|
| Pittsburgh (US) | 150-300 | 10 | 1.4-1.9 | 6.2 |
| Pocahontas (US) | 420-600 | 2-9 | 4.5 | 12.1 |
| Bulli (Australia) | 480-610 | 3-35 | 2.6-4.2 | 13.0 |
| Deep Soft (UK) | 900-1000 | <0.01 | 1.2 | 8.0 |

Table 2.1. Comparative coal seam characteristics.

Strata gas drainage can thus be split into 3 broad categories ;

- (i) drainage from surface boreholes.
- (ii) drainage during underground development.
- (iii) drainage during underground extraction.

Gas capture from virgin or undisturbed coal seams, or during roadway driveage, is termed pre-drainage whereas gas capture during the coal winning process is often known as post-drainage.

2.2 Drainage From Surface Boreholes

Properties of coal fields in areas such as the U.S.A. and Canada with high permeability, shallow seams and high seam gas pressure permit degasification from surface operations. Tax incentives offered by the respective governments, particularly in the U.S.A. during the 1980's, has also meant viable commercial operations taking place without there ever being an intention to begin mining operations. Over \$1

billion was invested spurning over 200 wells. Many Canadian seams, for instance in Alberta, are not an economic thickness for mining but the high gas contents has further induced surface degasification operations.

In most cases however surface boreholes will be drilled to capture gas during or prior to mining activity. Not requiring any mine openings for installation, surface operations can be used to pre-drain virgin or undisturbed coal seams. Pre-drainage with surface boreholes would appear to be a universal panacea. However the early stages of the operation will produce very little gas and a long period of dewatering.

The gas in a coal seam is usually saturated with water. The surface borehole will extract this water and as the water phase is depleted, the relative permeability to gas improves and is reflected in increased production of gas.

The production of gas has generally been improved through hydraulic fracturing [32] [33]. Water at high pressure is pumped down the borehole to break the rock. The fissures produced are filled with sand to improve the permeability to gas. This technique of hydrofracturing undisturbed coal seams must be monitored when applied to mineable coal. The damage suffered to roof and floor could produce difficulties into any subsequent mining operation. Hydraulic fracturing in these cases is generally not recommended.

The use of surface boreholes for pre-drainage, although needing long lead times (up to 5 years [34]) for any significant degassing to take place, do provide valuable information as to the geology of the proposed mining area.

The greatest benefit from surface boreholes is achieved when draining gas from above active goafs. As the over and underlying strata relaxes, fractures will open and permeability increase. The goaf behind a longwall face will become a reservoir for methane.

Surface boreholes will intercept these fractures and capture the methane released. Boreholes will often be spaced every 250-500 metres apart. Vacuum pumps will often be necessary on each borehole to improve the flow rates [35].

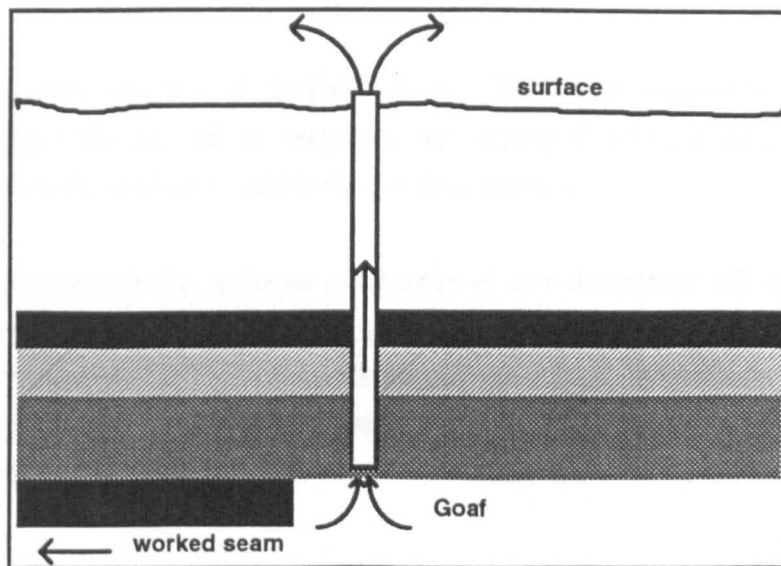


Figure 2.1. Methane drainage above an active goaf using surface boreholes.

The drilling of deep boreholes is expensive and not possible in all geological conditions. A vacuum pump required on each borehole will add even greater expense. The severe cost and safety aspect will restrict the use of surface boreholes in the U.K. and other European Countries where mining often takes place at depths of over 400 metres and sometimes of depths up to 900-1000 metres. The low permeabilities and seam gas pressures will restrict any pre-drainage.

Difficulties may also be encountered in drilling holes and laying pipes from the surface. The surface environmental implications mean that surface boreholes are unlikely to represent a viable solution in densely populated, environmentally sensitive countries such as the U.K.

2.3 Drainage During Underground Development

The risk and occurrence of methane emissions during the development of underground mining operations, particularly from the worked seam, has made it necessary to introduce methods of pre-drainage prior to the start of full scale mining activity. The problem is particularly prevalent in shallow seams with a low overburden pressure and high permeability and is further exacerbated by the development of virgin ground.

The current trends towards the use of fewer retreat longwall mining units with higher production levels has necessitated the development of longer roadway driveages. In such conditions extremely large surface areas of coal seam are exposed and in many cases the only answer to the problem of gas emission from the worked seam has been to develop an in-seam methane drainage system.

In-seam boreholes need not be used in isolation. Boreholes inclined to intersect over and underlying strata will still be necessary, particularly if workings enter the emission zone of previously worked or currently working districts.

Applying methane drainage systems in advance of coal extraction will reduce the gas content and gas pressure of the seam and hence lessen the burden on the drainage system when full scale mining begins. Obviously the longer the drainage period before full scale mining, the better. Reductions in gas pressures will also reduce the risk of gas outbursts, a problem particularly prevalent in Australia [36] and Poland.

A number of methods have been developed to de-gas the seam being worked. In general all will involve the drilling of horizontal boreholes of various lengths and various angles to the roadway driveages. The earliest drilling of these holes will ensure the maximum time for de-gassing to take place not only for the proposed panel but also the development of any future panels. In some cases the maximum time available for drainage can be up to two years [32].

When driving headings boreholes will commonly be drilled in both sides of the roadway at small angles to its axis. Lengths will be chosen such that they project beyond the face of the heading.

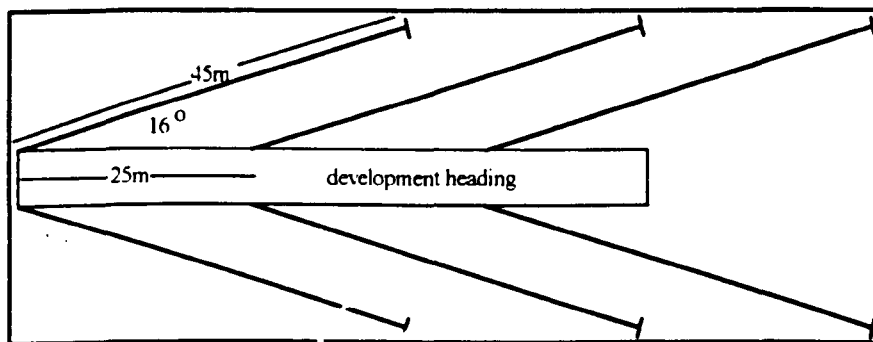


Figure 2.2. Typical arrangement for the pre-drainage of a development heading
(after Gluckauf [34])

Highton [37] has described some particular problems experienced at U.K. collieries and the drainage layouts that were subsequently developed under various conditions including virgin, previously overworked and inclined seams. Figure 2.3 shows a development heading of a retreating face in virgin ground.

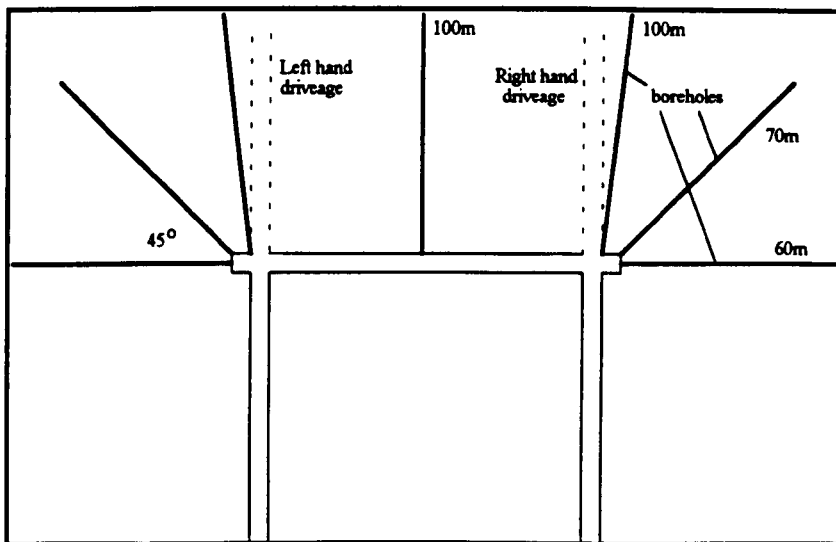


Figure 2.3. A development heading at Point of Ayr colliery. (after Highton [37])

These cases were also compared with drainage methods employed in the Bulli seam in New South Wales, Australia. Suggestions were made for the drainage layout to obtain the maximum degassing effect. Boreholes should be drilled at right angles to the development road and the length of holes should be sufficient to drain future workings. These holes should be on suction for at least 6 months prior to working.

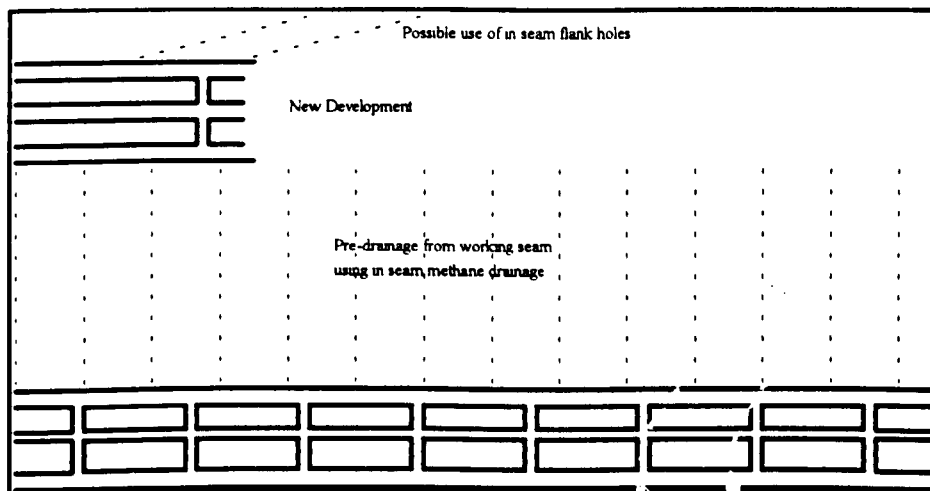


Figure 2.4a. Methane drainage from the working seam. (after Highton [37])

Hungerford [38] has also described conventional pre-drainage techniques used in Australia but stated the time period may be too short for effective drainage to take place.

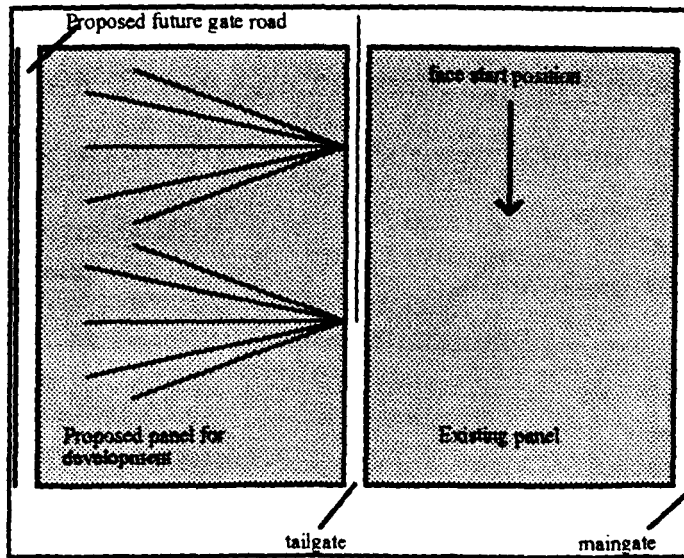


Figure 2.4b. Methane drainage from the working seam. (after Hungerford [38])

An alternative method described, now frequently used in Australia and U.S.A. was that of long hole drilling. Hebblewhite [39] has described the introduction of longhole drilling at West Cliff Colliery, N.S.W. during 1981. Boreholes are drilled in the seam being developed to lengths of up to 1000 metres. Marshall [40] along with Hebblewhite have detailed some of the particular problems of longholes. These include :

- (i) The maintenance of horizon and direction.
- (ii) The risk of gas blow backs in zones liable to outbursts.

The success of the method is critically dependent on the high permeability of the coal seam and although many are used in the United States their application for drainage of methane ahead of development has been prolific only in the Pittsburgh seam.

Long, in-seam boreholes will substantially reduce the amount of drilling required for drainage. Estimated gas flows need to be accurately predicted to assess the required borehole diameter. If gas flow is too high or borehole diameter too small, pressure build up will significantly retard flow.

Longholes have also been drilled into adjacent seams [38], not only providing uniform pre-drainage from those seams but also providing a suitable post-drainage installation.

Longwall methods require level fault free seams. Any information provided from longholes as to faults in the seam would be valuable for future mine planning.

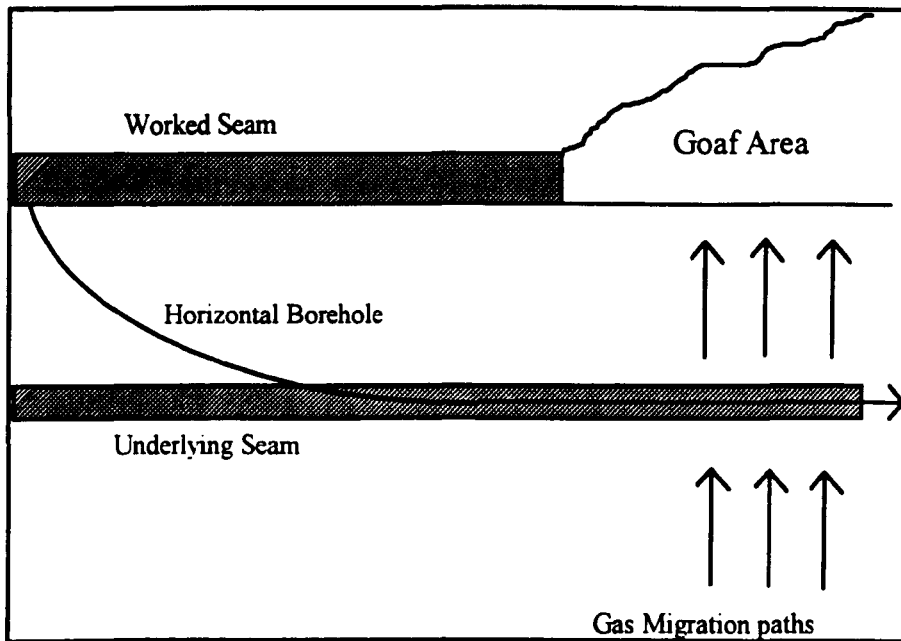


Figure 2.5. Longhole drainage of an adjacent seam.

Once coal extraction begins and extensive fracture systems are created gas will migrate from other seams into the working area. Drainage techniques now need to be developed to capture this gas before its emission into the ventilating airstream.

2.4 Drainage During Extraction

2.4.1 Background

As mentioned previously, one method of draining gas from relaxed zones during mining operations has been to sink surface boreholes into the strata immediately above longwall goaves. Although suitable for shallow seams this method becomes prohibitively expensive with no guarantee of success in the deeper seams of lower permeability common to European countries.

An alternative method of reducing methane emissions is to position the new longwall panel in the emission zones of previously worked districts. The gas emissions will be substantially lower than if the conditions were virgin. This is a consequence of the removal of the gas source and the already partial de-gassing of the strata.

However, whether the strata be virgin or previously worked, methane drainage will still be needed and significant gas capture is commonly achieved through the use of cross-measure boreholes.

Cross-measure methane drainage was first used in the Ruhr coalfields of Germany some 50 years ago and is now the most common form of methane post-drainage in Germany, United Kingdom, France and other E.E.C. countries. In 1952 Bromilow [46] recorded the results of trials at 8 British Collieries and by 1959 firedamp drainage was common to most divisions of the National Coal Board [41]. By 1974 there were some 8000 boreholes in British Coal mines with a total of 320 Km in length. Morris [42] reported in 1982 that 60% of British mines employed methane drainage with an annual gas capture of some 500 Mm³.

| | West Germany | United Kingdom | Belgium | France | E.E.C. |
|--|-----------------|-------------------|---------|---------|-----------|
| No. of Boreholes | 4.059 | 7.861 | 261 | 679 | 12.860 |
| Total Length (m) | 201.885 | 320.993 | 14.585 | 31.927 | 569.390 |
| Total Methane Drained (Mm ³) | 575.036 | 381.031 | 62.610 | 152.211 | 1.170.888 |
| % utilised | 59.5 | 29.9 | 95.8 | 88.1 | 55.5 |

Table 2.2. Firedamp drainage data for the European Community in 1974
(after Gluckauf [34]).

This technology has been tried in other countries such as the United States [43] [45] and South Africa [33] but the use is limited due to other simpler alternatives available. However the continued development of longwall mining techniques and the associated rapid rates of face advance means the method is becoming increasingly popular.

Boreholes are drilled above and below the active goaf to capture gas from the relaxed zone immediately behind the face line. Advantage is taken of the increased flows from the enhanced permeability and bed separation cavities experienced in this region. Emission values indicate other gas sources commonly seams above and below the working horizon. The length and inclination of boreholes must be chosen such that these gas sources are intersected.

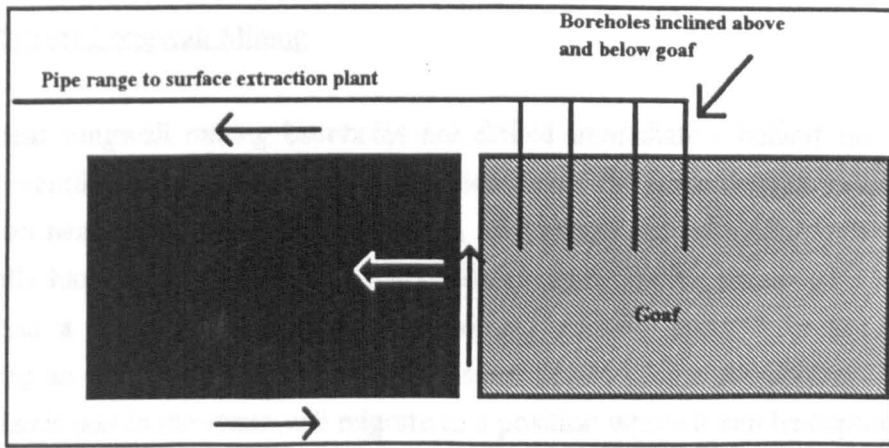


Figure 2.6. 'Retreat longwall' methane drainage using cross measure boreholes.

2.4.2 Advancing Longwall Mining

For advancing longwall mining boreholes will be drilled from the return gate roadway. The ventilation pressure differences between intake and return roadways will create migration paths in the goaf and strata. Any gas released into the goaf will be diluted by the air leakage and forced, by the pressure difference, into the return roadway airstream. Gas in the strata will migrate to a position near the return roadway where it can be effectively captured by methane drainage boreholes.

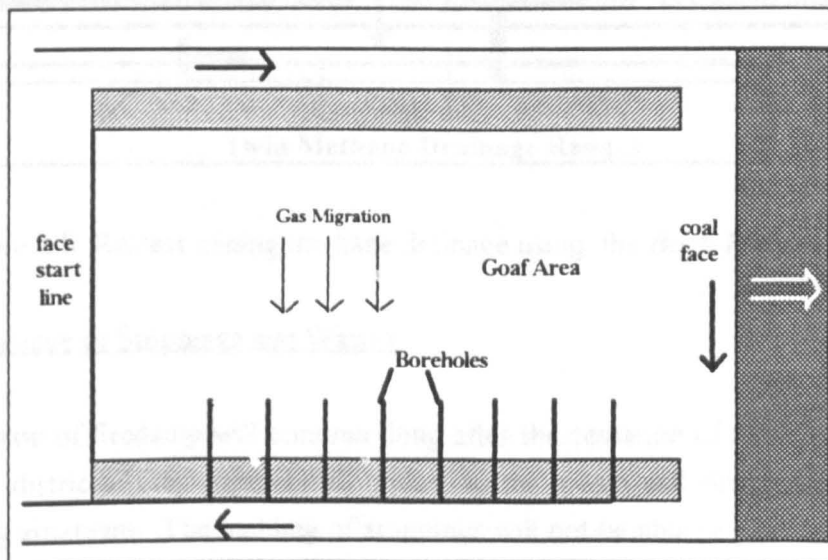


Figure 2.7. Methane drainage in advancing longwall mining.

2.4.3 Retreat Longwall Mining

For retreat longwall mining boreholes are drilled immediately behind the face line. With no ventilation pressure difference applied across the goaf, the gas will migrate to a position near the return gate of the face. To direct gas migration away from the potentially hazardous face line a **back return** system may be employed. Using coal pillars and a pack cavity system air is coursed initially away from the face thus simulating an advancing set up. Boreholes are drilled across the coal pillar into the strata. Again gas in the strata will migrate to a position where it can be captured by the drainage boreholes.

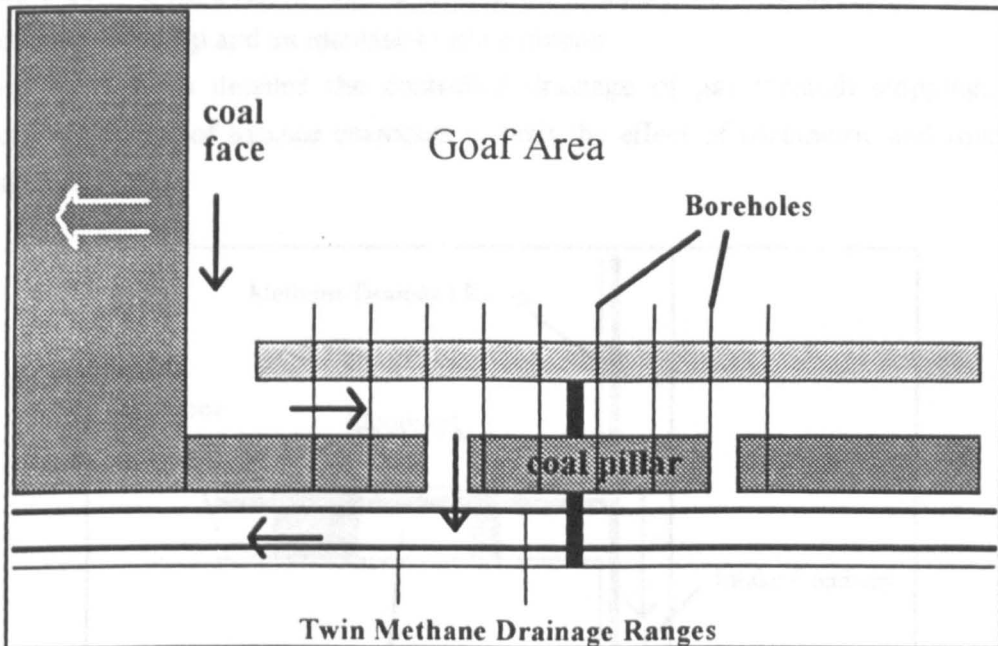


Figure 2.8. Retreat mining methane drainage using the **Back Return** system

2.4.4 Drainage of Stoppings and Wastes

The emission of firedamp will continue long after the cessation of mining activity in a particular district. Gas emitted will collect in the waste and finally emerge in the ventilating airstream. The building of stoppings will not be able to prevent this and so this gas must be drained from these stopped off areas.

Pipes are positioned through the stoppings as the latter are built and coupled into the firedamp drainage range. To prevent air entering the stopping, and hence the methane drainage range, the pressure of the ventilating airstream is kept slightly less than that in the stopping.

Although changes in barometric pressure have negligible effect when considering cross measure methane drainage they are greatly significant when considering gas emission from stoppings [44]. When barometric pressure falls, the extra volume of gas created will emerge into roadways unless captured by the drainage pipe in the stopping. Conversely for increasing barometric pressure drainage will need to be stopped following the possible ingress of air into the waste.

The problem of gas emission from wastes will commonly dictate the use of exhausting ventilation systems as a fail safe control. A main fan stoppage would be accompanied , initially, by a pressure rise in underground roadways thus inhibiting gas emission from waste areas. Conversely a forcing ventilation system would be accompanied by an initial pressure drop and an increase in gas emission.

Wood [44] has detailed the controlled drainage of gas through stoppings and described the use of balance chambers to limit the effect of barometric and roadway pressure changes.

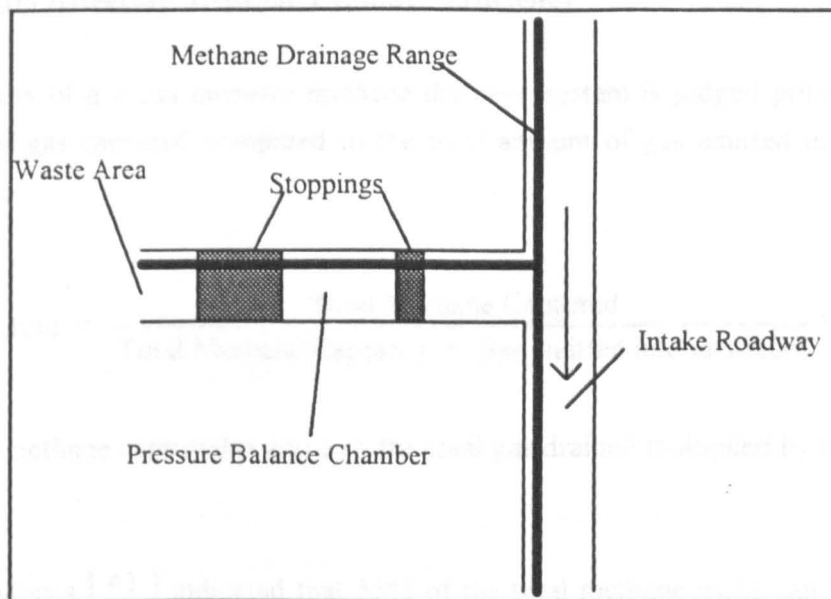


Figure 2.9. Methane drainage from stopped off areas.

Another method of draining gas from the waste, employed successfully in Germany, is through the use of pack cavities. This involve the building of a pipe into a cavity created in the waste. A small suction applied to the pipe will drain gas. With this method there is the obvious possibility of leakage of air into the gas range and it is, of course, not suitable where total caving is practised. However it does move the gas fringe away from the hazardous face line and further into the goaf.

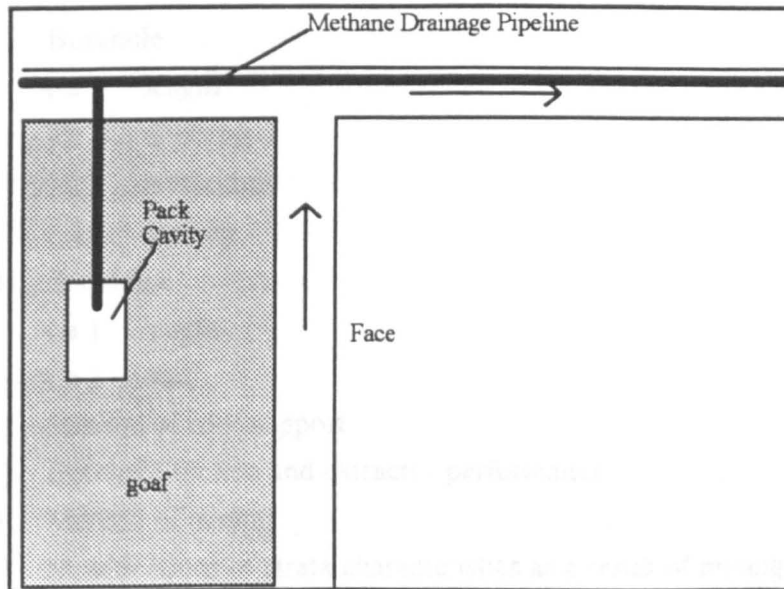


Figure 2.10. Methane Drainage using the pack cavity system.

2.5 Factors Affecting Methane Drainage Efficiency

The success of a cross measure methane drainage system is judged primarily on the amount of gas captured compared to the total amount of gas emitted in the current district. i.e.

$$\% \text{ capture} = \frac{\text{Total Methane Captured}}{\text{Total Methane Captured} + \text{Gas emitted into airstream}} * 100\%$$

The total methane captured is equal to the total gas drained multiplied by the purity of that gas.

In 1961 Morris [41] indicated that 55% of the total methane make can be captured and in 1982 the same author [42] reported the overall effectiveness to be commonly between 40% and 60% and frequently between 70% and 80%.

Swift [47] reported in 1970 that the 41 retreating longwall faces then operational in U.K. mines had capture efficiencies of between 30% and 75%.

These figures, if anything, demonstrate the variations that exist in the efficiency of gas capture. This efficiency will depend on many factors. These include ;

- (i) Borehole
 - (a) length
 - (b) diameter
 - (c) inclination
 - (d) spacing
- (ii) Standpipe
 - (a) length
 - (b) seal
- (iii) Method of roof support
- (iv) Borehole suction and extractor performance
- (v) Method of mining
- (vi) Modifications to strata characteristics as a result of mining
- (vii) Pipe network design and integrity

2.5.1 Borehole Configuration

Boreholes are the actual gas draining apparatus and therefore careful monitoring of their performance and the parameters influencing their performance is essential for a successful and effective methane drainage operation.

Bromilow [46], in 1952, studied the performance of methane drainage operations in the U.K. and drew conclusions as to the optimum configuration of borehole parameters for an effective drainage system. These conclusions were drawn from practical results of the few methane drainage installations that were in operation at the time.

The optimum position, length and inclination of boreholes will, of course, depend on the strata and its structural behaviour during and after mining activity. Firedamp horizons, strata formation and gas emission zones all combine to determine the optimum combination of borehole parameters. Borehole length and inclination need to be selected such that the relaxed strata, particularly above waste areas is intersected. Boreholes will commonly be inclined from between 35° and 70° to the horizontal for holes drilled parallel to the face line. Shallower angled holes may be affected by rock fissures and bed separation cavities [41] [34]. Some boreholes have been found to give better results when given a forward lead i.e. inclined towards the face [41]. However this is not always the case [46]. Forward lead may be necessary if drilling close to the face is not possible.

General guidelines exist for the spacing of boreholes and are usually based on past colliery experience. This distance is usually between 20 metres and 25 metres. The spacing ultimately depends on the zone of influence of the borehole, which in turn is dependent again on the strata characteristics and the suction applied to the borehole. Boreholes should be positioned such that their zones of influence just overlap [34]. Too close a spacing will induce mutual interference between holes as noticed by Wharton [50] and Morris [41]. Boreholes spaced too far apart will allow gas to migrate into mine workings.

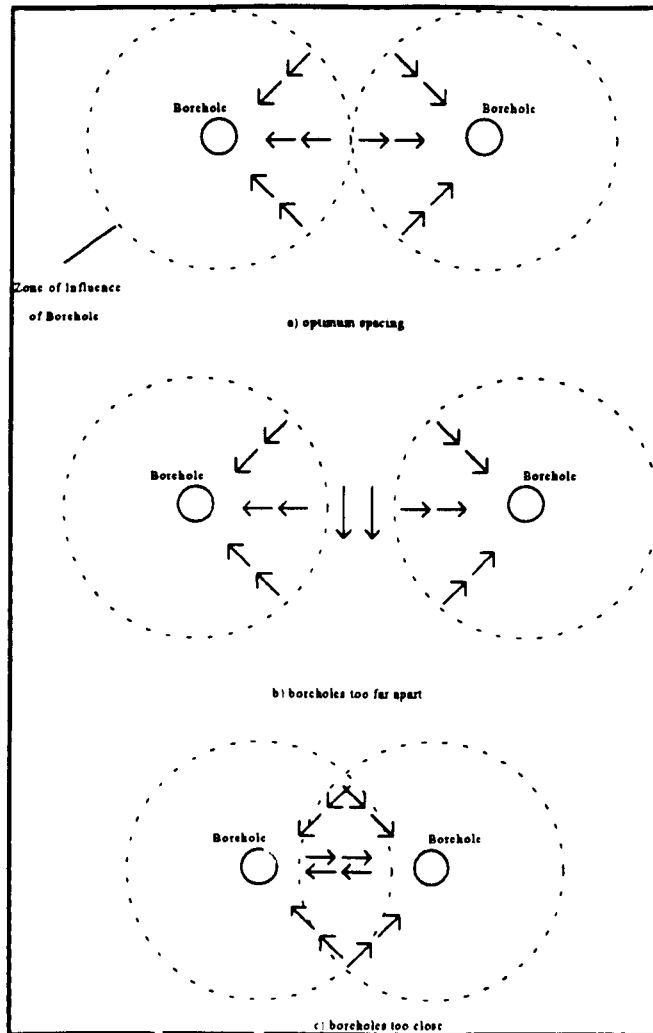


Figure 2.11. Selection of an optimum borehole spacing. (after Gluckauf [34])

The most productive boreholes will usually be situated closest to the face. The first hole will commonly be some 10 metres to 40 metres outbye of an advancing face [41]. For retreating faces boreholes will always be drilled in the relaxed zone behind the face line through the pillars in the 'back return' and never in front [49]. If a back

return is not employed boreholes can be given a forward lead to intersect the relaxed zone.

As stated earlier the quantity of gas captured is dependent on the suction achieved at the borehole which in turn depends on the resistance of the borehole. The typical pressure loss along a borehole can be written, after Morris [42], as ;

$$\Delta p = \frac{1}{2} \rho \lambda \frac{l Q^2}{d A^2}$$

where Δp is the pressure loss, ρ the density in kg/m^3 , λ the friction coefficient, Q the volume flow rate in m^3/s , A the cross-sectional area in m^2 , d the pipe diameter in metres and l the pipe length.

As can be seen, the diameter is an important factor in determining pressure loss. Typical borehole diameters will vary between 50mm and 70mm. Increasing the suction along a borehole, either through increasing diameter or uprating exhausters , however will also increase the risk of air inleakage and thus reduce the purity and total gas capture.

2.5.2 Standpipe Configuration

The initial length of a borehole will be sleeved with a standpipe. This will not only reduce damage to the borehole passing through the relaxed and fissured ground, but, if sealed properly, will reduce air inleakage. The actual length of standpipe will depend on the thickness and nature of the relaxed strata. Shallower angled holes, drilled through increasingly fissured ground will require longer standpipe lengths.

Steele and Yates [48] described a method of determining the optimum standpipe length through examination of gas purities on successive boreholes with the same vacuum but altered standpipe lengths.

Many seals are used today to reduce the air inleakage in the annular gap between standpipe and strata. These include cement, rubber sealing sleeves, Densotape, polyurethane foam and Bentonite.

2.5.3 Pipe Network Configuration

Once drilled and sealed all boreholes are connected to a pipe range and thence to an exhauster installed either underground or on the surface.

The maximum suction that can be applied at boreholes will be the difference between exhauster suction and the suction lost through the pipe network. This suction will vary with each individual borehole having a regulating valve for control purposes. In 1982 there were 55 surface extractor installations in the U.K. with suctions ranging from 20 kPa to 60 kPa and flows from 300 l/s to 3000 l/s. There were 54 underground extractors with suctions ranging from 10 kPa to 50 kPa and flows from 150 l/s to 1200 l/s [42]. Wharton [50] commented that the ideal arrangement would be to have extractors at the pit top. Underground extractors could be used for experimental drainage and in areas of high gas emission but surface exhausters will allow the complete coverage of the mine. The large suction pressures needed to drain gas to the surface for utilisation necessitates sizes and numbers of extractors which could only be installed at a surface plant. In 1974 29.9% of drained gas in the U.K. was utilised (see Table 2.2.).

In the U.K. extractors must be approved by the Mines Inspectorate and are normally Nash Hytor, water seal, L, HL, or CL designs. The characteristic curves of these extractors generally show linear relationships up to about 60 kPa . Flexibility of performance is introduced by arranging exhausters in parallel. This will allow flow capacity to be altered whilst maintaining suction.

Before providing suction at boreholes an extractor will need to overcome losses in the pipe network connecting the surface installation. Consideration must therefore be given to extractor duty and network layout in any attempt to design a system to supply specified borehole suctions.

Many methane drainage pipe ranges have a small initial layout which grows with the extended development of the mine. The use of the correct size of pipe range to permit the drainage of specified gas quantities is essential. Steele and Yates [48] remarked that the pipe size specified should depend upon the quantity of gas expected to be passed through the system, its capacity and permissible pressure loss.

Bromilow [46] , in his review of firedamp drainage in Great Britain stated that, at Stafford Colliery, if an exhauster and gas-main of adequate capacity had been installed,

the gas production could probably have been doubled. He observed at Windsor Colliery that further holes drilled and coupled into the main gave no further gas flow owing to the resistance of the gas main.

The planning of pipe ranges will begin with the determination of the gas content of the surrounding strata and an estimate of the potential emission quantity and pattern due to mining activity. The drainage system will be designed to maximise the capture of gas in the surrounding strata. The design fresh air level will be set to dilute the remainder of the gas to below statutory threshold limiting values. Additional capacity is often included in the design of the drainage installation.[34].

The pipe range is commonly constructed of steel (although glass reinforced plastic (GRP) is now becoming popular) and is usually between 150mm and 500mm in diameter. Pipelines will be phosphate treated and red lead lined to reduce the risk of corrosion. Each borehole connected to the pipe range will be fitted with a regulating valve and each branch or district fitted with a full way valve to allow isolation for maintenance, extension or emergency purposes.

Capture and purity will be improved by careful monitoring and regulation of each individual borehole. Capture is likely to be inferior on retreat faces due to the inability to carry out this monitoring process. In this case two pipe ranges are commonly installed in the gate road and joined by a suitable Y-piece outbye. Batches of boreholes can then be connected to the alternate ranges (see Figure 2.8). This " leap frogging" system gives a coarse form of purity control and allows for the total isolation of one range without losing the whole drainage capacity.

The gradient of the pipe range needs to be kept as uniform as possible. This will allow traps to be positioned at low points to drain water ingested into the system from the surrounding strata.

The size, capacity, layout and integrity of the pipe networks, the inclusion of valves, water traps and other fittings plus the presence of water and the inleakage of air will all affect the pressure loss and capacity of a drainage network.

2.5.4 Pressure, Flow and Purity Measurement

The continued performance of a methane drainage system will therefore only be achieved through monitoring at appropriate and carefully considered positions.

Regular measurement of pressures, flow and purity will all give indications as to the performance of a range.

Pressure measurements will give indications of suction (with the use of a ring balance), flow through the measurement of differential pressures and absolute pressures. Purity measurements can be made with instruments developed using a number of different principles e.g. thermal conductivity, oxygen absorption, refractive index, infra red and acoustic analyses. All these parameters will give different results for methane and air thus allowing determination of purity.

Flow measurements are commonly made via orifice plates or venturis placed in straight pipe sections free from any obstruction.

Pressure and purity measurements can be taken with hand-held instruments for quick analysis or with fixed instruments which will log results for later analysis or, in many cases, transmit them to remote monitoring stations at the surface. These stations will collect, process and present data received from the many parts of the mine. Measurements can be rapidly assessed and anomalies detected. Data can be inspected from a central position, along with ventilation measurements, to provide an accurate assessment of not only the drainage range in isolation but also its effect on the complete mine ventilation system. Each underground logging station will be interrogated in a sequential manner by Time Division Multiplexing (TDM) systems.

Gas purities have been previously tested by transmitting samples to the surface along a tube bundle system. The gas samples were inspected at a central location by an infra red analyser. These are now taken using high concentration methane monitors and in many cases are attached to the mine MINOS system. These purity measurements, apart from giving warnings of potentially dangerous conditions will, along with pressure measurements and flows give indications of anomalies in the performance of the range.

2.6 Pipe Network Modelling

Measured data is invaluable if a simulation model is to provide an accurate assessment of performance, particularly pressure losses and capacity of the system.

Estimation of pressure drops along pipes was originally carried out with purpose designed disc calculators [50], using formulae derived for compressible gas flow.

Examples of these are the NCB/Mears *Methane Drainage Pipe Calculator* and the Gaz de France *Methane Flow Calculator* . The pressure loss can be read from the calculator knowing the absolute pressure, friction coefficient, diameter of the pipe and the flow rate. These calculators, still used today, are quick, easy to use and can be used anywhere but suffer from limited accuracy. When used throughout a drainage pipe network, the computation could become laborious and the inherent inaccuracies propagate errors through the calculation.

2.6.1 Previous Modelling Programs

Computer programs have been written, particularly by Cerchar in France and Ruhrkohle AG (RAG) and TU Clausthal in Germany. All assume compressible flow and adopt equations for compressible flow pressure losses.

The Reglagaz program, written by Cerchar, calculates one of five parameters (upstream pressure, downstream pressure, flow rate, pipe diameter and pipe length) in each pipe, given values of the other four. The program will proceed sequentially through a small branching network but will not be suitable for a larger, more complex network with, for instance, pipes in parallel.

The Resogaz computer program, again developed by Cerchar, also examines each junction throughout a network in a sequential manner. Pressures at junctions are treated as unknowns, and an iterative solution technique is used to find these and the flows in each branch. The program will deal with complex networks and considers the flow/pressure characteristics of the exhaustor and gas capture regions. The program however is limited to 100 nodes.

The Ruhrkohle AG adopts a similar solution technique, calculating pressure and volume flow throughout the network. Branches can be specified as constant flow or constant pressure drop in which case only the other variable will be calculated. The program is limited to 320 branches and assumes the same roughness in all pipes and the same composition of gas throughout the network.

Harper [51] in the U.K. constructed a simulation model again considering branches sequentially. This model was very similar to the ones mentioned above. Calculations would begin outbye and work towards the surface or exhaustor branch. Results for limbs with common outlet junctions would indicate the amount of regulation needed to

be applied. More complex networks were again dealt with by resorting to iterative procedures.

2.6.2 Analysis of Previous Methods

Analysis of the models discussed above, highlighted the need for the development of a new program which will form the basis of a methane drainage optimisation model. The model should be capable of dealing with complex networks and place no restriction on the number of junctions or pipes in the network. The program developed should employ a more suitable solution procedure which although still iterative, will consider the complete network and not each junction in a sequential manner. The program will assume isothermal conditions but allows the roughness factor to vary from pipe to pipe. Pressures and flow rates will again be the unknown quantities. These quantities will be specified at the boundary junctions together with gas composition (purity), that is those routinely measured in a methane drainage range. Unlike the previous models the purity throughout the network can then be calculated. These model results can then be used , along with measured data, to accurately predict air inleakage, hence the true flow rates and thus the 'in-situ' equivalent values of the resistance coefficients. Only when these factors have been determined can the conditions within the pipe network be realistically simulated. The model may then be used as an analytical optimisation tool with which to investigate any remedial measures necessary in order to maintain the operational performance of the network or assess the effect altering pipe characteristics, such as diameter and roughness, will have on system performance and capacity.

2.7 Summary and Conclusions

This chapter has discussed the varying methods of methane drainage and recovery used throughout the world. The applicability and success of each method is dependent on the characteristics of the gas bearing strata and the method of mineral recovery.

Conditions in the U.K. have dictated gas drainage during, and in the immediate vicinity of, the mineral extraction operations.

Gas capture is achieved through cross measure boreholes with each borehole being connected to a pipe range for transmission to the exhausting point. The suction available at boreholes and hence the gas capture is dependent on the configuration and condition of the pipe network.

The pipe network is thus an integral component of the drainage system and the ability to model the pipe network is necessary for a continued, successful and effective methane drainage operation. This chapter has analysed previous models, discussed their limitations and suggested the need for a new model.

The continued performance of the drainage range, and the accuracy of any simulation model, can only be achieved through the monitoring of pressures, flow and purity at appropriate and carefully considered positions in the range. Only then can the pipe network model be used to ascertain the improved performance that can be gained from selective changes to the range.

Chapter 3 will discuss the development of the computer model in depth and chapter 4 will proceed to discuss how the model results, along with measurements made, can be combined to produce a correlated, accurate simulation of the drainage range.

Chapter 3

The Pipe Network Model

3.1 Introduction

This chapter will describe the mathematical model employed in the computer simulation program developed as part of the study into the optimum performance of methane drainage ranges.

A brief overview of the principles of fluid flow is given and this is followed by a description of how these principles are employed in the measurement of pressure and flow in methane drainage ranges. Once simplifying assumptions have been outlined, equations describing the pressure/flow relationship for a single pipe are developed. These equations are then generalised to form a system of equations whose solution will describe the flow regime within the complete pipe network.

Where appropriate an attempt has been made to give a physical interpretation of the analyses which may be performed using the derived mathematical model and the observations which may be drawn as to the nature of the flow which is predicted.

3.2 Principles of Fluid Flow

3.2.1 Conservation of Mass

A fluid is a substance, either gas or liquid, which deforms continuously, offering no permanent resistance, under the action of a deforming force. If a fluid is considered made up of layers then this force acting on one of the layers will cause the fluid to shear and is known as a shearing force. If the neighbouring layers offer no resistance to the deformation then this fluid is frictionless and ideal, otherwise the fluid is described as real. If the fluid is at rest then there can be no shearing forces acting on it and the only forces acting will be compressive or body forces.

In any moving fluid, mass can neither be created or destroyed. Considering steady flow in a fixed volume then this law can be expressed simply as ;

$$\text{mass flow into volume} = \text{mass flow out of volume}$$

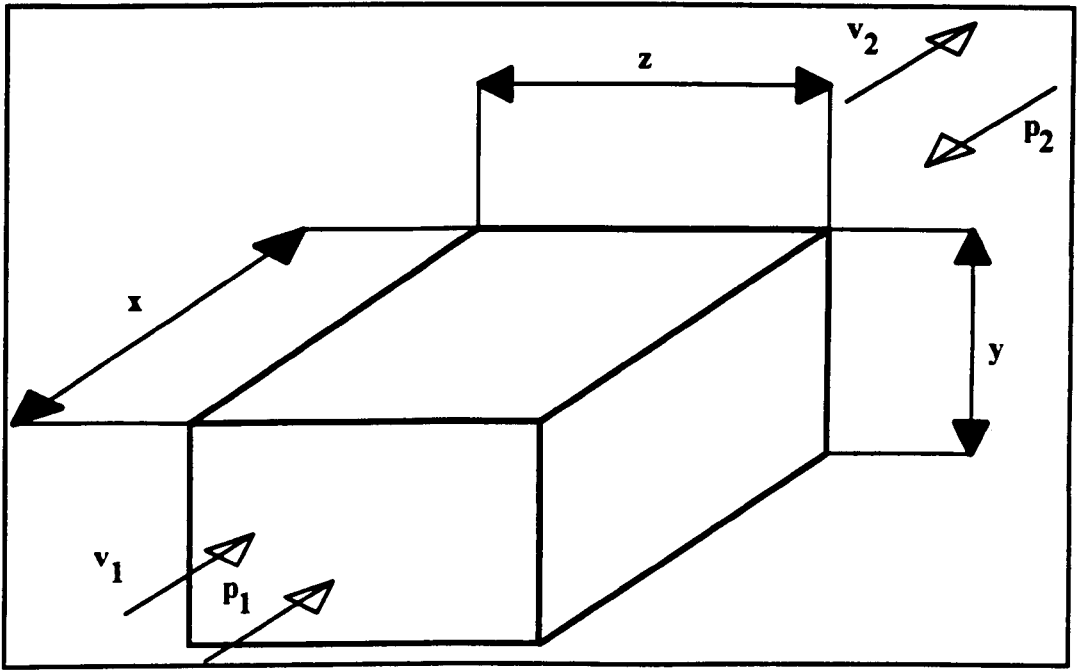


Figure 3.1. Flow through a fixed control volume.

For the fluid to move through the fixed volume forces must be applied. These forces are the pressures which act on each face of the fixed volume. The pressure difference in each direction will cause the fluid to flow, the magnitude of the pressure difference will determine the rate at which the fluid flows

3.2.2 Conservation of Momentum

Newton's second law of motion states that the rate of change of momentum of a body is equal to the force acting on it. i.e.

$$F = \frac{d(mv)}{dt} \quad (3.1)$$

where F is the force acting on a body of mass m travelling at velocity v .

If m remains constant then ;

$$F = m \frac{dv}{dt} = ma \quad (3.2)$$

where a is the acceleration of the body.

If pressures p_1 and p_2 act on the two opposite faces of a control volume as illustrated in Figure 3.1. the corresponding forces are $p_1 yz$ and $p_2 yz$. In addition to these surface forces the fluid element may also be subjected to body forces. If b is the body force per unit mass and ρ the density then ;

$$F = p_1 yz - p_2 yz + b \rho x yz \quad (3.3)$$

The mass of the fluid element is $\rho x yz$ and if x is a very small distance then $a = \frac{v_2 - v_1}{t}$ where t is the time taken to travel across the fluid element. Equation (3.2) can now be written as ;

$$(p_1 - p_2)yz + b \rho x yz = m \frac{(v_2 - v_1)}{t} \quad (3.4)$$

The average velocity across the fluid element can be written as $\frac{v_1 + v_2}{2} = \frac{x}{t}$ and equation (3.4) now becomes ;

$$p_1 - p_2 + b \rho x = \rho \frac{(v_2^2 - v_1^2)}{2} \quad (3.5)$$

Taking the vertical z direction then the only body force acting is gravity and $b = -g$ and if the difference in height of the fluid element is $z_1 - z_2$ then ;

$$p_1 + \frac{\rho v_1^2}{2} + \rho g z_1 = p_2 + \frac{\rho v_2^2}{2} + \rho g z_2 \quad (3.6)$$

This is Bernoulli's equation. written in terms of pressure. Dividing by ρg will give the equation in terms of heads.

3.2.3 Conservation of Energy

From Bernoulli's equation it can be seen that the total mechanical energy of a system is made up of components of potential, kinetic and pressure energies. The addition of extra energy to the system in terms of heat, δq , or mechanical energy, δw , must alter

the total energy. Including the internal energy of the system, U , the steady flow energy equation can be written as ;

$$\delta w + \delta q + \left(\frac{p}{\rho} + U + \frac{1}{2}v^2 + gz \right) = \frac{p}{\rho} + \frac{dp}{\rho} + U + dU + \frac{1}{2}(v + \delta v)^2 + g(z + \delta z)$$

or more simply as ;

$$\delta w + \delta q = \frac{dp}{\rho} + dU + v\delta v + g\delta z \quad (3.7)$$

The sum of the $\frac{p}{\rho}$ term and the internal energy is known as the enthalpy, h , of the fluid.

$$dh = \frac{dp}{\rho} + dU$$

The internal energy term, dU , represents the heat added to the fluid and is equal to $\delta q + \delta F$, where δF is the frictional energy loss.

Integrating equation (3.7) now gives ;

$$W = \int \frac{dp}{\rho} + F + \frac{1}{2}(v_1^2 - v_2^2) + g(z_1 - z_2) \quad (3.8)$$

This is the steady flow energy equation and describes the relationship between the energy added to a system and the energy lost through frictional resistance.

The three laws discussed are fundamental fluid flow laws and are the starting point of any attempt to investigate the pressure losses and gas flows in a methane drainage pipe range (or a mine ventilation circuit).

3.2.4 Measurement of Pressure and Flow

On a methane drainage range measurements are commonly made of static pressures, differential pressures and purity. All measurements are routinely taken manually on a

frequent basis. However the increased importance of methane drainage operations has been accompanied by an increased application of remotely monitored continuous measurement devices.

Static pressures are measured from tappings in the pipeline and differential pressures across orifice plates (from which values of flow can be determined). Orifice plates should be positioned outbye of each district and prior to any major branching in the pipe range.

Recalling Bernoulli's equation ;

$$p + \frac{1}{2}\rho v^2 + \rho gz = \text{constant}$$

then the sum of the pressure components on the left hand side is known as the total pressure, p is the static pressure and $\frac{1}{2}\rho v^2$ the dynamic pressure. In a level pipe ρgz will be zero and commonly will be small compared to the other terms so we can write ;

$$\text{total pressure} = \text{static pressure} + \text{dynamic pressure}$$

Figure 3.2. shows how the different pressure components are measured using a simple U-tube manometer. Indications of the magnitude of pressures will be given by the difference in height of the two columns of each manometer.

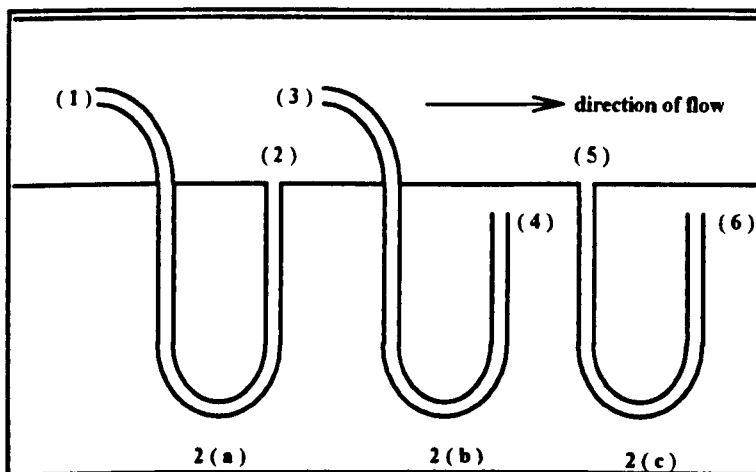


Figure 3.2. Measurement of dynamic, total and static pressures.

Points (1) and (3) in the diagram will measure the total pressure of the fluid flow. Points (2) and (5) will not be able to measure any dynamic or velocity pressure but will measure static pressure. Points (4) and (6) will not measure any pressure related to the flow in the pipe but merely the atmospheric pressure.

Therefore manometer (a) will measure total - static = dynamic pressure, manometer (b) will measure total pressure and manometer (c) will measure static pressure.

The atmospheric pressure measured at points (4) and (6) will vary and therefore the total, static and dynamic pressures measured will be relative to this datum. These are called gauge pressures and the absolute pressure is the sum of the atmospheric and gauge pressures.

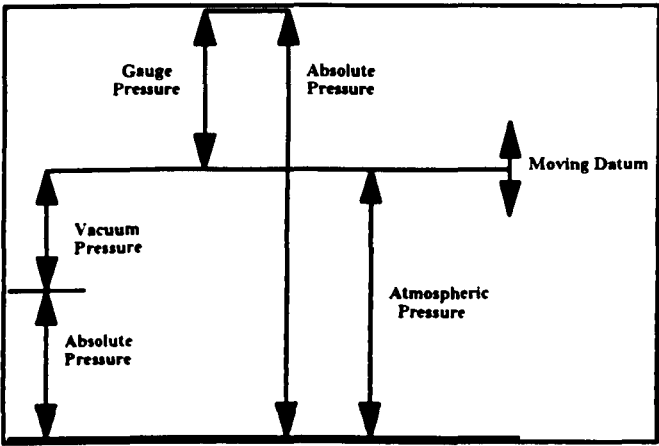


Figure 3.3. Relationship between gauge, absolute and atmospheric pressures.

3.2.5 The Orifice Plate

An orifice plate is able to calculate fluid flow by measuring the pressure drop across a known obstruction placed in the flow.

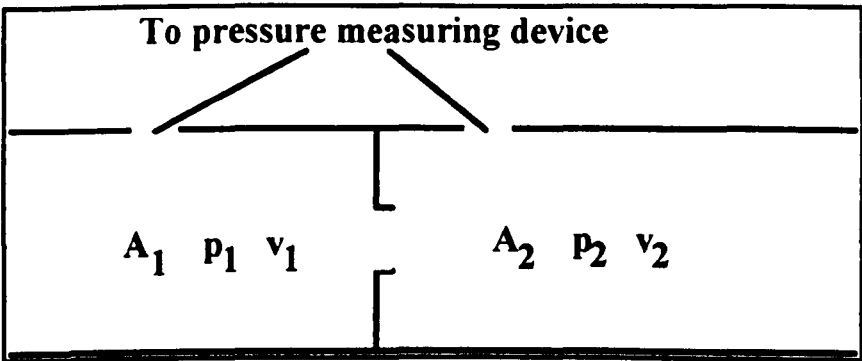


Figure 3.4. An orifice plate measurement station.

Tappings are placed a distance d upstream and $d/2$ downstream where d is the bore of the pipe.

Using Bernoulli's equation (3.6) once again, and noting that there is no change in elevation across the orifice unit, then ;

$$v_2^2 - v_1^2 = 2 \frac{(p_1 - p_2)}{\rho} \quad (3.9)$$

As mass must be conserved ;

$$\rho A_1 v_1 = \rho A_2 v_2$$

and therefore, using equation (3.9) ;

$$v_1^2 \left(\left(\frac{A_1}{A_2} \right)^2 - 1 \right) = \frac{2}{\rho} (p_1 - p_2) \quad (3.10)$$

The ratio $\frac{A_1}{A_2}$ will be known and so, from knowledge of the pressure difference, v_1 and hence the flow rate can be calculated. There will be other losses as a result of the restriction placed in the flow and can be included in the equations developed. These losses are well documented and further reference should be made to British Standard BS1042.

3.3 Flow in Methane Drainage Ranges

Gas flows through methane drainage ranges are accompanied by large pressure drops. These large pressure, and hence density, changes are too great to be neglected and the flow must be modelled as compressible.

Temperature will also vary through a typical underground pipe network. However for the purposes of the current study the temperature is assumed constant throughout the network. This constant value will be set prior to any analysis being carried out. Both pressure and density will be affected by temperature. If the flow process is considered

adiabatic then $\frac{p_1}{p_2} = \left(\frac{T_1}{T_2} \right)^{\frac{\gamma}{\gamma-1}}$ and $\frac{\rho_1}{\rho_2} = \left(\frac{T_1}{T_2} \right)^{\frac{1}{\gamma-1}}$, where γ is the ratio of specific heats, $\frac{c_p}{c_v}$, (see Table 3.1). If the temperature in the network was set at 25°C (298K) but

actually varied 5°C either side of this value then the error introduced in pressure and density (hence flow rate) calculations would be no greater than 6%. This error was considered small enough to allow the application of an isothermal model.

Although strata water may be present in the pipe network it is assumed that most of this would be collected by suitably positioned water traps. Two phase flow may exist in regions of the pipe but because of the difficulties in taking corroborative measurements this was not included in the derivation of the equations or the pipe network model. Any water that does remain in the pipes would be modelled by a subsequent reduction in the effective diameter of the pipes.

The Reynolds number for flow in pipes can be written as ;

$$Re = \frac{\rho v d}{\mu} \tag{ 3.11 }$$

where ρ is the density of the fluid in kg/m^3 ,
 μ the absolute viscosity in kg/ms ,
 v the velocity in m/s and
 d the diameter of the pipe in m .

| | Methane (CH ₄) | Air |
|--|-----------------------------|-------|
| Density, ρ (kg/m^3) | 0.7168 | 1.20 |
| Specific Heat, C_p (kJ/kgK) | 2.216 | 1.005 |
| Specific Heat, C_v (kJ/kgK) | 1.697 | 0.718 |
| Gas Constant, R (kJ/kg K) | 0.519 | 0.287 |
| Expansion Index, (adiabatic constant), γ | 1.306 | 1.400 |
| Absolute viscosity, $\mu \times 10^5$ (Ns/m^2) | 1.34 | 1.80 |

Table 3.1 Properties of methane and air at standard atmospheric pressure.

If the transition from laminar to turbulent flow is at a Reynolds number of 10^5 then for air the velocity would be approximately 3 m/s in a 16 inch pipe and 6 m/s in an 8 inch pipe. For methane these figures would be 4 and 8 m/s respectively. Flow in methane drainage ranges frequently exceeds these values and it would seem appropriate to assume a fully developed turbulent flow regime.

Therefore in the model developed, and discussed in the subsequent sections, the flow is assumed to be ;

- (i) compressible.
- (ii) isothermal.
- (iii) a fully mixed methane/air mixture.
- (iv) turbulent.
- (v) single phase

3.4 The Single Pipe Model

D'Arcy's equation for the frictional pressure losses, Δp Pascals, along a pipe of length ΔL metres and circular cross section can be written as ;

$$\Delta p = \frac{-4f\rho v^2}{2d} \Delta L \quad (3.12)$$

where f is the dimensionless friction factor.

At this point it may be useful to note that the value of friction factor quoted in many texts, λ , is $4f$ in the notation employed here. In this text however the UK recognised value of the friction factor, f , will be used.

If the pipe is inclined at an angle θ , then the change in elevation along the length ΔL is $\sin\theta \Delta L$ and the pressure loss due to this change ;

$$\Delta p = \rho g \sin\theta \Delta L \quad (3.13)$$

Combining equations (3.12) and (3.13) then the pressure loss, dp , along an increment of pipe length, dl , is ;

$$dp = \frac{-4f\rho v^2}{2d} dl - \rho g \sin \theta dl \quad (3.14)$$

With the flow being considered compressible, density will be varying with the changes in pressure occurring. Equation (3.14) must therefore be re-written in terms of mass flow which will be constant along the length of the pipe.

The mass flow at any point can be written as ;

$$m = \rho A v \quad (\text{kg/s}) \quad (3.15)$$

where A is the cross-sectional area of the pipe (m²)

Therefore ;

$$\rho v^2 = \frac{16m^2}{\rho A^2} = \frac{16m^2}{\rho \pi^2 d^4} \quad (3.16)$$

Using the equation of state, $\frac{p}{\rho} = RT$, for an ideal gas, equation (3.16) can be rearranged as ;

$$\rho v^2 = \frac{16m^2}{\pi^2 d^4} \frac{RT}{p} , \quad (3.17)$$

where R is the gas constant of the mixture and T the temperature.

Eliminating ρ and v from equation (3.14) gives ;

$$dp = \frac{-k_1}{p} dl - k_2 p dl , \quad (3.18)$$

or after separating terms ;

$$\frac{p dp}{k_1 + k_2 p^2} = -dl \quad (3.19)$$

where $k_1 = \frac{32f\mu^2RT}{\pi^2d^5}$, and $k_2 = \frac{g\sin\theta}{RT}$.

Equation (3.19) can now be integrated to give the total pressure loss along a pipe of length L ;

$$\frac{1}{2k_2} \int \frac{2pdp}{\frac{k_1}{k_2} + p^2} = - \int dl \quad (3.20)$$

$$\log_e \frac{(\frac{k_1}{k_2} + p_2^2)}{(\frac{k_1}{k_2} + p_1^2)} = -2k_2L \quad (3.21)$$

$$\boxed{p_2^2 = e^{-2k_2L} \left(\frac{k_1}{k_2} + p_1^2 \right) - \frac{k_1}{k_2}} \quad (3.22)$$

Equation (3.22) gives an expression for the outlet pressure p_2 for compressible fluid flowing in a pipe of length L, with inlet pressure p_1 . For level pipes this equation can be simplified to give ;

$$\boxed{p_2^2 = p_1^2 - 2k_1L} \quad (3.23)$$

3.5 Combinations of Pipes in Series and Parallel

Equation (3.23) can be rewritten in the form ;

$$p_1^2 - p_2^2 = r \cdot m^2 \quad (3.24)$$

where r, the resistance coefficient, can be written as ;

$$r = \frac{64f\mu^2RTL}{\pi^2d^5} \quad (3.25)$$

Equation (3.24) can be used to demonstrate the effect on resistance of combining pipes in series and parallel.

3.5.1 Pipes in Series

If a mass of air, m , is flowing through pipes in series then the same mass will have to flow through each pipe in turn. Therefore ;

$$p_1^2 - p_2^2 = r_1 \cdot m^2, \quad p_2^2 - p_3^2 = r_2 \cdot m^2,$$

and so ;

$$p_1^2 - p_3^2 = (r_1 + r_2)m^2$$

The equivalent resistance of the pipe combination is given by ;

$$r = r_1 + r_2$$

or more generally for n pipes in series ;

$$\boxed{r = r_1 + r_2 + \dots + r_n} \quad (3.26)$$

3.5.2 Pipes in Parallel

If two pipes are connected in parallel with mass flows m_1 and m_2 flowing then the total flow will be $m_1 + m_2$. However the pressure drop through both pipes will be the same and so using equation (3.24) ;

$$r \cdot m^2 = r_1 \cdot m_1^2 = r_2 \cdot m_2^2$$

But $m = m_1 + m_2$ and ;

$$\sqrt{\frac{(p_1^2 - p_2^2)}{r}} = \sqrt{\frac{(p_1^2 - p_2^2)}{r_1}} + \sqrt{\frac{(p_1^2 - p_2^2)}{r_2}}$$

or ;

$$\frac{1}{\sqrt{r}} = \frac{1}{\sqrt{r_1}} + \frac{1}{\sqrt{r_2}}$$

More generally for n pipes in parallel ;

$$\boxed{\frac{1}{\sqrt{r}} = \frac{1}{\sqrt{r_1}} + \frac{1}{\sqrt{r_2}} + \dots + \frac{1}{\sqrt{r_n}}} \quad (3.27)$$

3.6 Generalisation to Pipe Networks

Having considered the single pipe we can now apply the equations developed to a combination of pipes in a network. To do this we need to recall that ;

$$e^x = 1 + x + \frac{x^2}{2!} + O(x^3)$$

for $|x| \leq 1$ then we can write ;

$$e^{-2k_2L} = 1 - 2k_2L + O((2k_2L)^2)$$

If the denominator, RT, of k_2 is sufficiently large rapidly reduce powers of $2k_2L$ then equation (3.12) can be re-stated as ;

$$p_2^2 = (1 - 2k_2L)\left(\frac{k_1}{k_2} + p_1^2\right) - \frac{k_1}{k_2} \quad \text{or,}$$

$$p_2^2 - (1 - 2k_2L)p_1^2 = -2k_1L \quad (3.28)$$

If $-2k_1L$ is written as k_3m^2 then equations (3.23) and (3.28) will give two statements describing the pressure loss along a level and inclined pipe respectively ;

$$\begin{aligned} p_2^2 - p_1^2 &= k_3m^2 \\ p_2^2 - (1 - 2k_2L)p_1^2 &= k_3m^2 \end{aligned} \quad (3.29a \text{ \& } 3.29b)$$

3.6.1 The Linear Theory Method

Kirchhoff's first law states that the algebraic sum of mass flows at any junction in the pipe network must equal zero. i.e.

$$\sum_{j=1}^n m_j = 0, \quad (3.30)$$

where n is the number of branches incident at the current junction.

Writing m^2 as $|m_{i-1}|m_i$ equations (3.29a & b) can be rewritten thus ;

$$\frac{p_2^2 - p_1^2}{k_3 |m_{i-1}|} = m_i$$

(3.31a & 3.31b)

$$\frac{p_2^2 - (1 - 2k_3 L)p_1^2}{k_3 |m_{i-1}|} = m_i$$

where $()_i$ is the current iteration and

$()_{i-1}$ the previous iteration.

Equations (3.31a) and (3.31b) can now be combined with Kirchhoff's first law to provide a system of equations to be solved for the pressure squared value at each junction in the network ;

$$A p = 0 \quad (3.32)$$

This procedure of linearising the mass flow term and resorting to an iterative method of solution is known as the **Linear Theory Method (LTM)**. An initial, arbitrary, estimate is made of the flows in the pipe network and the system of equations (3.32) solved for the pressure at each junction. These values can then be used in (3.31a) and (3.31b) to provide new estimates of the mass flows. A revised coefficient matrix, A , can then be formed and the solution procedure repeated. This will continue until the mass flows between consecutive iterations converge below an acceptable level.

3.6.2 Specification of the Problem

A typical methane drainage system will be an open network of pipes with gas flowing in at each of the boundary or open junctions and flowing out at the extraction plant junction. The model assumes only one exhausting point at junction 1.

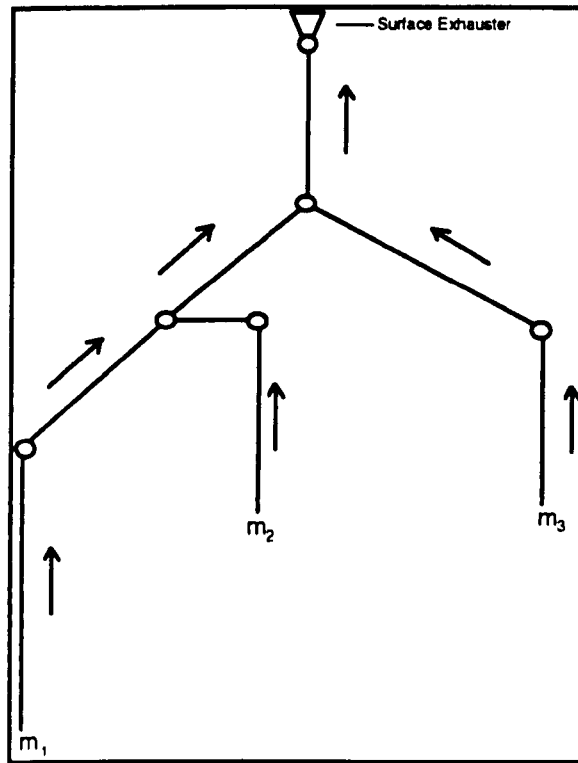


Figure 3.5. A typical methane drainage range.

The mass flow into the system must be defined at each boundary junction. One boundary pressure however is enough to specify the problem, all other junction pressures will be calculated in the solution process described above.

Underground measurements are commonly made of volume, rather than mass, flow rates and suctions rather than pressures. This is catered for in the solution process, with the volume flow rates being converted to mass flow rates after pressures have been calculated and an estimate made of the density of the fluid at each of the boundary junctions.

The boundary pressure is given by ;

$$\text{pressure in pascals} = 101325 - \text{suction in pascals}$$

where $101325 \text{ Pa} = 1 \text{ atmosphere}$.

The one specified pressure can just as easily be the surface pressure generated by the vacuum pumps or the pressure at a particular underground boundary junction.

The solution can either ;

- (i) Find the suction generated at underground boundaries given the suction of the surface exhauster or,
- (ii) Find the exhauster suction required to give a specified suction at the underground boundaries of the network.

3.6.3 Calculation of Purity

The purity of methane in a methane/air mixture will again be measured on a volumetric basis. The model developed will calculate the purity for each pipe in the network given the purity of the gas flowing into the network at boundary junctions.

The gas flowing out of a junction, in any pipe is assumed to be perfectly mixed and have the same purity.

At any junction ;

$$\sum m_{in} = \sum m_{out}$$

or,

$$\sum \rho_{in} Q_{in} = \sum \rho_{out} Q_{out} \quad (3.33)$$

where Q is measured in (m³/s)

The pressure, and hence density, will be constant at the junction under consideration and so ;

$$\sum Q_{in} = \sum Q_{out} \quad ,$$

for the mixture.

The purity, P, of the gas is the actual amount of methane flowing in the methane/air mixture and can be written ;

$$P = \frac{Q_{\text{meth}}}{Q_{\text{meth}} + Q_{\text{air}}} * 100\%$$

where Q_{meth} is the volume of methane flowing and Q_{air} the volume of air.

i.e. $Q_{\text{meth}} = PQ_{\text{tot}}$ where Q_{tot} is the total volume of gas flowing.

Therefore, as the methane flow into a junction will equal the methane flow out ;

$$\sum P_{\text{in}} Q_{\text{in}} = P_{\text{out}} \sum Q_{\text{out}} \quad (3.34)$$

The purity of methane flowing in any pipe away from the current junction can be written ;

$$P_{\text{out}} = \frac{\sum P_{\text{in}} Q_{\text{in}}}{\sum Q_{\text{out}}} \quad (3.35)$$

Again the purity of the gas entering the network at each boundary node will need to be specified and a series of equations formed describing the purity of the gas in each pipe in the network ;

$$\mathbf{B} \mathbf{P} = \mathbf{0} \quad (3.36)$$

\mathbf{B} is the matrix of coefficients and \mathbf{P} the column vector of purity values for each pipe in the network.

Therefore, once a solution for the pressures at each junction has been found, the mass flow rates and hence the volume flow rates for each pipe entering a junction can be found and the purities calculated from equation (3.36)

3.6.4 Solution Method

The system of equations (3.32) and (3.36) are both solved using the method of triangular decomposition. This method depends on a result of matrix algebra which states that a square matrix **C** can be expressed in the form ;

$$\mathbf{C} = \mathbf{L} \mathbf{U} \quad (3.37)$$

where **L** is a lower triangular matrix and **U** an upper triangular matrix. A general system of equations ;

$$\mathbf{C} \mathbf{X} = \mathbf{D} \quad (3.38)$$

can then be written as ;

$$\mathbf{L} \mathbf{U} \mathbf{X} = \mathbf{D} \quad (3.39)$$

or ;

$$\mathbf{L} \mathbf{Y} = \mathbf{D} \quad (3.40a)$$

$$\mathbf{U} \mathbf{X} = \mathbf{Y} \quad (3.40b)$$

where **Y** is an intermediate solution stage.

As **L** is a lower , and **U** an upper, triangular matrix equations (3.40a) and (3.40b) can be solved for **Y** by forward substitution and then **X** by backward substitution

As an example consider a (3 x 3) system of equations ;

Equation (3.38) can now be written as ;

$$\begin{pmatrix} a_{11} & a_{12} & a_{13} \\ a_{21} & a_{22} & a_{23} \\ a_{31} & a_{32} & a_{33} \end{pmatrix} \begin{pmatrix} x_1 \\ x_2 \\ x_3 \end{pmatrix} = \begin{pmatrix} d_1 \\ d_2 \\ d_3 \end{pmatrix} \quad (3.41)$$

and equation (3.39) as ;

$$\begin{pmatrix} 1 & 0 & 0 \\ l_{21} & 1 & 0 \\ l_{31} & l_{32} & 1 \end{pmatrix} \begin{pmatrix} u_{11} & u_{12} & u_{13} \\ 0 & u_{22} & u_{23} \\ 0 & 0 & u_{33} \end{pmatrix} \begin{pmatrix} x_1 \\ x_2 \\ x_3 \end{pmatrix} = \begin{pmatrix} d_1 \\ d_2 \\ d_3 \end{pmatrix} \quad (3.42)$$

For convenience the diagonal elements of L are chosen to be unity.

The general formulae for calculating the components of L and U when C is an $(n \times n)$ matrix are ;

$$\begin{aligned} u_{1j} &= c_{1j} \\ l_{i1} &= c_{i1} / u_{11} \\ u_{ij} &= c_{ij} - \sum_{s=1}^{i-1} l_{is} u_{sj} \quad 1 < i \leq j \\ l_{ij} &= (c_{ij} - \sum_{s=1}^{j-1} l_{is} u_{sj}) / u_{jj} \quad i \geq j > 1 \end{aligned}$$

Equation (3.40a) for the (3×3) system now becomes ;

$$\begin{aligned} l_{11}y_1 &= d_1 \\ l_{21}y_1 + l_{22}y_2 &= d_2 \\ l_{31}y_1 + l_{32}y_2 + l_{33}y_3 &= d_3 \end{aligned}$$

y_1 can be found simply from the first equation and substituted into the second to give y_2 and hence into the third to give y_3 . This method is known as forward substitution and more generally for an $(n \times n)$ system ;

$$\begin{aligned} y_1 &= d_1 / l_{11} \\ y_i &= \frac{1}{l_{ii}} (d_i - \sum_{j=1}^{i-1} l_{ij} y_j) \quad i = 2 \rightarrow n \end{aligned}$$

The computed values of y_1 , y_2 and y_3 can now be used to rewrite equation (3.40b) as ;

$$\begin{aligned}
u_{11}x_1 + u_{12}x_2 + u_{13}x_3 &= y_1 \\
u_{22}x_2 + u_{23}x_3 &= y_2 \\
u_{33}x_3 &= y_3
\end{aligned}$$

Back substitution will now give the required values of x_1 , x_2 and x_3 . Generally for an $(n \times n)$ system ;

$$\begin{aligned}
x_n &= \frac{y_n}{u_{nn}} \\
x_i &= \frac{1}{u_{ii}}(y_i - \sum_{j=i+1}^n u_{ij}x_j) \quad i = n-1 \rightarrow 1
\end{aligned}$$

This method is often used in computer programs due to the economy of storage space. It is unnecessary to store the zeros of L and U and the 1's on the diagonal of L . Furthermore as each element of C is used only once in the calculation of L and U the results can replace the elements of C as the solution proceeds.

3.6.5 Calculation of the Gas Constant, R.

The gas constant, R , used in equations (3.22) and (3.23) will vary according to the purity of the mixture flowing in each pipe in the network.

The gas constant can be written as ;

$$R = \frac{R_o}{M} \text{ (kJ/kg K)},$$

where R_o is the Universal Gas Constant (= 8.314 kJ/kmol K) and M is the relative molecular mass of the gas (kg/kmol).

For a mixture of gases this relationship becomes ;

$$R = \sum \frac{m_i}{m} R_i \tag{ 3.43 }$$

where R_i is the gas constant of the i 'th constituent of the mixture and $\frac{m_i}{m}$ the mass fraction of that constituent.

For a methane/air mixture, equation (3.43) can be expanded to give ;

$$R = \frac{m_{\text{meth}} R_{\text{meth}} + m_{\text{air}} R_{\text{air}}}{m_{\text{meth}} + m_{\text{air}}}$$

or in terms of volume flow rates,

$$R = \frac{\rho_{\text{meth}} Q_{\text{meth}} R_{\text{meth}} + \rho_{\text{air}} Q_{\text{air}} R_{\text{air}}}{\rho_{\text{meth}} Q_{\text{meth}} + \rho_{\text{air}} Q_{\text{air}}} \quad (3.44)$$

Using the equation of state, $\frac{P}{\rho} = RT$, at a constant temperature and pressure, then

$$\frac{\rho_{\text{meth}}}{\rho_{\text{air}}} = \frac{R_{\text{air}}}{R_{\text{meth}}} \quad (3.45a)$$

$$\text{Also} \quad Q_{\text{meth}} = P Q_{\text{tot}} \quad (3.45b)$$

$$\text{and} \quad Q_{\text{air}} = (1 - P) Q_{\text{tot}} \quad (3.45c)$$

Equations (3.45a,b and c) can now be substituted into equation (3.44) to give ;

$$R = \frac{1}{\frac{P}{R_{\text{meth}}} + \frac{(1 - P)}{R_{\text{air}}}} \quad (3.46)$$

The relative molecular mass of methane is 16 and of air 29. Therefore $R_{\text{air}} = \frac{R_o}{29}$, and

$R_{\text{meth}} = \frac{R_o}{16}$, and equation (3.46) becomes ;

$$R = \frac{R_o}{16P + 29(1 - P)} \quad \text{kJ/kg K} \quad (3.47)$$

Equation (3.47) gives the gas constant as a function of the purity of the mixture flowing in each pipe. Hence once purities in the pipe network are known the gas constants can be updated and used in equations (3.22) and (3.23).

3.6.6 The Inclusion of Valves and Pipe Fittings.

The pressure losses incurred across valves, other pipe fittings or as a result of bends in the pipe network are all modelled as an equivalent length of pipe incurring the same pressure loss.

The friction coefficient, ζ , is defined (after [34]) by ;

$$\Delta p = \frac{\zeta \rho v^2}{2g}$$

Equating this with D'Arcy's equation (3.12) for the incompressible pressure loss along a pipe will give ;

$$\zeta = \frac{4f\Delta L}{d},$$

and the equivalent length of pipe is ;

$$\Delta L = \frac{\zeta d}{4f} \quad (3.48)$$

| Type of Fitting | Friction Coefficient (ζ) |
|-----------------------------------|----------------------------------|
| Globe Valve, Fully Open | 10.0 |
| Angle Valve, Fully Open | 5.0 |
| Swing Check Valve, Fully Open | 2.5 |
| Gate Valve, Fully Open | 0.19 |
| Gate Valve, 3/4 Open | 1.15 |
| Gate Valve, 1/2 Open | 5.6 |
| Gate Valve, 1/4 Open | 24.0 |
| 90 ⁰ elbow | 0.9 |
| 45 ⁰ elbow | 0.4 |
| Large Radius 90 ⁰ bend | 0.6 |
| Tee Junction | 1.8 |

Table 3.2. Friction coefficients for a selection of valves located in pipe networks.

3.6.7 Calculation of the Friction Factor.

D'Arcy's equation, (3.12), gives an expression for the frictional losses along a length of pipe. It includes a term, f , the friction factor which will dictate the magnitude of these losses. Generally this friction factor will be dependent on both the Reynolds Number, Re , and the relative surface roughness, ϵ , of the pipe boundary.

$$f = \Phi(Re, \epsilon) \quad (3.49)$$

The relative surface roughness is the ratio of the height of the roughness elements to the diameter of the conduit ;

$$\epsilon = \frac{k}{d} \quad (3.50)$$

The friction factor for fully developed laminar flow can be derived from first principles and can be shown to be independent of the surface roughness ;

$$f = \frac{16}{Re} \quad (3.51)$$

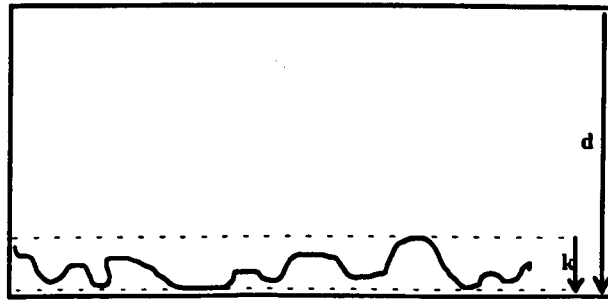


Figure 3.6. Roughness elements.

The mechanism of turbulent flow is far more complex and empirical relationships have been derived to evaluate the friction factor.

If the ratio $\frac{k}{d}$ is small the surface can be considered smooth and the flow regime one of 'smooth turbulent'. In 1913 Blasius proposed a relationship, still independent of surface roughness, of the form ;

$$f = \frac{0.079}{Re^{1/4}} \quad (3.52)$$

This has been found to give reasonable values up to a Reynolds number of 10^5 .

Based on extensive work by Nikuradse, Karmen, in 1933, established a relationship of the form ;

$$\frac{1}{\sqrt{f}} = 4.07 \log_{10}(Re\sqrt{f}) - 0.6 \quad (3.53)$$

This expression has been verified for Reynolds numbers in the range $5000 < Re < 3 \times 10^6$.

For rough pipes the friction factor will depend on the relative surface roughness as well as the Reynolds number. Nikuradse's experiments showed that for sufficiently high values the friction factor becomes independent of the Reynolds number and can be written as ;

$$\frac{1}{\sqrt{f}} = 4 \log_{10}\left(\frac{d}{k}\right) + 2.28 \quad (3.54)$$

For the transitional flow regime between rough and smooth turbulence a relationship of the form ;

$$\frac{1}{\sqrt{f}} = -4\log_{10}(\frac{k}{3.71d} + \frac{1.26}{Re\sqrt{f}}) \tag{ 3.55 }$$

can be used. This is known as the Colebrook equation and may be seen to converge to equations (3.53) and (3.54) for fully smooth ($k \rightarrow 0$) or rough ($Re \rightarrow \infty$) pipes.

The most common source of reference for the calculation of friction factors is the Moody Chart. The three distinct flow regimes can be distinguished from the chart. Friction factors for laminar and smooth turbulent flow are represented by single lines. For rough turbulence a number of lines are drawn each representing a specified relative roughness, $\frac{d}{k}$.

Methane Drainage pipe networks are usually of steel construction and between 8 and 16 inches in diameter. The value of $\frac{d}{k}$ will typically vary between 5000 and 10,000. This will place the flow regime in the transition zone between smooth and rough turbulent for the typical velocities experienced. However as the pipes age the relative surface roughness will decrease and the flow will become completely rough turbulent. Therefore, in the current model, equation (3.54) is used to calculate the value of the pipe friction factor.

| Boundary Material (new) | Surface Roughness, k, (mm) | Relative Roughness, d/k, for a 250mm pipe. |
|-----------------------------|---------------------------------|---|
| Glass, Brass, Copper, Lead | ' Smooth ' | $\rightarrow \infty$ |
| Steel Pipe | 0.045 | 5555 |
| Galvanised Iron | 0.1524 | 1640 |
| Steel Pipe with Sand Grains | 0.381 | 656 |
| Cast Iron | 0.411 | 608 |

Table 3.3. Typical values of surface roughness, k.

3.7 Sensitivity Analysis Applied to Governing Equations.

3.7.1 Dependence on Diameter

Equations (3.22) and (3.23) show that ;

$$p_1^2 - p_2^2 \propto \frac{1}{d^5}.$$

This indicates large variations in pressure drop are experienced for only small changes in the pipe diameter. It would therefore seem advisable to use as large a pipe diameter as possible when constructing or modifying a gas drainage range, and that all existing pipes should be kept as clean and free from obstruction as possible. Any build up of solid on the internal walls of a pipe will, apart from increasing the frictional resistance, reduce the effective diameter of the pipe which will in turn dramatically increase the pressure losses.

3.7.2 Dependence on Absolute Pressure

Equation (3.23) describing the pressure loss along a single level pipe can be rewritten to give ;

$$p_1 - p_2 = \frac{-2k_1 L}{p_1 + p_2} \quad (3.56)$$

Hence the pressure loss $\Delta p = p_1 - p_2$ is dependent on the absolute value of the pressures $p_1 + p_2$.

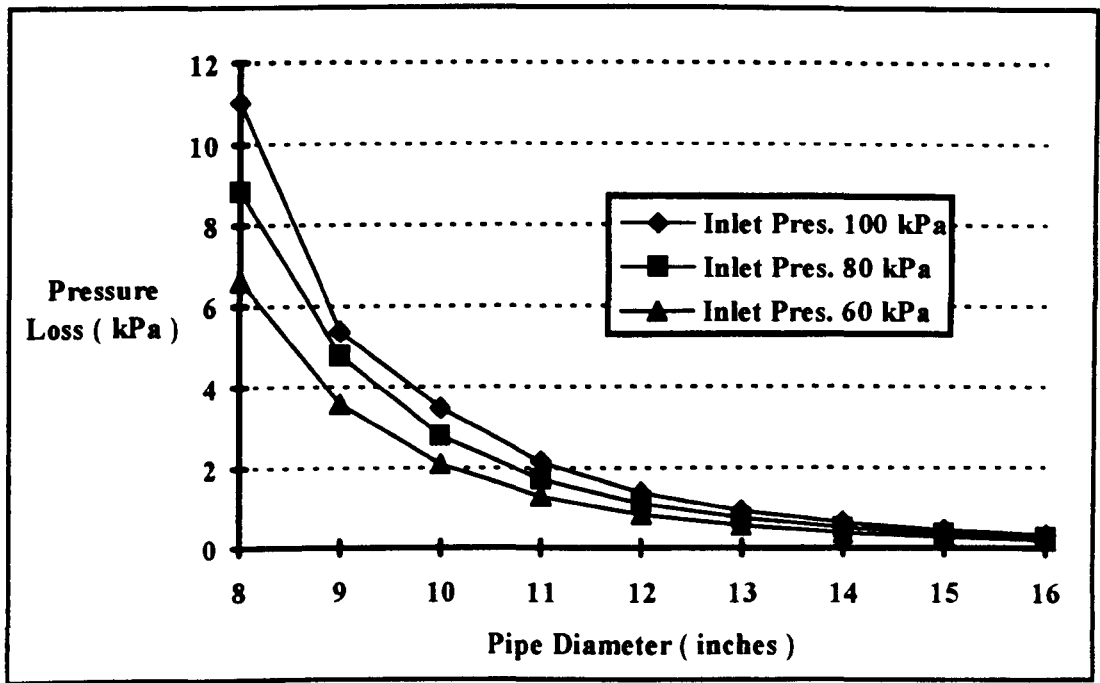


Figure 3.7. Variation of pressure losses with diameter and inlet pressure.

3.7.3 The Effect of Pressure Loss Changes on Pipes in Series.

Consider the two pipes in series shown in Figure 3.8.

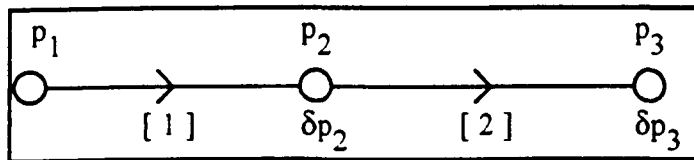


Figure 3.8. The effect of pressure loss changes on pipes in series.

An alteration is made to pipe (1) such that the pressure at node 2, p_2 , is raised by an amount δp_2 . i.e. the pressure loss has dropped by an amount δp_2 . This has the effect of raising the pressure at p_3 by an amount δp_3 . For incompressible flow δp_2 would equal δp_3 . However for compressible flow in pipe (2) ;

$$p_2 - p_3 = \frac{2k_1 L}{p_2 + p_3} \quad (3.57)$$

in the original case and ;

$$(p_2 - \delta p_2) - (p_3 - \delta p_3) = \frac{2k_1 L}{(p_2 - \delta p_2) + (p_3 - \delta p_3)}$$

or ;

$$(p_2 - p_3) - (\delta p_2 - \delta p_3) = \frac{2k_1 L}{(p_2 + p_3) - (\delta p_2 + \delta p_3)} \quad (3.58)$$

in the modified case.

As $\delta p_2 + \delta p_3 > 0$ then, from (3.57) and (3.58), $\delta p_2 - \delta p_3 < 0$ i.e. $\delta p_3 > \delta p_2$ and a greater pressure saving will be seen further downstream in the series of pipes.
i.e. the total pressure saving made outbye, through maintenance or reconfiguration, will not be detected by measurements made inbye in the methane drainage range.

3.7.4 Larger Diameter vs. Pipes in Parallel

Re-arranging equation (3.23) we can write ;

$$p_1^2 - p_2^2 = \frac{km^2}{d^5} \quad (3.59)$$

where ;

$$k = \frac{64fRTL}{\pi^2}$$

If the diameter of a pipe section is now modified such that the inlet pressure is still p_1 but the outlet pressure is now p_3 then ;

$$p_1^2 - p_3^2 = \frac{km^2}{d_n^5}$$

where d_n is the new pipe diameter.

If n of these pipes are added in parallel then the mass flowing through each pipe will be m/n . Therefore ;

$$p_1^2 - p_3^2 = \frac{k(m/n)^2}{d_n^5} \quad (3.60)$$

Re-arranging equations (3.59) and (3.60) we get ;

$$p_3^2 = p_1^2 (1 - (\frac{d}{d_n})^5 \frac{1}{n^2}) + p_2^2 (\frac{d}{d_n})^5 \frac{1}{n^2} \quad (3.61)$$

Therefore the ventilation engineer has the option to either replace the existing pipe with one of a larger diameter or paralleling the existing installed pipe with one of same or larger diameter.

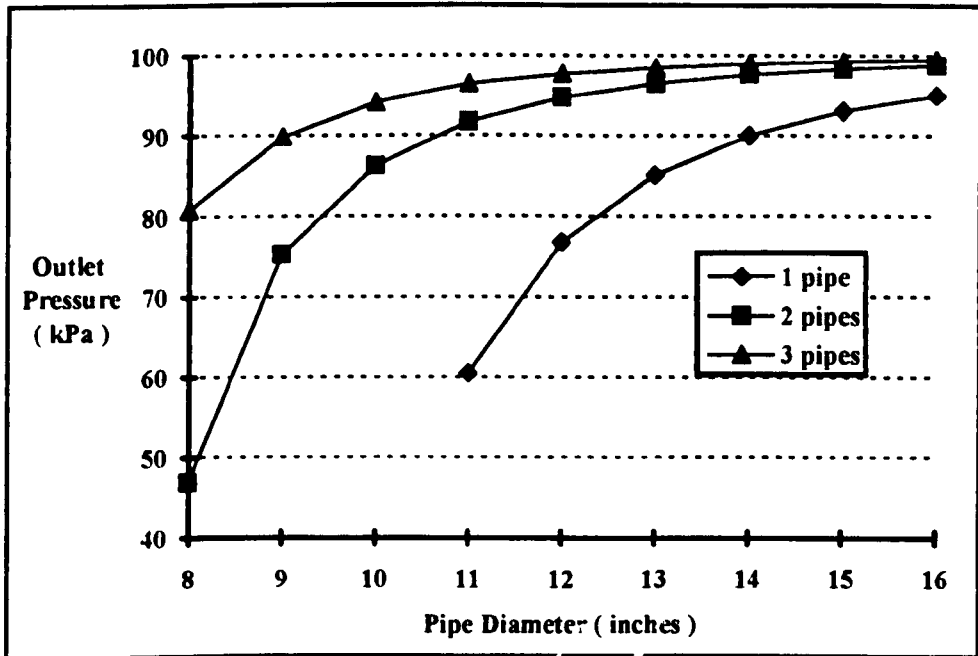


Figure 3.9. A comparison of pressure losses for pipes in parallel and an inlet pressure of 100 kPa.

The mathematical model discussed in this chapter has been developed into a computer model capable of simulating flows in methane drainage ranges. The detailed construction of the computer model may be found in appendix 1.

3.8 Summary and Conclusions

This chapter has discussed some basic principles of fluid flow and how these principles are applied to instrumentation for the monitoring of flow and pressure in methane drainage ranges.

Beginning with D'Arcy's Law, equations were derived for compressible flow pressure losses along a single pipe. These were then combined to form a system of equations to be solved for the pressure distribution throughout the whole range.

Using a new method, the *Linear Theory Method*, these equations were solved thus enabling subsequent calculation of the volume flow and velocity of gas in each pipe. A system of equations was also formed to calculate the purity of gas in each pipe. Purity will affect the gas constant, R , and hence the pressure drop along each pipe.

The pressure loss is dependent on the absolute value of pressures and, more critically, on pipe diameter. Any water or sedimentation present in pipes, apart from increasing the frictional resistance of the pipe, will reduce the effective diameter and rapidly increase the pressure losses. Any network reconfiguration or maintenance carried out to reduce the pressure losses in outbye sections of the range will not be transmitted through the network to have the same effect inbye. This is a consequence of the pressure losses being dependent on the absolute value of pressures.

Before the model can be used to assess the effect changing parameters such as diameter and roughness will have on system performance it must be accurately simulating the current drainage configuration. The accuracy of the model will be dependent on air leakage and correct values for frictional resistance being used.

The current model assumes no air leakage. Chapter 4 will present the arguments which demand that only when the model is supplied with accurately measured underground data can it be used to effectively simulate the flow regime within the methane drainage range. The principles behind the correlation of actual and predicted data are discussed and how these principles have been applied, (1) to effectively model the performance of the drainage ranges at two representative U.K. collieries and (2) to provide an assessment of the improvements in system performance which may be obtained by considering the selective reconfiguration of the drainage range.

Chapter 4

Correlation Exercises and the Development of an Optimisation Strategy

4.1 Introduction

Chapter 2 discussed the various methods of methane drainage and the rationale behind adopting each of these techniques. Drainage methods employed in advance of mining will attempt to capture gas at a high purity. The objective of any optimisation, therefore, would be to maximise the purity, P , and hence the gas capture.

The primary objective of methane drainage during mining operations has been to maximise the gas capture and thus minimise the gas migration into the mine airways. In this case the objective of an optimisation problem would be to maximise the volume flow rate of methane, Q_m (= $Q \cdot P$, where Q is the total volume flow rate). Once the maximum gas capture has been determined this will enable the ventilation engineer to calculate the minimum fresh air quantities required in the working areas

With the current trends towards the concentration of coal extraction to fewer but higher production units there has been an increase in the volume of gas liberated. This has been accompanied by an increase in the application of methane drainage techniques. Mines have realised they are tapping an extensive, second, energy source and recognised there is a potential for the possible future utilisation of this source. However, the overriding objective of underground methane drainage ranges together with the ventilation system will continue to be the maintenance of a safe working environment.

The maintenance of the purity, and hence the volume of gas capture, such that coal production targets are achieved, and that there is potential to utilise the gas, has increased the need to accurately monitor and simulate the operation of the drainage network. The accurate monitoring, together with the development of an optimisation model, will allow recognition of potential problems within the drainage network.

Air leakage, previously and reluctantly tolerated by mines and pipe manufacturers, is no longer accepted due to the reduced capture potential in the working areas. Water, sedimentation, the poor operation and deterioration in the performance of fittings, the deterioration in pipe linings and the operation of surface extraction plants, all need to be monitored to ensure the correct management of a methane drainage system.

During the development of the computer model a range of correlation exercises were performed on a number of real mine drainage networks. These exercises contributed to the development of the model and the identification of the subsequent optimisation strategies.

4.2 Case Study 1 - Harworth Colliery

4.2.1 Background

Harworth Colliery is situated in the Nottinghamshire coalfield, some 35 miles north of Nottingham. It has long been known to have particular environmental problems including unusually high virgin strata temperatures and high makes of methane gas. It has extensive reserves with 36 million tonnes of classified coal (i.e. that which could be recovered using current technology and market prices) and another 45 million tonnes unclassified in the seams currently being worked. If all the possible workable seams are considered there are approximately 200 million tonnes of reserves.

Production is currently concentrated in the Deep Soft seam at a depth of approximately 960 metres. Workings are situated on the north east flank of the Ranskill anticline. The axis of the anticline has a north west to south east orientation and plunges to the north west. The dip of current workings is about 2° with intake slightly down dip of returns.

Sandstone beds are known to lie both above and below the Deep Soft workings (see Figure 4.1). These bands cap gas released from seams above and below the Deep Soft. They have low permeability, between 0.16 mD and 0.19 mD, and will only yield significant amounts of gas when fractured. The sandstone beds below will also cap gas released from underlying sources, particularly the Parkgate seam, and the pressure build up, linked with high porosity, increases the risk of severe unpredictable gas emissions.

Coal is mined from 4 faces, 3 in the Deep Soft seam (see Figure 4.2) and 1 in the Swallow Wood seam. All panels are mined using advancing longwall methods and current production levels are between 1.8 and 2 million tonnes per year.

Methane emissions from the Swallow Wood seam were originally around 13 m³ per tonne of coal mined. This figure has almost doubled since the face has begun to work under virgin ground rather than the previously exploited Top Hard seam.

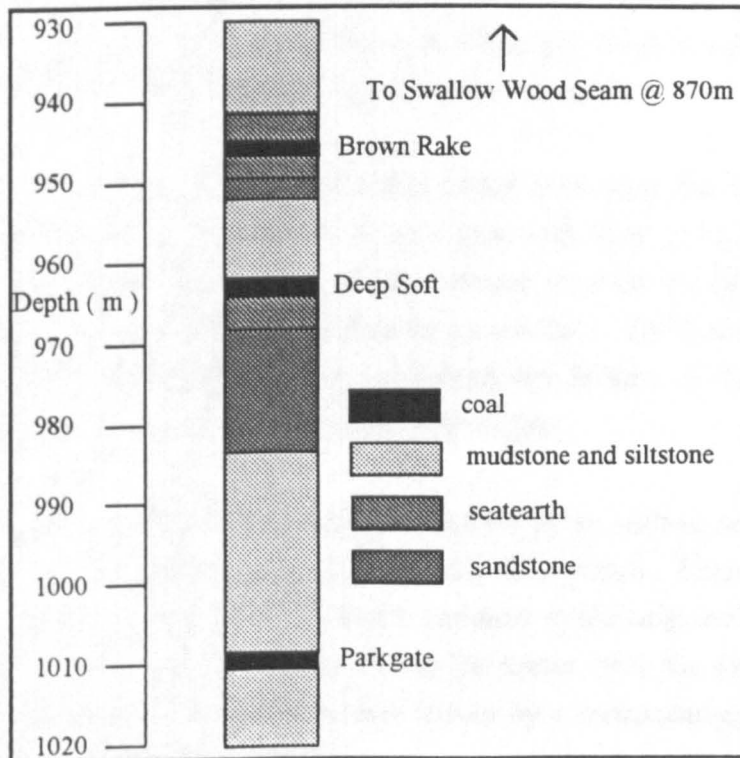


Figure 4.1. Stratigraphic section of Harworth colliery from the Low Farm borehole.

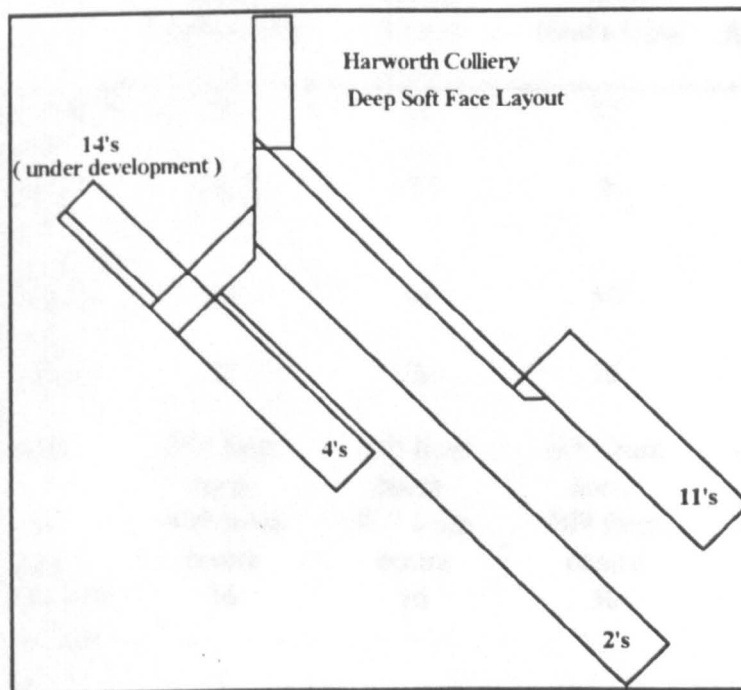


Figure 4.2. Harworth colliery face layout of the Deep Soft seam.

Gas emissions from the Deep Soft seam are of the order of 42 m³ per tonne of coal mined. These large quantities are attributed to the virgin conditions of the ground and other gas bearing strata additional to the coal seams themselves.

Gas is extracted through 2 inch roof holes drilled from both the intake and return roadways. These are complemented on all faces with floor holes drilled from the intake roadway to ensure the capture of gas desorbed from the Parkgate seam and not allow it to accumulate below the capping sandstone bed. The holes will relieve the pressure build up and reduce the risk of intermittent failures of the sandstone and sudden emissions of large quantities or 'blowers' of gas.

All holes are connected to 14 inch ranges for delivery to the surface extraction plant. The surface extraction plant consists of 8 Nash CL3002 pumps. These provide 65 kPa of suction of which approximately 52 kPa is currently available at the shaft head. The current duty is 3000 l/s at 50% purity. Until December 1992 the extracted methane was fed to boilers and a 500 kW alternator driven by a reciprocating gas engine, the remainder being vented to atmosphere.

| | 11's Roof Holes Intake Gate | 11's Roof Holes Return Gate | 11's Floor Holes Intake Gate | 11's Floor Holes Return Gate |
|--|-----------------------------------|--------------------------------------|------------------------------------|------------------------------------|
| Borehole Length (m) | 61 | 61 | 55 | 55 |
| Standpipe Length (m) | 13.7 | 13.7 | 6 | 6 |
| Borehole Diam. (mm) | 50 | 50 | 50 | 50 |
| Standpipe Diam. (mm) | 52 | 76 | 52 | 52 |
| Inclination | 55° from horiz. | 55° from horiz. | 60° from horiz. | 60° from horiz. |
| Angle to Roadway | 90° from centre | 90° from centre | 90° from centre | 90° from centre |
| Max. distance of last hole to face (m) | 36 | 36 | 50 | 50 |
| Max. spacing between holes (m) | 25 | 25 | 40 | 40 |

Table 4.1. Borehole parameters and configuration on 11's face, Harworth colliery.

Today all extracted methane is utilised to both fuel the colliery boilers and produce electricity. This is done by two 4mW alternators driven by gas turbines. The waste heat from the turbine exhaust is used in boilers producing steam to drive a 10mW alternator. The plant as a whole will produce about 14mW of useful power.

Figure 4.4 shows the typical operational characteristic curves of the extractor pumps used at Harworth Colliery. To exhaust 3000 l/s with a system resistance of 9000 Ns^2m^{-8} indicates that 6, or possibly 7, extractors would have to be used supplying 65 kPa of suction. If the resistance could be dropped to 7000 Ns^2m^{-8} in order to extract 3000 l/s, 6 pumps would be necessary delivering 60 kPa.

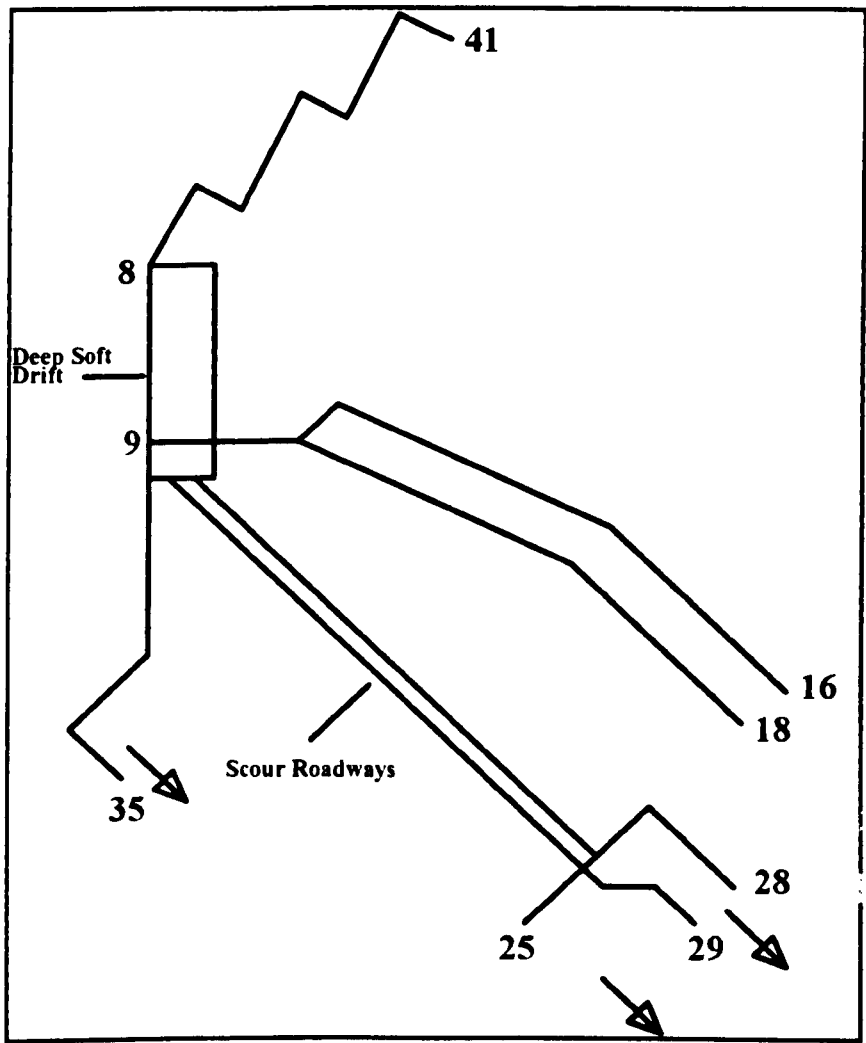


Figure 4.3. Harworth colliery methane drainage pipe layout.

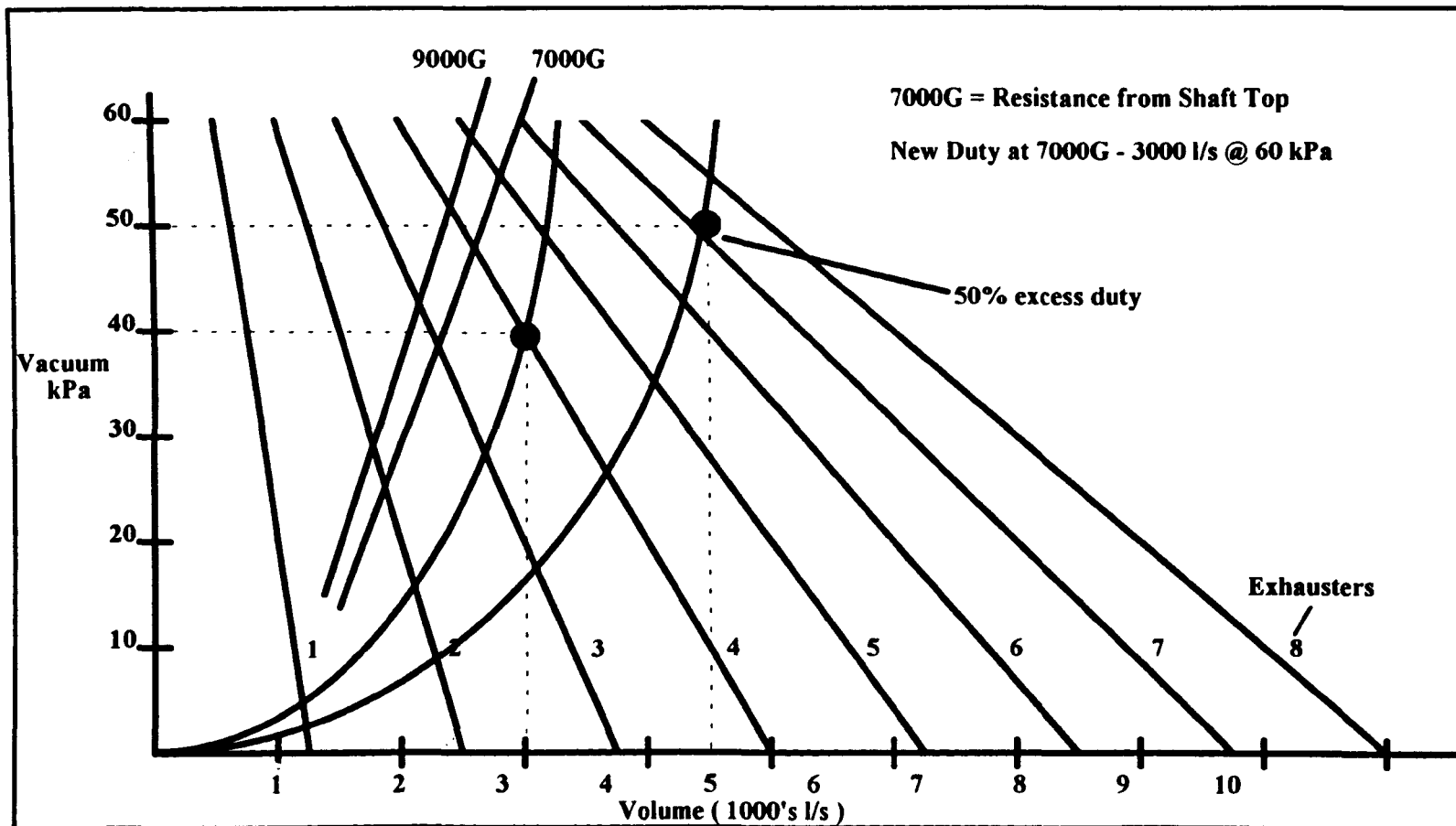


Figure 4.4. Performance curves for 8 CL3002 methane vacuum pumps.

4.2.2 Application of the Model to Harworth's Network

With the end utilisation of the gas, the monitoring of the drainage range is essential to ensure a large enough quantity at the correct purity is being supplied to the electricity generating plant. Since 1988 continual modifications have been made to increase the capacity of the range (see Figure 4.3). A 16 inch Glass Reinforced Plastic (GRP) shaft range has been installed in parallel with the existing 14 inch steel one. More recently a second 14 inch steel range has been installed in the scour roadways servicing the faces. All production faces now have 14 inch pipes installed in the return gate to cope with current drainage volumes. Typical borehole configurations are listed in Table 4.1.

Water traps are installed at suitable locations, particularly along the twin 14 inch ranges in the scour roadways. As stated earlier water has a detrimental effect on the operating efficiency of a system and, at Harworth, the water originates primarily from floorholes drilled to intersect the Parkgate seam.

At this point in the simulation exercise the pipe friction coefficients and loss coefficients across fittings were adjusted to correlate with the measured data obtained by colliery staff [52]. Any differences between measured and predicted performance of pipe sections was attributed to a combined error in the values of both the friction factors and the loss coefficients across fittings. This data indicated losses of 16 kPa in the 14 inch drift range.

It was predicted that this configuration would be unable to cope with any desired, further, increases in drainage capacity. Subsequent to the inclusion of the 16 inch GRP shaft range and paralleling the 14 inch range in the scour roadways the third stage planned at the colliery was to install a 16 inch GRP drift range in parallel with the existing 14 inch steel drift range. This was to take place in mid 1992.

The pipe network model was used to simulate conditions at the colliery and then assess the benefit that could be obtained by installing the 16 inch pipe. The results of this simulation are illustrated in Table 4.2. The inclusion of a 16 inch GRP pipe reduced the predicted pressure losses in the drift to approximately 2 kPa. The predicted suction pressures at the boundary junctions inbye were almost doubled. An improvement in suction may improve gas capture from boreholes and could be accompanied by an increase of air inleakage into the pipe range. Both these factors will increase volume flows in the pipe range thus increasing the losses in the network.

The example modelled above assumed the same volume flows entering the network for both cases and does not model air leakage into the range. It will therefore give a qualitative guideline as to the effect of altering the pipe network topology. Further correlation and development of the program is necessary to include air leakage.

| Measured Data | | Predicted Results | |
|---------------|-----------------|-------------------|-----------------|
| JUNCTION | SUCTION (kPa) | JUNCTION | SUCTION (kPa) |
| 1 | 50.00 | 1 | 50.00 |
| 2 | 49.40 | 2 | 49.40 |
| 3 | 49.38 | 3 | 49.38 |
| 4 | 43.28 | 4 | 43.28 |
| 5 | 43.46 | 5 | 43.46 |
| 6 | 43.26 | 6 | 43.26 |
| 7 | 43.43 | 7 | 43.43 |
| 8 | 42.90 | 8 | 42.90 |
| 9 | 25.28 | 9 | 40.85 |
| 10 | 41.24 | 10 | 42.64 |
| 11 | 25.44 | 11 | 39.45 |
| 12 | 24.78 | 12 | 40.27 |
| 13 | 24.78 | 13 | 40.26 |
| 14 | 24.10 | 14 | 39.41 |
| 15 | 22.10 | 15 | 36.94 |
| 16 | 23.58 | 16 | 38.76 |
| 17 | 21.18 | 17 | 35.80 |
| 18 | 16.33 | 18 | 29.96 |
| 19 | 24.92 | 19 | 39.59 |
| 20 | 24.92 | 20 | 39.38 |
| 22 | 14.69 | 22 | 27.06 |
| 25 | 13.67 | 25 | 25.87 |
| 26 | 14.58 | 26 | 26.93 |
| 27 | 14.47 | 27 | 26.80 |
| 28 | 14.69 | 28 | 27.06 |
| 29 | 14.27 | 29 | 26.57 |
| 30 | 25.05 | 30 | 39.37 |
| 31 | 14.69 | 31 | 27.06 |
| 32 | 23.27 | 32 | 37.57 |
| 33 | 22.82 | 33 | 37.02 |
| 34 | 21.13 | 34 | 34.96 |
| 35 | 19.89 | 35 | 33.47 |
| 36 | 41.99 | 36 | 41.99 |
| 37 | 39.50 | 37 | 39.50 |
| 38 | 29.00 | 38 | 29.00 |
| 39 | 28.26 | 39 | 28.26 |
| 40 | 26.62 | 40 | 26.62 |
| 41 | 24.36 | 41 | 24.36 |
| 42 | 14.63 | 42 | 26.99 |

Table 4.2. Comparison of Measured and Predicted Pressure distributions.

Measurements taken in the range after installation of the 16 inch G.R.P. drift range showed that losses along the new paralleled section were reduced to approximately 4

kPa. The borehole suction available near the face line were improved by up to 10 kPa.

The surface extraction plant gained some 400 l/s but there was a drop in purity from 57% to 54% which indicated that this could be attributed in part to inleakage in the newly installed range. At the drift top the gas purity had reduced to 35%.

4.3 Use of The Program as an Optimisation Tool

4.3.1 Network Monitoring

Before the pipe network model could be utilised to assess the optimal performance of an existing methane drainage range, or the effect modifications to the drainage range will have on its performance then the user must be confident the model is accurately simulating the current drainage range set up.

Using the example of Harworth Colliery, friction coefficients were adjusted until pressure drops calculated in the simulation model were similar to those that had been measured in the drainage range. This method gave adequate results in order that an assessment of the effect of introducing a new 16 inch GRP pipe could be made. However another factor, namely the inleakage of air, will affect pressure drops through the system, an assumption confirmed by greater volume flows and lower purities than expected at the surface extraction plant.

To improve predictions produced by the computer model a data base needs to be collated from measurements made on installed drainage systems in order to assess the range taken by certain system parameters. For example the friction factor of pipes of different material type and age, an assessment of the amount of leakage experienced for a given pressure range, the pressure losses actually experienced across installed pipe fittings and an assessment of the efficiency of manual or automatic water traps in removing strata water from the drainage range.

The primary operational objective of the drainage range is to maximise gas capture for the capacity and suction pressure of the surface plant. However, as mentioned previously, surface utilisation of the gas requires that purity levels be maintained and hence there may be a second, complementary, objective.

It is evident that the optimal performance of a methane drainage range is influenced by a complex interaction of factors. The simulation model may be employed to assess the operational performance of an existing range by comparing the differences between the predicted performance and the measured data. The availability of good measured data, made at suitable locations, is therefore essential if a worthwhile attempt is to be made at accurately modelling the range.

An analysis of significant differences may be used to highlight, for example, where major pressure losses are occurring. Once these sections are located the ventilation engineer may make further measurements to identify the cause which may be : the presence of strata water, the deterioration of the inner surface of the pipe, the deterioration in the performance of pipe fittings or the occurrence of measurable leakage. The ventilation engineer may then be able to enact remedial maintenance measures to improve the system performance.

4.3.2 Analysis of Measured and Predicted Data

Any discrepancy between the measured and predicted data sets can, justifiably, be put down to a combination of an incorrect initial estimate of friction factor for the pipes and fittings or the presence of air inleakage into the range.

An analysis comparing each branch of the network, to produce a correlated simulation, will begin at the boundary junctions on the districts and work towards the extraction plants. Using Figure 4.5 as a simple example pipes will be considered in the sequence shown, firstly to assess inleakage and thence to assess the true frictional resistance of pipes and fittings.

In order to assess the relative effect which these parameters have on the performance of the drainage range the relationship between the flow regime (which includes the air inleakage) and the physical network model needs to be determined. Only when these

relationships have been determined can a correct analytical method of making a comparison between measured and predicted data be devised.

The flow regime within the range is described by a combination of gas purity, pressure and flow rate measurements made throughout the network (see Figure 4.7). The physical pipe network model is described by the topology of the network (i.e. pipe connections), the physical pipe characteristics, and the position of pipe fittings.

The measured and predicted data needs to be analysed in such a way that the end product will provide a true simulation of the drainage range (see Figure 4.6). The model may then be used to identify remedial maintenance measures which will improve system performance.

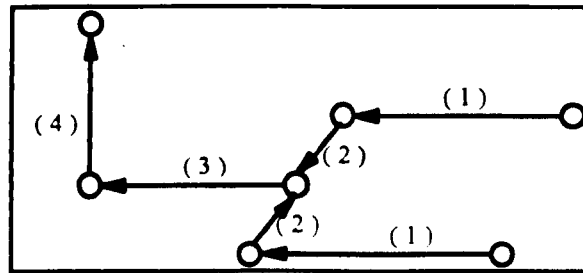


Figure 4.5. A simple network for the comparison of measured and predicted data.

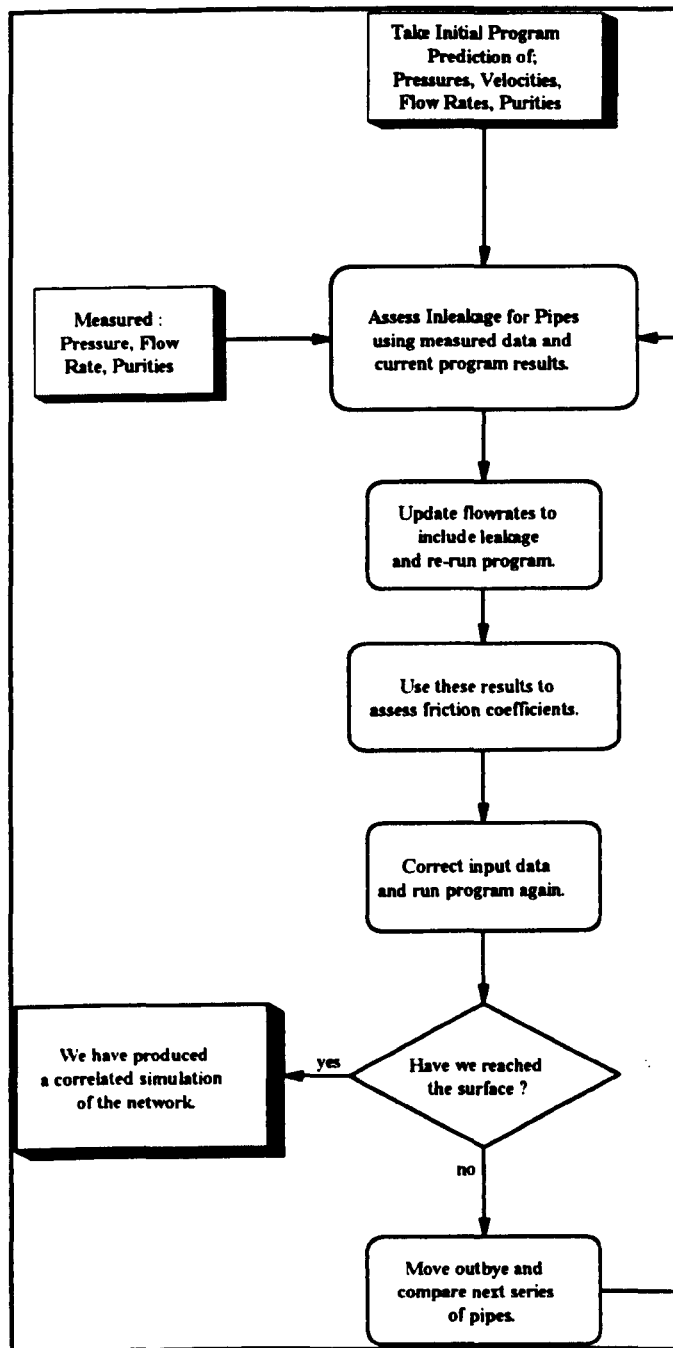


Figure 4.6. Using the measured data to effectively simulate the drainage range.

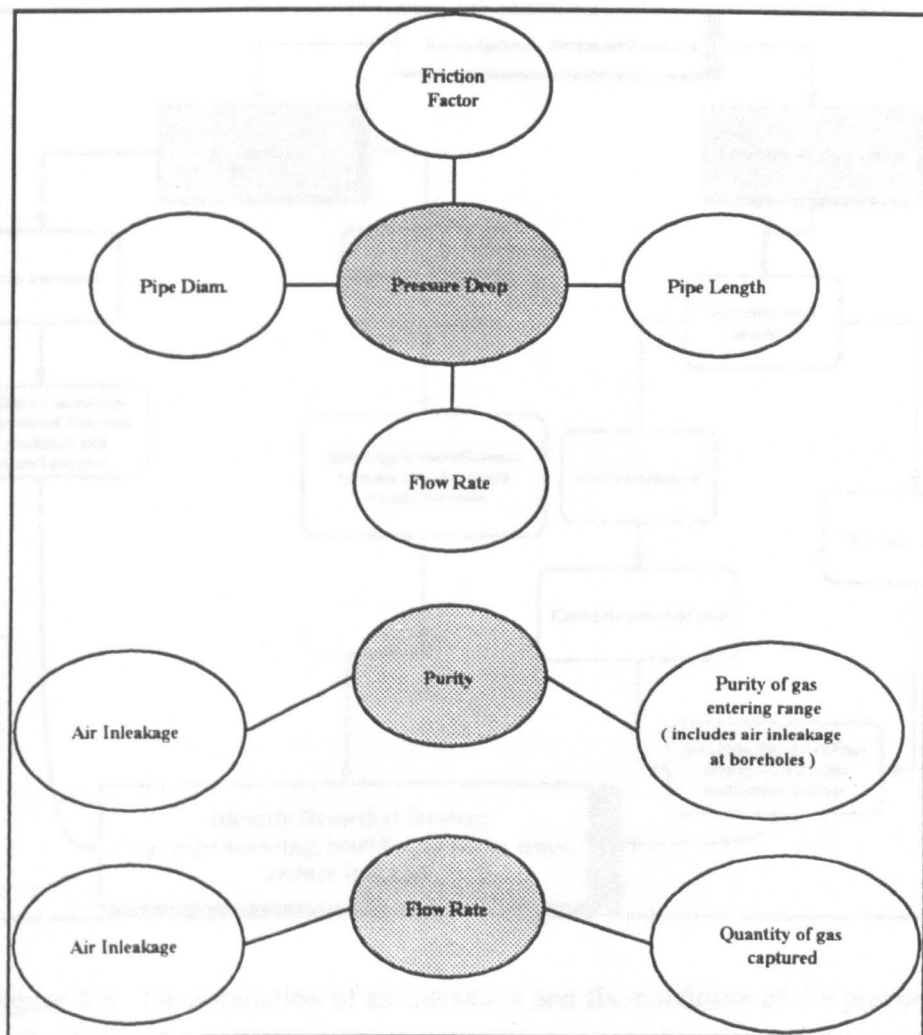


Figure 4.7. Factors affecting the flow parameters

4.3.2.1 Air Inleakage

Air inleakage into sections of the drainage range will manifest itself as increased flow rates of lower purity gas mixtures than expected (see Figure 4.8). Hence estimates of inleakage can be determined by a knowledge of one of these measured values together with the predicted purity and flow rate.

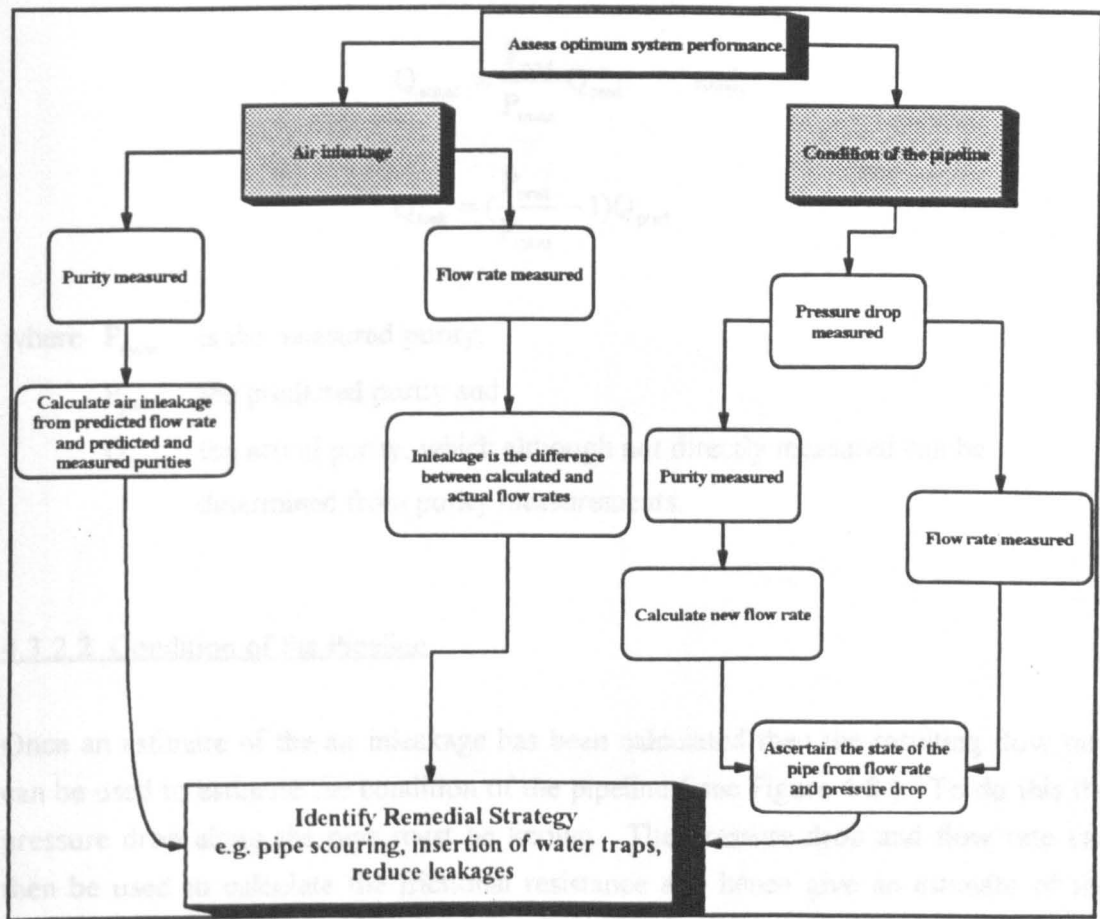


Figure 4.8. Determination of air leakage and the condition of the pipeline.

4.3.2.1.1 Flow Rate Measured

The Air leakage will simply be the difference between measured and predicted flow rates. i.e.

$$Q_{\text{leak}} = Q_{\text{meas}} - Q_{\text{pred}}$$

where Q_{leak} is the leakage volume flow rate,

Q_{meas} is the measured volume flow rate and

Q_{pred} is the predicted volume flow rate.

4.3.2.1.2 Purity Measured

Using the measured purity and the predicted flow rate and purity then ;

$$Q_{\text{actual}} = \frac{P_{\text{pred}}}{P_{\text{meas}}} Q_{\text{pred}} \quad \text{and,}$$

$$Q_{\text{leak}} = \left(\frac{P_{\text{pred}}}{P_{\text{meas}}} - 1 \right) Q_{\text{pred}}$$

where P_{meas} is the measured purity,
 P_{pred} the predicted purity and
 Q_{actual} the actual purity, which although not directly measured can be determined from purity measurements.

4.3.2.2 Condition of the Pipeline

Once an estimate of the air inleakage has been calculated then the resulting flow rate can be used to estimate the condition of the pipeline (see Figure 4.8). To do this the pressure drop along the pipe must be known. The pressure drop and flow rate can then be used to calculate the frictional resistance and hence give an estimate of the state of the pipe.

Increased values of the pipe resistances can be attributed to a number of causes as shown in Figure 4.9.

Careful monitoring of the 'effective' frictional resistance of a pipe over a period of time will reveal the relative effect of the parameters shown above.

Water can enter the pipeline from the surrounding strata and as the result of wet drilling operations. This, together with the presence of any sedimented particles, will decrease the active cross section of the pipelines (in the lowest part of the network) and hence rapidly increase the resistance to flow. This will result in a reduction of the efficiency and hence reduce the capacity of the system. Efficient and competent water removal mechanisms are essential for the accurate determination of actual friction factors in the pipelines (see Figure 4.10).

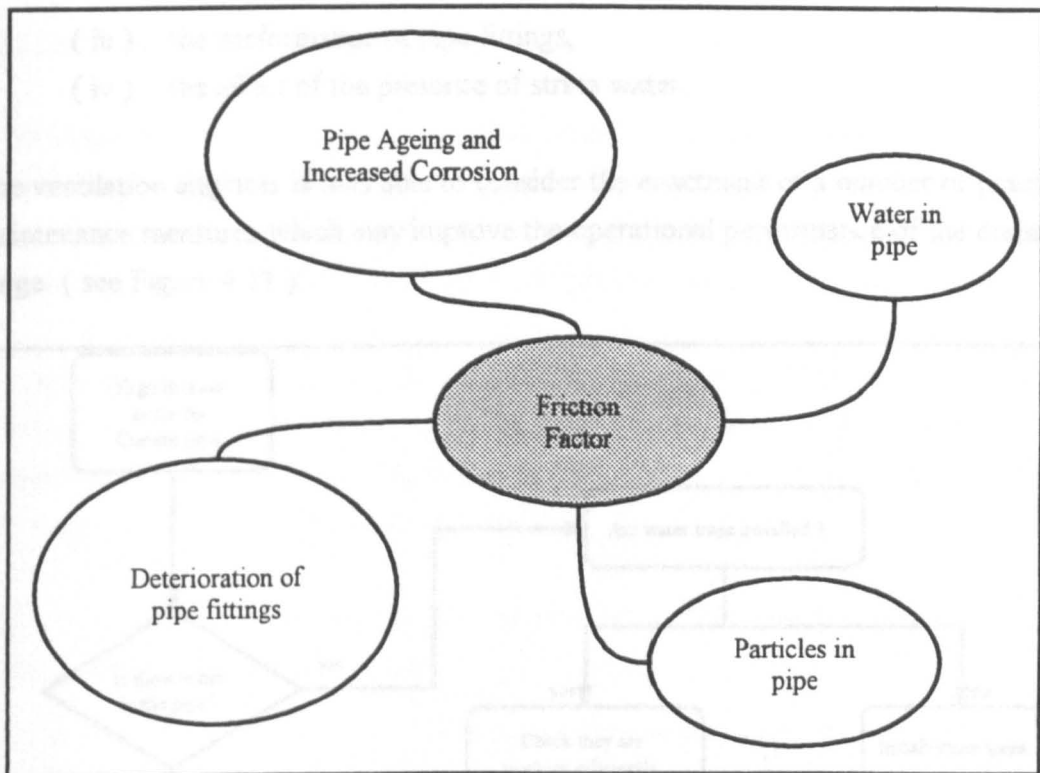


Figure 4.9. Some factors affecting the friction factor.

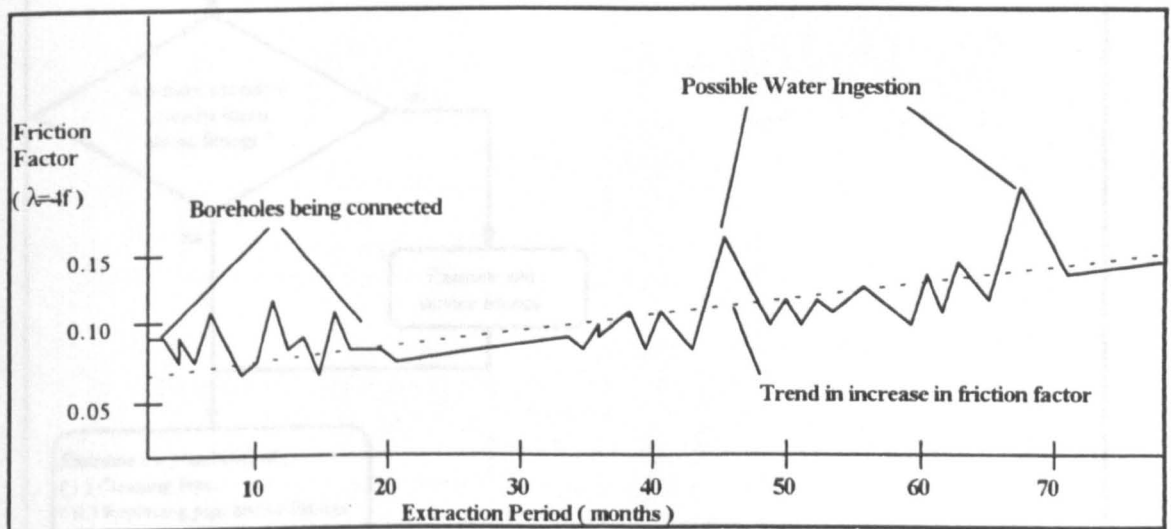


Figure 4.10. Variation of 'effective' resistance over the extraction period (after Pawinski et al [53]).

By performing the above systematic analysis this will enable the identification of ;

- (i) the magnitude and location of air inleakage,
- (ii) the extent in the deterioration of the pipe lining,

- (iii) the performance of pipe fittings,
- (iv) the effect of the presence of strata water.

The ventilation engineer is thus able to consider the enactment of a number of practical maintenance measures which may improve the operational performance of the drainage range. (see Figure 4.11)

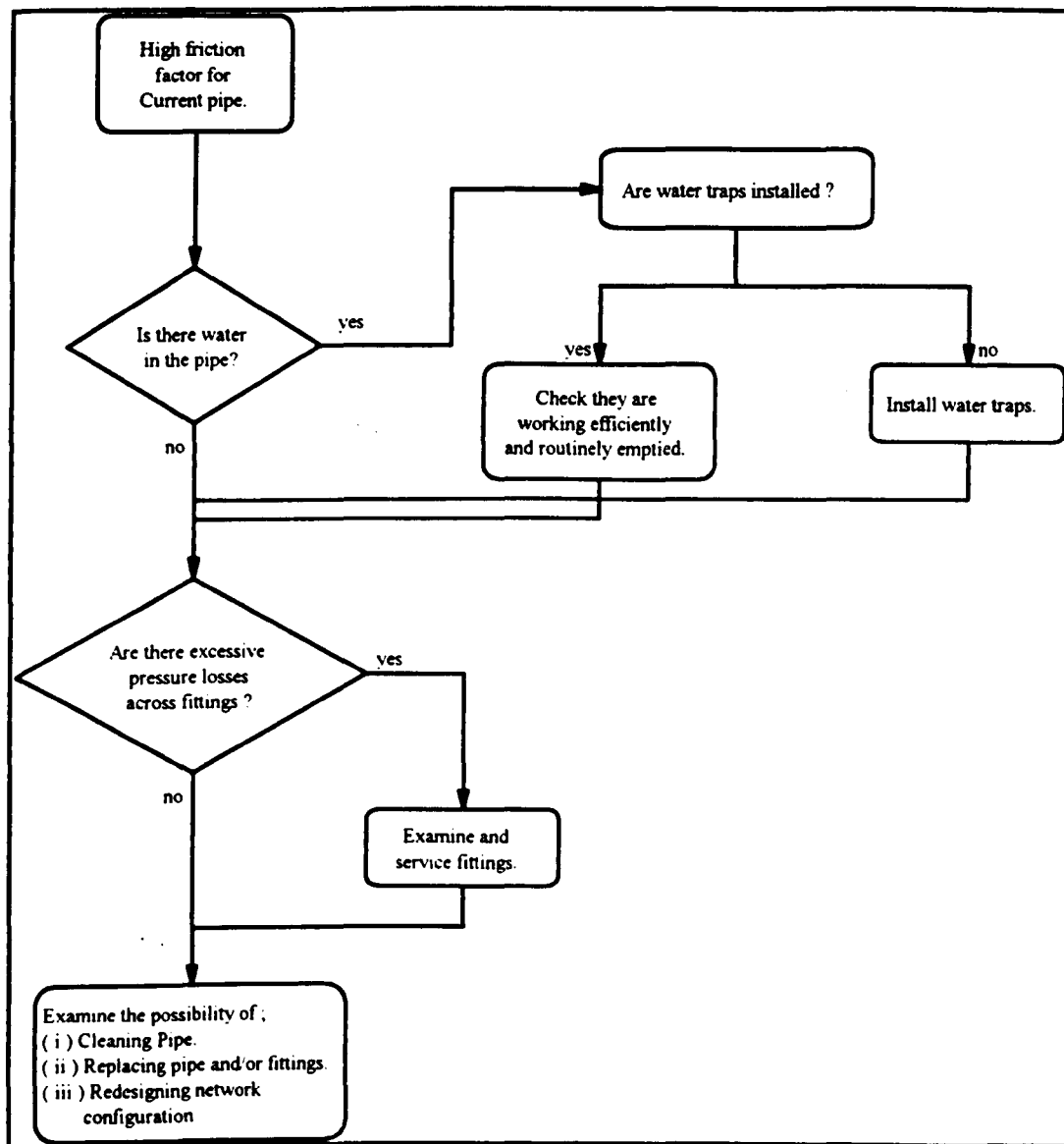


Figure 4.11. Routine maintenance of the pipe network.

4.3.3 Network Reconfiguration

In the event that required suction and flows cannot be achieved, even with the careful maintenance of the current network, the ventilation engineer may use the model to assess the improvement which may be obtained in the performance of the installed system by making changes to the system configuration (see Figure 4.12).

This may involve achieving a reduction in the total pressure losses experienced, by installing a larger diameter pipe to either replace or parallel an existing section of pipeline which is experiencing a significant pressure drop, or by examining alternative pipe materials with lower frictional resistances.

This analysis is demonstrated in the second case study used to examine the effectiveness of the simulation model.

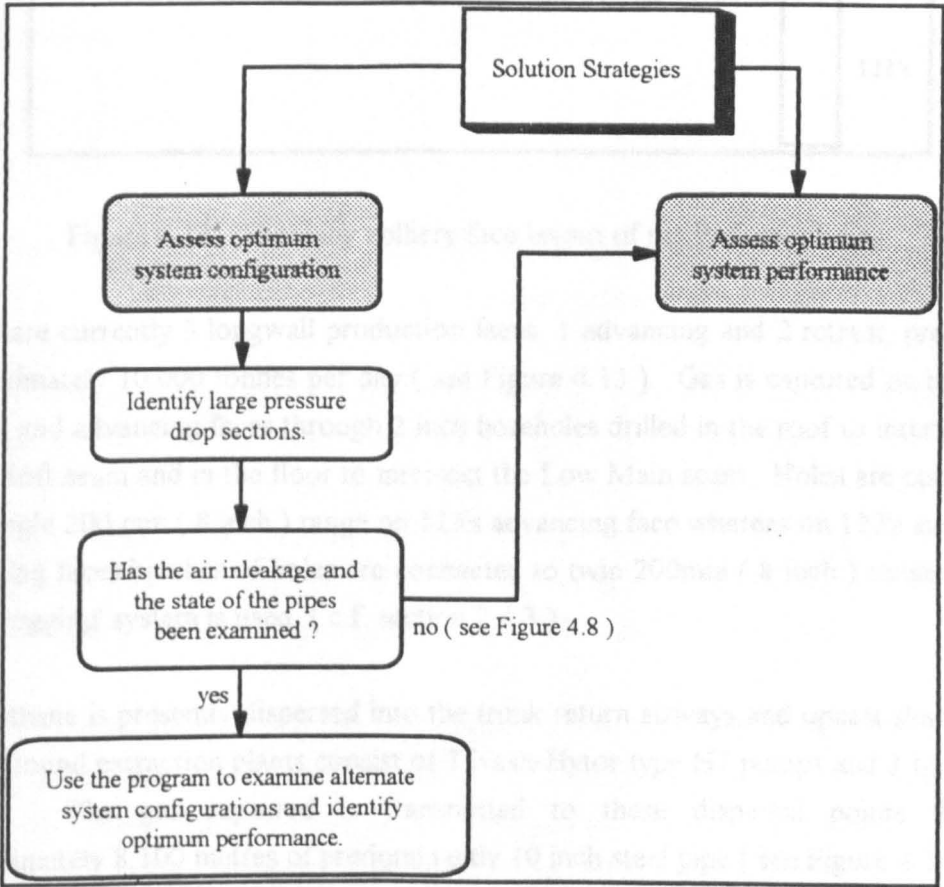


Figure 4.12. Examination of alternative network configurations.

4.4 Case Study 2 - Thoresby Colliery

4.4.1 Background

Thoresby Colliery is situated in the Nottinghamshire coalfield, some 25 miles north of Nottingham. The colliery commenced production in 1928, mining the Top Hard seam but today all mining is from the Parkgate seam which commenced production in 1977.

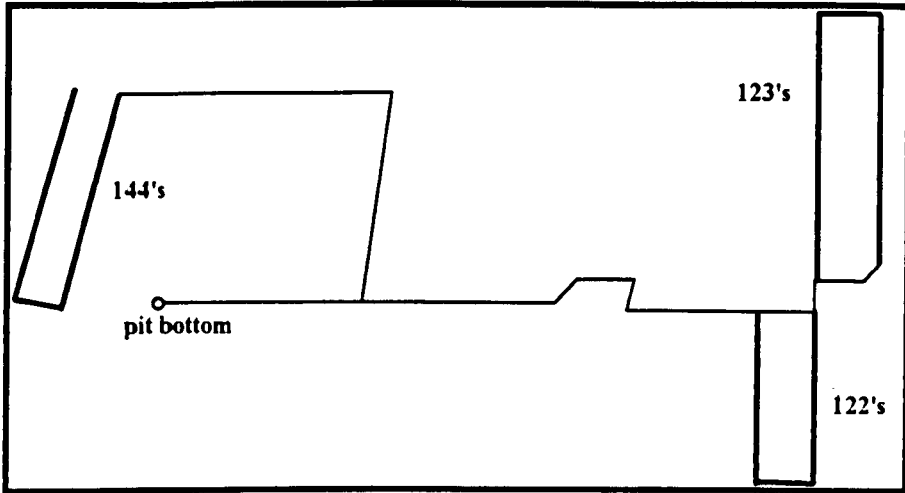


Figure 4.13. Thoresby colliery face layout of the Parkgate Seam.

There are currently 3 longwall production faces, 1 advancing and 2 retreat, producing approximately 10,000 tonnes per day (see Figure 4.13). Gas is captured on both the retreat and advancing faces through 2 inch boreholes drilled in the roof to intersect the Deep Soft seam and in the floor to intersect the Low Main seam. Holes are connected to a single 200 mm (8 inch) range on 123's advancing face whereas on 122's and 144's retreating faces batches of holes are connected to twin 200mm (8 inch) ranges and a 'leap frogging' system is used. (c.f. section 2.4.3)

All methane is presently dispersed into the trunk return airways and upcast shaft. The underground extraction plants consist of 3 Nash-Hytor type H7 pumps and 3 type SC7 pumps. The gas captured is transmitted to these dispersal points through approximately 8,100 metres of predominantly 10 inch steel pipe (see Figure 4.14).

| | 123's Roof (Advance) | 123's Floor (Advance) | 144's and 122's Roof (Retreat) | 144's and 122's Floor (Retreat) |
|---|---------------------------|----------------------------|--|---|
| Borehole Length (m) | 44 - 48 | 19 - 22 | 44 - 48 | 19 - 22 |
| Standpipe Length (m) | 21 | 3 | 21 | 3 |
| Borehole Diam. (mm) | 50 | 50 | 50 | 50 |
| Method of sealing standpipe | resin or densotape | hardstop | resin or densotape | hardstop |
| Inclination | 55 - 65° from horiz. | 45 - 55° from horiz. | 55 - 65° from horiz. | 45 - 55° from horiz. |
| Angle to Roadway | 90° from centre | 90° from centre | 90° from centre | 90° from centre |
| Max. distance of last hole to face. (m) | 50 | 50 | 15 | 50 |
| Max. spacing between holes (m) | 15 | 45 | 10 | 40 |

Table 4.3. Thoresby colliery manager's rules for borehole patterns on both retreat and advance faces.

Twenty three per cent of the methane emission at Thoresby Colliery is captured by methane drainage [54] , the remainder being diluted by the fresh air flow. The current methane levels in the airstream along with planned future increases in production targets has necessitated the examination of the re-location of the underground methane drainage plants on the surface. It is proposed to install 4 CL3002 Nash methane pumps capacity of up to 2700 l/s at 45 kPa suction.

The re-siting of the methane plant on the surface will require the uprating of the main underground ranges to ensure the increased suction being made available will not be dissipated in the ranges. The ranges have been analysed by the Ventilation Department of British Coal, Nottinghamshire Group and the current computer prediction model was used to assist in the analysis and prediction of future performance.

The surface plant, in addition to providing a safer underground environment, will allow possible utilisation of the captured gas. This could take one of two forms ;

- (i) Colliery boilers which can be fired using methane above 30% purity.
- (ii) Power generation by turbines. In this case the methane must be above 40% purity.

4.4.2 Thoresby's Current Drainage Range

The majority of the pipe range consists of 10 and 12 inch steel pipe installed over a period of time ranging from April 1977 until January 1988 (see Figure 4.14). The pressure losses experienced are higher than those normally expected from rough steel pipes and 80 % of the available vacuum is absorbed in overcoming the losses in these trunk ranges. There is no water problem indicated in the ranges but appears to be a general problem due to the presence of silt and corrosion which is indicative of the age of pipe range [54].

4.4.3 Application of the Model to Thoresby's Network

The modelling was carried out in three stages ;

- (i) The development of an initial model assuming rough pipes and no air leakage.
- (ii) The production of a correlated model of the actual range using measured data, supplied by colliery staff, from various positions on the range.
- (iii) The development of a reconfigured model to predict the effect of inserting new 14 inch pipes in parallel with sections of the existing installation and the with the extraction plant being moved to surface.

The present computer model assumes only one exhausting point at junction 1. The operation of the 3 H7 pumps, effectively in parallel with the 3 SC7 pumps, was modelled by inserting a parallel 'imaginary' pipe from the position of the H7 pumps to the exhausting location. This pipe will carry a total flow equal to that which is currently being exhausted at the H7 pumps. The exhausting of gas using 144's outbye diffuser was modelled in a similar way with pipe (19).

4.4.3.1 Initial Model

The current drainage range configuration was modelled as shown in Figure 4.14.

The model consists of 19 junctions and 20 pipes. The resistances of the 'imaginary' pipes inserted to mimic the action of the O/B diffuser and the H7 pumps were adjusted until the flows along these pipes was equal to the flows actually being exhausted at these points.

In this initial model friction factors assumed are that for a normal rough steel pipe and there is no air inleakage along the drainage range.

| JUNCTION | SUCTION (kPa) |
|----------|-----------------|
| 1 | 33.0 |
| 2 | 29.5 |
| 3 | 21.9 |
| 4 | 12.1 |
| 5 | 11.4 |
| 6 | 24.2 |
| 7 | 23.7 |
| 8 | 23.5 |
| 9 | 23.4 |
| 10 | 20.6 |
| 11 | 20.6 |
| 12 | 20.4 |
| 13 | 20.3 |
| 14 | 20.2 |
| 15 | 20.1 |
| 16 | 32.3 |
| 17 | 29.5 |
| 18 | 32.2 |
| 19 | 18.0 |

Table 4.4. Predicted pressure drops for the initial model of Thoresby colliery.

| PIPE | CORR. VOL. FLOW (l/s) | VELOCITY (m/s) | PURITY |
|------|----------------------------|------------------|--------|
| 1 | 1042 | 14.3 | 46 |
| 2 | 491 | 9.7 | 50 |
| 3 | 491 | 9.7 | 50 |
| 4 | 621 | 12.3 | 50 |
| 5 | 423 | 8.4 | 39 |
| 6 | 423 | 8.4 | 39 |
| 7 | 423 | 4.3 | 39 |
| 8 | 423 | 4.3 | 39 |
| 9 | 423 | 8.4 | 39 |
| 10 | 226 | 1.7 | 34 |
| 11 | 198 | 3.9 | 45 |
| 12 | 198 | 3.9 | 45 |
| 13 | 198 | 3.9 | 45 |
| 14 | 198 | 3.9 | 45 |
| 15 | 546 | 7.5 | 42 |
| 16 | 124 | 2.5 | 50 |
| 17 | 367 | 5.0 | 50 |
| 18 | 497 | 6.8 | 50 |
| 19 | 130 | 2.6 | 50 |
| 20 | 621 | 12.3 | 50 |

Table 4.5. Pipe flows, velocities and purities for the initial model of Thoresby colliery.

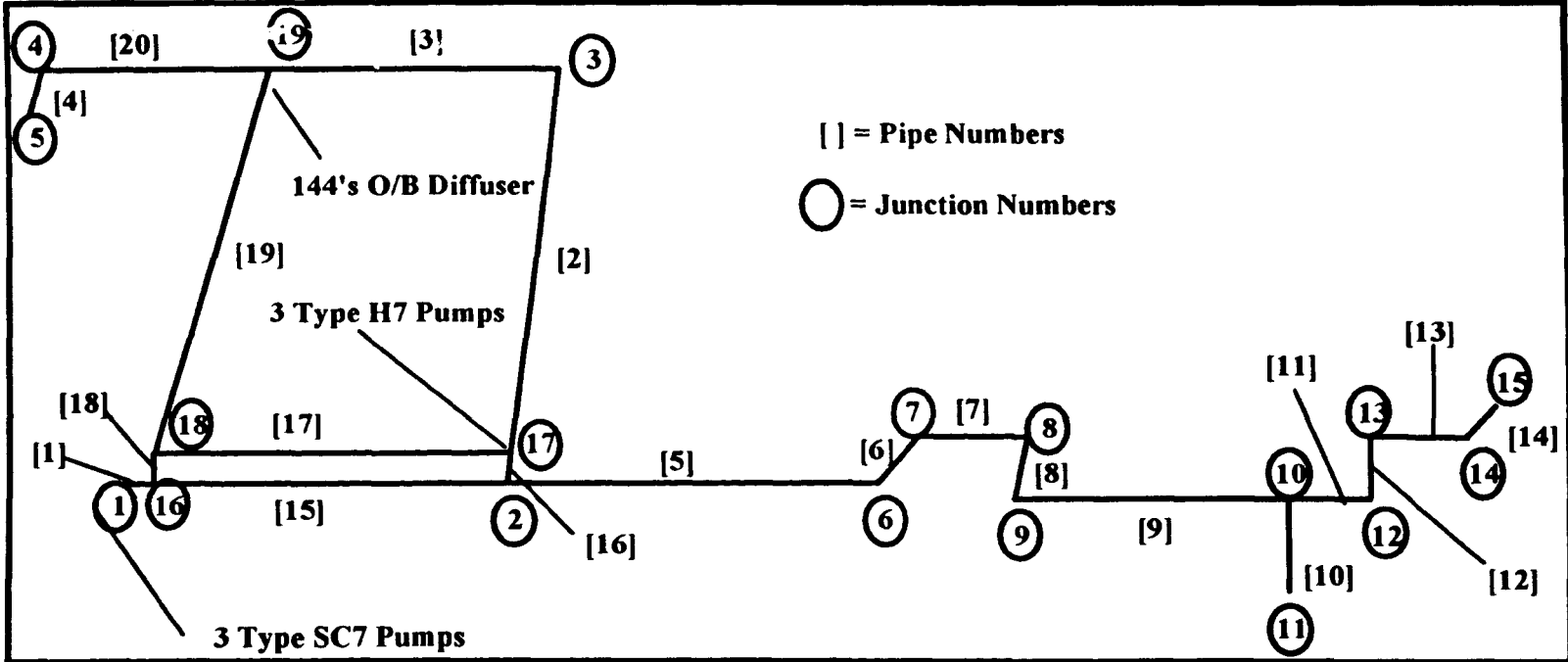


Figure 4.14. Schematic of Thoresby colliery methane drainage range.

4.4.3.2 Correlated Model

The actual measurements of purity and flow taken by colliery staff combined with the initial prediction model now enabled calculation of the air inleakage. The measured pressure drops enabled calculation of the actual resistance factors through the pipe range.

| Pipe Number | Air Inleakage (l/s) | Cumulative Air Inleakage in Current District |
|----------------|-----------------------|---|
| 14, 13, 12, 11 | 64 | 64 |
| 10, 9 | 63 | 127 |
| 8,7,6 | 39 | 166 |
| 5 | 46 | 210 |
| 2 | 164 | 164 |

Table 4.6. Air inleakage determined from the initial model and measured data.

The increase in resistances of selective pipes in the range are shown below as a factor of the resistance value assumed for a normal rough steel pipe.

| Pipe Number | Increase in Resistance |
|-------------|------------------------|
| 2 | 0.50 |
| 5 | 0.55 |
| 6, 7 | 3.30 |
| 9 | 2.00 |
| 15 | 0.80 |
| 3, 20 | 1.25 |

Table 4.7. Increase in resistance values in comparison with a normal rough steel pipe.

These changes gave the results for the correlated model shown in Tables 4.8 and 4.9

| JUNCTION | SUCTION (kPa) |
|----------|-----------------|
| 1 | 33.0 |
| 2 | 26.0 |
| 3 | 19.0 |
| 4 | 6.7 |
| 5 | 6.1 |
| 6 | 19.4 |
| 7 | 16.0 |
| 8 | 14.7 |
| 9 | 14.2 |
| 10 | 5.6 |
| 11 | 5.5 |
| 12 | 5.2 |
| 13 | 5.1 |
| 14 | 4.9 |
| 15 | 4.8 |
| 16 | 31.7 |
| 17 | 26.0 |
| 18 | 31.5 |
| 19 | 15.2 |

Table 4.8. Pressure drops for the correlated model of Thoresby colliery.

| PIPE | CORR. VOL. FLOW (l/s) | VELOCITY (m/s) | PURITY |
|------|----------------------------|------------------|--------|
| 1 | 1417 | 19.4 | 34 |
| 2 | 657 | 13.0 | 38 |
| 3 | 493 | 9.7 | 50 |
| 4 | 621 | 12.3 | 50 |
| 5 | 634 | 12.5 | 26 |
| 6 | 588 | 11.6 | 28 |
| 7 | 588 | 5.9 | 28 |
| 8 | 549 | 5.5 | 30 |
| 9 | 549 | 10.9 | 30 |
| 10 | 226 | 1.7 | 34 |
| 11 | 262 | 5.2 | 34 |
| 12 | 262 | 5.2 | 34 |
| 13 | 262 | 5.2 | 34 |
| 14 | 198 | 3.9 | 45 |
| 15 | 848 | 11.6 | 29 |
| 16 | 214 | 4.2 | 38 |
| 17 | 443 | 6.1 | 38 |
| 18 | 571 | 7.8 | 40 |
| 19 | 128 | 2.5 | 50 |
| 20 | 621 | 12.3 | 50 |

Table 4.9. Pipe flows, velocities and purities for the correlated model of Thoresby colliery.

4.4.3.3 Reconfigured Model

Changes were now made to the network by moving the exhaustor to the surface, removing the underground pumps and paralleling areas of the range with 14 inch pipe. This is illustrated in Figure 4.15. The model is unable to predict the suction-capture potential of the borehole configurations from the strata and hence the results shown below assume the same volume of gas is captured as for the previous drainage range configuration.

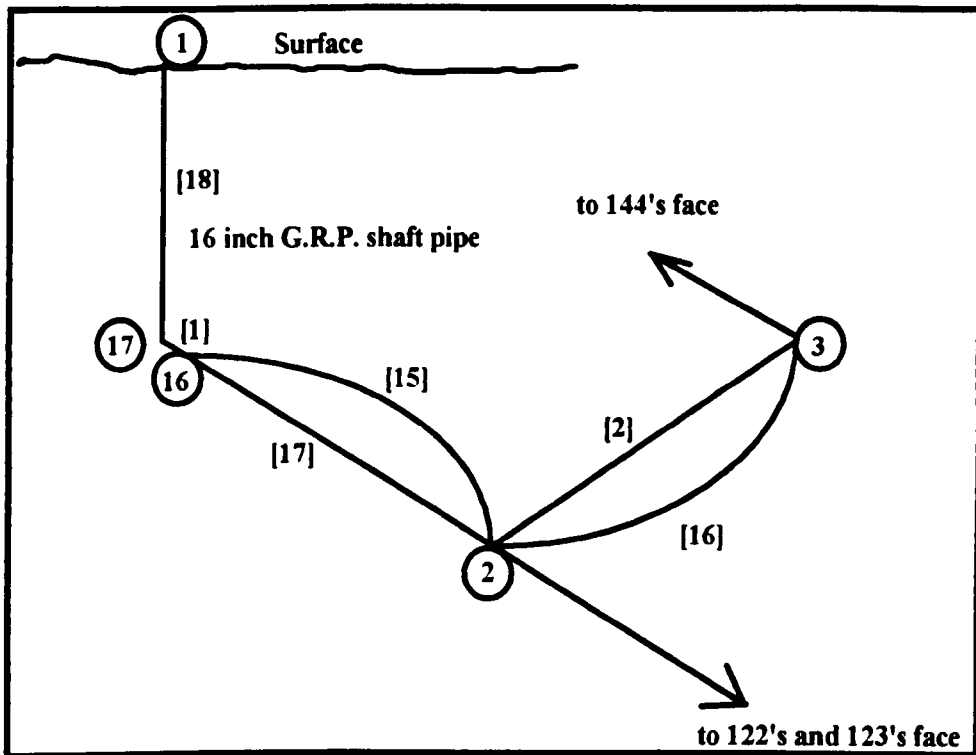


Figure 4.15. Paralleled section of the Thoresby colliery methane drainage network.

The surface exhaustor is assumed to be delivering a suction of 45 kPa and the diameter of the shaft pipe is 16 inch, is 700 metres long and has the same resistance factor of a new steel pipe. Results for this configuration are shown in Tables 4.10 and 4.11

The correlation exercises performed using the model for the reconfigured network have predicted an increase in suction to approximately 12 kPa available on 144's district and 11 kPa on 123's district. The commissioning of this new system is now under consideration by the mine management.

| JUNCTION | SUCTION (kPa) |
|----------|-----------------|
| 1 | 45.0 |
| 2 | 34.5 |
| 3 | 32.9 |
| 4 | 13.3 |
| 5 | 12.6 |
| 6 | 27.1 |
| 7 | 23.4 |
| 8 | 22.0 |
| 9 | 21.4 |
| 10 | 12.1 |
| 11 | 12.0 |
| 12 | 11.7 |
| 13 | 11.6 |
| 14 | 11.3 |
| 15 | 11.3 |
| 16 | 37.7 |
| 17 | 38.4 |

Table 4.10. Predicted pressure drops for the network with a surface exhaustor and 14 inch pipes in parallel

| PIPE | CORR. VOL. FLOW (l/s) | VELOCITY (m/s) | PURITY |
|------|----------------------------|---------------------|--------|
| 1 | 1417 | 14.3 | 34 |
| 2 | 298 | 5.9 | 40 |
| 3 | 621 | 12.3 | 50 |
| 4 | 621 | 12.3 | 50 |
| 5 | 634 | 12.5 | 26 |
| 6 | 588 | 11.6 | 28 |
| 7 | 588 | 5.9 | 28 |
| 8 | 550 | 5.5 | 30 |
| 9 | 550 | 10.9 | 30 |
| 10 | 226 | 1.7 | 34 |
| 11 | 262 | 5.2 | 34 |
| 12 | 262 | 5.2 | 34 |
| 13 | 262 | 5.2 | 34 |
| 14 | 198 | 3.9 | 45 |
| 15 | 614 | 8.4 | 34 |
| 16 | 488 | 4.9 | 40 |
| 17 | 805 | 8.1 | 34 |
| 18 | 1417 | 10.9 | 34 |

Table 4.11. Predicted flows, velocities and purities for the network with a surface exhaustor and 14 inch pipes in parallel.

4.5 Summary and Conclusions

This chapter has described the development and application of the computer simulation model in the analysis of the operational performance of methane drainage ranges installed at two British Coal collieries. Both of the analyses performed were divided into three stages ;

- (i) Production of an initial model.
- (ii) Production of a correlated model using measured underground data.
- (iii) Assessment of the predicted performance of a reconfigured network.

In the first case, the absence of sufficient measured data meant that the resulting predictive analysis was only able to provide an approximation as to the improvement which may be produced in the system performance by the introduction of a parallel 16 inch G.R.P. pipe.

However the measured flow, purity and pressure data provided for the second case study enabled a more accurate determination of the air inleakage and the true resistance using the solution strategy developed in this chapter.

The correlated model was employed to provide an assessment of the effect of re-locating the underground extraction plant to the surface and the introduction of a 16 inch shaft pipe and paralleling sections of the range with 14 inch pipe.

The correlation and analytical exercises performed on the representative drainage networks has highlighted the need, for accurate measured data in order to provide realistic model predictions of the performance of methane drainage ranges. The wider application of remotely monitored, precise, measurement transducers in the drainage range will greatly enhance the applicability of the computer model.

Chapter 5

General Conclusions and Suggestions for Further Work

5.1 General Conclusions

The objective of the research work carried out as the first part of this thesis, was the development of a computer simulation model to assist the ventilation engineer in the assessment of the optimum operational performance and design of a methane drainage system.

Chapter 2 presents a discussion of the various methods of methane drainage and recovery employed around the world. The applicability and success of each method is dependent on the characteristics of the gas bearing strata and the method of mineral recovery. Conditions within U.K. collieries have dictated gas drainage during, and in the immediate vicinity of, the mineral extraction operations.

Gas capture is achieved through cross measure boreholes with each borehole being connected to a pipe range for transmission to the exhausting point. The suction available at boreholes and hence the gas capture is dependent on the configuration and condition of the pipe network.

The pipe network is thus an integral component of the drainage system and the ability to model the pipe network is necessary for a continued, successful and effective methane drainage operation. Chapter 2 presents a critical analysis of previous models, discusses their limitations and suggests the need for development of an alternative model.

Chapter 3 presents some of the basic principles of fluid flow and illustrates how these principles are applied within instruments used in the monitoring of flow and pressure in methane drainage ranges.

Gas flows through methane drainage ranges are accompanied by large pressure drops. The large pressure, and hence density, changes are significant and therefore cannot be neglected. The simulation model developed assumed compressible flow pressure losses. This model was generalised to represent the compressible flow distribution throughout an entire drainage range. The resultant system of non-linear equations was solved using a new method, the *Linear Theory Method*, enabling subsequent

calculation of the volume flow and velocity of gas in each pipe. A system of equations was also formed to calculate the purity of gas in each pipe.

The pressure loss is dependent on the absolute value of pressures and, more critically, on pipe diameter. Any water or sedimentation present in pipes, apart from increasing the frictional resistance of the pipe, will reduce the effective diameter and rapidly increase the pressure losses. Any network reconfiguration or maintenance carried out to reduce the pressure losses in outbye sections of the range will not be transmitted through the network to have the same effect inbye. This is a consequence of the pressure losses being dependent on the absolute value of pressures.

The maintenance of the optimal performance of the drainage range, and the subsequent accuracy of the simulation model, can only be achieved through the accurate monitoring of pressures, flow and purity at appropriate positions in the drainage range. The accuracy of the model will be dependent on air inleakage and correct values for frictional resistance being used. Once air inleakage is quantified from both purity and flow measurements made on a range it may be included in the simulation model in order to ascertain the true values of friction coefficients in all sections of the network. The resulting correlated model may then be used to ascertain whether any gain in performance can be made from remedial maintenance or selective alterations in system configuration.

Chapter 4 describes the development and application of the computer simulation model in the analysis of the operational performance and design of methane drainage ranges installed at two British Coal collieries. Both of the analyses performed were divided into three stages ;

- (i) Production of an initial model;
- (ii) Production of a correlated model using measured underground data;
- (iii) Assessment of the predicted performance of a reconfigured network.

In the first case study, the absence of sufficient measured drainage range data meant that the resulting predictive analysis was only able to provide an approximation as to the improvement which may be produced in the system performance by the

introduction of a 16 inch G.R.P. pipe in parallel with an existing drainage pipe in a major inter-measure drift.

However, in the second case study, the measured flow, purity and pressure data enabled a more accurate determination of the air inleakage and the true resistance coefficients.

During the correlation exercises conducted on these representative colliery networks a subsequent solution strategy was developed. The details of this strategy are presented in this Chapter. The strategy has two components ;

- (i) the enactment of remedial measures to improve system performance.
- (ii) the incorporation of alternative system configurations to improve system performance.

The computer model may be used to predict the improvements which may be obtained by the enactment of the above strategy.

5.2 Suggestions for Further Work.

5.2.1 Further Correlation Studies

An initial further development of this work should be further correlation exercises on representative drainage networks to gain confidence in the accurate predictive performance of the simulation model. This further development should be in close conjunction with the practising mine ventilation engineers.

5.2.2 The Development of a Decision Support System

A future expansion of this work should be the development of an Expert or Decision Support System [1]. This would provide an intelligent interface between the user and the existing simulation program. The rationale behind the development of this Decision Support System would be twofold ;

- (i) the management of input and output data to the program.

- (ii) the provision of advice to the ventilation engineer in the selection of practical design and operational modifications to existing ranges, to increase the capture efficiency.

The Decision Support System would, in addition, be able to explain the rational behind the remedial strategies proposed and hence be a useful training package.

5.2.3 The Incorporation of a CAD Package

Another extension would be the incorporation of a Computer Aided Design package (e.g. AutoCad) which would enable an on-screen representation of the network. Data input and output could then be managed using this representation. This would also allow the drainage network to be overlayed on a ventilation plan (e.g. Vent 5, British Coal Corporation).

PART 2

THE OPTIMISATION OF MINE VENTILATION

Chapter 6

Mine Ventilation Systems

6.1 Introduction

The principal objective of a mine ventilation engineer is to provide a safe and comfortable environment in all working areas of an underground mine. The primary tool available to the engineer is the provision of a suitable quantity of fresh air at a correct velocity to enable rapid dispersal and removal of pollutants from the mine. If this is not sufficient then additional methods, such as gas drainage may need to be considered.

Not even a finely tuned, well designed and well managed methane drainage system will capture all methane liberated as a result of mining operations. A capture efficiency (the ratio of methane captured by the drainage system to the total methane liberated) of 70% is considered to be about the maximum that can be attained in practice. The remainder of the gas will enter the workings and must still be diluted by the ventilating airstream to bring general body concentration levels to below statutory threshold limit values (TLV's). In addition the ventilating airstream should be sufficient to dilute other noxious gases, respirable dusts and unacceptable levels of heat and humidity.

During the extensive lifetime of many underground U.K. coal mining operations the working areas have become more remote from the surface connections. The higher productivity rates required of these mining operations has led to an increase in pollutant emissions and increased load on the ventilation systems. Larger quantities of fresh air flows are entering the mine through narrow shafts and inadequately sized roadways, thus incurring large pressure drops and increased operating costs of the ventilation system.

6.2 Optimisation Strategies

There are a number of formal strategies the ventilation engineer may employ in order to maintain the efficiency of the ventilation system. These include the sealing of leakage paths, the installation of booster fans or regulating doors and the sinking of additional surface connections. The remedial measures employed will have varying capital and operating costs associated with them and should at all times be safe, reliable and economic. The strategy to be followed may include (after [55]) ;

- (i) improving the maintenance of doors and stoppings to minimise leakage and the uncontrolled recirculation of any mine air.
- (ii) where appropriate, the opening of additional airways parallel to existing roadways to reduce the power consumed in providing the required airflow distribution.
- (iii) installing booster fans of the correct duty in strategic locations to increase the air quantity into particular sections of the mine to the desired level.
- (iv) the review of the number, siting and duty of fans within the network.
- (v) the review of the number siting and size of regulators within the network.

Any strategy will commonly be restricted by practical constraints and include ;

- (i) having to maintain air velocities below 4 m/s in order to prevent pick up of dust,
- (ii) having to install booster fans or regulators in specific trunk airways.

In the U.K., Legislation requires that every mine must have a surface standby fan which is capable of providing ventilation adequate for the safe withdrawal of men from underground workings in emergencies [4]. In some countries booster fans are not permitted and mines are ventilated solely by a surface fan. In these cases regulators are the only means of flow control and in networks with a large imbalance in the pressure requirements of different sections, regulators are used in the low pressure districts to consume the excess fan pressure and air power. This power dissipating method of flow control results in inflated ventilation operating costs.

In simple terms the air power required to ventilate an underground mine with a single surface fan is proportional to ;

- (i) the total effective resistance of the mine.
- (ii) the cube of the air quantity supplied through the fan.

If either of these two factors could be reduced, whilst still maintaining the required fresh airflows in working areas, then there will be a corresponding reduction in the cost of ventilation.

6.2.1 Air Leakage

The layout of the ventilation network is usually dictated by the nature of the mineral deposit and the chosen method of mining which takes place over a long period covering many years. Many interconnections in the network are superfluous to ventilation requirements and result in some air short circuiting the desired ventilation route through these, what are termed, 'leakage paths'.

The flow rate through a leakage path is controlled by the resistance of the path and the pressure difference across it. The resistance of some leakage paths can be increased through maintenance of doors and stoppings.

Leakages are normally responsible for the major power transmission loss in a ventilation network. Leakage minimisation through improved airflow control should be an essential feature of good ventilation system design. In ventilation networks with a large number of leakage paths, improved pressure control will greatly influence the operating costs of the system.

As stated earlier, with mines becoming more extensive and with the increase in the concentration of production to fewer but more productive faces, the increased fresh airflow quantities demanded in the more remote locations has increased the pressures required of the surface fans. This has increased the pressure differences and hence airflows across leakage paths with a corresponding reduction in the efficiency and an increase in the cost of the ventilation system. In some cases the ventilation pressure required will become so high that to achieve this by the use of the surface fan alone would create problems at the surface airlock may endanger the health of the workforce and furthermore would become uneconomic. For these reasons the application of booster fans have become an integral part in the ventilation system of present day U.K. coal mines.

6.2.2 Reduction in Effective Resistance

Reduction in the effective resistance can be achieved by the opening of parallel trunk airways. However a far cheaper option, if applicable, would be to reduce the roadway surface friction with suitable materials such as wooden boarding, sheet metal or spray concrete lining. Before any design is considered the ventilation engineer must know the airflow the roadway is expected to carry.

6.2.3 Airflow Control

Far greater benefits, however, can be obtained by careful management of the air quantity distribution and leakage. The control of the distribution of airflow can be achieved by the selective addition of *passive* and/or *active* regulation. Passive regulation is the addition of resistance commonly in the form of a regulating door. Active regulation is the addition of pressure sources in the form of underground booster fans.

6.3 The Use of Underground Booster Fans

The addition of an underground booster fan or fans has become a necessary, and an energy efficient, way of regulating a ventilation network. The total pressure, and hence energy, requirement is now shared between surface and remote booster fans. Not only will the booster fan installations assist in the supply of the energy required to deliver the pre requisite fresh airflow, but they will be able to deliver and control the airflow at the required locations of the ventilation network. The input of power at a number of carefully chosen positions can be readily shown to be more efficient than a single point input [56]. Today, 25% of all power supplied to ventilating systems in U.K. collieries comes from booster fans [57].

Practical considerations apart, booster fans are commonly positioned ;

- (i) to increase the fresh air flows within high resistance, remote sections, of the ventilation circuit in order to improve environmental conditions.
- (ii) to reduce or balance pressure differences across leakage paths to minimise the air lost across these paths.
- (iii) to keep the pressure generated by the surface fans to a minimum.

(iv) to assist the surface fan in the ventilation of the mine.

A single surface fan will operate at a pressure necessary to meet the needs of the highest resistance split in the network. The requirements of the other splits, as stated earlier, are met by using regulators to control the flow of air. This is a method of flow control which is wasteful of energy and expensive to run and alternatively a booster fan may be used to control the flow of air in the high resistance split. The flow of air in all the other splits will be reduced. The surface fan has to perform the additional duty of passing extra air along the trunk airways, and a certain proportion of pressure previously available for ventilating the outbye splits is now absorbed by the trunk airways. Under such conditions the action of a booster fan is that of controlling the distribution of airflow by an addition of a fixed amount of energy to all the air passing through it.

To assist a surface fan in the ventilation of a mine, and hence reduce the power consumption, an exhausting booster fan is commonly situated in a return trunk airway. Care must be taken that the combination of pressure and location of a booster fan, whether it be in a trunk airway or high resistance split, does not induce flow recirculation across leakage paths. It would therefore be desirable to operate the booster fan at a pressure and location which minimised air leakage but did not cause flow reversal. This point is commonly known as the neutral point and is the position at which the pressure difference between intake and return is equal to the booster fan pressure. If the fan is sited inbye of this point, flow recirculation will occur across leakage paths and if sited outbye the fan will only serve to increase leakage.

Underground booster fans can be purpose built single fan units or be modular in design, a number of fans being assembled together in a series and/or parallel cluster arrangement to produce the required duty. Booster fans have become a necessary part of the ventilation systems of present day U.K. coal mines and when properly designed, installed and maintained form an effective part of the ventilation control strategy.

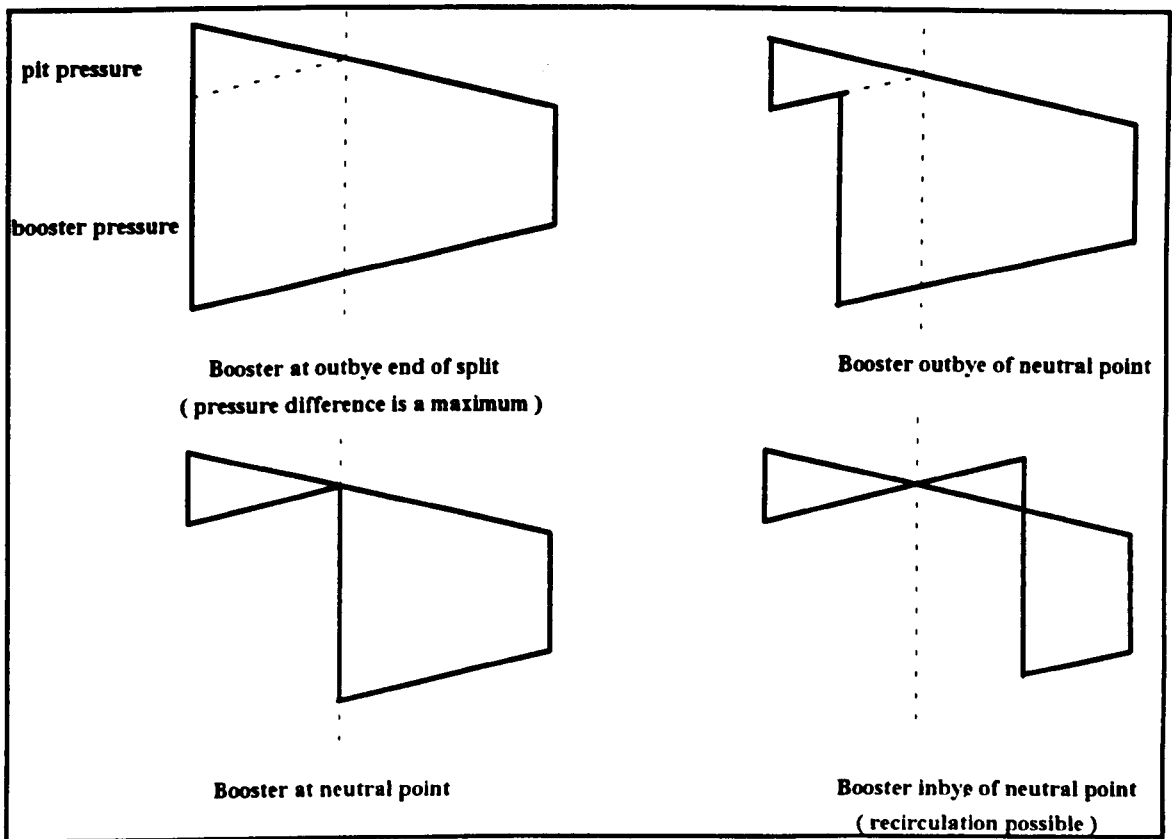


Figure 6. 1. The effect of booster fan location on ventilating pressure (after [58]).

6.4 Mine Ventilation Calculations

6.4.1 Assumptions

Bernoulli's equation, discussed in chapter 3, was developed assuming constant density in the fluid i.e. incompressible flow. Fluid density is affected by a combination of temperature and pressure. If the ranges of temperature and pressure caused by variations in elevation, heat transfer or moisture content produce changes in air density in excess of 5% then the application of Bernoulli's equation will produce consistent errors. Velocities in excess of 100 m/s or elevation changes of 500 m will produce errors of this order. In this case appeal must be made to the more thermodynamically based steady flow energy equation

6.4.1.1 Natural Ventilation

Natural ventilation will occur whenever heat is added to an airstream. Considering the steady flow energy equation around a complete mine cycle then ;

$$\sum w = \oint \frac{dp}{\rho} + \sum f = -\sum q$$

where $\sum w$ is the mechanical energy input into the system and $\sum q$ the net heat transfer.

$\oint \frac{dp}{\rho}$ is the natural ventilating energy (NVE) which will assist the fans providing the mechanical energy to overcome the resistance terms $\sum f$. The more commonly used natural ventilating pressure (NVP) can be written as ;

$$NVP = NVE \cdot \rho$$

An alternative, approximate, method of writing the natural ventilating pressure is by considering the mean densities of upcast and downcast shafts. The difference in 'weights' of these two components of the mine circuit will promote airflow. The NVP can be written as ;

$$NVP = g(z_1 - z_2)(\rho_d - \rho_u)$$

where $(z_1 - z_2)$ is the depth of the two shafts, ρ_d the mean density in the downcast shaft and ρ_u the mean density of the upcast shaft.

For the purposes of mine ventilation calculations and network analysis the flow is considered incompressible and therefore adiabatic with no heat transfer between the airstream and the surroundings. The effects of natural ventilating pressure have therefore also been ignored and specific conditions, such as those experienced in shafts, must be considered on their own merit.

McPherson [59] stated the Reynolds number can be approximated by ;

$$Re = 261000 * (Q/P)$$

where Q is the volume flow rate and P the perimeter of the airway. Flow is therefore considered fully turbulent with most mine airways having a Reynolds number in excess of 5000

6.4.2 Atkinson's Equation

The quantity of air flowing in an airway of a mine ventilation network will be determined by the resistance, both frictional and added in the form of regulators, of that airway. This airflow resistance will induce pressure energy losses which must be overcome for the air to flow.

John J. Atkinson's classic paper of 1854 [60] could be said to have laid the foundations for the study into mine ventilation analysis. He was to postulate a law of the form ;

$$\Delta p = RQ^2 \quad (6.1)$$

R is the resistance factor (in Ns^2m^{-8}) and will indicate the pressure loss, Δp Pascals, along a mine airway with a quantity, $Q \text{ m}^3/\text{s}$, of air flowing. Conversely Δp can be considered as the pressure which must be supplied to the airway for a quantity Q to flow. This law is empirically based and is valid for turbulent flows with a Reynolds number $\gg 5000$.

As stated in chapter 3, D'Arcy's law for predicting the friction losses in a circular conduit can be written as ;

$$\Delta p = \frac{4fL\rho v^2}{2d} \quad (6.2)$$

where f is the dimensionless friction factor, L the length and D the diameter of the circular conduit in metres, ρ the density in kg/m^3 and v the velocity in m/s of the fluid flowing in the conduit

Friction losses are principally determined by the amount of fluid in contact with the conduit walls and this equation can be readily applied to conduits and airways of any shape if the concept of hydraulic radius is considered. The hydraulic radius, R_h , is the ratio of the cross sectional area, A of a conduit to the perimeter, P . Therefore for a circular conduit ;

$$R_h = \frac{A}{P} = \frac{\pi r^2}{2\pi r} = \frac{r}{2} = \frac{d}{4},$$

and D'Arcy's equation can be written as ;

$$\Delta p = \frac{fPL\rho v^2}{2A} \quad (6.3)$$

The velocity of the flow can be written as Q/A and equation (6.3) can be re-stated as ;

$$\Delta p = \frac{kPLQ^2}{A^3} = RQ^2 \quad (6.4)$$

where $k = \frac{\rho f}{2}$. Equation (6.4) is known as *Atkinson's formula* and K is the Atkinson friction factor which unlike f is dependent on density and has the dimension density.

6.4.3 Shape Factors

Equation 6.4 reveals that R is proportional to $\frac{P}{A^3}$. However for any given type of cross-section $\frac{P}{\sqrt{A}}$ is constant and this is commonly termed the *shape factor*. The ideal shape of a mine airway (i.e. the shape with the maximum ratio of area to perimeter) is a circle. The shape factor of other cross sectional areas is often quoted relative to the circular shape factor and this is known as the *relative shape factor*. If all other parameters remain constant, the resistance of a mine ventilation airway varies with respect to its shape factor.

| Mine Airway | k (kg/m ³) |
|---|-------------------------|
| <u>Shafts</u> | |
| Smooth, concrete-lined, unobstructed | 0.0030 |
| Brick-lined, unobstructed | 0.0037 |
| Smooth, concrete-lined, with rope guides and pipe ranges on buntons | 0.0065 |
| Brick-lined, with rope guides and pipe ranges on buntons | 0.0074 |
| Tubbing lined with no guides or cages | 0.0139 |
| Timber-lined, no middle buntons | 0.0167 |
| Brick-lined, two lines of side buntons, without tie girders | 0.0176 |
| Brick-lined, two lines of side buntons, one tie girder to each buntion | 0.0223 |
| Timber-lined with middle buntions | 0.0223 |
| <u>Steel arched roadways</u> | |
| Smooth, concrete all round | 0.0037 |
| Concrete slabs or timber lagging between flanges all round | 0.0074 |
| Concrete slabs or timber lagging between flanges to spring | 0.0093 |
| Lagged behind arches, good condition | 0.0121 |
| Rough conditions with irregular roof, sides and floor | 0.0158 |
| <u>Rectangular roadways</u> | |
| Smooth, concrete lined | 0.0037 |
| Girders on brick or concrete walls | 0.0093 |
| Unlined airways with uniform sides | 0.0121 |
| Unlined airways, irregular conditions | 0.0158 |
| Girders or bars on timber props | 0.0186 |

Table 6.1. The coefficients of friction, k, of typical mine airways
(after McPherson [61])

| Shape of roadway or shaft | Shape Factor | Relative Shape Factor |
|--------------------------------|--------------|-----------------------|
| Circular | 3.5449 | 1.00 |
| Arched, straight legs | 3.8285 | 1.08 |
| Arched, splayed legs | 3.8639 | 1.09 |
| Square | 4.0 | 1.13 |
| Rectangular (width : height) | | |
| 1.5 : 1 | 4.0825 | 1.15 |
| 2 : 1 | 4.2426 | 1.20 |
| 3 : 1 | 4.6188 | 1.30 |
| 4 : 1 | 5.0000 | 1.41 |

Table 6.2. Relative shape factors.

6.4.4 Airways in Series and Parallel.

Mine ventilation calculations can be vastly simplified by combining the resistances of airways operating in series or parallel. This has already been discussed in section 3.5 and the results for the 'effective' resistance of airway combinations are identical.

For n airways in series ;

$$R = R_1 + R_2 + \dots R_n \quad (6.5)$$

and for n airways in parallel ;

$$\frac{1}{\sqrt{R}} = \frac{1}{\sqrt{R_1}} + \frac{1}{\sqrt{R_2}} + \dots \frac{1}{\sqrt{R_n}} \quad (6.6)$$

By selective paralleling and serialising of branches some mine ventilation circuits can be reduced to a single equivalent resistance and the straightforward application of Atkinson's equation will reveal the total airflow entering the mine for a given pressure input from the fans.

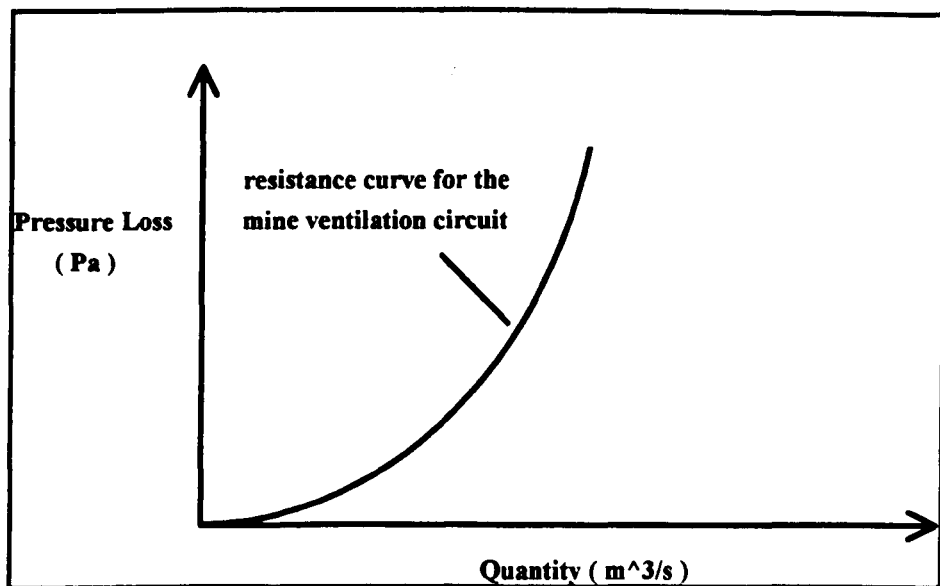


Figure 6.2. Resistance curve of the complete mine ventilation circuit.

6.4.5 Fans and Fan Selection

Fans will provide energy to an airflow in which they are placed. This energy will manifest itself in the form of a pressure rise across the fan. The greater the flow of air the less energy per unit volume the fan can impart on the flow and the less will be the pressure rise. The theoretical pressure/volume relationship for a fan will be of the form $PQ = \text{constant}$. However the airflow is subject to frictional and shock losses through the fan and the pressure volume relationship is as shown in Figure 6.3.

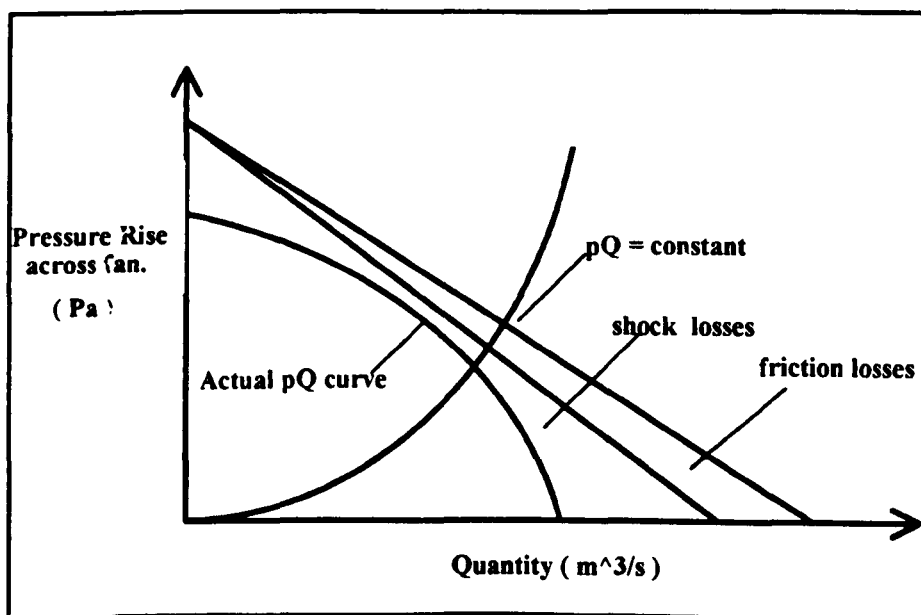


Figure 6.3. A typical p-Q fan characteristic.

Figures 6.2 and 6.3 can now be superimposed on each other to find the quantity of air, and at what pressure, that will be supplied to the mine

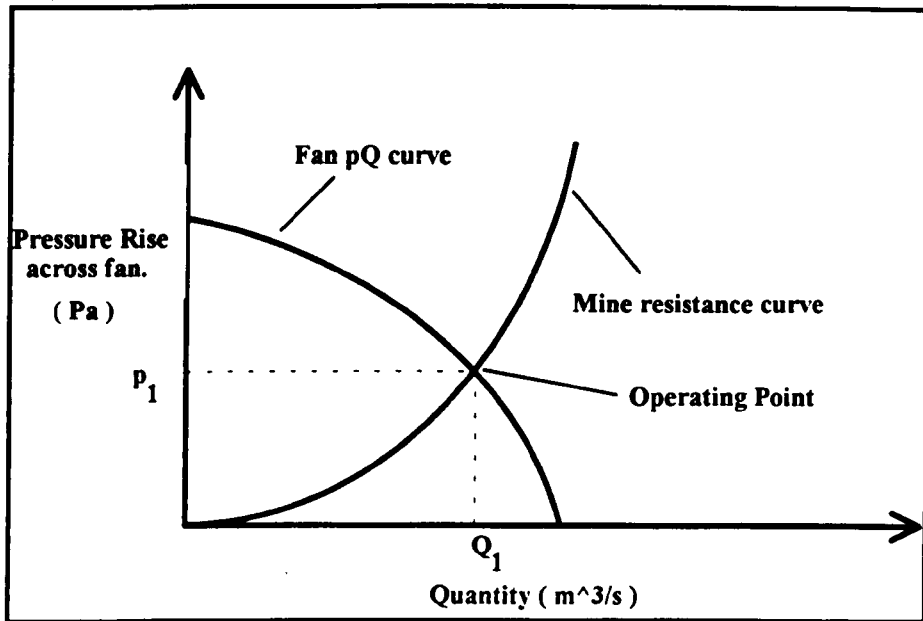


Figure 6.4. Intersection of fan characteristic and mine resistance curve to find the operating point.

Mining is a dynamic process and the system resistance will be constantly changing. A fan must be chosen which will supply the required quantity of air at near peak efficiency over the specified resistance range. The shape of the fan curve will vary according to the type of fan selected. A fan will need to be selected whose quantities will not vary substantially with the small system resistance changes that could ensue from the dynamic nature of the mining process. i.e. the slope of the fan characteristic should be quite steep at or near the operating point.

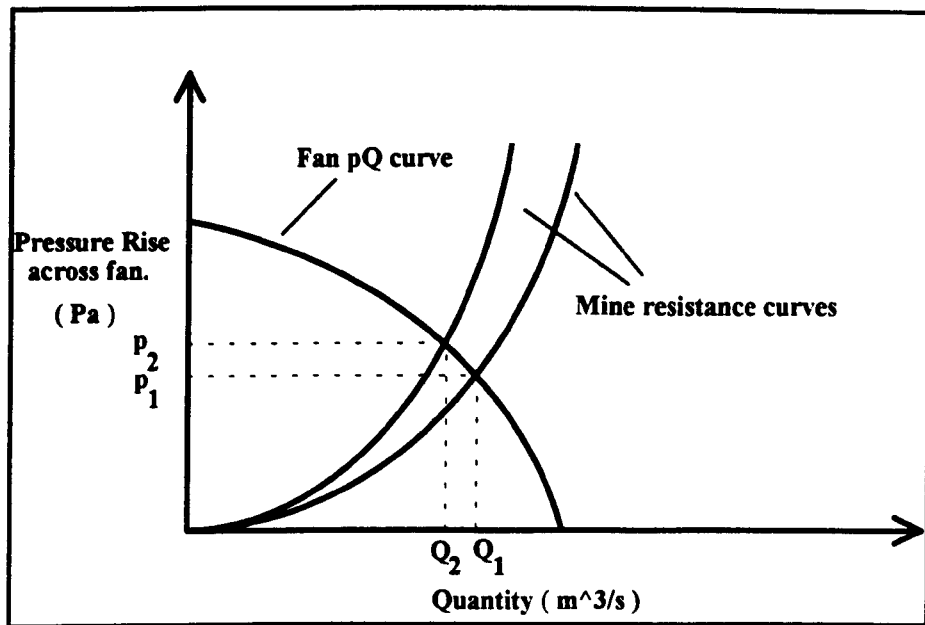


Figure 6.5. Changing fan operating points with varying mine resistance.

6.4.6 Fans in Parallel and Series

As discussed earlier the required pressure and quantity need not be supplied by a single fan. Booster fans can be installed in underground airways to provide extra pressure energy and a better airflow distribution for particular areas of a mine. Fan installations can be constructed from a number of fans in series and parallel thus allowing flexibility in their operation.

An improved quantity of air can be provided by a fan in parallel. A fan in series will maintain the same airflow with an increase in the pressure delivered. New characteristic curves are generated by simply adding the pressures at a given quantity for fans in series or adding the quantities at a given pressure for fans in parallel.

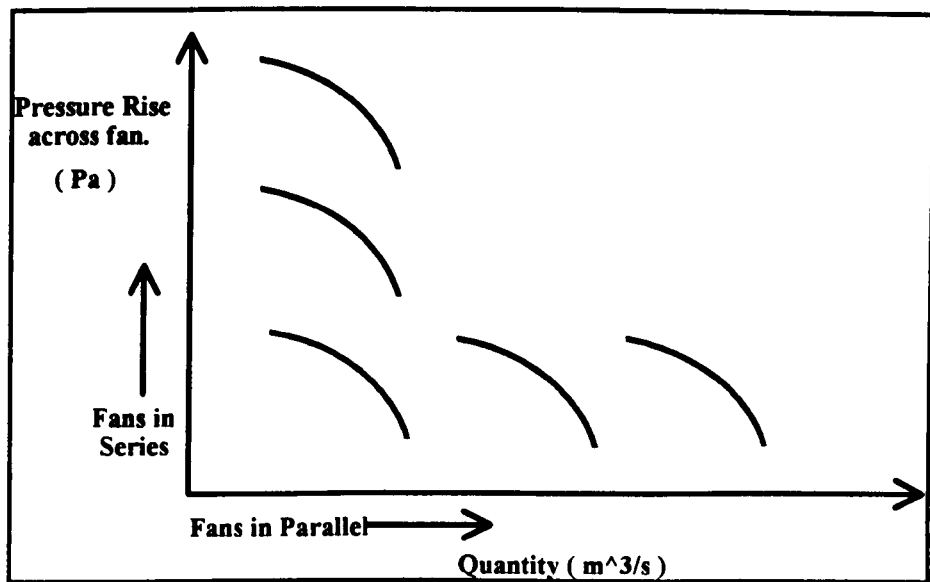


Figure 6.6. Combinations of fans in series and parallel.

6.5 Summary and Conclusions

This chapter has discussed the assumptions, particularly incompressible and turbulent flow, used in mine airway calculations. Atkinson's equation has been introduced describing the turbulent flow pressure loss in a single mine airway. This was then used to combine airways and develop a statement describing the airflow-pressure loss characteristic or system characteristic for a complete mine ventilation circuit. Operating points of fans can then be found by examination of the intersection of fan and system characteristics.

Some networks however cannot be simplified into a single effective resistance and graphical techniques for finding airflows and pressures do not exist. One has to resort to numerical solution techniques.

A number of commercial programs using these techniques are currently available. VENTFLO W developed by the Chamber Of Mines Research Organisation (COMRO) in South Africa takes density changes into account and is widely applicable to the deep, hot workings experienced in that country. VNETPC developed by Mine Ventilation Services Inc. (MVS) in the U.S.A. and VENT, the British Coal program both use an incompressible approach with air being injected should any deviation from this assumption take place.

The theory behind the network analysis of mine ventilation is discussed in the next chapter. The different methods that have been developed and the reason for their adoption is also discussed.

The Mathematical Analysis and Optimisation of Mine Ventilation Networks

7.1 Introduction

A typical mine ventilation network (MVN) can consist of several hundred interconnected roadways, shafts and working areas. These form the principal components of the mine ventilation system, together with the surface and underground fans and regulating doors. The equations governing flow along a mine airway can now be extended to a complete MVN. These equations will then describe the complete airflow and pressure distribution in the mine. The solution to the equations will involve representing the ventilation network topographically with the interconnecting roadways and shafts being described by branches and the positions where the roadways meet by junctions. With each branch there will be an associated frictional resistance to airflow. The object of any analysis is to determine the steady state airflows, pressure distribution around the network, energy or power losses in branches and the operating points for the chosen positions of fans and regulating doors. In this study flow is assumed to be unidimensional and incompressible thus simplifying any analysis schemes used.

The optimisation strategy developed in the previous chapter needs to be mathematically formulated. The objective of this construction becomes the selection of the duty and position of fans and regulators within the network to minimise the total air power consumption whilst maintaining pre-assigned airflows at working areas. Past research work in this area is critically reviewed and the subsequent adoption of a particular method is discussed. The development and application of a computer simulation model based on this method is presented.

By selective paralleling and serialising of branches some networks can be reduced to a single compound resistance and the straightforward application of Atkinson's law will give the required results. However more complex networks cannot be simplified in this manner and one has to resort to numerical solution techniques. These techniques will vary depending on the airflow constraints placed upon the network.

If no airflow constraints are placed on any branches then the airflow will distribute itself according to the resistance characteristics of the airway, i.e. it will be allowed to split naturally. However if there exists specifically required airflows on some of the

branches then booster fans and regulators may be necessary to control the splitting of the airflow. If all airflows in the network are specified the problem is termed 'pure controlled' otherwise it is termed 'generalised controlled'.

Along with Atkinson's equation, Kirchhoff's Laws of mass and energy conservation are used to describe flow in a mine ventilation network. Appeal is made to the mathematical subject of *graph theory* to construct the system of equations governing the flow and pressure distribution.

7.2 Kirchhoff's Laws

7.2.1 Kirchhoff's First Law

Kirchhoff's first law states that , for each of the j junctions in the network, the algebraic sum of mass flow must equal zero ;

$$\sum_{i=1}^n m_i = 0 \quad (7.1)$$

where m_i is the mass flow in branch i and n the number of branches incident at the current junction. As the flow is being considered incompressible then equation (7.1) can be written in terms of the volume flow rate, Q , in each branch ;

$$\sum_{i=1}^n Q_i = 0 \quad (7.2)$$

7.2.2 Kirchhoff's Second Law

Kirchhoff's second law states that the algebraic sum of the pressure drops for all the branches around any closed mesh in the network must equal zero ;

$$\sum_{i=1}^m \Delta p_i = 0 \quad (7.3)$$

where Δp_i is the pressure drop along a branch i and m the number of branches in the loop. Using Atkinson's equation to describe the frictional resistance losses along a branch then we can write;

$$\Delta p_i = r_i Q_i^2 - h_i(Q_i) + \rho g \Delta z_i \quad (7.4)$$

where,

r is the frictional resistance losses along the branch,

Q is the flow in the branch,

h is the pressure - flow characteristic of a fan positioned in the branch.

ρ is the density of the air.

g is the acceleration due to gravity

Δz is the increase in elevation from one end of the branch to the other

Around a closed circuit $\sum_{i=1}^n \Delta z_i = 0$, therefore we can write ;

$$\sum_{i=1}^n r_i Q_i^2 - h_i(Q_i) = 0 \quad (7.5)$$

7.3 Application of Graph Theory

Kirchhoff's two laws (equations 7.2 and 7.5) can now be used to formulate a system of equations for the flow rates in each of the branches of the MVN.

Kirchhoff's first law provides linear equations for the flow rates in branches. If there are j junctions in the ventilation network then j equations can be formulated. However only $j-1$ will be linearly independent i.e. the final equation will just be a linear combination of the previous equations. Therefore if there are b airways in the network $b-j+1$ equations are still required from Kirchhoff's second law in order for there to be enough equations to solve for the flow in each branch of the network.

7.3.1 The Junction-Branch Incidence Matrix

Each branch in the MVN will have a direction associated with it, determined by the direction of airflow along the branch. The Junction-Branch Incidence Matrix, A , is a matrix of order j by b such that if $A = [a_{st}]$, then ;

$a_{st} = 1$ if branch t is incident at junction s and directed away from it.

$a_{st} = -1$ if branch t is incident at junction s and directed towards it.

$a_{st} = 0$ if branch t is not incident at junction s

Each column of this incidence matrix represents a branch and thus contains exactly two non-zero elements 1 and -1, confirming that not all rows of A are linearly independent.

Kirchhoff's first law (7.2) can now be stated more rigorously as ;

$$\sum_{s=1}^{j-1} \sum_{t=1}^b a_{st} Q_t = 0 \quad (7.6)$$

7.3.2 The Spanning Tree

A *spanning tree*, simply referred to as the *tree*, of a network is a connected subnetwork of branches which contains all the junctions in the network but no meshes. A mesh is a closed sequence of branches in which all the junctions j_1, j_2, \dots, j_{n-1} are distinct but with $j_1 = j_n$. If there are j junctions then there will be $j-1$ branches in the tree. Any of the remaining branches when added to the branches of the tree will complete a mesh. These branches belong to the *cotree* and are called *chords* of the network. A chord will belong to only one fundamental mesh. Therefore the number of chords, c , and hence the number of meshes generated from the spanning tree will be equal to $b - j + 1$.

This, as shown above, is the number of equations required from Kirchhoff's second law to formulate a set of equations to solve for the flows in each branch.

Spanning Tree Algorithm

The algorithm used for the calculation of the spanning tree has been described by Minieka [52] and was chosen, primarily, for its simplicity to program. The algorithm examines the branches of the network in any arbitrary sequence and decides whether a branch shall be included in the spanning tree. It examines each branch only once and therefore has a finite number of steps to completion. This is termed a *greedy* algorithm.

The spanning tree constructed obviously depends on the order in which the branches are examined. If a list of branches are examined sequentially a consequence of the algorithm is that the majority of the chords will be found from branches last in the list. Once the spanning tree has been found the problem reduces to one of finding the fundamental meshes of the network and formally stating Kirchhoff's second law.

A simple mine ventilation network is shown in Figure 7.1a. Three alternative spanning trees are shown by the solid lines in Figures 7.1b, 7.1c, 7.1d. The chords are the remaining branches shown by dotted lines.

- Step 1:** Select any branch. Place this branch in the spanning tree and place both its endpoints into an empty bucket.
- Step 2:** Select any branch not yet considered (If all branches have been considered then no spanning tree exists). One of four different situations must occur.
- Both endpoints are in the same bucket.
 - One endpoint is in a bucket, the other endpoint is not in any bucket.
 - Neither endpoint is in any bucket.
 - Each endpoint is in a different bucket.
- If item a) occurs mark the branch as a chord and return to step 2.
- If item b) occurs mark the branch in the spanning tree and place the unbucketed endpoint in the same bucket.
- If item c) occurs mark the branch in the spanning tree and place both endpoints in an empty bucket.
- If item d) occurs mark the branch in the spanning tree and combine the contents of both buckets leaving the other bucket empty.
- Step 3:** If all endpoints are in one bucket, the spanning tree has been found. Otherwise return to step 2.

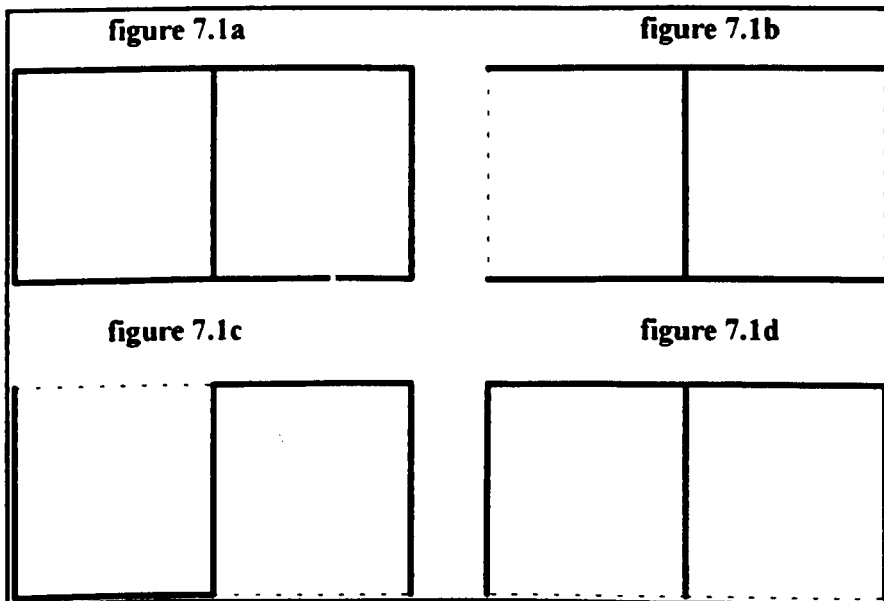


Figure 7.1. A simple mine ventilation network with alternative spanning trees.

7.3.3 The Mesh-Branch Incidence Matrix

The mesh-branch incidence matrix, **B**, of a directed network is a matrix of order (total number of meshes) by n such that if $\mathbf{B} = [b_{st}]$ then ;

$b_{st} = 1$ if branch t is contained in mesh s and their directions coincide.

$b_{st} = -1$ if branch t is contained in mesh s and their directions do not coincide.

$b_{st} = 0$ if branch t is not in mesh s .

The mesh-branch incidence matrix contains many duplicated meshes. The number of meshes required to describe the network however is given by $c = b - j + 1$. This, as shown above, is also the number of chords in the network and hence the number of meshes generated from the spanning tree. The fundamental mesh-branch incidence matrix, **B**, is therefore a matrix of order c by b .

Kirchhoff's second law (7.5) can now be stated more rigorously as ;

$$\sum_{s=1}^c \sum_{t=1}^b b_{st} \{ r_t Q_t^2 - h_t(Q_t) \} = 0 \quad (7.7)$$

The construction of **A** is straightforward and the construction of **B** is also straightforward if the branches are ordered such that the chords of the network are last in the list of branches. With only $j-1$ equations derived from Kirchhoff's first law being linearly independent a reduced junction-branch incidence matrix, **A_{red}**, can be formed by simply deleting an arbitrary row from the complete incidence matrix.

With **A_{red}** and **B** ordered in the same branch order and . s each chord will appear in only one fundamental mesh, then mesh-branch and junction-branch incidence matrices can be partitioned to give ;

$$\mathbf{B} = [\mathbf{B}_1 : \mathbf{I}] \quad (7.8a)$$

$$\mathbf{A}_{red} = [\mathbf{A}_1 : \mathbf{A}_2] \quad (7.8b)$$

where $[I]$ is the unit matrix of order c , B_1 is of order c by $(b - c) = (j - 1)$, A_1 is of order $(j - 1)$ by $(j - 1)$ and A_2 is of order $(j - 1)$ by c .

The junction-branch and the transpose of the mesh-branch incidence matrices are orthogonal (Christofides [63]). Therefore we can write ;

$$A_{red} B^t = 0 \quad (7.9)$$

i.e.

$$[A_1 : A_2] [B_1 : I]^t = 0$$

$$A_1 B_1^t + A_2 = 0$$

$$B_1 = -A_2^t [A_1^{-1}]^t \quad (7.10)$$

A_1 is a square matrix and so the calculation of its inverse is possible and hence the mesh-branch incidence matrix can be found from the junction-branch incidence matrix if the chords of the network are ordered last in the list. Once the two incidence matrices have been found a system of equations can be formulated from Kirchhoff's two laws (7.6) and (7.7) to find the flow rate in each branch of the network.

One problem still remains however. Equation (7.7) contains non-linear terms in Q^2 and methods have had to be derived to effectively linearise these terms and permit solutions to the equations.

7.4 Solutions to the Network Equations

The penalty in removing the non-linearity from the mesh equations is having to resort to an iterative method of solution. Iterative techniques involve making an initial estimate of the branch flows and then calculating a new, improved, flow. This continues until a satisfactory degree of accuracy has been achieved and the solution is said to have converged.

A number of methods have evolved since the first systematic attempt at analysing flow distribution networks by Hardy Cross in 1936 [64]. The applicability of each of the methods depends on the criteria laid down governing their selection. The Hardy Cross method, for instance, is widely applicable for hand calculations and calculates the flow

corrections to be made for each mesh in the network during the iterative procedure. Alternative methods may be able to calculate the junction pressures or flow rate in each branch directly in the iterative calculation.

Mathematical correctness, guaranteed and speed of convergence, or the ease of programming may all be considered important and all would be considered when selecting the appropriate solution method for the mine ventilation network. The network topology and size will also affect the performance of each of the methods evolved. Kim [65] discussed performance of a variety of methods against ;

- (i) The interconnection of airways.
- (ii) The distribution of resistances.
- (iii) The size of the network.
- (iv) The density of the network - (the number of nodes compared to the number of branches).

The proceeding discussion will explain in detail several methods that have evolved and discuss the advantages and disadvantages of each of the methods in the solution to mine ventilation network problems.

7.4.1 The Relationship Between Mesh and Branch Flows

Each chord of the network will be in one, and only one, fundamental mesh. The flow through this chord will therefore be the same as the flow around the fundamental mesh in which it is contained. The flow in the non-chord branches i.e. the branches contained within the spanning tree can therefore be calculated as the sum of the flows around all the meshes in which that branch is contained.

If (q_1, q_2, \dots, q_c) are the flows around each of the c meshes in the network then ;

$$Q = B^t q \quad (7.11)$$

where Q is the vector of branch flows, q the vector of mesh flows and B the mesh-branch incidence matrix. Partitioning B as previously then ;

$$[Q_1 : Q_2] = [B_1 : I]^t q$$

i.e.

$$Q_2 = q$$

and

$$Q_1 = B_1^t q = B_1^t Q_2 \quad (7.12)$$

where Q_2 is the vector of chord flows and
 Q_1 is the vector of non-chord or tree branch flows.

Using equation (7.10), then equation (7.12) can be restated as ;

$$Q_1 = -A_1^{-1} A_2 Q_2$$

$$A_1 Q_1 + A_2 Q_2 = 0$$

or

$$[A_1 : A_2] [Q_1 : Q_2] = 0$$

i.e. equation (7.12) is just another statement of Kirchhoff's First Law of flow conservation at each junction in the MVN.

7.4.2 The Hardy Cross Method

The Hardy Cross method considers the mesh flows as unknown parameters and sequentially finds a correction for each of these flows throughout the network after an initial estimate has been made. Branch flows are subsequently found using equation (7.12).

If an initial estimate, Q , is made for the flows in each branch then the actual flow, Q_a , can be written as ;

$$Q_a = Q + \delta Q$$

From equation (7.4) the pressure loss along an airway can be written as ;

$$\Delta p = r(Q + \delta Q)^2 - h(Q + \delta Q) + \rho g \Delta z$$

Expanding these terms and neglecting terms of order δQ^2 (effectively linearising the equation) gives ;

$$\Delta p = rQ^2 + 2rQ \delta q - h(Q) - \delta q \frac{dh}{dQ}(Q) + \rho g \Delta z. \quad (7.13)$$

or ;

$$\delta q = \frac{\{\Delta p - rQ^2 + h(Q) - \rho g \Delta z\}}{\{2rQ - \frac{dh}{dQ}(Q)\}} \quad (7.14)$$

Doing this for each branch in the mesh and noting that the pressure drop around a closed mesh is zero then a mesh flow correction factor can be found as ;

$$\delta q_m = \frac{-\{\sum_{i=1}^n r_i(Q^2)_i - h(Q)_i\}}{\{\sum_{i=1}^n 2r_i(Q)_i - \frac{dh}{dQ}(Q)_i\}} \quad (7.15)$$

Once each mesh correction has been found, the new branch flows can be determined and the iterative procedure repeated again.

The Hardy Cross method is particularly suitable for hand calculations but can also be incorporated quite easily into a computer program. Tominaga [66] and Jeppson [67] noted that the convergence can be accelerated by adjusting each of the flow rates of all the airways in the current mesh immediately the mesh correction has been calculated. Kim et al [65] pointed out that the speed of convergence is directly affected by mesh selection and mesh ordering. Scott and Hinsley [68] alluded to this when stating that high resistance branches should form the chords of the network and not branches common to meshes. Wang and Li [69] confirmed this when stating (in more graph theoretic terms) that constructing a minimal spanning tree, i.e. the spanning tree with lowest resistance branches, is known to improve convergence. Wang and Saperstein [70] also suggested that fixed quantity branches and those containing fans should be included as chords.

Convergence is also affected, and proved difficult in some cases, when large networks are being considered [71]. The method also suffers with initial estimates of the branch flows having to satisfy continuity and inaccurate estimates slowing convergence [72] [73].

7.4.3 The Newton-Raphson Method

The advent of the computer era, allowing solutions to large systems of simultaneous equations, has spawned a number of alternative methods. One such method is the Newton-Raphson method [74] [75] [69]. Wang and Li [69] commented that the second order convergence and simultaneous correction for all mesh flows give it great potential for the solution of MVN's. Not only mesh flows, but branch flows or junction pressures can be considered unknown. When mesh flows are considered, one sees that the Hardy Cross method is just a mathematical variation of the Newton-Raphson Method. Again initial estimates are required to satisfy continuity and the accuracy of this estimate will affect the speed of convergence. [72].

Recalling that for a single function, $f(Q)$, an approximation to one root of the equation $f(Q) = 0$ is given by ;

$$Q_{n+1} = Q_n - \frac{f(Q_n)}{f'(Q_n)} \quad (7.16)$$

where Q_n is the original estimate of the root,
 Q_{n+1} the new estimate of the root,
 n the iteration number,

and $f'(Q_n) = \frac{df(Q_n)}{dQ}$, the function derivative.

This equation can be applied to a series of functions to give ;

$$Q_{n+1} = Q_n - D^{-1} F(Q_n)$$

or

$$D Q_{n+1} = D Q_n - F \quad (7.17)$$

where **D** is the Jacobian matrix of derivative elements ;

$$\frac{\partial F_i}{\partial (Q_n)_i} \quad (7.18)$$

The functions, **F**, are generated from Kirchhoff's first and second laws. The system of equations (7.17) can be solved using standard techniques such as Gauss Siedel iteration or Cholesky decomposition. These algorithms have proved to be efficient when considering sparse matrices as is the case with MVN's [76] [71]. The Newton Raphson method will always converge, and rapidly, but requires a significant amount of time in the generation of the system matrix, **D** [75] [77].

With large networks, although the number of iterations to solution may not increase substantially, the time required to generate **D** and **F** will certainly increase. The consideration of branch flows directly, rather than mesh flows, will increase the number of equations still further and increase the time of the matrix generation.

7.4.4 The Linear Theory Method

A new method was proposed, called the *Linear Theory Method* (**LTM**), arising out of the study of hydraulic distribution networks by civil engineering practitioners [73] [78] and applied to mine ventilation networks by Bhamidipati and Procarione [79].

The non-linear terms in the mesh equations are effectively linearised without having to resort to Taylor Series expansions of the functions. These terms rQ^2 are written as KQ_{n+1} where ;

$$K = r | Q_n | \quad (7.19)$$

where *n* is the iteration number.

Using Kirchhoff's First and Second Laws a system of linear equations can now be generated to solve for the branch flows.

$$K Q_{n+1} = 0 \quad (7.20)$$

where **K** is the system matrix generated from the junction-branch incidence matrix, mesh-branch incidence matrix and the coefficients from equation (7.19). In

comparison with the Newton-Raphson method (equation (7.17)) it can be seen that there is no right hand side of the system of equations to be generated and that the only difference between **D** and **K** is the factor of 2 in the terms generated from the mesh equations.

i.e. if $f = rQ^2$ then $\frac{\partial f}{\partial Q} = 2rQ$ whereas equation (7.19) gives $k = r|Q|$.

This method can adequately deal with large systems of equations and has the advantage that the first approximation to the solution does not need to satisfy continuity conditions and the initial values may be arbitrary.

Wood and Charles [73] observed an oscillatory nature in successive estimates close to the converged solution and suggested the next trial solution to be the average of the previous two solutions.

$$Q_n = \frac{Q_{n-1} + Q_{n-2}}{2} \quad (7.21)$$

Bhamidipati and Procarione [79] suggested ;

$$Q_n = \sqrt{Q_{n-1} Q_{n-2}} \quad (7.22)$$

works just as satisfactorily in removing the oscillatory nature of successive solutions.

Other methods have been derived for the solution of MVN's such as second order approximations [77] and non-linear programming techniques [80] [81] but it was considered they offered no more simplification or accuracy to the method of solution of MVN's than those discussed above. In the computer model subsequently developed to calculate the pressure and flow distribution in MVN's it was decided to use the Linear Theory Method ahead of the Hardy Cross or Newton-Raphson methods for three main reasons ;

- (i) Ease of Programming.
- (ii) No need for reasonable initial estimates satisfying continuity.
- (iii) It was considered the most appropriate method when solving for branch flows.

7.4.5 Fan Characteristics and Fixed Flow Branches

Fan characteristics and fixed flow branches can be easily incorporated into a system of equations using the linear theory method. Fan characteristics are frequently assumed to be of the form ;

$$p = aQ^2 + bQ + c \quad (7.23)$$

where p is the pressure rise across the fan,

Q is the flow rate and,

a, b, c are constants describing the pressure-flow characteristic.

These constants may be determined by the application of a suitable numerical curve fitting routine applied to pressure/flow characteristic points of a given fan.

Equation (7.19) describing the linearisation of the mesh terms in the system matrix can be re-written to give ;

$$K = r | Q | - a | Q | - b \quad (7.24)$$

with the term c being written on the right hand side of the equations (7.20).

Fixed flow branches are incorporated by eliminating the appropriate column from the system matrix, K , and moving the fixed flows to the right hand side of the system of equations.

i.e. consider the junction with branches 1 and 2 entering and branch 3 leaving.

Kirchhoff's First Law can be stated as ;

$$Q_1 + Q_2 - Q_3 = 0 \quad (7.25)$$

or in matrix form ;

$$(1, 1, -1) \begin{pmatrix} Q_1 \\ Q_2 \\ Q_3 \end{pmatrix} = 0 \quad (7.26)$$

With a fixed flow of $10 \text{ m}^3/\text{s}$ in branch 2 equation (7.26) becomes

$$(1, 0, -1) \begin{pmatrix} Q_1 \\ Q_2 \\ Q_3 \end{pmatrix} = 10 \quad (7.27)$$

The mesh equations which contain the fixed quantity branch will reveal the pressure change necessary to achieve this desired quantity. i.e. when considering the pressure loss, rQ^2 , r as opposed to Q , will become the branch unknown still leaving a system of b equations in b unknowns to be solved.

i.e. consider a mesh with 4 branches. Kirchhoff's second law can be written as ;

$$r_1 Q_1^2 + r_2 Q_2^2 + r_3 Q_3^2 + r_4 Q_4^2 = 0 \quad (7.28)$$

Linearising this equation using equation (7.19) gives ;

$$(K_1, K_2, K_3, K_4) \begin{pmatrix} (Q_1)_{n+1} \\ (Q_2)_{n+1} \\ (Q_3)_{n+1} \\ (Q_4)_{n+1} \end{pmatrix} = 0 \quad (7.29)$$

With a fixed flow of $10 \text{ m}^3/\text{s}$ in branch 2 equation (7.29) becomes ;

$$(K_1, 100, K_3, K_4) \begin{pmatrix} (Q_1)_{n+1} \\ (r_2)_{n+1} \\ (Q_3)_{n+1} \\ (Q_4)_{n+1} \end{pmatrix} = 0 \quad (7.30)$$

7.5 The Categorisation of the Controlled Flow Problem

The methods so far discussed have been able to calculate the flow distribution in a network given the branch resistances and the positions and characteristics of any fans placed in the network. The branch flows will assign themselves according to the

resistance of individual branches i.e. will be allowed to split naturally. The specification of airflows in selected branches will control the splitting of the air to some degree. This is commonly achieved with the use of underground booster fans and regulating devices (thus changing the resistance characteristics of individual airways). If a large enough number of branches have pre-assigned flows then the airflow around the MVN will be completely controlled by these booster fans and regulating devices and the problem becomes one of finding the positions of these devices to achieve the required pressure drops and hence airflows in each branch of the network. In some cases however some airflows will be assigned and the others will be allowed to split naturally. The problem now includes finding the remaining airflows but still requires the determination of the position and pressure of underground fans and the position and resistance of regulators to achieve the prescribed flows.

The airflow distribution problem can therefore be categorised in one of three ways ;

- (i) Natural Splitting and fixed fan positions.
- (ii) Controlled Flow where all airflows are prescribed.
- (iii) Semi-Controlled Flow where some airflows assign themselves through natural splitting and some are controlled.

7.5.1 Pure Controlled Flow

If the number of branches whose airflow is preassigned is equal to or larger than the number of fundamental meshes in the network then all airflow quantities can be evaluated. With the chords of the network described by the preassigned airflows then by using equation (7.12) all flows in the network will be defined. This, of course, assumes a spanning tree can be formed using the remaining branches. If this is not the case then the flows specified cannot be achieved and the problem will need to be reconfigured.

For the 'pure controlled' flow problem, since the airflow quantities are known, the problem becomes one of finding the position and characteristics of fans and regulators to achieve the required pressure drops such that Kirchhoff's Second Law is satisfied (Kirchhoff's First Law is satisfied when finding the remaining, non-assigned, branch flows).

With the inclusion of regulators Kirchhoff's Second Law (equation (7.5)) can be written as ;

$$\sum_{i=1}^n (r_i + R_i) Q_i^2 - h(Q_i) = 0 \quad (7.28)$$

where R_i is the regulator resistance in branch i

7.5.1.1 Linear Programming Methods

This type of ventilation problem lends itself naturally to formulation as a linear programming model [82]. The linear objective function, to be minimised, is the total air power supplied by the fans. i.e. ;

$$\sum_{j=1}^b Q_j h(Q_j) \quad (7.29)$$

This will be subject to a variety of conditions imposed by the user ;

- (i) Any solution must satisfy Kirchhoff's Second Law.
- (ii) Location restrictions. If a branch does not allow a fan then $h(Q_j) = 0$ and similarly if a regulator is not permitted then $R_i = 0$.
- (iii) Non-negativity constraints. If a fan should not be installed in a branch against the normal direction of flow then $Q_i \cdot h(Q_i) > 0$.

This formulation can be applied to many standard operations research algorithms with the Simplex Method being the most widely used technique [55]. However, treating the problem as a standard linear program is very inefficient and ignores the network structure [83]. An alternative method was proposed using the 'Out-of-Kilter' algorithm [83] [84].

The 'Out-of-Kilter' algorithm is a general and widely used algorithm for dealing with network flows [85]. The algorithm uses the concepts of linear programming duality theory. It can effectively deal complex constraints and is computationally fast.

7.5.1.2 Critical Path Methods

Another method, also computationally fast and used in operations research for network flows, but more easily understood is the *Critical Path Method* [85] [86] [87]. The critical, or longest, path through a network is the path starting at the entrance junction and finishing at the exit junction with the largest pressure drop. This is known as the free-split of the network. The pressure drop along this path is the pressure, for the specified flow distribution, which has to be developed by the surface fan. The pressure drops required in the non free-split branches in order to maintain the required airflows, and hence satisfy Kirchhoff's Second Law, are achieved by the use of suitable regulation.

In calculating the longest path, the cumulative pressure drops, relative to the entry junction are calculated at each junction. An algorithm for this calculation has been given by Price [88].

| | |
|--------|---|
| Step 1 | Initially let all junctions bear the label (0 , 0) |
| Step 2 | Search for a branch (i , j) such that $p(i) + r(i, j) > p(j)$ where $p(i)$ is the cumulative pressure at junction i and $r(i, j)$ is the resistance loss along branch (i , j) |
| Step 3 | Replace the label on junction j with (i , $p(i) + r(i, j)$) Return to step 2 |

i.e. the cumulative pressure drop at each junction is the maximum of the pressure at the upstream end of the branch plus the pressure loss along the branch for all branches incident at the current junction. The algorithm requires that the node numbering is such that flow is directed from i towards j and that $i < j$. A junction numbering algorithm can be found in Fulkerson [89].

Once all cumulative pressures have been found the free-split can be traced back through the junction labelling and the magnitude of the regulation required in each branch is ;

$$p(i) - p(j) - r(i, j) \tag{ 7.30 }$$

As an example consider the network shown in Figure 7.2.

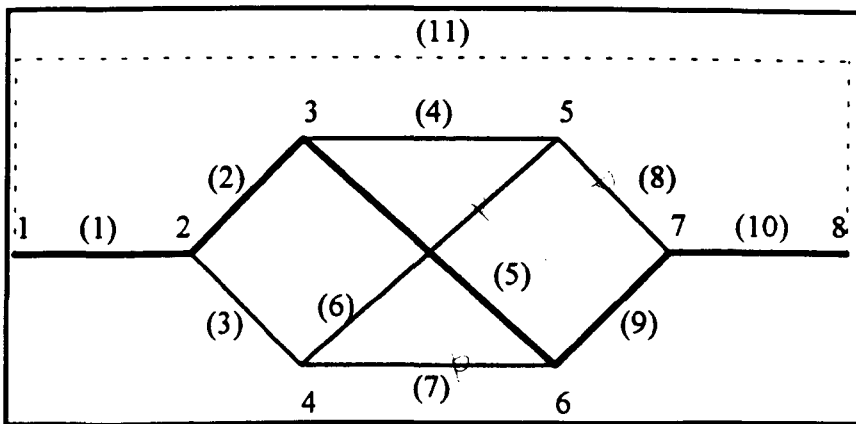


Figure 7.2. A controlled flow test network. [after Wang [86]]

The branch resistance losses are given by,

| Branch No. | Resistance | Flow Rate. (m^3/s) | Pressure loss (Pa) |
|------------|------------|--------------------------------------|----------------------|
| 1 | 0.0516 | 50.0 | 129 |
| 2 | 0.218 | 30.2 | 199 |
| 3 | 0.827 | 17.0 | 239 |
| 4 | 0.541 | 22.7 | 239 |
| 5 | 2.462 | 5.7 | 331 |
| 6 | 1.900 | 13.2 | 80 |
| 7 | 0.610 | 19.8 | 189 |
| 8 | 0.951 | 14.1 | 279 |
| 9 | 0.458 | 27.3 | 341 |
| 10 | 0.060 | 50.0 | 149 |
| 11 | 0.000 | 50.0 | 0 |

Table 7.1. Branch resistances and flows for the controlled flow test network.

The critical path is shown by the bold line. The nodal pressures were calculated as shown in Table 7.2.

The maximum pressure loss through the network is 1149 Pascals. This is the pressure which must be supplied by the fan with $50\text{m}^3/\text{s}$ flowing through it. The regulation required in each branch can now be calculated.

| junction. | branch numbers flowing in | start junction | start pressure | branch loss | nodal pressure | maximum nodal pressure |
|-----------|---------------------------|----------------|----------------|-------------|----------------|------------------------|
| 1 | --- | --- | --- | --- | --- | 0 |
| 2 | 1 | 1 | 0 | 129 | 129 | 129 |
| 3 | 2 | 2 | 129 | 199 | 328 | 328 |
| 4 | 3 | 2 | 129 | 239 | 368 | 368 |
| 5 | 4 | 3 | 328 | 239 | 567 | 567 |
| | 6 | 4 | 368 | 80 | 448 | |
| 6 | 5 | 3 | 328 | 331 | 659 | 659 |
| | 7 | 4 | 368 | 189 | 557 | |
| 7 | 8 | 5 | 567 | 279 | 846 | |
| | 9 | 6 | 659 | 341 | 1000 | 1000 |
| 8 | 10 | 7 | 1000 | 149 | 1149 | 1149 |

Table 7.2. Cumulative pressure losses for the controlled flow test network.

| Branch Number | Pres. loss at first node | Pres. loss at second node | Regulation required(Pa) |
|---------------|--------------------------|---------------------------|-------------------------|
| 1 | 0 | 129 | 0 |
| 2 | 129 | 328 | 0 |
| 3 | 129 | 368 | 0 |
| 4 | 328 | 567 | 0 |
| 5 | 328 | 659 | 0 |
| 6 | 368 | 567 | 119 |
| 7 | 368 | 659 | 102 |
| 8 | 567 | 1000 | 154 |
| 9 | 659 | 1000 | 0 |
| 10 | 1000 | 1149 | 0 |

Table 7.3. Regulation required from the forward pass procedure.

One such solution for the position and magnitude of regulators to provide the specified airflows is illustrated in Table 7.2. An alternative solution can be generated by starting at the exit junction and working towards the entrance junction. This is the backward, as opposed to forward, pass procedure [86] [87].

The critical path method is simple to understand and easy to implement, but cannot in the form discussed so far, deal effectively with booster fans or restrictions on the locations of regulators.

The inclusion of booster fans in a controlled flow network has been considered by Wang [90] using network cut-set operations. An alternative simpler method was proposed by Longson and Hu [91].

Any booster fan included in the network must be positioned in the longest path if it is to reduce the pressure supplied by the main fan. The pressure supplied by the booster fan will be equal to the pressure loss along the original longest path minus the pressure loss along the new longest path excluding the booster fan branch. This is effectively equalising the pressure drops along each path through the network and hence the power supplied by the fans [92] [93].

The inclusion of booster fans in a controlled flow network will, of course, alter the resistance characteristics of the network. The Critical Path Method of Wang would therefore need to be re-used to ascertain the location and amount of regulation in the non-critical path branches.

An alternative solution proposed is a combination of the CPM for the positioning of regulators and the work of Longson and Hu in finding booster fan pressures to equalise pressure drops through the network. This method would be easy to implement and understand and also readily amenable to hand calculations.

As an example consider the network shown in Figure 7.2 once again. The critical path is given by branches (1, 2, 5, 9, 10), the total loss along this path is 1150 Pa and hence the power required by a single fan is 57.5 kW (=1150*50 Watts). Placing a booster fan in branch 5 will result in a new critical path along branches (1, 3, 7, 9, 10) and a total loss along this path of 1049 Pa. The booster fan will therefore supply a pressure of 101 Pa to equalise the losses along the original and new critical paths. The new power consumption by both fans is 53.783 kW (=101*13.2 + 1049*50 Watts). The resistance in branch 5 can now be reduced by $101/(13.2*13.2) \text{ N s}^2\text{m}^{-8}$. The forward pass procedure of the CPM gives regulator values of 119 $\text{N s}^2\text{m}^{-8}$ in branch 6, 1 $\text{N s}^2\text{m}^{-8}$ in branch 7 and 54 $\text{N s}^2\text{m}^{-8}$ in branch 8.

The complete specification of the airflow distribution only occurs in very small number of mine ventilation networks. This greatly limits the application of the powerful yet simple solution algorithms discussed above. In most MVN's the number of branches with preassigned flows is less than the number of fundamental meshes and hence a complete flow specification is not possible. The remainder of the flows must be found along with the optimum location and characteristics of fans and regulators.

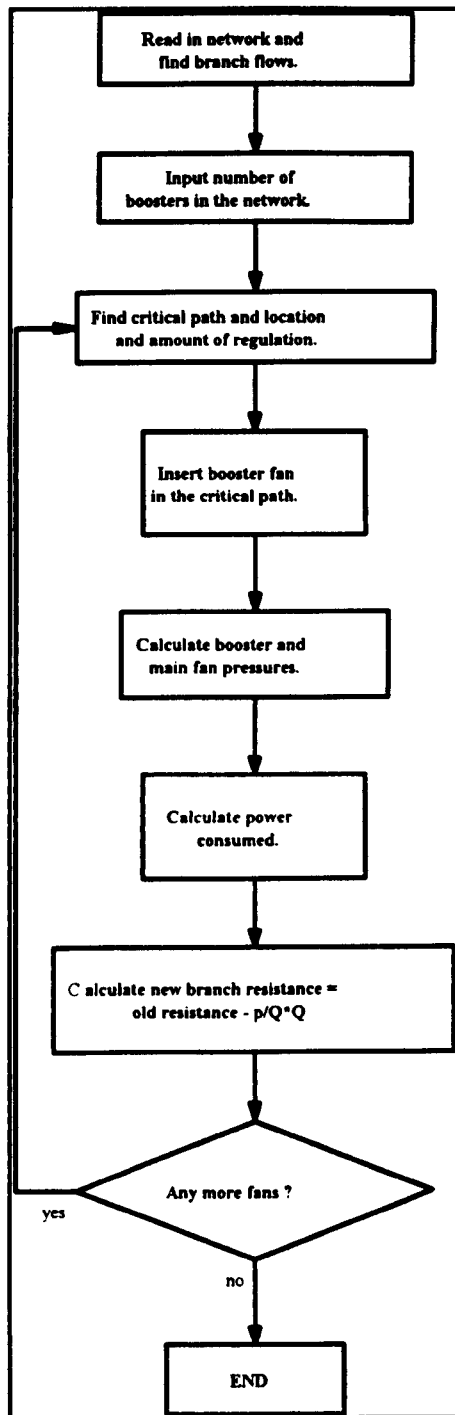


Figure 7.3. Algorithm for the positioning of fans and regulators in a controlled flow network.

7.5.2 Semi Controlled Flow

With the controlled flow problem the positioning of fans and regulators was made to maintain the flow distribution. In the case of the more general mine ventilation network where some airflows are prescribed, the remainder which distribute themselves according to natural splitting are dependent upon the location and characteristics of the fans and regulators and will therefore influence the optimum location.

The problem therefore has now become twofold ;

- (i) To find the optimum location and characteristics of fans and regulators.
- (ii) To evaluate the remaining airflows in the network.

This is known as a 'generalised' or 'semi-controlled' flow network and the current research work identified as its objective the development of a solution to this problem.

The maintenance of pre-designed airflows using regulation alone has also been considered by Wang and Yao [94]. For a single fan system, regulation would conventionally be applied to the low pressure loss sections until losses along all flow paths were the same and equal to the loss along the free-split. A more suitable method would be to regulate the branches which have air entering a free-split branch thus reducing airflow into the free-split and the pressure loss through the system. The optimum form of control is to therefore, once again, equalising the pressure losses along each path but at a pressure lower than the original longest path.

Wu and Topuz [95] and Longson and Hu [96] have considered the use of constrained Non-Linear Programming (NLP) optimisation models for analysis of semi-controlled networks. These methods require fan positions to be fixed, are not user interactive and, as with the case of the NLP methods developed for the natural splitting problem, are mathematically complex and hence not easy to interpret or mathematically program.

An alternative method developed by Calizaya et al [97] [98], which although still requires fan locations to be fixed, is mathematically far simpler and is graphically based which enables the user to analyse the results easily and to maintain control of the solution process.

As stated earlier, in order to maintain a system of b equations in b unknowns the resistance of fixed quantity branches must be allowed to vary. The added resistance, AR , required to maintain the airflow distribution is the difference between the natural resistance, r , and the calculated or effective resistance, ER , of the branch. i.e.

$$AR = ER - r \quad (7.31)$$

The regulation required for each fixed flow branch, will vary with the pressure supplied by fans in the network. There are two forms of regulation which may be employed namely 'active' regulation or 'passive' regulation. Active regulation is the addition of a pressure source such as a booster fan and would be indicated by the analysis as a negative added resistance. Passive regulation is the addition of a regulating device such as doors and would be indicated by the analysis as a positive added resistance.

These relationships, for fan pressures which do not induce airflow recirculation through leakage paths can be written as ;

$$P_m = b \cdot AR + c \quad (7.32)$$

for a single fan system, or ;

$$P_m = a P_b + b \cdot AR + c \quad (7.33)$$

for a two fan system,

where P_m is the main fan pressure,

P_b the booster fan pressure,

a the rate of change of main with booster fan pressure,

b the rate of change of main fan pressure with added resistance,

c the intercept.

The constants a , b , and c are found by performing a linear regression analysis on sets of results obtained from executing the solution program with varying fan pressures. This must be done at least a number of times equal to the number of fixed flow faces in the network. However the greater the number of solutions the more accurate will be the results of the linear regression analysis.

7.5.2.1 The Single Fan System

As an example consider the representative network shown below. A single fan is placed in branch 12 to 13. There are 16 branches and 13 junctions in the network.

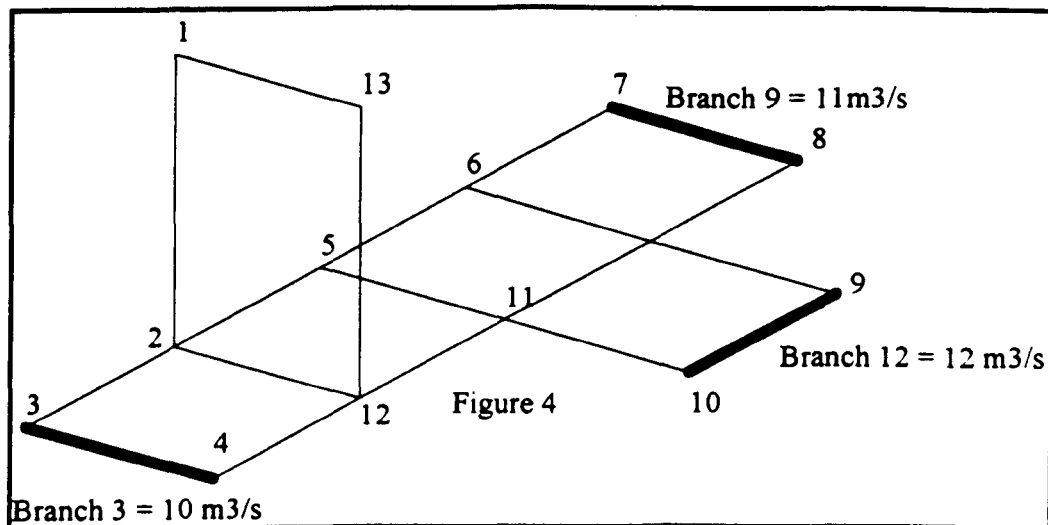


Figure 7.4. A semi-controlled flow test network. [after Calizaya [97]]

There are three fixed flow branches, but to fully specify the flow distribution would require $16-13+1=4$. Running the program for 11 varying fan pressures gave the results shown in Tables 7.4 and 7.5.

| Fan Pressure (Pa) | Added Resistance (Branch 3) | Added Resistance (Branch 9) | Added Resistance (Branch 12) |
|---------------------|-------------------------------|-------------------------------|--------------------------------|
| 1000 | -0.015 | -2.151 | -2.277 |
| 1100 | 0.571 | -1.752 | -1.941 |
| 1200 | 1.188 | -1.316 | -1.575 |
| 1300 | 1.829 | -0.855 | -1.188 |
| 1400 | 2.487 | -0.374 | -0.784 |
| 1500 | 3.160 | 0.122 | -0.367 |
| 1600 | 3.845 | 0.630 | 0.060 |
| 1700 | 4.541 | 1.150 | 0.497 |
| 1800 | 5.245 | 1.679 | 0.942 |
| 1900 | 5.957 | 1.216 | 1.393 |
| 2000 | 6.676 | 2.761 | 1.850 |

Table 7.4. Added resistance of the fixed flow branches, to maintain the specified airflows, for the single fan system.

| Fixed Flow Branch | b | c |
|-------------------|---------|----------|
| 3 | 148.623 | 1020.571 |
| 9 | 201.735 | 1461.303 |
| 12 | 240.088 | 1573.991 |

Table 7.5. Calculated linear regression coefficients for the single fan system.

These results are shown more succinctly in Figure 7.5. From this figure it can be seen that to maintain the specified flows on all three faces using a single fan system would require a pressure of 1574 Pascals. Faces 3 and 9 would then be regulated to maintain the required pressures of 1021 and 1462 Pascals respectively.

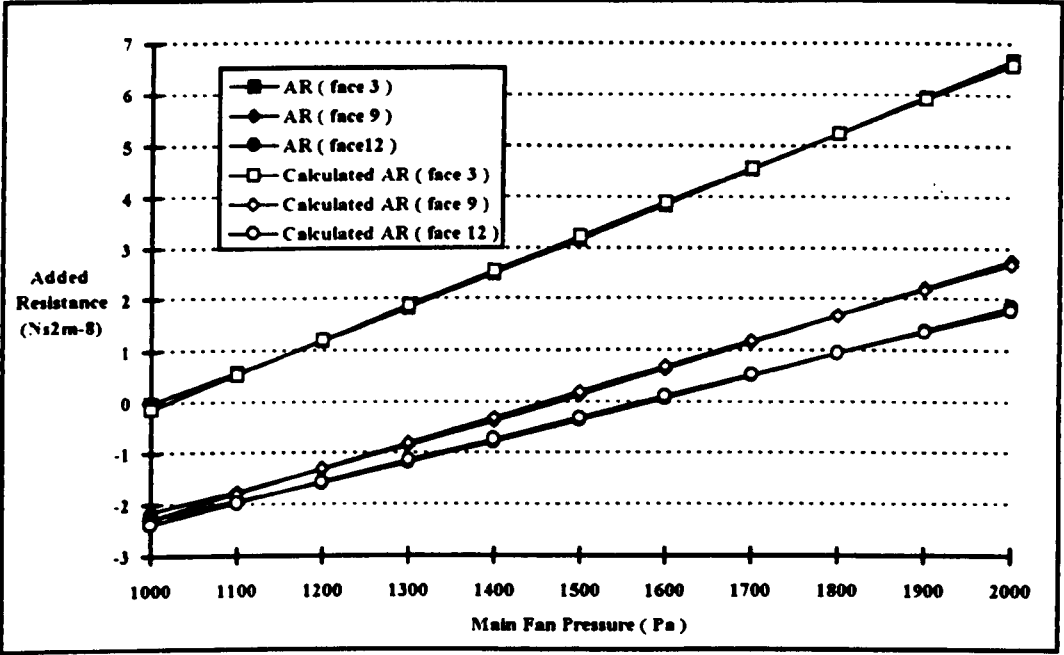


Figure 7.5. Added resistance required, on each fixed flow branch, to maintain the specified airflows, for increasing fan pressure.

7.5.2.2 The Two Fan System

The single fan system is now modified by the addition of a booster fan in branch 15. Running the program again for 10 varying pairs of fan pressures gave the results shown in Tables 7.6 and 7.7.

| Main Fan Pressure (Pa) | Booster Fan Pressure (Pa) | Added Resis. (Branch 3) | Added Resis. (Branch 9) | Added Resis. (Branch 12) |
|-----------------------------|--------------------------------|------------------------------|------------------------------|-------------------------------|
| 900 | 400 | -1.440 | -0.321 | -0.739 |
| 1300 | 300 | 1.288 | 0.961 | 0.338 |
| 1100 | 250 | 0.055 | -0.325 | -0.742 |
| 1000 | 350 | -0.750 | -0.181 | -0.622 |
| 1200 | 200 | 0.792 | -0.150 | -0.596 |
| 1300 | 350 | 1.209 | 1.276 | 0.603 |
| 1100 | 400 | -0.195 | 0.600 | 0.035 |
| 1200 | 250 | 0.705 | 0.154 | -0.340 |
| 1000 | 300 | -0.664 | -0.486 | -0.877 |
| 900 | 200 | -1.078 | -1.505 | -1.734 |

Table 7.6. Added resistance of the fixed flow branches for the two fan system.

| Fixed Flow Branch | a | b | c |
|-------------------|--------|---------|----------|
| 3 | 0.270 | 156.551 | 1020.371 |
| 9 | -1.291 | 212.439 | 1486.709 |
| 12 | -1.291 | 252.847 | 1605.490 |

Table 7.7. Calculated linear regression coefficients for the two fan system.

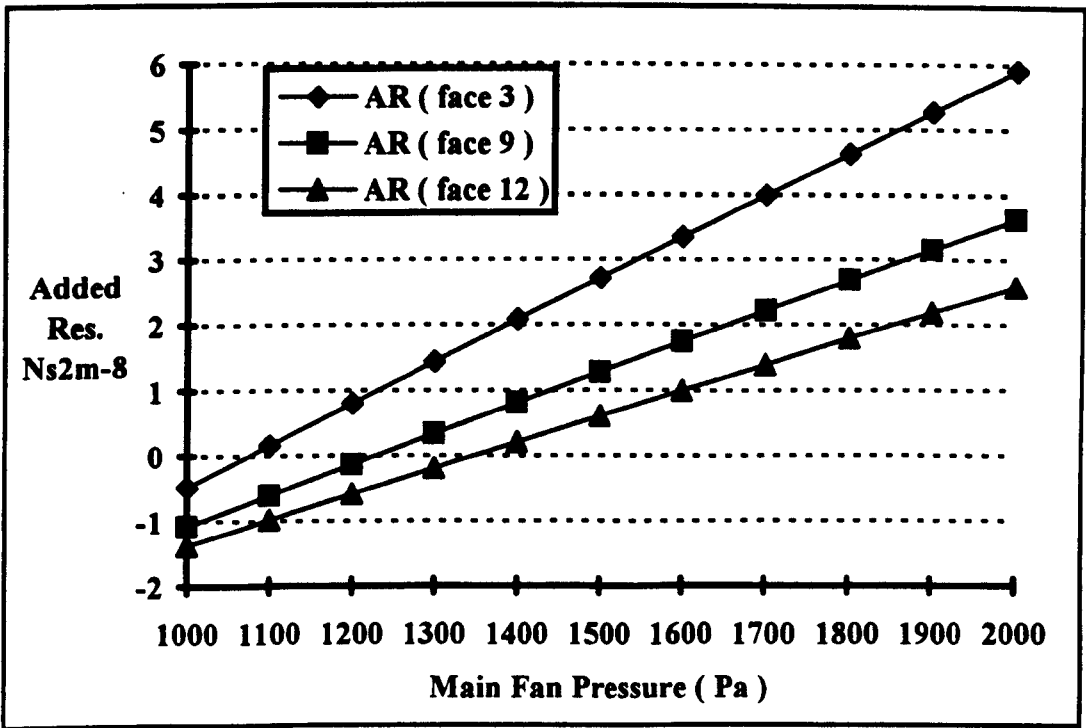


Figure 7.6. Added resistance required to maintain the specified airflows for a varying main fan pressure and a booster fan pressure of 200 Pa.

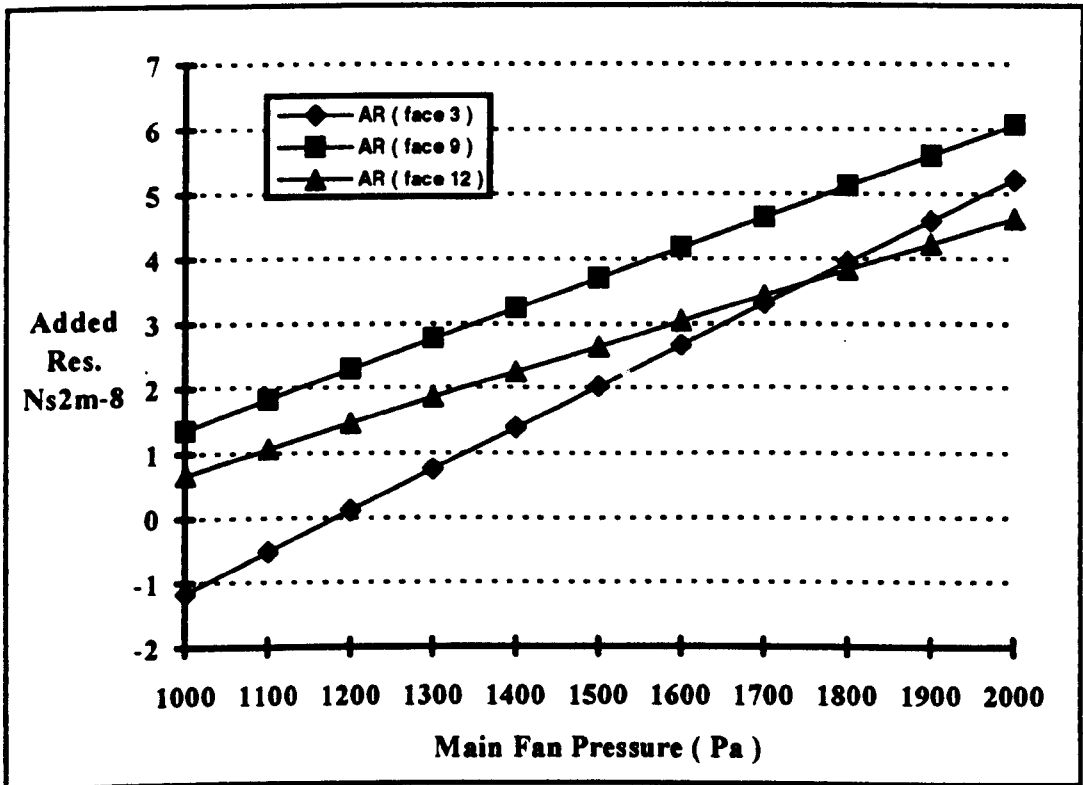


Figure 7.7. Added resistance required to maintain the specified airflows for a varying main fan pressure and a booster fan pressure of 600 Pa.

The optimum combination of main and booster fan pressures will be such that

- (i) The added resistance on faces is zero.
- (ii) The power consumed by fans is a minimum.

Using equation (7.33) then, for zero added resistance on a face;

$$P_m = aP_f + c \quad (7.34)$$

The lines of main fan pressure against booster fan pressure can now be plotted for each fixed flow face. The graphical method of solution reveals at the intersection of two lines the main and booster fan pressures required for zero added resistance on those two faces.

For the solution to be valid, the added resistance on all other faces must be positive indicating that no more pressure is required in the network, just regulation to achieve the pre-assigned airflows.

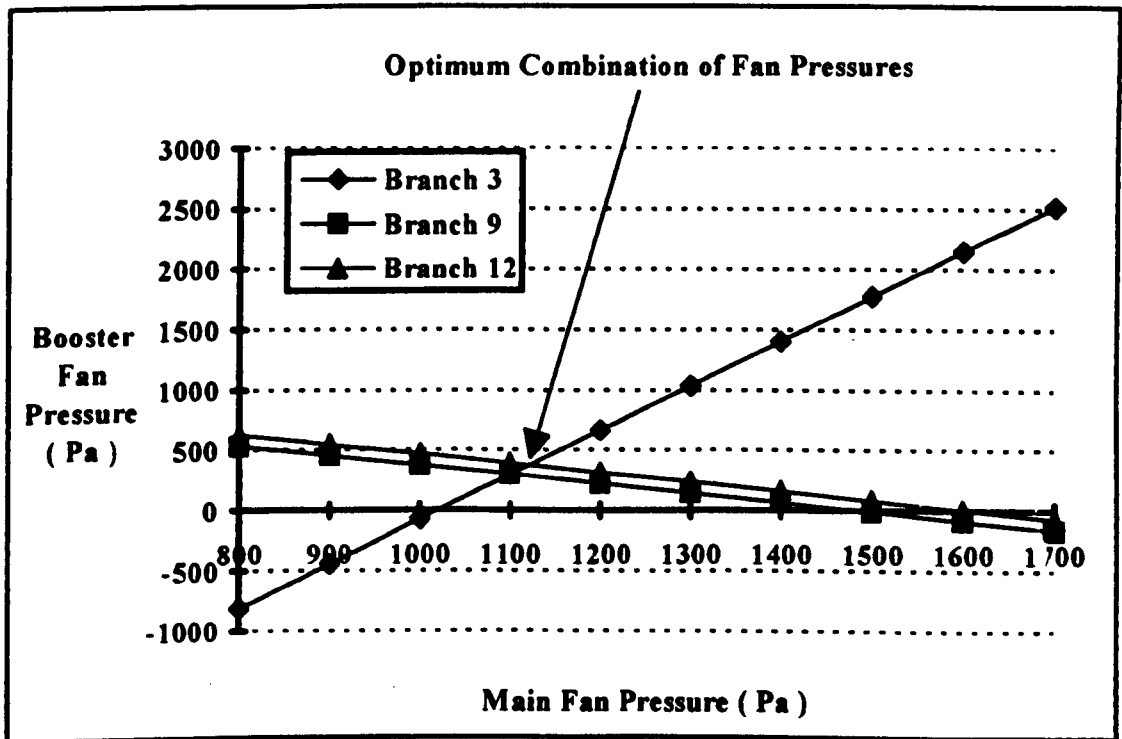


Figure 7.8. Main and booster fan pressures required for zero added resistance on each fixed flow face.

The optimum combination of fan pressures in this example case is a main fan pressure of 1122 Pascals and 41.66 m³/s of air and a booster fan pressure of 375 Pascals and 28.10 m³/s of air. The total power consumption is therefore 57.28 kW (=1122*41.66 + 375*28.10 Watts). This compares with the power requirement for the single fan case of 68.69 kW (=1574*43.64 Watts).

This method, described briefly here, is simple to understand and easy to program but restricted by the graphical nature of the solution process, whereby one can only optimise between two fans and two faces. It also suffers from the need to input specified booster fan locations and fixed fan pressures rather than characteristics. The choice of fan pressures chosen for the regression analysis is critical to the accuracy of the solution. It is obvious that fan pressures chosen in the region of the optimum solution will provide better results and, in addition, fan pressures chosen which may induce recirculation in a network will affect reliability of the linear relationship between added resistance and fan pressures which has been assumed.

However, the simplicity of the method, as opposed to the complicated mathematical Non-Linear Programming techniques, makes it a powerful tool and this method was adopted for the development of the computer program subsequently employed in the analysis of realistic mine ventilation networks. The method was extended to include ;

- (i) Analysis to find possible booster fan locations.
- (ii) Analysis of all the intersection points of zero added resistance lines.
- (iii) Analysis of total network leakage.

Extra fans can be included in the model but the optimisation can only be carried out between two fan installations at a time. For example a main fan characteristic could be fixed and the optimisation be carried out between two underground booster fan installations.

7.5.2.3 Analysis of Booster Fan Locations

The location of booster fans will be dependent on the ventilation methods employed in the network. An exhausting ventilation system will require the booster in a return branch otherwise a forcing one would require it in an intake.

The booster fan, if it is to assist the main fan, will also need to be installed in a branch of the critical path through the network. The program will calculate the critical path and state which branches are return branches and which are intake.

Each fixed flow branch will be made a chord of the network and hence will appear in only one mesh. The program will analyse all the possible branches available from the analysis so far and state in how many meshes each of those branches are contained and in what direction. Placement of the booster fan in the same mesh as a fixed flow branch and in the same direction will have a greater effect on the added resistance required.

Consider the network shown in Figure 7.9

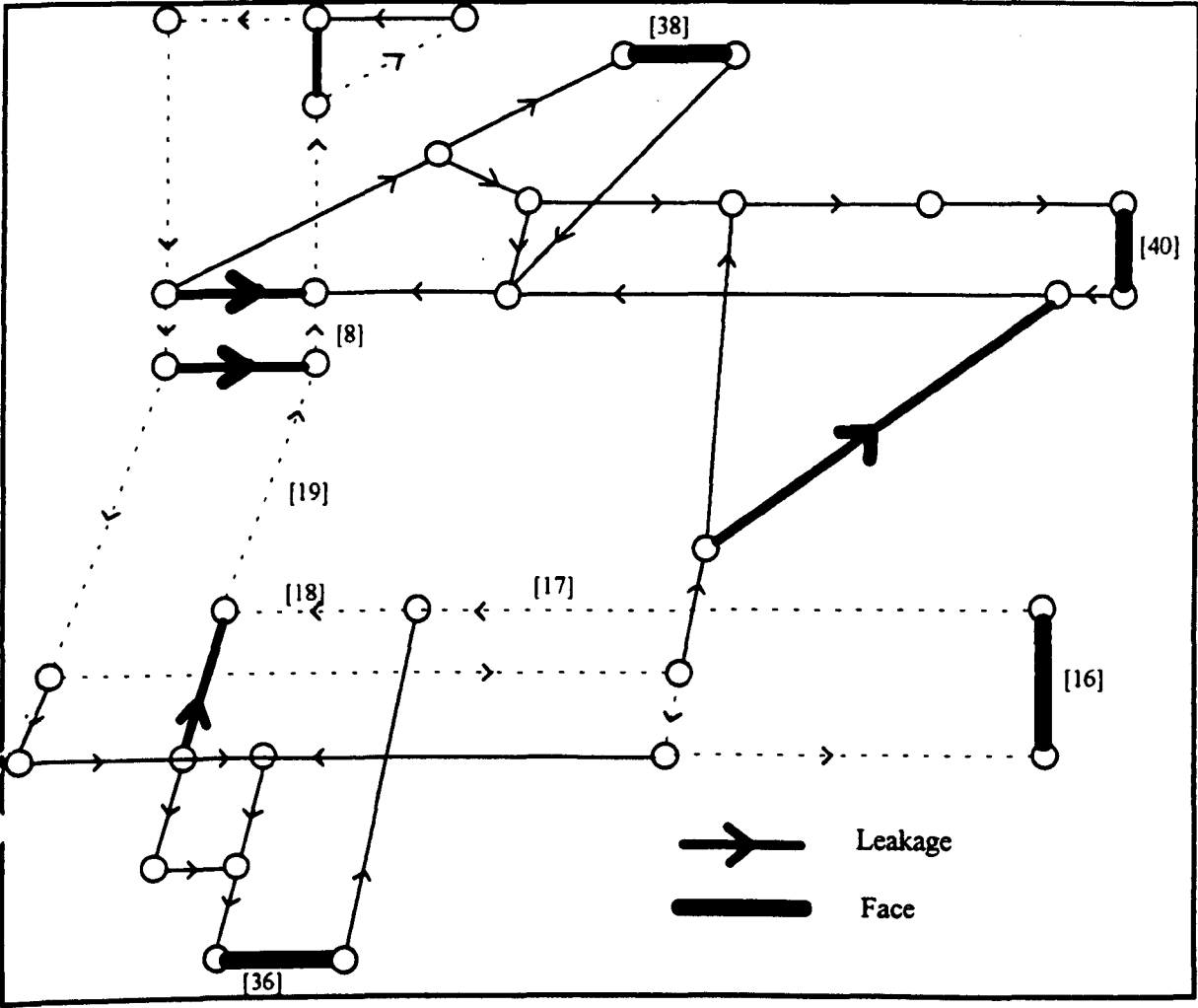


Figure 7.9 Network for the example of optimum booster fan location .
(after Calizaya [98])

The critical path is shown by the dotted line and for an exhausting system the booster fan could be positioned in branches 8, 17, 18 or 19. The simulation model was run with the booster fan in each of these positions and the results are displayed in Table 7.8

The ventilation engineer now has to investigate the most practical and suitable location for the booster fan.

7.5.2.4 Analysis of Intersection Points

The general mathematical model will produce a number of solutions not all of which are practicable. The program is able to analyse all the points of intersection and reject all the non practicable solutions where ;

- (i) Main fan pressure is negative.
- (ii) Booster fan pressure is negative.
- (iii) Negative added resistance is still required in another fixed flow branch, indicating pressure is still needed.

Solutions to the combinations that still remain will be calculated and printed in a results file.

7.5.2.5 Analysis of Total Leakage

The flows through all specified leakage branches will be added to give a total leakage value for the network.

7.5.2.6 A General Strategy for Network Analysis

The exercises performed on the example ventilation networks have indicated, and led to the development of a general strategy with which to analyse the optimum ventilation configurations. This strategy is shown in Figure 7.10.

| Booster Branch | Main Fan Pressure (Pa) | Booster Fan Pressure (Pa) | Zero Added Resistance Faces | Regulation Required on Other Faces (Ns^2m^8) | Power Consumed in the Network. (kW) |
|----------------|--------------------------|-----------------------------|-----------------------------|--|---------------------------------------|
| 8 | 1498 | 1299 | 16 and 40 | Face 36 - 7.094 Face 38 - 0.080 | 170.2 |
| 8 | 1476 | 1312 | 16 and 38 | Face 36 - 7.086 Face 40 - -0.109 | 168.5 |
| 17 | 1689 | 1035 | 16 and 36 | Face 38 - 1.704 Face 40 - 1.925 | 145.0 |
| 17 | 1044 | 8474 | 38 and 40 | Face 16 - 49.133 Face 36 - -2.536 | 171.8 |
| 18 | 1256 | 1284 | 16 and 40 | Face 36 - 7.153 Face 38 - 0.018 | 120.4 |
| 18 | 1039 | 13414 | 38 and 40 | Face 16 - 83.427 Face 36 - 90.603 | 391.6 |
| 19 | 1427 | 1295 | 16 and 40 | Face 36 - 7.153 Face 38 - 0.141 | 152.6 |
| 19 | 1408 | 1307 | 16 and 38 | Face 36 - 7.158 Face 40 - -0.015 | 151.2 |

Table 7.8. Optimum combination of main and booster fan pressures for varying booster fan locations.

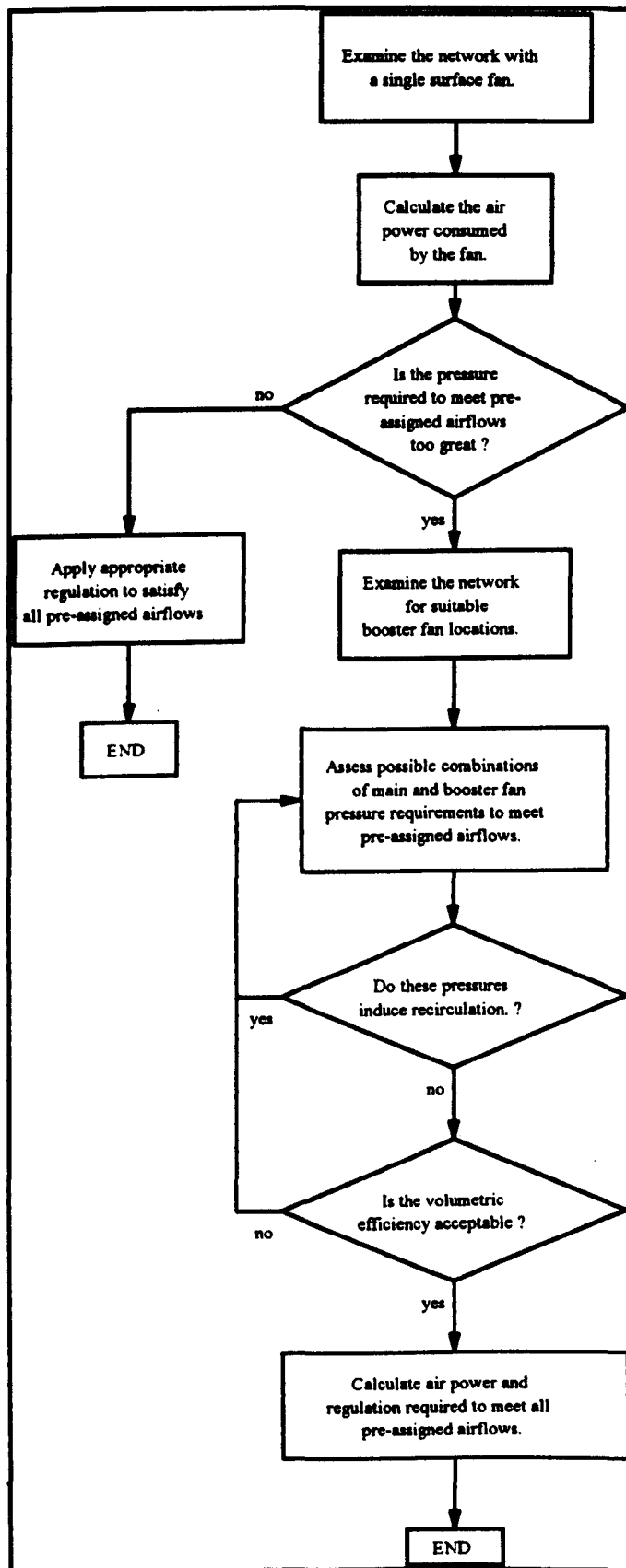


Figure 7.10 A strategy with which to perform an analysis of a general mine ventilation network.

7.6 Summary and Conclusions

Only when appeal is made to the mathematical topic of graph theory can a concise statement be made of the topographical arrangement of mine ventilation networks and Kirchhoff's first and second laws.

The adoption of Atkinson's equation describing the pressure loss along a mine airway means the system of equations arising from Kirchhoff's laws are non linear and can only be solved for airflows and pressure distributions after resorting to an iterative method of solution. These solution methods are discussed.

The specification of branch flows has redefined the problem and a number of solution techniques have arisen out of past research. These vary according to whether the fixed flows define the complete flow distribution in the network or whether some branch flows are still undetermined. The mathematical complexity of some methods makes them difficult to implement and a more graphically based, user interactive, approach was adopted to analyse the ' generalised controlled flow ' problem. This method determines the optimum position of fans and regulators whilst, at the same time, not fixing the complete flow distribution in the network

The application of this method to a number of existing mine ventilation networks is discussed in the following chapter.

A discussion and listing of all the computer programs developed for the analysis of the varying types of mine ventilation networks may be found in Appendix 2.

Chapter 8

Program Results and Correlation Exercises

8.1 Case Study 1 - Bilsthorpe Colliery

Bilsthorpe colliery is situated in the Nottinghamshire coalfield some 15 miles north of Nottingham and 10 miles east of Mansfield. The colliery commenced production from the Top Hard seam in 1928, and continued wholly in that seam until 1946 when part of the output was obtained from the Low Main Seam. Access to the Low Main seam is via twin drifts down from the Top Hard pit bottom. In November 1966 part of the output was obtained from the Parkgate seam, access to this seam being from the Low Main drifts. Output from the Top Hard seam ceased in August 1968 and the product since that date has been a blend of Parkgate and Low Main coals.

Two 6.15 metre shafts were sunk during the period 1925 to 1928. The downcast shaft is 442 metres deep and the upcast shaft is 460 metres deep.

The colliery ventilation network is shown in Figures 8.1 and 8.2. There are 4 production faces requiring specified air quantities to be passed through them. These airflows are shown in Table 8.1 and in subsequent discussion these faces will be referred to as the fixed flow branches.

| Branch | Quantity (m ³ /s) |
|--------|--------------------------------|
| 107 | 24.4 |
| 123 | 14.6 |
| 133 | 15.6 |
| 134 | 14.6 |

Table 8.1. The airflow quantities specified for the Bilsthorpe network.

The computer simulation model was executed with these fixed quantities, firstly with a single surface fan and then with a booster fan inserted in the return branch from junction 83 to 44.

8.1.1 The One Fan System

The regulation required for each fixed flow branch, will vary with the pressure supplied by fans in the network. There are two forms of regulation which may be employed namely 'active' regulation or 'passive' regulation. Active regulation is the addition of a pressure source such as a booster fan and would be indicated by the analysis as a negative added resistance. Passive regulation is the addition of a regulating device such as doors and would be indicated by the analysis as a positive added resistance.

The main fan pressure was varied between 3 kPa and 10 kPa. This gave the added resistances (i.e. the extra resistance required by suitable regulation) to maintain the fixed flows shown in Table 8.1. This resistance is added to the branch of the network having the fixed flow specified. The required resistances for varying fan pressure are shown in table 8.2. or more graphically in Figure 8.3.

Below a main fan pressure of approximately 5.5 kPa the assumption of a linear relationship between fan pressure and added resistance becomes invalid. This is the result of observed recirculation flows occurring through leakage paths for fan pressures in the region below 5.5 kPa. A negative added resistance is equivalent to the addition of a booster fan pressure of $|AR|Q^2$ on the gateroads of each fixed quantity branch. If these pressures become large enough, recirculation will occur through the leakage paths, outbye of the fixed quantity branches, rendering the linear assumption invalid. The regression analysis was therefore carried out using main fan pressures above 5.5 kPa. This gave the linear regression coefficients shown in Table 8.3 and illustrated graphically in Figure 8.4.

| Main Fan Pressure (Pa) | Added Resistance Branch 107 (Ns^2m^{-8}) | Added Resistance Branch 123 (Ns^2m^{-8}) | Added Resistance Branch 133 (Ns^2m^{-8}) | Added Resistance Branch 134 (Ns^2m^{-8}) |
|-----------------------------|--|--|--|--|
| 3000 | -2.450 | -3.360 | -2.762 | -3.155 |
| 3500 | -2.084 | -2.753 | -2.249 | -2.570 |
| 4000 | -1.740 | -2.370 | -1.931 | -2.207 |
| 4500 | -1.391 | -2.004 | -1.634 | -1.867 |
| 5000 | -1.042 | -1.669 | -1.391 | -1.588 |
| 5500 | -0.663 | -1.148 | -0.969 | -1.106 |
| 6000 | -0.262 | -0.496 | -0.426 | -0.484 |
| 6500 | 0.153 | 0.234 | 0.190 | 0.219 |
| 7000 | 0.579 | 1.021 | 0.857 | 0.981 |
| 7500 | 1.014 | 1.853 | 1.565 | 1.790 |
| 8000 | 1.457 | 2.722 | 2.307 | 2.638 |
| 8500 | 1.907 | 3.622 | 3.077 | 3.517 |
| 9000 | 2.363 | 4.549 | 3.871 | 4.424 |
| 9500 | 2.823 | 5.499 | 4.686 | 5.355 |
| 10000 | 3.289 | 6.471 | 5.521 | 6.308 |

Table 8.2. Added resistance required, to maintain specified airflows, for each fixed flow branch with increasing fan pressure.

| | b | c |
|------------|------|------|
| Branch 107 | 1135 | 6312 |
| Branch 123 | 584 | 6328 |
| Branch 133 | 685 | 6333 |
| Branch 134 | 599 | 6332 |

Table 8.3. Coefficients from linear regression analysis of data presented in Table 8.2.

The almost point intersection of the 4 lines in Figure 8.4 indicate that the network has already been appropriately regulated to achieve the specified quantities. A fan pressure of 6333 Pascals would give zero added resistance for branch 133 and require only a small amount of regulation on the remaining districts for the preassigned airflows to be maintained. This fan pressure would provide 177 m³/s of airflow and the air power necessary would be 1122 kW.

This pressure and quantity combination, however, does not lie on the characteristic of the existing surface fan at the colliery. The high fan pressures required in this case has meant the necessary consideration of the use of booster fans in the ventilation network.

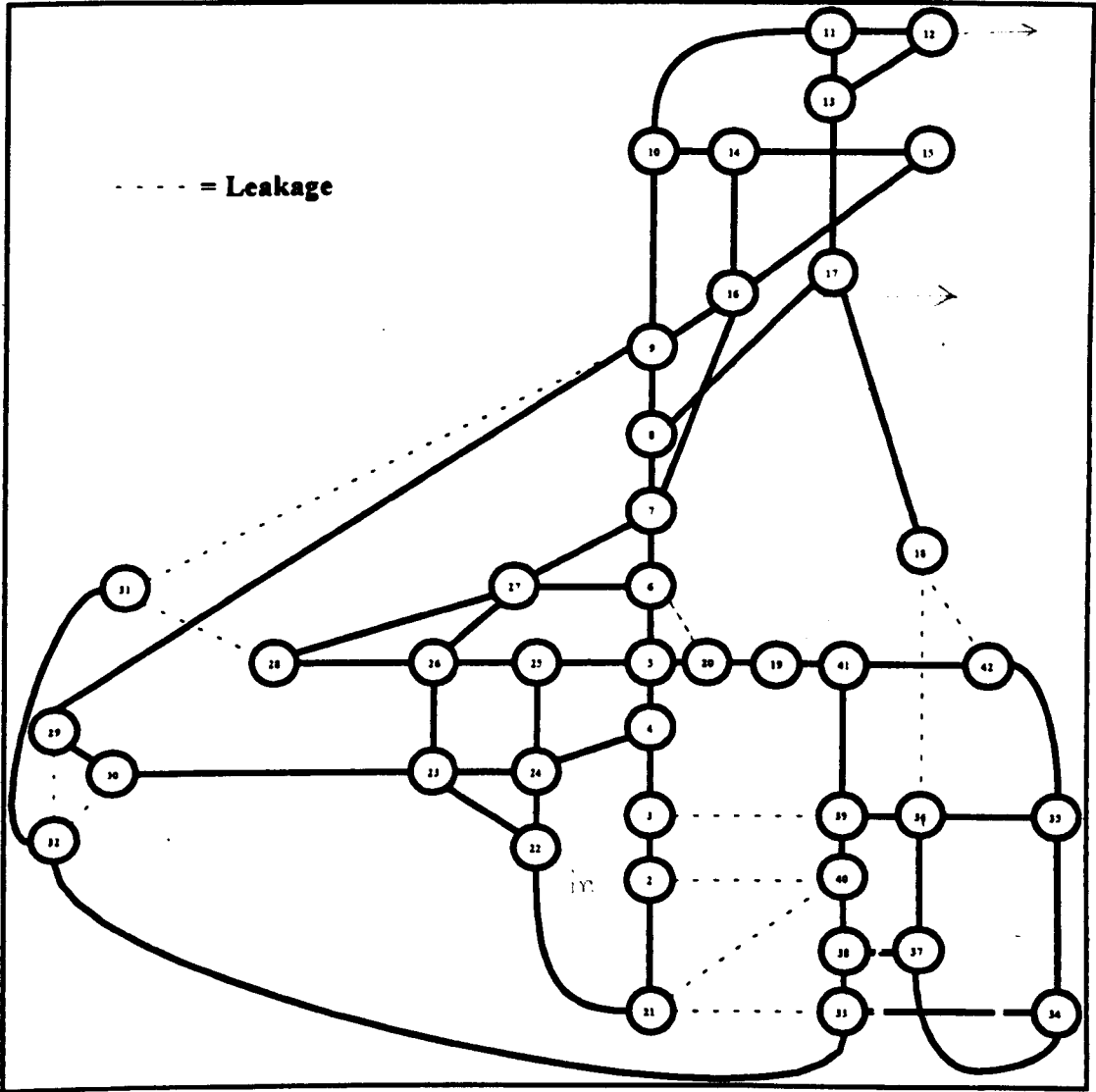


Figure 8.1. Schematic of the Bilsthorpe colliery pit bottom area.

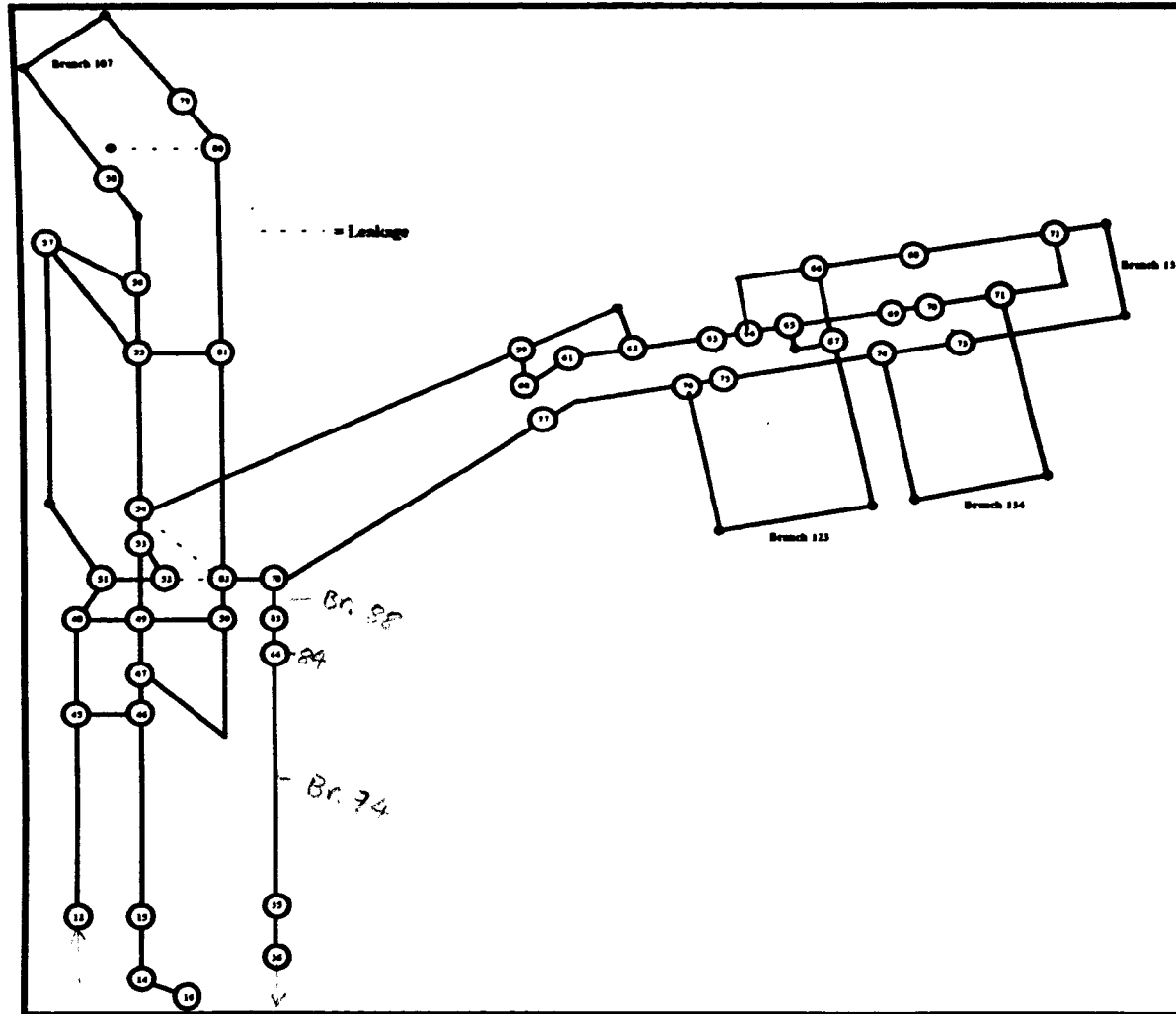


Figure 8.2. Schematic of the Bilsthorpe colliery Face Layout.

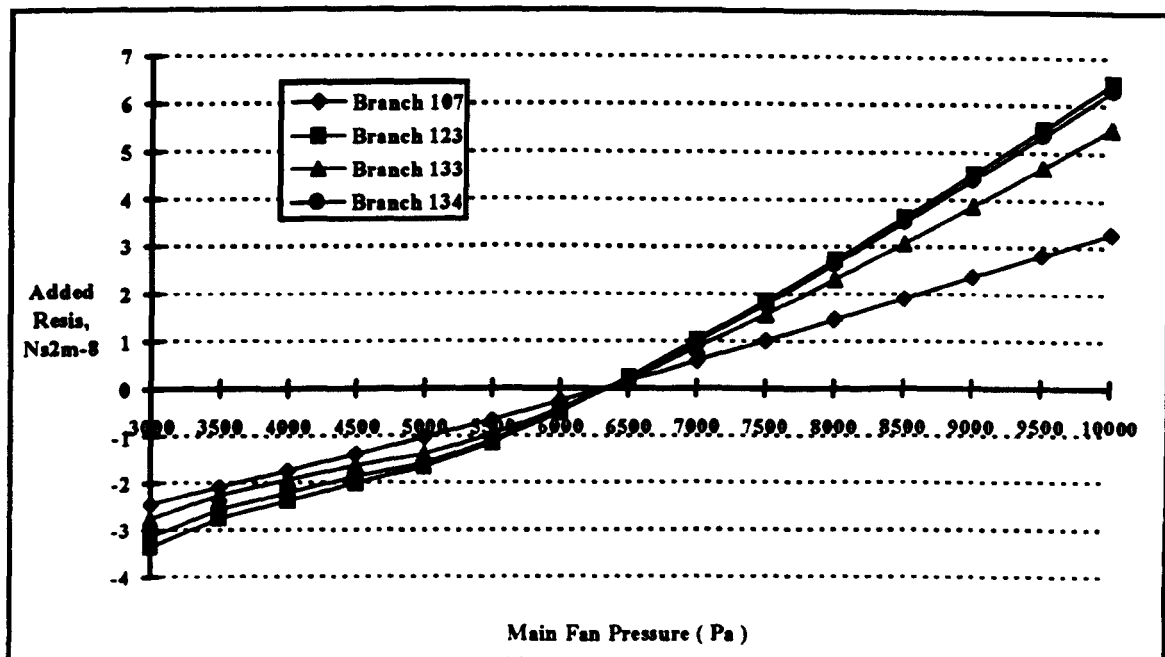


Figure 8.3. Actual added resistance required to maintain specified airflows with increasing fan pressure.

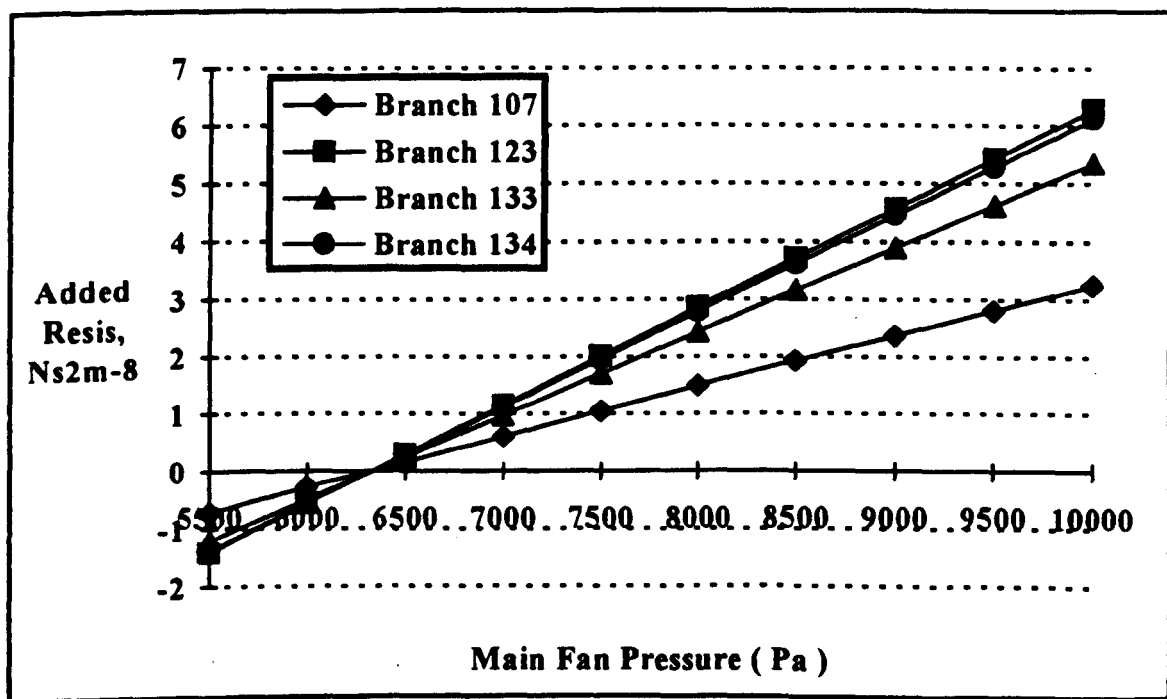


Figure 8.4. Calculated added resistance required to maintain specified airflows with increasing fan pressure.

8.1.2 The Two Fan System

Due to the large pressure differences across the network, resulting in excessive leakage, that occur with a single surface fan means realistically a booster fan must be installed to reduce the ventilation costs and control the air lost through leakage. At Bilsthorpe colliery a modular bank of Davidson booster fans are installed in the branch from junction 83 to 44 and configured in 4 banks and 2 stages. The characteristics of the main and combined booster fan characteristics are shown in Tables 8.4 and 8.5 and illustrated graphically in Figures 8.5 and 8.6 respectively..

| Pressure (Pa) | Quantity (m ³ /s) |
|-----------------|--------------------------------|
| 2752 | 0.0 |
| 2802 | 23.6 |
| 2877 | 47.2 |
| 2989 | 70.8 |
| 3139 | 94.4 |
| 3163 | 118.0 |
| 2939 | 141.6 |
| 2553 | 165.2 |
| 2030 | 188.8 |
| 1370 | 212.4 |
| 623 | 236.0 |
| 0 | 251.0 |

Table 8.4. Duty points for the Bilsthorpe colliery main fan.

| Pressure (Pa) | Quantity (m ³ /s) |
|-----------------|--------------------------------|
| 3900 | 103 |
| 3850 | 105 |
| 3720 | 110 |
| 3560 | 115 |
| 3380 | 120 |
| 3180 | 125 |
| 2940 | 130 |

Table 8.5. Duty points for Davidson booster fans - 4Banks , 2 Stages

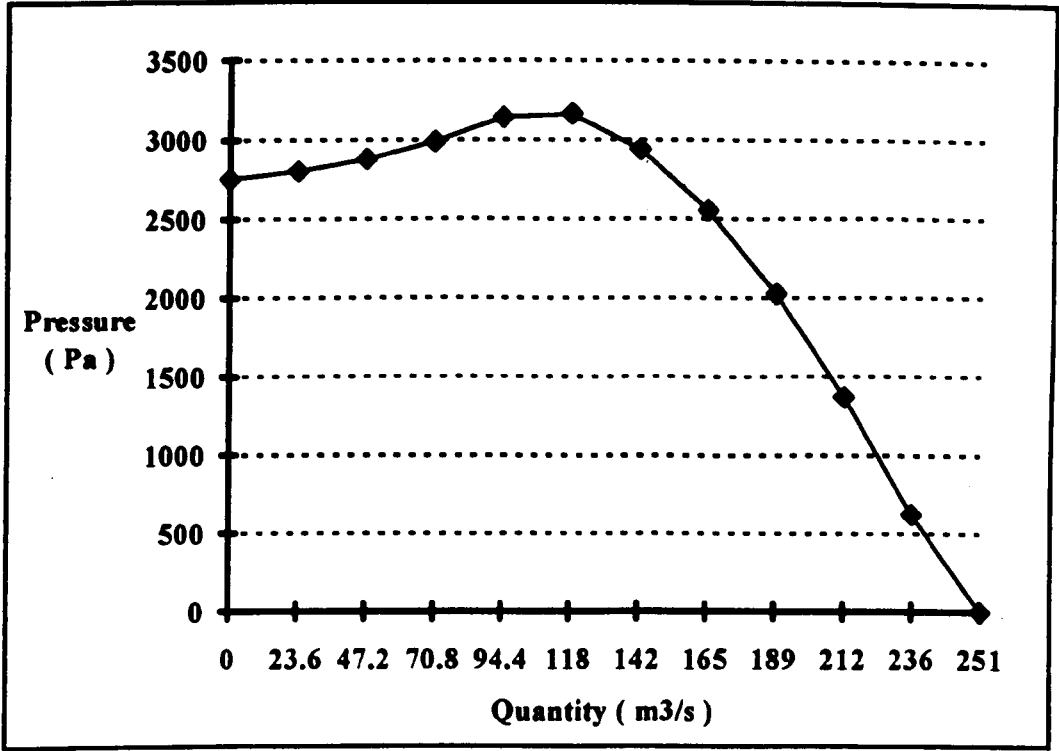


Figure 8.5. Performance characteristic for the Bilsthorpe colliery main fan.

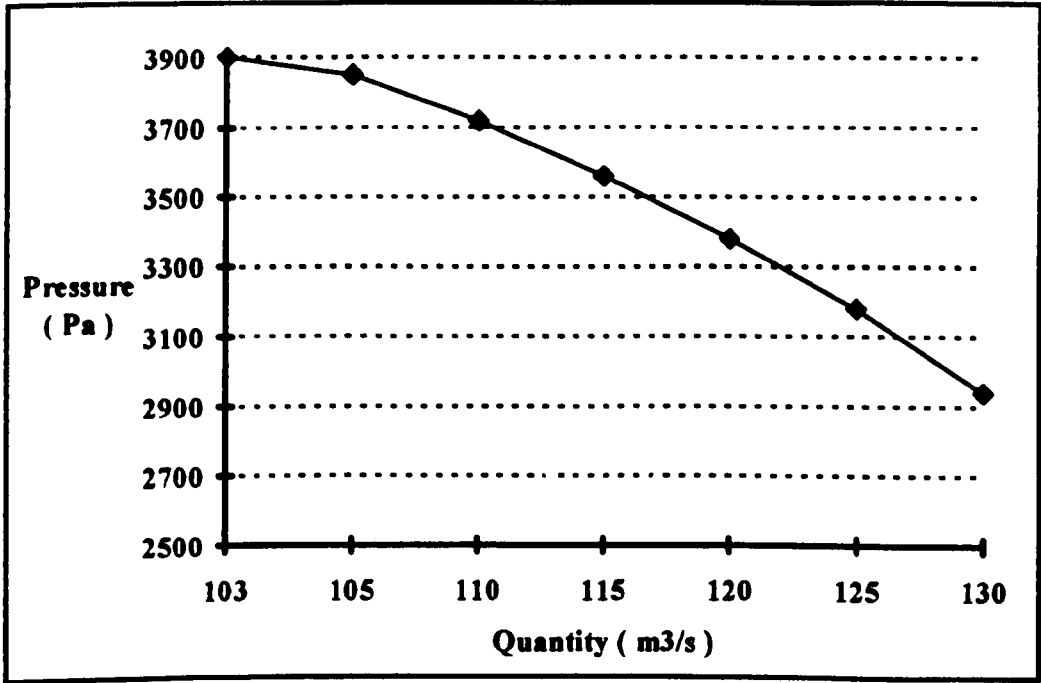


Figure 8.6. Performance characteristic for Davidson booster fans - 4 Banks, 2 Stages.

Within the normal operating range, as indicated by the data in Tables 8.4 and 8.5, the fan pressures can usually be represented by a second order relationship of the form ;

$$p = aQ^2 + bQ + c$$

A non-linear regression analysis performed on the above data produced a main fan characteristic ;

$$p = 2507 + 17.37Q - 0.11Q^2$$

and ;

$$p = 929 + 79.67Q - 0.49Q^2$$

for the booster fan configuration.

The initial analysis, however, was to execute the computer simulation program for the two fan system with varying fan pressure combinations. Analysis of the results will determine the optimum fan pressure/quantity combinations to maintain the pre-assigned airflows. Subsequent analysis will find the fan pressure/quantity combinations which lie on the characteristics discussed above. Results of the trials are shown in Tables 8.6 and 8.7.

| Main Fan Pressure (Pa) | Booster Fan Pressure (Pa) | Added Resistance Branch 107 | Added Resistance Branch 123 | Added Resistance Branch 133 | Added Resistance Branch 134 |
|--------------------------|-----------------------------|-----------------------------|-----------------------------|-----------------------------|-----------------------------|
| 2000 | 3000 | -1.013 | -1.635 | -1.365 | -1.558 |
| 2500 | 3250 | -0.432 | -0.779 | -0.663 | -0.755 |
| 3000 | 2750 | -0.440 | -0.793 | -0.675 | -0.769 |
| 2750 | 4000 | 0.409 | 0.704 | 0.598 | 0.674 |
| 1500 | 2500 | -1.718 | -2.361 | -1.925 | -2.199 |
| 2250 | 3500 | -0.427 | -0.771 | -0.556 | -0.748 |
| 1750 | 4000 | -0.416 | -0.754 | -0.642 | -0.731 |
| 1500 | 3750 | -0.812 | -1.368 | -1.151 | -1.313 |
| 3000 | 3250 | -0.024 | -0.082 | -0.078 | -0.087 |
| 2000 | 2750 | -1.188 | -1.785 | -1.467 | -1.675 |

Table 8.6. Added resistance required to maintain the specified airflows for varying main and booster fan pressure combinations.

| | a | b | c |
|------------|--------|------|------|
| Branch 107 | -1.009 | 1299 | 6315 |
| Branch 123 | -0.921 | 844 | 6052 |
| Branch 133 | -0.902 | 1015 | 5994 |
| branch 134 | -0.902 | 888 | 5993 |

Table 8.7. Coefficients from Linear Regression Analysis of Data presented in Table 8.6.

Figures 8.7a, 8.7b and 8.7c give the lines, for each fixed flow face, which describe the various values of added resistance or regulation which must be applied for a range of main fan pressures, given that the booster fan pressure is fixed at 3000, 3500 and 4000 Pascals. The equation of the regression lines may be represented in the form ;

$$p_m = b * AR + (a * p_r + c)$$

where $(a * p_r + c)$ is now constant and represents the intercept on the vertical axis.

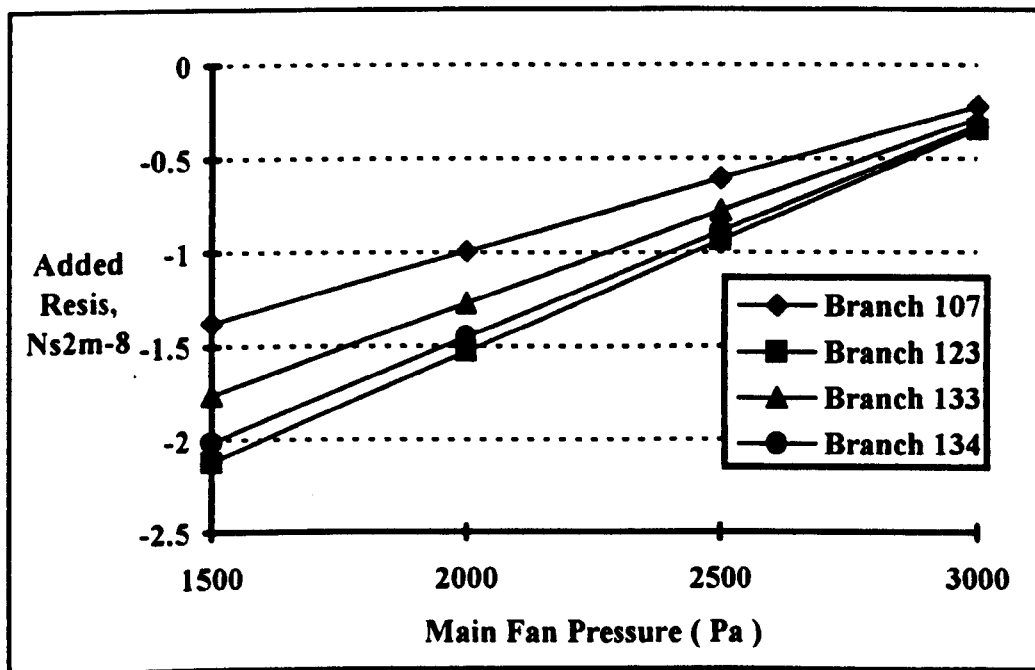


Figure 8.7a. Added resistance required to maintain specified airflows with increasing main fan pressure and a booster fan pressure of 3000 Pa.

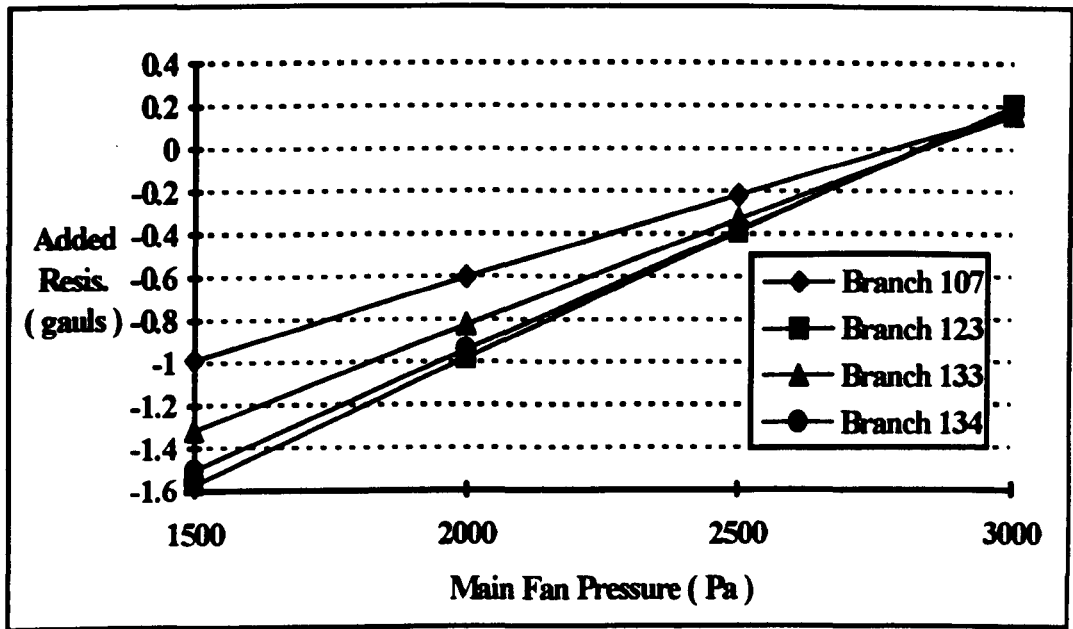


Figure 8.7b. Added resistance required to maintain specified airflows with increasing main fan pressure and a booster fan pressure of 3500 Pa.

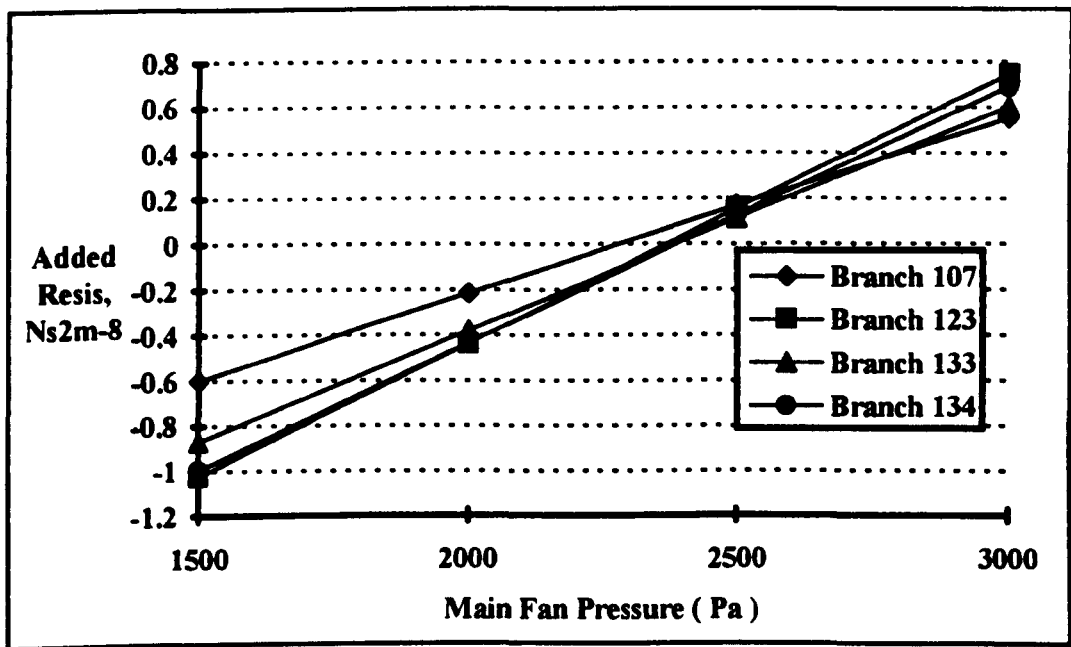


Figure 8.7c. Added resistance required to maintain specified airflows with increasing main fan pressure and a booster fan pressure of 4000 Pa.

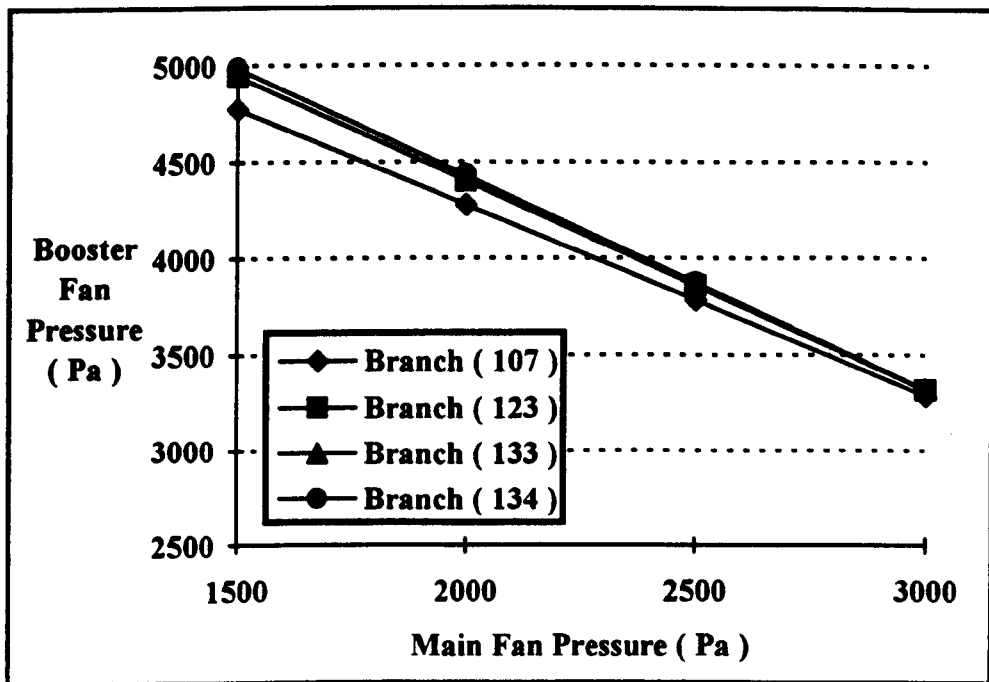


Figure 8.8. Main and booster fan pressure combinations for zero added resistance on each fixed flow branch.

Figure 8.8 shows the variation of main fan pressure plotted against the required booster fan pressure for no regulation or zero added resistance on the fixed flow branches. i.e.

$$p_m = a * p_b + c$$

It becomes apparent from Figure 8.8 that this network has been pre-regulated to satisfy the required airflows on all faces for the given main and booster fan positions. The lines of zero added resistance are all similar and any combination of main and booster fan pressures along these lines would give the required quantities in all the specified branches without any extra regulation being required. Using the results obtained for branch 134 and tabulated on Table 8.6 then ;

$$p_m = -0.902p_b + 5993$$

This relationship produces the range of main and booster fan combinations shown in Table 8.8.

| Main Fan Pressure (Pa) | Main Fan Quantity (m ³ /s) | Booster Fan Pressure (Pa) | Booster Fan Quantity (m ³ /s) |
|-----------------------------|--|--------------------------------|---|
| 0 | 103.9 | 6644 | 119.1 |
| 250 | 118.4 | 6366 | 118.5 |
| 500 | 127.0 | 6089 | 118.0 |
| 750 | 132.0 | 5812 | 117.6 |
| 1000 | 135.8 | 5535 | 117.2 |
| 1250 | 139.1 | 5258 | 116.8 |
| 1500 | 142.0 | 4981 | 116.4 |
| 1750 | 144.7 | 4703 | 115.9 |
| 2000 | 147.1 | 4426 | 115.5 |
| 2250 | 149.3 | 4149 | 115.1 |
| 2500 | 151.5 | 3872 | 114.7 |
| 2750 | 153.5 | 3595 | 114.3 |
| 3000 | 155.3 | 3318 | 113.9 |
| 3250 | 157.1 | 3041 | 113.4 |
| 3500 | 158.9 | 2763 | 113.0 |
| 3750 | 160.5 | 2486 | 112.5 |
| 4000 | 162.1 | 2209 | 112.0 |

Table 8.8. Main and booster fan pressures required to maintain the specified airflows.

The problem now is to find a main fan and booster fan pressure combination such that ;

- (i) recirculation is avoided
- (ii) the air power consumed by fans in the network, whilst still maintaining the pre-assigned airflows, is minimised.

Figure 8.9 demonstrates the air power consumed by the main and booster fan combinations specified in Table 8.8. Recirculation occurs with main fan pressures below 500 Pascals and the fan pressure combination minimising the air power consumption would be one with a main fan pressure just above 500 Pascals. This however would require too great a pressure to be supplied by the booster fan and give a main fan duty point not lying on the characteristic curve (Figure 8.5).

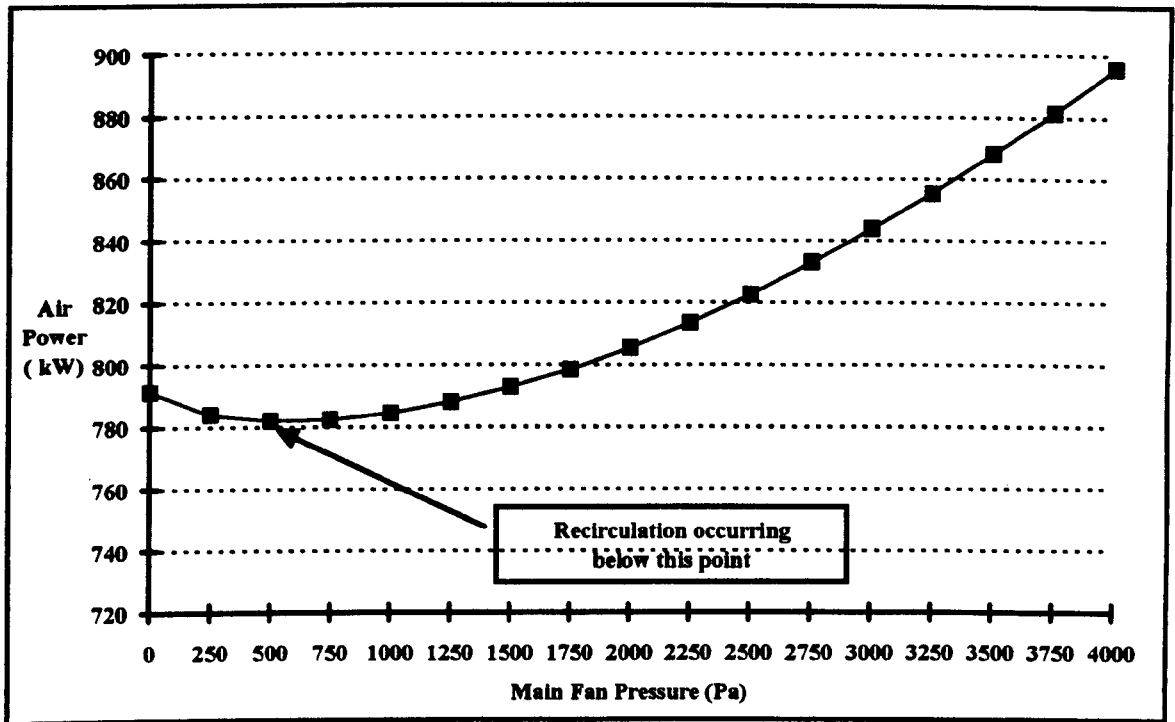


Figure 8.9 Air power consumed for main and booster fan combinations shown in Table 8.8

A delivered fresh air quantity of $152 \text{ m}^3/\text{s}$ entering the mine would, from the characteristic curve (Figure 8.5), result in a main fan pressure of 2606 Pascals. This would also satisfy the requirements of the fan pressure combinations demonstrated in Table 8.8. The required booster fan pressure would therefore be 3755 Pascals ($= (2606 - 5993)/-0.902$ Pascals) delivering approximately $114.5 \text{ m}^3/\text{s}$ of air. The power required for this configuration is 826.1 kW (as opposed to 1122 kW for the one fan system).

By analysing the booster fan characteristic (Figure 8.6) it can be seen that for a pressure of 3775 Pascals the air delivered would be $109.5 \text{ m}^3/\text{s}$. This booster configuration is therefore delivering approximately $5 \text{ m}^3/\text{s}$ too little air for the current mine ventilation network configuration. The network would need to be adjusted to overcome this shortfall in air delivery.

8.1.3 Leakage and Volumetric Efficiency

Variations in the main and booster fan pressures will of course produce variations in the pressure differences across leakage paths. These pressure differences are the driving force behind leakage flows and therefore the program was also developed to quantify these leakage flows against the variations in fan pressures. The total leakage is given by the total air quantity moving through the main fan minus the sum of all the required fresh air quantities delivered to the working areas. The reduction in leakage at low main fan pressures is due, once again, to recirculation.

A more effective measure of the effect of leakage is the volumetric efficiency or the ratio of leakage to total flow through the main fan. This is shown in Figure 8.11 and at 2606 Pascals the volumetric efficiency is 47%

The example of Bilsthorpe colliery , although an already well regulated and balanced network, has shown how the method discussed is a simple tool for the effective analysis of mine ventilation networks. An optimum fan pressure combination was found which removed the risk of recirculation and reduced the total air power requirement of the network from 1122 kW to 826.1 kW (i.e. by 26 %).

| Main Fan Pressure (Pa) | Main Fan Quantity (m ³ /s) | Booster Fan Pressure (Pa) | Booster Fan Quantity (m ³ /s) | Air Power (kW) |
|-----------------------------|--|--------------------------------|---|---------------------|
| 2606 | 152 | 3755 | 114.5 | 826 |

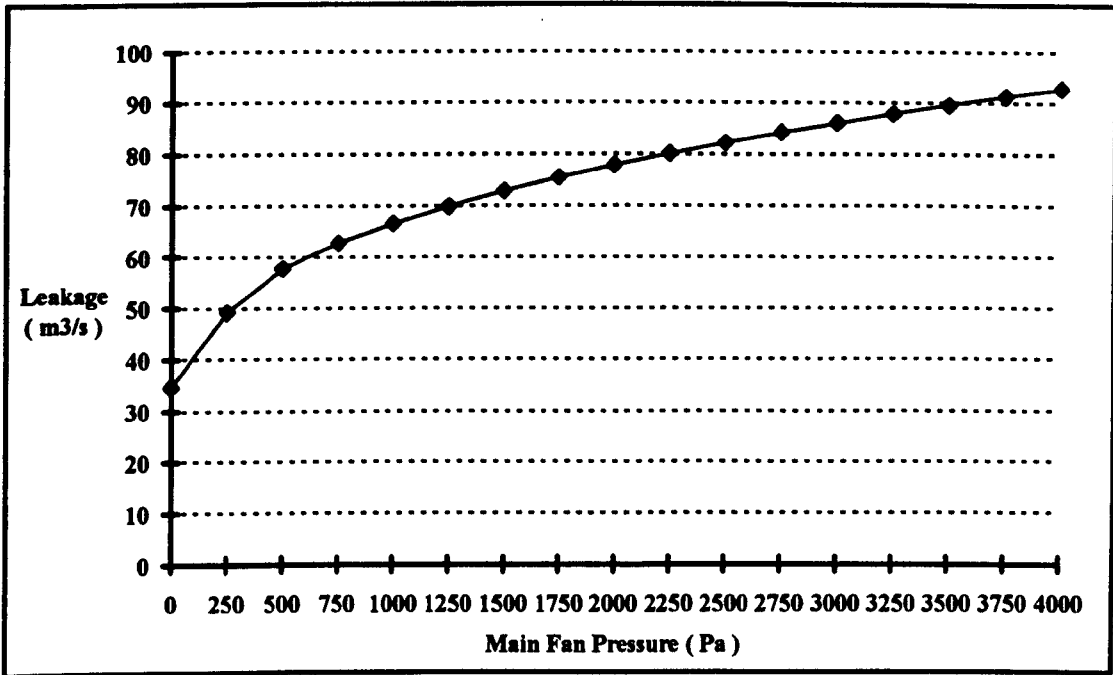


Figure 8.10. Total leakage in the two fan system for increasing main fan pressure.

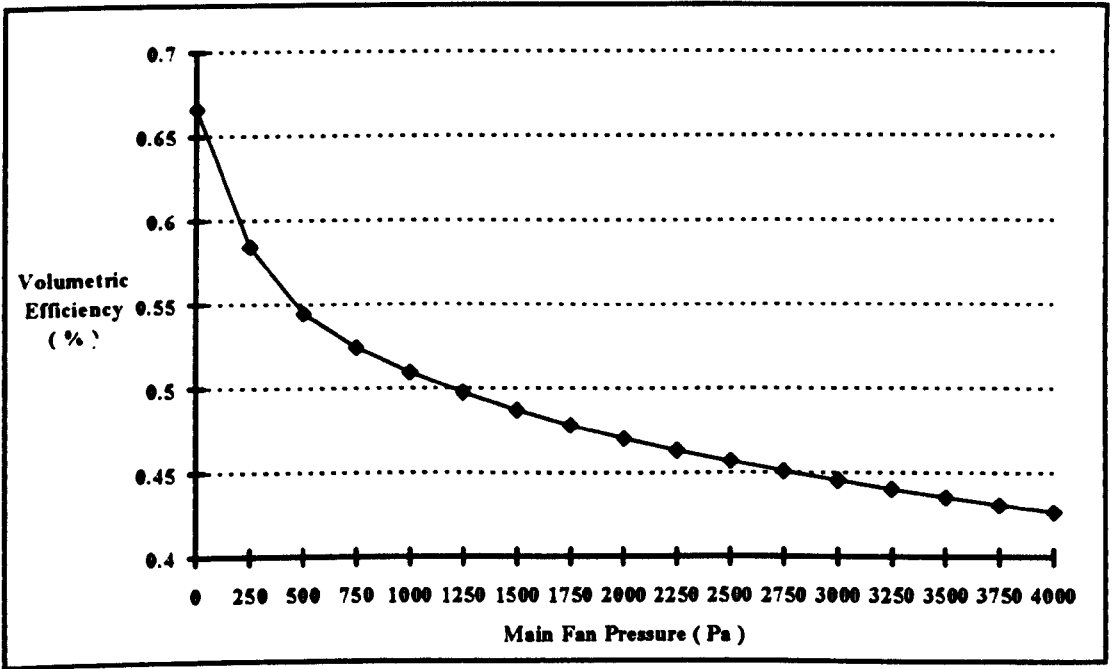


Figure 8.11. Volumetric Efficiency in the two fan system for increasing main fan pressure.

8.2 Case Study 2 - Clipstone Colliery

Clipstone colliery is situated in the Nottinghamshire coalfield, 5 miles north east of Mansfield. Shafts were first sunk in 1920 and 1922, and these are two of the deepest in the country at 920 metres. Coal is mined from the Yard and Deep Soft seams.

The exercises carried out were based on the ventilation plan from July 1991 (see Figure 8.12). The network at this time had one division of flow with air ventilating 3 advancing longwall faces (107's, 110's and 118's) in the eastern split of the mine and 1 advancing longwall face (204's) and one face currently under salvage (202's) in the split to the west. These splits have been designated 100's split for the 3 faces and 200's split for the single face and salvage.

| Face(Branch) | Quantity (m^3/s) |
|----------------|------------------------------------|
| 107's (78) | 13.6 |
| 202's (148) | 10.3 |
| 204's (157) | 19.6 |
| 110's (163) | 14.9 |
| 118's (173) | 12.9 |

Table 8.9 The airflow quantities specified in the Clipstone network.

The approach to this network, as opposed to the Bilsthorpe network, is more general with no pre-regulation obvious from the data and no characteristics considered for fans already present in the network.

The computer simulation exercises performed on the network, using the fixed face airflow quantities specified in Table 8.9, considered in turn the application of ;

- (i) A single surface main fan only.
- (ii) The installation of a booster fan in the split of highest resistance.
- (iii) The installation of a booster fan in the split of lowest resistance
- (iv) The installation of a booster fan in both splits.

Figure 8.12. Diagrammatic layout of Clipstone colliery.

8.2.1 The One Fan System

The ventilation simulation was again run initially with a single surface fan. Results for the added resistance of regulation required to maintain flow on these faces for varying fan pressures, between 2.5 and 8.5 kPa, are shown in Table 8.10 and Figure 8.13.

| Main Fan Pressure (Pa) | Added Resis. (107's) | Added Resis. (202's) | Added Resis. (204's) | Added Resis. (110's) | Added Resis. (118's) |
|--------------------------|------------------------|------------------------|------------------------|------------------------|------------------------|
| 2500 | -2.475 | -10.912 | -1.257 | -1.636 | -0.637 |
| 3000 | -2.168 | -9.043 | -0.854 | -1.469 | -0.516 |
| 3500 | -1.969 | -7.099 | -0.417 | -1.334 | -0.444 |
| 4000 | -1.869 | -5.114 | 0.039 | -1.266 | -0.403 |
| 4500 | -1.700 | -3.079 | 0.513 | -1.186 | -0.340 |
| 5000 | -1.459 | -0.999 | 1.004 | -1.050 | -0.280 |
| 5500 | -1.165 | 1.114 | 1.507 | -0.895 | -0.252 |
| 6000 | -0.832 | 3.256 | 2.020 | -0.724 | -0.225 |
| 6500 | -0.464 | 5.426 | 2.542 | -0.535 | -0.163 |
| 7000 | -0.067 | 7.618 | 3.073 | -0.330 | -0.076 |
| 7500 | 0.353 | 9.831 | 3.611 | -0.113 | 0.028 |
| 8000 | 0.795 | 12.062 | 4.156 | 0.114 | 0.148 |
| 8500 | 1.254 | 14.310 | 4.706 | 0.351 | 0.279 |

Table 8.10. Added resistance required, to maintain specified airflows, for each fixed flow branch with increasing fan pressure.

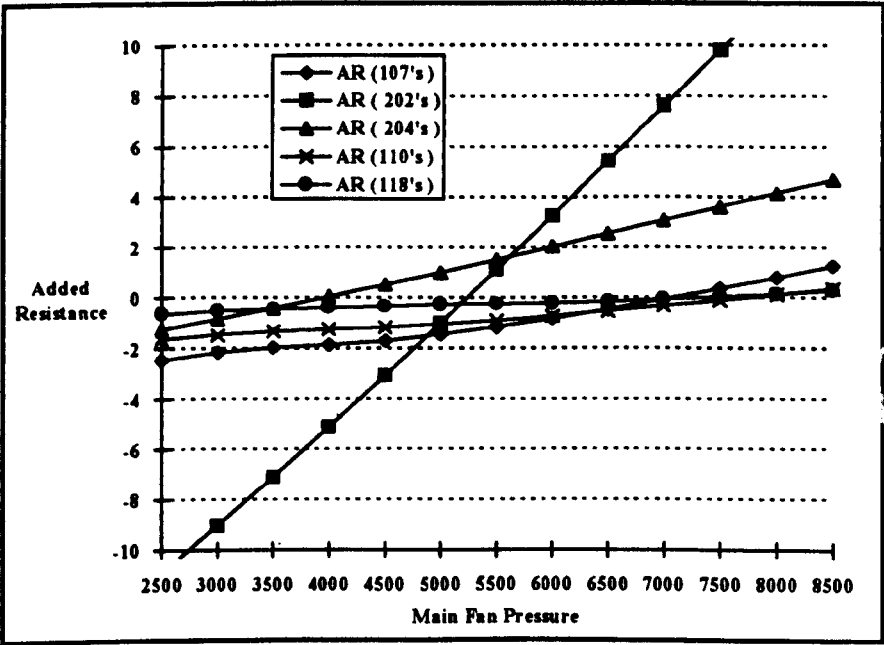


Figure 8.13. Actual added resistance required to maintain specified airflows with increasing fan pressure.

Results of the regression analysis to produce relationships of the form ;

$$P_m = b.AR + c$$

are shown in Table 8.11 and Figure 8.14.

| | b | c |
|------------|------|------|
| 107's Face | 1924 | 7476 |
| 202's Face | 242 | 5206 |
| 204's Face | 1032 | 3907 |
| 110's Face | 3579 | 8481 |
| 118's Face | 8806 | 7688 |

Table 8.11. Coefficients from linear regression analysis of data presented in Table 8.10.

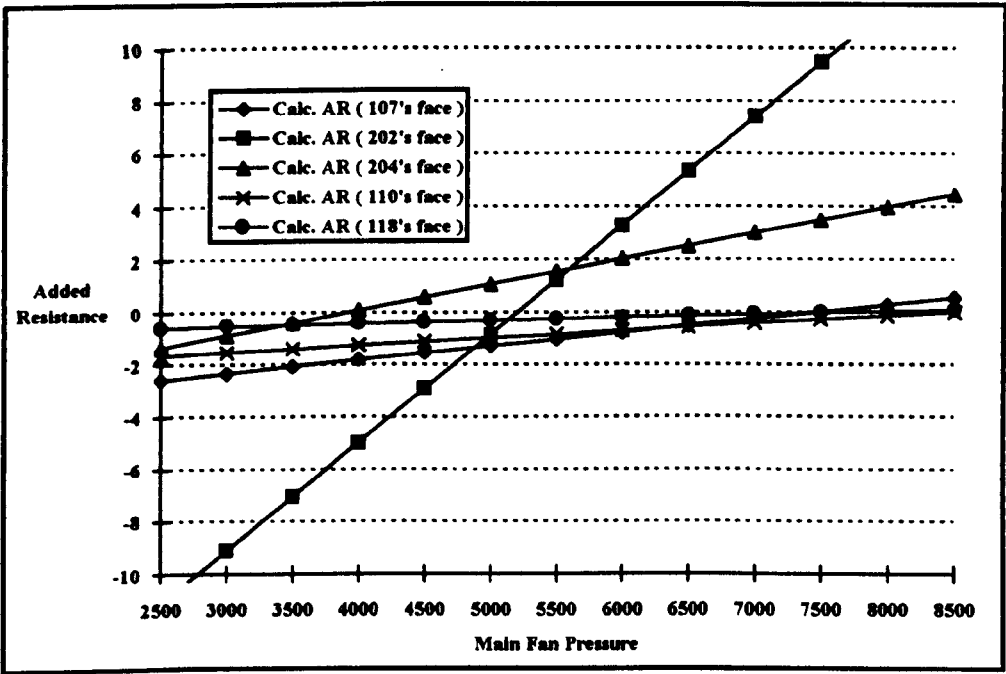


Figure 8.14. Calculated added resistance required to maintain specified airflows with increasing fan pressure.

The coefficient, c, in Table 8.11 indicates the main fan pressure required to give zero added resistance on each face. It can be deduced that the pressure differentials required to maintain the required airflows in the two splits of the network are 5206

Pascals (in 200's districts) and 8481 Pascals (in 100's districts). At a fan pressure of 8.5 kPa the air power delivered by the main fan is 2966 kW. It can be seen that the regulation required on the faces in 100's split are influenced very little by the main fan pressure. The significant changes in the added resistance on 202's face with increasing main fan pressure is explained by the face being in a low resistance path through the network and requiring a smaller fixed flow than the other faces. The extra pressure supplied by the main fan may be dissipated by increased leakage which is not desirable and by the term $AR.Q^2$, to maintain the fixed flow Q across the face. This is to be expected as an uprate of the main fan will produce an increase in the differential pressure across all parallel paths in the network inclusive of leakage paths. The simulation program will only apply regulation on the gate roads of the faces and not uprate the regulation required across leakage paths.

As leakage is an undesirable characteristic of any mine ventilation network it is necessary to quantify the leakage occurring in conjunction with increasing fan duty.

A conclusion of this simulation is that for all practicable purposes it is not possible to achieve the desired face airflows with the application of a single main surface fan. It is therefore necessary to consider the application of underground booster fans.

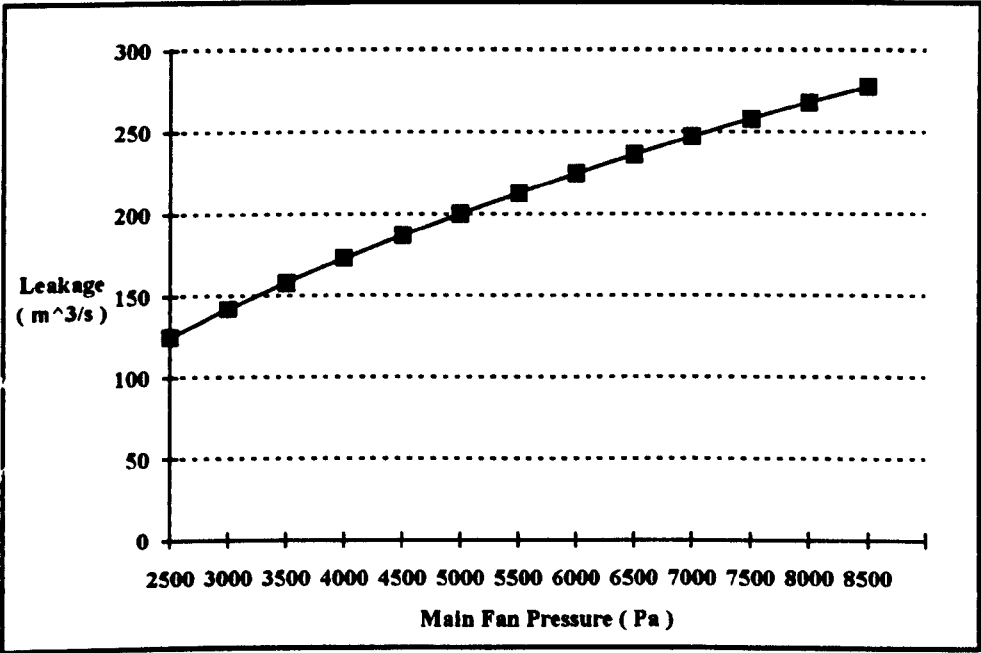


Figure 8.15. Total Leakage with increasing main fan pressure.

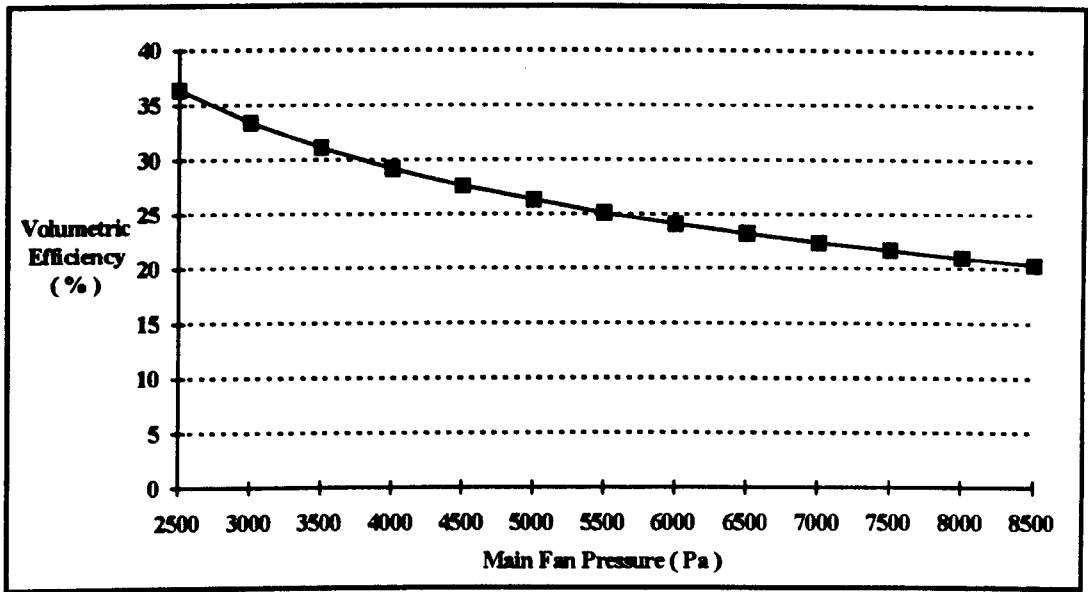


Figure 8.16. Volumetric efficiency with increasing main fan pressure.

8.2.2 The Two Fan System - Booster in High Resistance Split

In this case the ventilation was provided by a main surface fan in conjunction with a booster fan positioned in the return trunk roadway on 100's split close to the pit bottom (see Figure 8.12). Executing the program for this two fan system with varying fan pressure combinations produced the series of results shown in Tables 8.12 and 8.13 ;

| Main Fan Pressure (Pa) | Booster Fan Pressure (Pa) | Added Resis. (107's) Ns ² m ⁻⁸ | Added Resis. (202's) Ns ² m ⁻⁸ | Added Resis. (204's) Ns ² m ⁻⁸ | Added Resis. (110's) Ns ² m ⁻⁸ | Added Resis. (118's) Ns ² m ⁻⁸ |
|--------------------------|-----------------------------|---|---|---|---|---|
| 2500 | 3500 | -0.951 | -9.940 | -0.289 | -0.918 | -0.253 |
| 2750 | 3250 | -0.953 | -8.726 | -0.109 | -0.909 | -0.252 |
| 3000 | 4500 | 0.136 | -7.931 | 0.501 | -0.442 | -0.125 |
| 3250 | 4000 | -0.062 | -6.549 | 0.613 | -0.514 | -0.155 |
| 3500 | 2500 | -0.943 | -5.460 | 0.470 | -0.874 | -0.251 |
| 3750 | 3000 | -0.428 | -4.201 | 0.864 | -0.646 | -0.202 |
| 4000 | 2750 | -0.420 | -3.167 | 1.070 | -0.630 | -0.197 |
| 4250 | 3750 | 0.552 | -1.780 | 1.620 | -0.199 | -0.014 |
| 4500 | 4250 | 1.193 | -0.569 | 2.048 | 0.093 | 0.136 |
| 2500 | 4500 | -0.244 | -10.392 | -0.005 | -0.626 | -0.196 |

Table 8.12 Regulation for each fixed flow branch with varying main and booster fan pressure combinations.

| | a | b | c |
|------------|--------|------|------|
| 107's Face | -0.969 | 1281 | 7161 |
| 202's Face | 0.009 | 211 | 4603 |
| 204's Face | -0.272 | 944 | 3740 |
| 110's Face | -0.846 | 2619 | 7930 |
| 118's Face | -0.754 | 6299 | 7065 |

Table 8.13. Coefficients from linear regression analysis of data presented in Table 8.12.

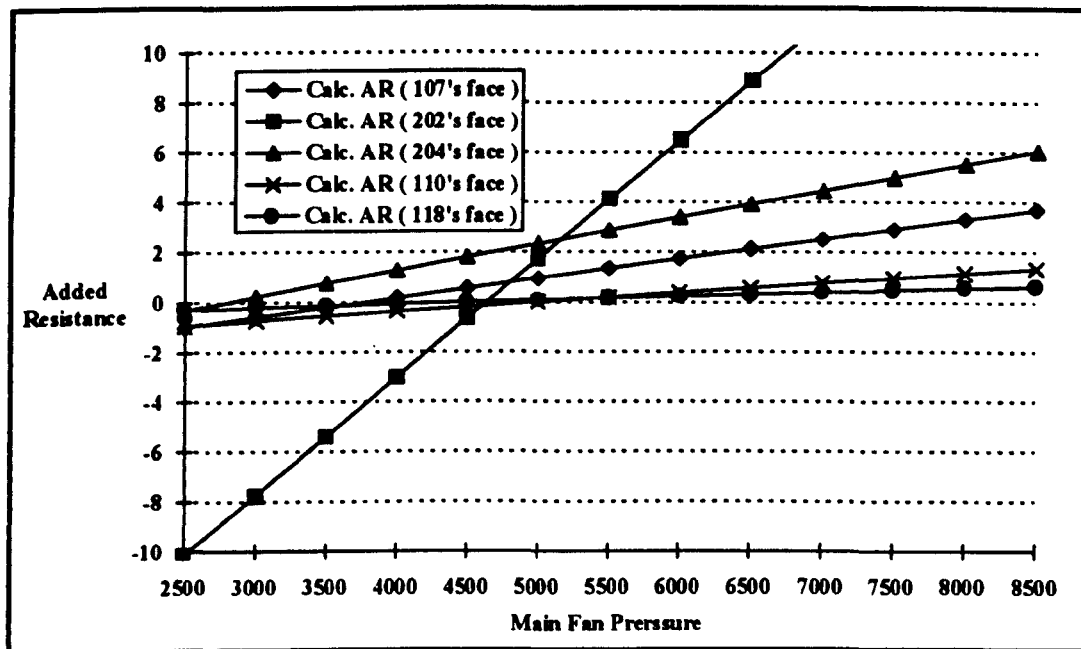


Figure 8.17. Added resistance required to maintain specified airflows with increasing main fan pressure and a booster fan pressure of 3500 Pa.

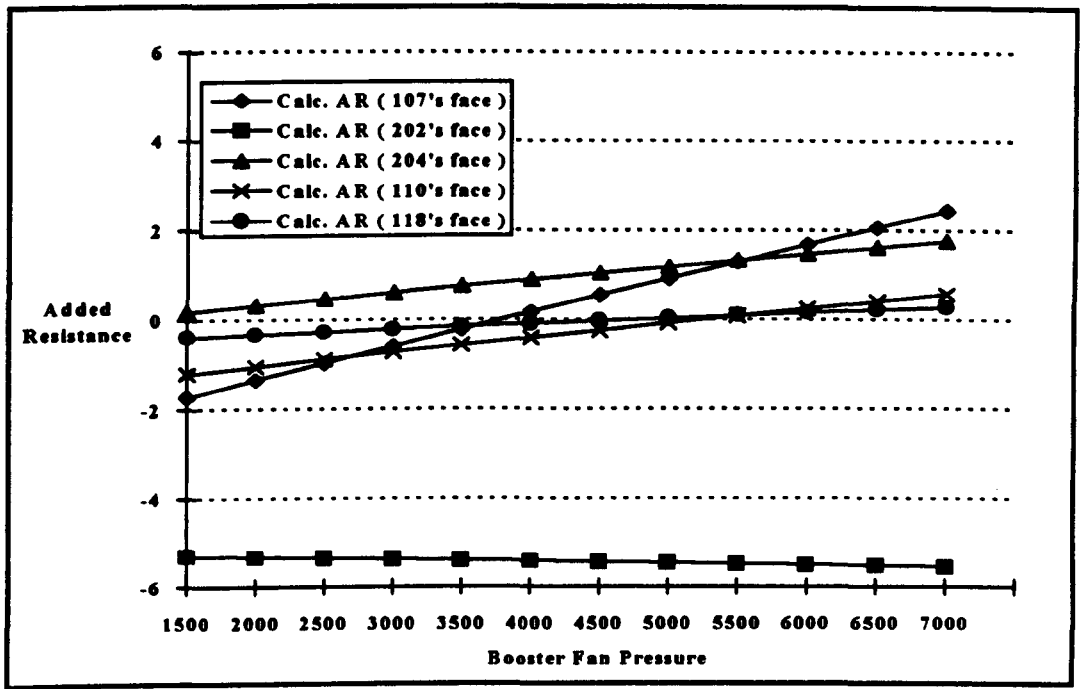


Figure 8.18. Added resistance required to maintain specified airflows with increasing booster fan pressure and a main fan pressure of 3500 Pa.

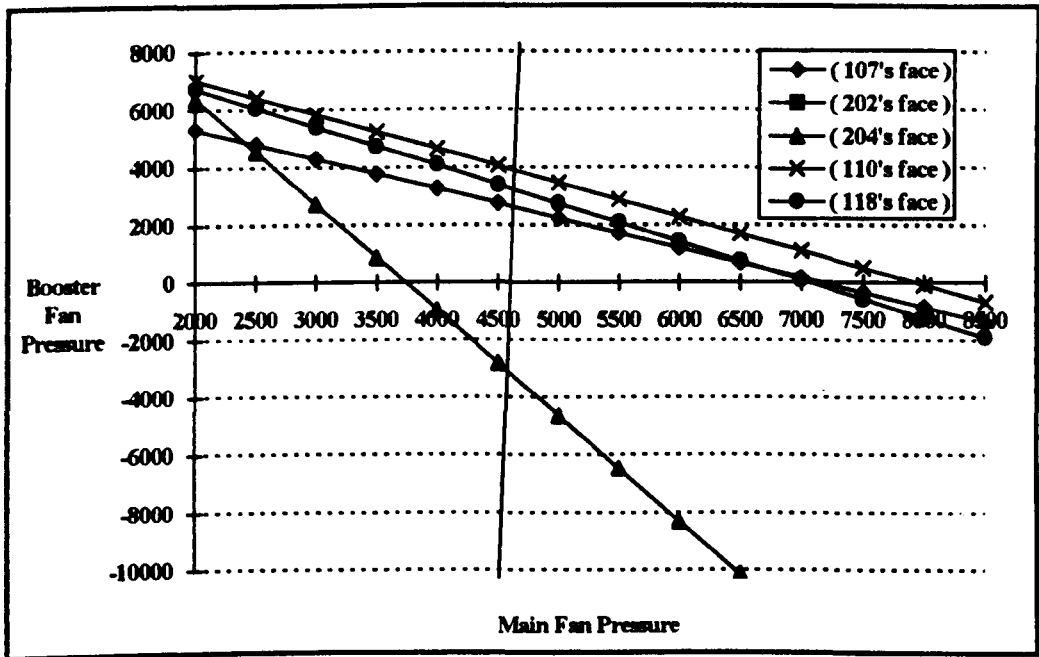


Figure 8.19. Main and booster fan pressure combinations for zero regulation on each fixed flow face.

Figure 8.18 demonstrates the effect of increasing the pressure of the booster fan in the high resistance split whilst maintaining the main fan pressure at 3.5 kPa. No variation is observed in the amount of regulation required on 202's face to maintain the specified

airflow. Very small changes are seen on 204's face and the 3 faces in the booster fan split. Figure 8.19 reinforces this point with the near vertical line indicating a main fan pressure of approximately 4.6 kPa required to maintain the flow on 202's face. However, as described in section 8.2.1, the one fan system suggested that a fan pressure of approximately 5.2 kPa would be necessary to maintain the flow on this face. As with any network problem careful analysis must be made to ensure that the redistribution of both pressure and airflow does not induce flow reversal and uncontrolled recirculation. The booster fan in 100's split is reducing the main fan pressure requirement of 202's face by 600 Pascals. Table 8.14 demonstrates all the practicable combinations of main and booster fan pressures to achieve the optimum flow distribution.

| Intersection of Faces | Main Fan Pressure (Pa) | Main Fan Quantity (m ³ /s) | Booster Fan Pressure (Pa) | Booster Fan Quantity (m ³ /s) | Air Power (kW) |
|-----------------------|--------------------------|---|-----------------------------|--|------------------|
| 107's, 202's | 4627 | 282 | 2614 | 134 | 1656 |
| 107's, 118's | 6725 | 315 | 450 | 119 | 2176 |
| 202's, 118's | 4633 | 286 | 3224 | 142 | 1784 |
| 202's, 110's | 4639 | 290 | 3888 | 150 | 1930 |
| 204's, 118's | 1860 | 227 | 6903 | 166 | 1568 |
| 204's, 110's | 1751 | 226 | 7302 | 169 | 1631 |

Table 8.14. Intersection points of the lines of zero added resistance.

The lines of zero added resistance (Figure 8.19) demonstrate that the three faces 107's, 110's and 118's in the same split all follow the same trends with varying fan pressure combinations. The fan pressure combination chosen, therefore, will nearly always satisfy the required airflows on the three faces in this split. However the combination chosen will have a noticeable effect on the added resistance required in the other split to maintain the pre-assigned airflows on those faces.

This is demonstrated in Table 8.15. The regulation required on the remaining faces is given for each fan pressure combination illustrated in Table 8.14

| Zero Regulation on Faces | Regulation required on remaining faces (Ns^2m^{-8}) | |
|--------------------------|--|---------|
| 107's, 202's | 204's Face | 1.730 |
| | 110's Face | -0.428 |
| | 118's Face | -0.119 |
| 107's, 118's | 202's Face | 6.820 |
| | 204's Face | 3.081 |
| | 110's Face | -0.281 |
| 202's, 118's | 107's Face | 0.450 |
| | 204's Face | 1.897 |
| | 110's Face | -0.220 |
| 202's, 110's | 107's Face | 1.007 |
| | 204's Face | 2.096 |
| | 118's Face | 0.098 |
| 204's, 118's | 107's Face | 1.285 |
| | 202's Face | -15.072 |
| | 110's Face | -0.005 |
| 204's, 110's | 107's Face | 1.569 |
| | 202's Face | -15.071 |
| | 118's Face | 0.147 |

Table 8.15 Regulation required to maintain pre-assigned airflows.

The optimum combination will involve zero regulation on 202's and another face indicated by an intersection of the regression lines (for example shown on Figure 8.19). From Table 8.15 the only practical intersection is between 202's and 110's faces which require no more pressure to be supplied to the system to maintain the flows on the remaining three faces. The main fan pressure will therefore be 4639 Pascals and the booster fan 3888 Pascals with an air power consumption of 1930 kW. This is a reduction of 1036 kW (35%) in the air power delivered by the single surface fan system.

To gain any further reduction in the pressure delivered by the surface fan requires the installation of a booster fan in the low resistance split. The following section will consider the case of a main surface fan and the installation of a booster fan in this low resistance split in isolation.

8.2.3 Two Fan System - Booster in Low Resistance Split

In this case the exhausting booster fan was positioned in a major trunk return roadway close to the pit bottom. Executing the program for this two fan system with varying fan pressure combinations produced results shown in Tables 8.16 and 8.17 ;

| Main Fan Pressure (Pa) | Booster Fan Pressure | Added Resis. (107's) | Added Resis. (202's) | Added Resis. (204's) | Added Resis. (110's) | Added Resis. (118's) |
|--------------------------|----------------------|------------------------|------------------------|------------------------|------------------------|------------------------|
| 2500 | 3500 | -2.440 | 0.942 | -0.877 | -1.554 | -0.574 |
| 2750 | 3250 | -2.275 | 1.051 | -0.645 | -1.471 | -0.517 |
| 3000 | 4500 | -2.129 | 6.503 | -0.360 | -1.378 | -0.462 |
| 3250 | 4000 | -2.021 | 5.705 | -0.136 | -1.322 | -0.443 |
| 3500 | 2500 | -1.952 | 1.468 | 0.060 | -1.291 | -0.432 |
| 3750 | 3000 | -1.903 | 4.224 | 0.334 | -1.265 | -0.401 |
| 4000 | 2750 | -1.847 | 4.379 | 0.570 | -1.236 | -0.371 |
| 4250 | 3750 | -1.754 | 8.921 | 0.868 | -1.163 | -0.327 |
| 4500 | 4250 | -1.643 | 11.748 | 1.149 | -1.083 | -0.292 |
| 4750 | 4750 | -1.513 | 14.606 | 1.438 | -0.996 | -0.265 |

Table 8.16 Added resistance of each fixed flow branch for varying main and booster fan pressure combinations.

| | a | b | c |
|------------|--------|------|------|
| 107's Face | -0.033 | 2671 | 8948 |
| 202's Face | 0.869 | 244 | 5319 |
| 204's Face | -0.047 | 996 | 3556 |
| 110's Face | -0.106 | 4578 | 9849 |
| 118's Face | -0.088 | 7907 | 7172 |

Table 8.17. Coefficients from linear regression analysis of results presented in Table 8.16.

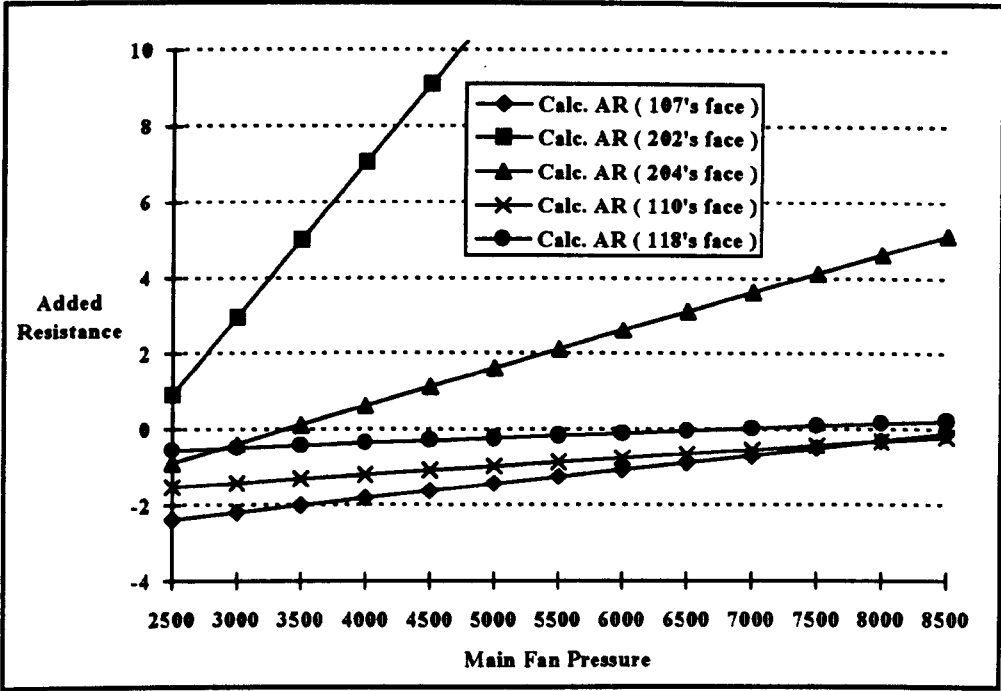


Figure 8.20. Added resistance required to maintain specified airflows for increasing main fan pressure and a booster fan pressure of 3500 Pa.

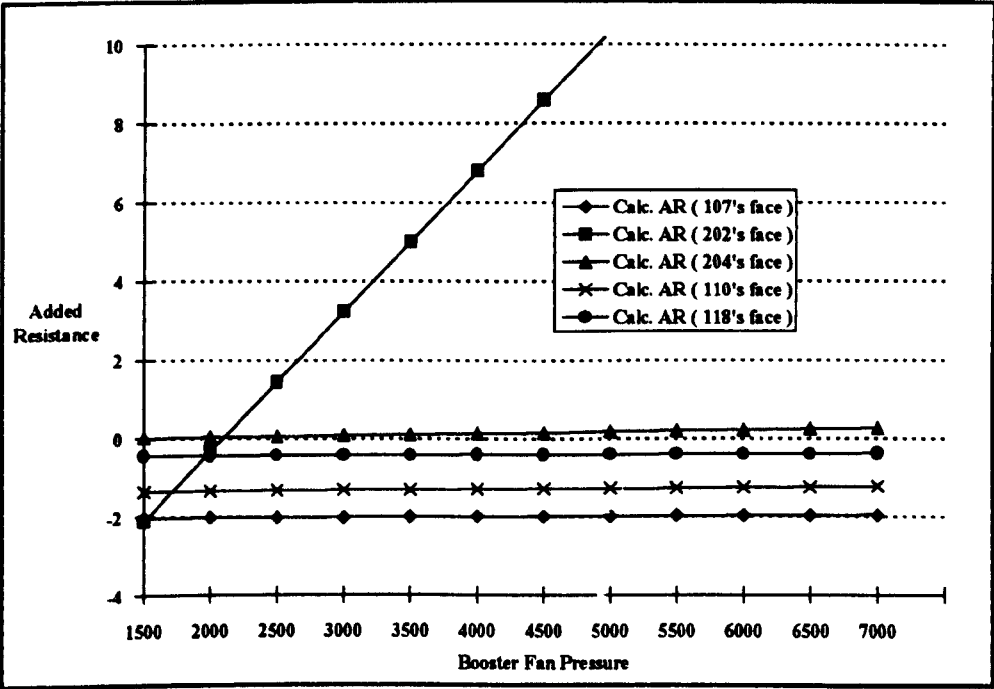


Figure 8.21. Added resistance required to maintain specified airflows for increasing booster fan pressure and a main fan pressure of 3500 Pa.

Figure 8.20 demonstrates a noticeable rate of change in the added resistances on 202's face and 204's face for increasing main fan pressure. Figure 8.21 demonstrates that the

booster fan has no influence on the extra regulation required to maintain the flows on faces in 100's split. All the pressure required to maintain flows on these faces would have to be supplied by the main fan. The booster fan in 200's split is therefore acting purely as a flow control as opposed to an energy saving device as would be expected for a booster fan not placed in the high resistance split. This booster fan is in fact widening the pressure requirements of the two individual splits. To achieve the objective of a reduction in the air power consumption in the network it is necessary to search for a combination of fans which will reduce the pressure requirements of each split in the network. Figure 8.21 indicates that majority of the main fan duty is being used to overcome the pressure drops in the high resistance split.

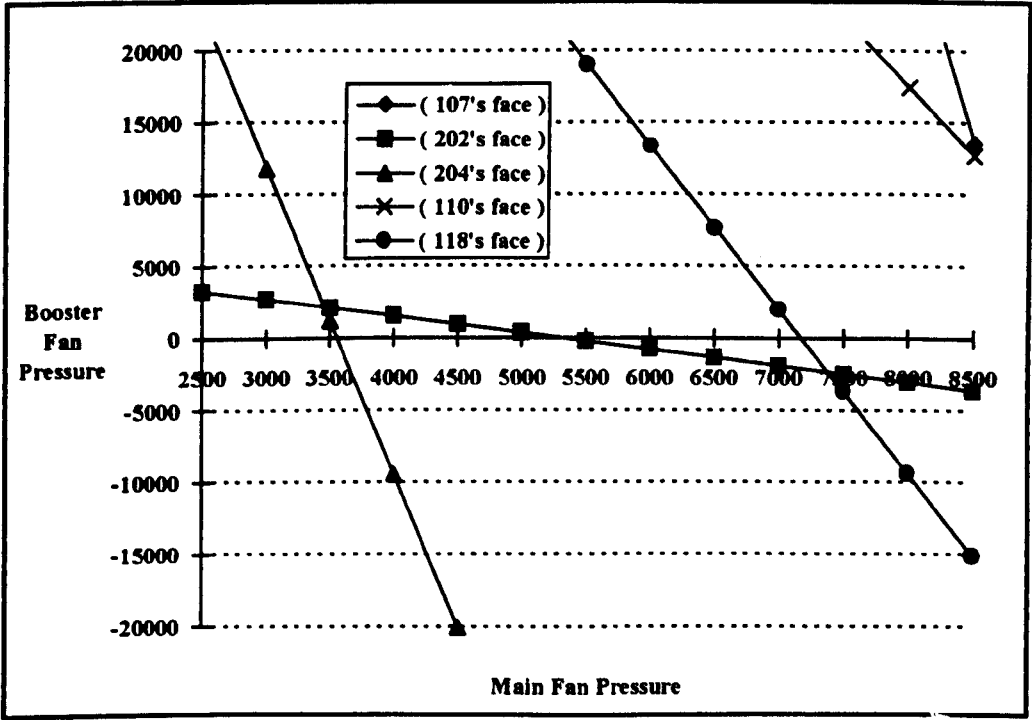


Figure 8.22. Main and booster fan pressure combinations for zero regulation on each fixed flow face.

Figure 8.22 demonstrates that the intersection of the lines of zero regulation necessary for 202's face and 204's face would give pressure requirements of the two fans shown in Table 8.18.

| Zero Regulation on Faces | Main Fan Pressure (Pa) | Main Fan Quantity (m ³ /s) | Booster Fan Pressure (Pa) | Booster Fan Quantity (m ³ /s) | Air Power (kW) |
|--------------------------|--------------------------|---|-----------------------------|--|------------------|
| 204's, 202's | 3455 | 236 | 2145 | 61 | 946 |

Table 8.18 Intersection Point for 202's and 204's Face.

However pressure is still needed to maintain the airflows in the high resistance split. The possibility of installing underground fans in both 100's and 200's split must now be examined.

8.2.4 Three Fan System - Booster Fan in Each Split

It should be noted that the optimisation analyses using this method can only be performed using two varying fan pressure combinations. Once a three fan system is considered it becomes necessary to specify one of the fan pressures. In the analysis performed for this system the main fan pressure was maintained at 3.5 kPa.

A booster fan was now installed in the same return trunk roadways (specified in sections 8.2.2 and 8.2.3) at the pit bottom in each split. The regression exercises were carried out on varying combinations of the two booster fan pressures. This gave the results shown in Tables 8.19 and 8.20.

| Booster Fan Pressure, 100's split (Pa) | Booster Fan Pressure 200's split (Pa) | Added Resis. (107's) (Ns ² m ⁻⁸) | Added Resis. (202's) | Added Resis. (204's) | Added Resis. (110's) | Added Resis. (118's) |
|--|---|--|------------------------|------------------------|------------------------|------------------------|
| 2500 | 3500 | -0.718 | 7.474 | 2.470 | -0.635 | -0.198 |
| 2750 | 3250 | -0.547 | 6.809 | 2.593 | -0.560 | -0.172 |
| 3000 | 4500 | -0.308 | 11.555 | 3.141 | -0.406 | -0.110 |
| 3250 | 4000 | -0.133 | 9.997 | 3.220 | -0.337 | -0.079 |
| 3500 | 2500 | -0.014 | 4.799 | 2.777 | -0.339 | -0.080 |
| 3750 | 3000 | 0.215 | 6.853 | 3.186 | -0.211 | -0.020 |
| 4000 | 2750 | 0.402 | 6.184 | 3.197 | -0.137 | 0.016 |
| 4250 | 3750 | 0.677 | 10.079 | 3.866 | 0.037 | 0.106 |
| 4500 | 4250 | 0.925 | 12.159 | 4.260 | 0.175 | 0.181 |
| 2500 | 4500 | -0.684 | 11.062 | 2.690 | -0.591 | -0.183 |

Table 8.19 Added resistance on each fixed flow face for varying booster fan combinations.

| | a | b | c |
|------------|--------|------|------|
| 107's Face | -0.077 | 1247 | 3699 |
| 202's Face | -3.693 | 1017 | 7845 |
| 204's Face | -0.485 | 1294 | 1081 |
| 110's Face | -0.173 | 2618 | 4807 |
| 118's Face | -0.199 | 5576 | 4417 |

Table 8.20 Results calculated from linear regression of data presented in Table 8.19

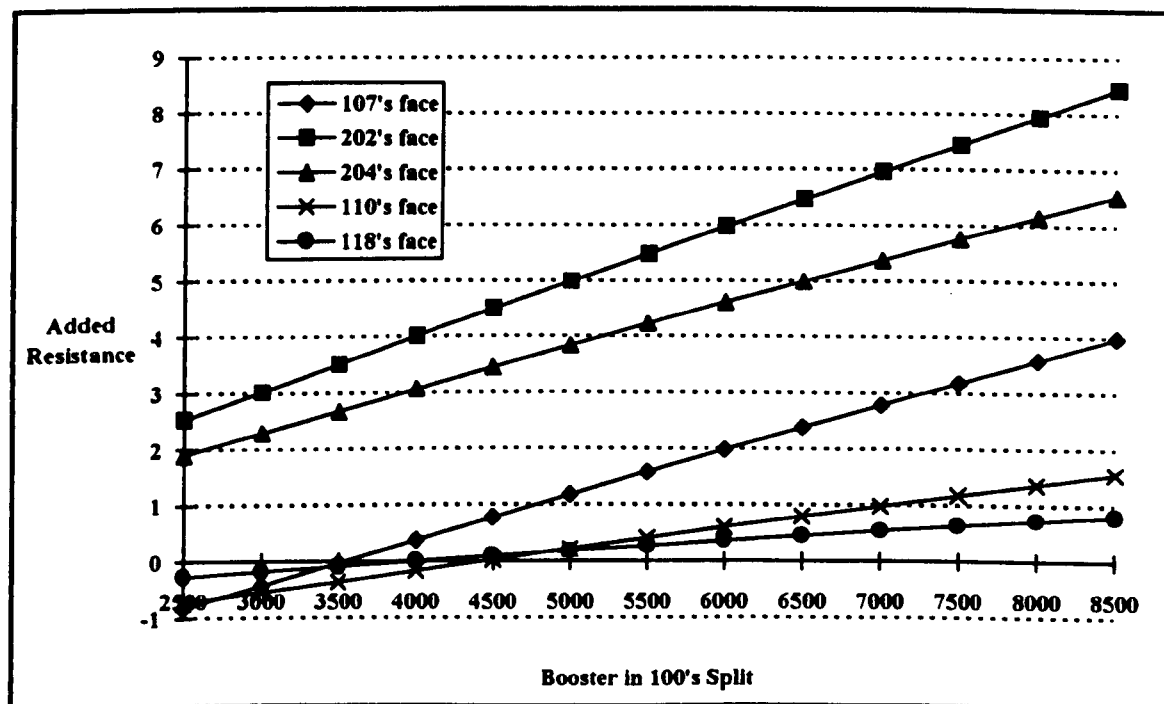


Figure 8.23. Booster fan in 200's split set at 2145 Pa

As an example of the analysis which must be performed the booster fan installed in 200's split was set at a value of 2145 Pascals as determined from section 8.2.3. From Figure 8.23 with this fixed booster fan pressure, the optimum booster fan pressure in 100's split to maintain the required airflows would be 4250 Pa.

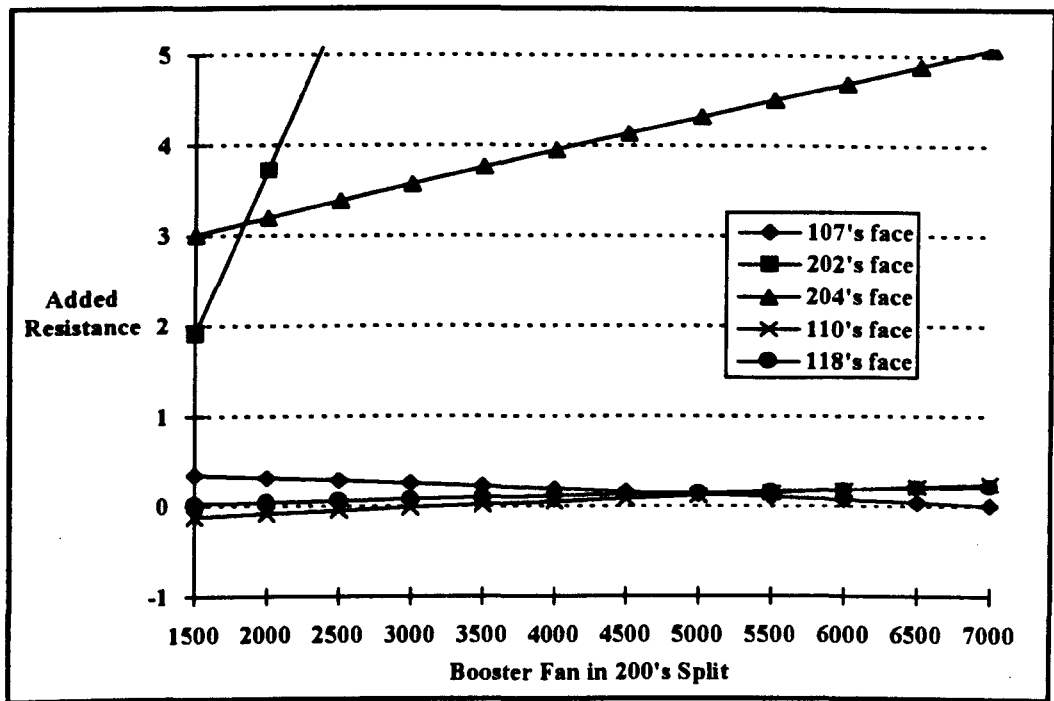


Figure 8.24. Booster fan in 100's split set at 4250 Pa

| Main Fan Pressure (Pa) | Main Fan Quantity (m ³ /s) | Boost. Fan Pressure 100's split (Pa) | Boost. Fan Quantity 100's split (m ³ /s) | Boost. Fan Pressure 200's split (Pa) | Booster Fan Quantity 200's split (m ³ /s) | Air Power (kW) |
|-----------------------------|--|--|---|--|--|---------------------|
| 3500 | 276 | 4250 | 138 | 2145 | 45 | 1675 |

Table 8.21 Suggested fan pressures for the 3 fan system

| Fixed Quantity Faces | Added Resis. (N s ² m ⁻⁸) |
|-------------------------|--|
| 107's | 0.560 |
| 202's | 4.223 |
| 204's | 2.907 |
| 110's | -0.099 |
| 118's | 0.035 |

Table 8.22 Regulation required for the 3 fan system results presented in Table 8.21

A solution for the three fan system is shown in Table 8.21. The quantity of air flowing through the two booster fans is 183 m³/s. The remaining 93 m³/s (= 276 - 183) is lost through leakage paths in the pit bottom and through the surface air lock. The air power consumed by the network has now been reduced to 1675 kW from the 1930 kW necessary in the two fan system discussed in section 8.2.2.

Further analyses may be performed on this 3 fan system by considering a range of fixed booster fan pressures in 200's split.

8.3 Summary and Conclusions

This chapter has illustrated the application of the optimisation program described in Chapter 7, by performing analyses on the mine ventilation networks of two representative British Coal collieries namely Bilsthorpe and Clipstone. Both of the collieries exhibit major splits in their ventilation networks.

A series of optimisation exercises were performed on these networks. In the first case the ventilation circuits were examined solely by the application of a single main surface fan. The required duties of these main fans, to maintain prescribed fresh airflows in the working areas, were determined. These exercises demonstrated that the selective application of underground booster fans in the major splits of the network were necessary to reduce the overall power consumption and afford better control of the airflow distribution.

For the case of Bilsthorpe colliery a single booster fan installation was able to service the power requirement of both splits in the network. Results demonstrated that the network was currently optimally regulated and the analysis became one of finding the optimum combination of main and booster fan duties. Installation of the single booster fan unit reduced the overall air power requirements of the network by 296 kW or (26.4 %).

The configuration of Clipstone colliery possesses an immediate splitting of the network at the pit bottom. Analyses were performed to investigate the effect of positioning a single booster fan installation in each split of the network in turn. Results demonstrated the small effect of booster fan installation on regulation requirements of faces in the other split. However when the booster fan was installed in the high resistance split the total air power delivered by fans in the network dropped significantly compared to that of a single main surface fan. When positioned in the split of low resistance the booster fan was shown to be acting purely as a flow control device in that split. The analyses demonstrated that in order to reduce the overall air power delivered further the installation of a booster fan in both splits becomes necessary.

Upon the installation of a booster fan in both splits of the network, the air power consumed was reduced to 1675 kW from 2966 kW for the one fan system and from 1930 kW for the two fan system.

In the general case the location of booster fan installations is another variable which may be included as part of the optimisation process. However in both of the case studies considered the booster fan location was severely restricted due to the complexity of the network at the pit bottom and the location of the network splits. This is a feature common to many of the older British Coal collieries.

These exercises have confirmed the applicability of this optimisation method for the comparison of main and booster fan combinations in order to investigate the optimum total air power requirements to maintain the prescribed fresh airflows at all working areas within the network.

The optimisation procedures are not automated but require the user to guide the processing of the data and any subsequent analysis. Therefore a knowledge of the rational behind the methods must be understood before any practical interpretation of the results may be made.

Chapter 2

General Conclusions and Suggestions for Further Work

2.1 General Conclusions

The objective of the research work carried out as the second part of this project, was to present a critical review of optimisation methods applied to the analysis of mine ventilation networks. Chapter 6 outlined mine ventilation planning strategies and followed this by presenting a discussion of previous research concerning the application of numerical optimisation techniques. A critical analysis of the previous research highlighted the suitability of one particular method. This method introduced by Calizaya et al [65] [66] was combined with the *linear theory method* in the development of a computer simulation program. The application of this program is illustrated by performing an optimisation analysis on the ventilation networks of two representative U.K. collieries.

Chapter 6 presented the basic principles which may be employed in mine airway calculations. These principles, together with simplifying assumptions, may be combined to provide a mathematical equation governing the turbulent, incompressible flow within a single mine ventilation airway. This equation may be generalised, by appealing to mathematical network theory, to simulate the flow and pressure distribution within an entire mine ventilation network. The subsequent equations may then be solved by the application of suitable numerical solution techniques.

A number of commercial programs are available to solve the conventional mine ventilation planning problems. VNETPC developed by Mine Ventilation Services (MVS) in the U.S.A. and VENT, the British Coal program both use an incompressible approach with air being injected should any deviation from this assumption take place. VENTFLOW developed by the Chamber Of Mines Research Organisation (COMRO) in South Africa takes density changes into account and is widely applicable to the deep, hot workings experienced in that country.

The principal objective in the design of a mine ventilation system is the provision of a sufficient quantity of fresh air at a correct velocity to all working areas. The maintenance and distribution of this airflow is controlled by the selective application of fans and regulators. There are a number of feasible solutions from which the ventilation engineer must select the ' best ' or most economic system configuration such

that pre-assigned airflow quantities are achieved with the minimum power consumption. This optimisation problem lends itself naturally to solution using operation research techniques.

The specification of branch air flows (e.g. the minimum required fresh airflow quantities in working areas) has resulted in the development of a number of optimisation techniques. These vary according to whether the specified flows define the complete flow distribution in the network or whether some branch air flows remain undetermined. The mathematical complexity of some methods makes them difficult to implement and a more graphically based, user interactive, approach was adopted to analyse the ' generalised controlled flow ' problem. This method determines the optimum position and duty of fans and regulators whilst, at the same time, not specifying the complete flow distribution in the network.

Chapter 8 illustrates the application of the optimisation program described in Chapter 7, by performing optimisation analyses on the mine ventilation networks of two representative British Coal collieries namely Bilsthorpe and Clipstone. Both of the collieries exhibit major splits in their ventilation networks.

Initially the ventilation circuits, for both Case Studies, were examined by the sole application of a single main surface fan. The required duties of these main fans, to maintain prescribed fresh airflows in the working areas, were determined. These exercises demonstrated that the selective application of underground booster fans in the major splits of the network were necessary to reduce the overall power consumption and afford better control of the airflow distribution.

For the case of Bilsthorpe colliery a single booster fan installation was able to service the power requirement of both splits in the network. Results demonstrated that the network was currently optimally regulated. The analysis determined the optimum combination of main and booster fan duties. Installation of the single booster fan unit reduced the overall air power requirements of the network by 296 kW (26.4 %).

The configuration of Clipstone colliery is more complex. The network possesses an immediate two way split at the pit bottom. Analyses were performed to investigate the effect of positioning a single booster fan installation in each split of the network in turn. Results demonstrated the small effect of booster fan installation on regulation requirements of faces in the other split. However, with a single booster fan installed in the high resistance split, the total air power delivered by the fans in the network

dropped significantly compared to that of a single main surface fan. When a single booster fan is positioned in the low resistance split it was shown to be acting purely as a flow control device in that split. The analyses demonstrated that in order to reduce the overall air power delivered and effect improved airflow and pressure control a booster fan in both splits of the network becomes necessary.

In the general case the location of booster fan installations is another variable which may be included as part of the optimisation process. However in both of the case studies considered the booster fan location was severely restricted due to the complexity of the pit bottom of the network and the location of the network splits. This is a feature common to many of the older British Coal collieries.

These exercises have confirmed the applicability of this optimisation method for the comparison of main and booster fan combinations in order to investigate the optimum total air power requirements to maintain the prescribed fresh airflows within the network.

The optimisation procedures are not automated but require the user to guide the processing of the data and any subsequent analysis. Therefore a knowledge of the rational behind the methods must be understood before any practical interpretation of the results may be made.

9.2 Suggestions for Further Work

9.2.1 Further Correlation Studies

An initial further development of this work should be further correlation exercises on other representative colliery ventilation networks. This further development should be in close conjunction with the operational mine ventilation engineers.

9.2.2 Automation of Analysis Procedure

The colliery ventilation networks investigated have serious restrictions on the choice of suitable booster fan locations. Other modern colliery networks may provide a number of alternative booster fan locations for analysis. The program may be further developed to automate the consideration of the number, duty and location of potential booster fan and regulator installations to achieve the desired air flow and pressure distribution.

ACKNOWLEDGEMENTS

Professor D. Potts, Head, Department Mineral Resources Engineering, University of Nottingham for the provision of the facilities with which to conduct this research.

Dr. I.S. Lowndes for his supervision, encouragement and advice.

Mr. I. Longson of the Department of Mineral Resources Engineering, University of Nottingham for his valuable input through discussions at various stages of the work.

Mr. F. Stout, Group Ventilation Engineer for the Nottinghamshire Group, British Coal and his support staff for their interest in the project and help in seeking suitable test sites.

The Managers at Harworth and Thoresby collieries for their permission to use underground methane drainage range data.

Mr. P. Shead, Head of Environment, Harworth Colliery, British Coal for his support with work carried out at that colliery.

Messrs. K. Mosely and C. Lane for their assistance in the measurement of data from the underground methane drainage range at Thoresby Colliery.

Messrs. S. Bennett, S. Kershaw and Dr. D. Creedy, Environment Branch, TSRE, Bretby, British Coal for their co-ordination of the project.

To the European Coal and Steel Community and to British Coal for the financial support to carry out the project.

REFERENCES

- [1] ' Time-Dependent Changes Associated With the Stopping and Re-Starting of Booster Fans. ', Final Report, ECSC 7258-05/08/129, British Coal Corporation
- [2] Hargraves A.J. 'Seam Gas and Seam Gas Drainage.' in Australasian Coal Mining Practice, Aus.I.M.M., Monograph Series no. 12, 1987, pp393-411.
- [3] Coward H.F. ' Explosibility of atmospheres behind stoppings '. Trans. of the Inst. of Mining Engineers, Vol. 77, 1928-29, pp94-115.
- [4] Mines and Quarries Act. 'The Law Relating to Safety and Health in Mines and Quarries. Part 1 The Act, Part 2 Regulations.' HMSO, 1954.
- [5] Zhao X. and Harpalani S. 'Investigation of Factors Affecting Release of Methane in Coalbeds.' Proceedings of the 4th U.S. Mine Ventilation Symposium, Berkeley, California, 1989, pp525-531.
- [6] Hargraves A.J. 'Review of Seam Gas Drainage in Australia.' Bull. Proc. Aus. I.M.M., Vol. 290, No. 1, Feb. 1985, pp55-70.
- [7] McPherson M.J. 'The Occurence of Methane in Mine Workings.' Journal of the Mine Ventilation Society of South Africa, Vol. 28, No. 8, 1975, pp118-125.
- [8] Ettinger I.L. et al 'Systematic Handbook for the Determination of the Methane Content of Coal Seams from the Seam Pressure of the Gas and the Methane Capacity of the Coal.' NCB Translations, A1606.
- [9] Jolly D.C., Morris L.H., Hinsley F.B. 'An Investigation into the Relationship Between the Methane Sorption Capacity of Coal and Gas Pressure.' The Mining Engineer, Vol. 127, No. 94, Jul. 1968, pp539-548.

- [10] Langmuir I. 'The Constitution and Fundamental Properties of Solids and Liquids.' *Journal of the American Chemical Society*, Vol. 38, 1916, pp2221-2295.
- [11] Curl S.J. 'Methane Prediction in Coal Mines' *IEA Coal Research*, 1978, 79p.
- [12] Gunther J. 'Investigation of the Relationship Between Coal and the Gas Contained in it.' *Revue de L'industrie Minerale*, Vol. 47, No. 10, 1965, 693p.
- [13] Graham J.I. 'The Measurement of the Quantity and Pressure of Methane in Coal.' *Trans. of the Inst. of Mining Engineers*, Vol. 94, 1937-38, pp122-135.
- [14] Kim A.G. 'Estimating the Methane Content of Bituminous Coalbeds from Adsorption Data.' *USBM, Report No. RI 8245*, 1977, 22p.
- [15] Kissell F.N. et al 'The Direct Method for Determining Methane Content of Coalbeds for Ventilation Design.' *USBM, Report No. RI 7767*, 1973, 22p
- [16] King R.L. 'Design of a Methane Control Expert System.' *Underground Mining Methods and Technology*, Elsevier Science Publishers, B.V. Amsterdam, 1987, pp11-19.
- [17] Creedy D.P. 'Methods for the Evaluation of Seam Gas Content from Measurements on Coal Samples.' *Mining Science and Technology*, Vol. 3, 1986, pp141-160.
- [18] Airey E.M. 'Gas Emission from Broken Coal : An Experimental and Theoretical Investigation.' *Int. Journal of Rock Mechanics and Mining Science*, Vol. 5, 1968, pp475-494.
- [19] Airey E.M. 'A Theory of Gas Emission in Mining Operations.' *MRDE Report No. 21*, 1971.

- [20] Lama R.D. and Bartosiewicz H. 'Determination of Gas Content of Coal Seams.' Symposium on Seam Gas Drainage with Particular Reference to the Working Seam, Aus. I.M.M., 1982, pp36-52.
- [21] Dunmore R. 'Prediction of Gas Emission from Longwall Faces.' The Mining Engineer, Vol. 140, Feb. 1981, pp565-572.
- [22] Klinkenberg L.J. 'The Permeability of Porous Media to Liquids and Gases', Drilling and Production Practice, Published by the American Petroleum Institute, 1941, pp200-211.
- [23] Gawuga J.K. 'Flow of Gas Through Stressed Carboniferous Strata.' Ph.D. Thesis, University of Nottingham, 1979.
- [24] Harpalani S. and McPherson M.J. 'Effect of Gas Pressure on the Permeability of Coal.' Proceedings of the 2nd U.S. Mine Ventilation Symposium, Reno, Nevada, 1985, pp369-375.
- [25] Fatt I. and Davies D.H. 'Reduction in Permeability with Overburden Pressure.' Transactions of the AIME, Petroleum Branch, Vol. 195, 1952, p329.
- [26] Mordecai M. and Morris L.H. 'The Effect of Stress on the Flow of Gas through Coal Measure Strata.', The Mining Engineer, Vol. 133, 1974, pp435-443.
- [27] Somerton W.H., Soylemezoglu I.M. and Dudley R.C. 'Effect of Stress on Permeability of Coal.' International Journal of Rock Mechanics Mining Science Geomechanics Abstracts, Vol. 12, 1975, pp129-145.
- [28] Durucan S. 'An Investigation into the Stress-Permeability Relationships of Coals and Flow Patterns Around Working Longwall Faces.' Ph.D. Thesis, University of Nottingham, Oct. 1981.
- [29] Keen T.F. 'The Simulation of Methane Flow in Carboniferous Strata.' Ph.D. Thesis, University of Nottingham, Oct. 1977.

- [30] O'Shaughnessy S.M. 'The Computer Simulation of Methane Flow Through Strata Adjacent to Working Longwall Coal Faces.' Ph.D. Thesis, University of Nottingham, May 1980.
- [31] Ediz I.G. 'An Application of Numerical Methods to the Prediction of Strata Methane Flow in Longwall Mining.' Ph.D. Thesis, University of Nottingham, October 1991.
- [32] Mills R. A. and Stevenson J.W. 'Improved mine safety and productivity through a methane drainage system.' Proc. 4th U.S. Mine Ventilation Symposium. , Berkeley , CA , U.S.A. 1989 , pp477-483
- [33] De Villiers A.W. ' Methane Drainage in Longwall Coalmining. ' J.S.Afr.Inst.Min.Metall. , Vol.89 , no.3 , Mar. 1989 , pp61-72.
- [34] ' Firedamp Drainage ; A handbook for the coalmining industry in the European Community. ' Verlag Gluckauf for the Coal Directorate of the Commission of the European Communities , 1980 , 415pp.
- [35] Thakur P.C. and Dahl H. D. ' Methane Drainage. ' In Mine Ventilation and Air Conditioning , Wiley, New York, 1982, pp69-83
- [36] Hargraves A. J. and Lunarzewski L. 'Review of Seam Gas Drainage in Australia', Proc.Aus.I.M.M. , Vol.290 , no.1 , Feb. 1985 , pp55-70.
- [37] Highton W. 'Experience with Pre-Drainage of Seam Gas in the Western Area of the National Coal Board.' Symposium on Seam Gas Drainage with particular reference to the Working Seam. , Aus.I.M.M., 1982, pp124-140.
- [38] Hungerford F. et al 'Long-Hole drilling for gas emission control at Appin Colliery NSW, Australia' Proc. 4th International Mine Ventilation Congress. , Brisbane, Queensland, 1988, pp207-216.
- [39] Hebblewhite B.K. et al ' Australian Experience in Long-Hole Drilling Technology for Seam Gas Drainage'. Symposium on Seam Gas Drainage with particular reference to the Working Seam. , Aus.I.M.M. , 1982 , pp202-217.

- [40] Marshall P. et al ' Experiences on Pre-Drainage of Gas at West Cliff Colliery '. Symposium on Seam Gas Drainage with particular reference to the Working Seam. , Aus. I.M.M., 1982 , pp141-156
- [41] Morris I. H. 'Firedamp Drainage.' The Min. Electr. Mech. Engr, vol.43 , Jan. 1963 , pp175-193.
- [42] Morris I.H. 'Firedamp Drainage Installations.' Symposium on Seam Gas Drainage with particular reference to the Working Seam, Aus. I.M.M. , 1982 , pp306-320
- [43] Thakur P.C. et al 'Methane Drainage with cross-measure boreholes on a retreat longwall face.' Mining Eng. (NY) , vol.37 , no.12 , Dec. 1985 , pp1375-1380.
- [44] Wood J. E. and Yates D.C. 'Controlled Drainage of Firedamp from Old Workings into a Firedamp Drainage System.' Transactions of the Institution of Mining Engineers, 1957-58, vol.117, pp4-22.
- [45] Cervik J. et al 'Experience with cross-measure boreholes for gob gas control on retreating longwalls.' Proc. 2nd U.S. Mine Ventilation Symposium , Reno , NV , 1985 , pp123-129
- [46] Bromilow J. G. 'Firedamp Drainage in Great Britain.' Trans. The Inst. of Mining Engineers, Vol. 111 , 1951-1952 , pp1012 -1040
- [47] Swift R. A. ' Methane Drainage in Great Britain.' Coal Age , vol.75 , Feb. 1970, pp94-99.
- [48] Steele E. and Yates D.C. ' The L evelopment and Application of Methane Drainage in the North Staffordshire Coalfield.' Transactions of the Institution of Mining Engineers, vol.119, Jan. 1960 , pp213-228.
- [49] Highton W. ' Retreat Mining Methane Drainage. ' Symposium on Seam Gas Drainage with particular reference to the Working Seam. , pp141-156. Aus.I.M.M.

- [50] Wharton P.B. ' Some Observations on the Drainage and Emission of Firedamp. ' The Mining Engineer , vol.121 , Jun. 1962 , pp577-589.
- [51] Harper P.J. and Harrison G. ' An Introduction to the Planning and Control of Methane Drainage Ranges Using Computers. ' The Mining Engineer , Vol.147 , Nov.1987 , pp255-260.
- [52] P. R. Shead , Head of Environment, Harworth Colliery, British Coal - Private Communication.
- [53] Pawinski J., Roszkowski J., Szlajak N. ' Nodal-Mesh Equations for the Methane Removal Network in Mines and their Practical Application ' . Archives of Mining Sciences, Polish Academy of Sciences, Vol. 37 , Issue 1, 1992, pp 3 - 19
- [54] F. Stout, Group Ventilation Engineer, British Coal, Nottinghamshire Group - Private Communication.
- [55] Lowndes I.S. , Hu W. ' The Application of Optimization Methods to Mine Ventilation Planning ' , University of Nottingham, Mining Department Magazine, vol. XL, 1988, pp 39-47.
- [56] Longson I. , Tuck M. ' Improving Mine Ventilation ' , Mining Magazine, October 1989, pp313 - 317.
- [57] Longson I. et al ' Booster Fans-Prediction and Measurement of the Ventilation System Response to Stopping and Re-starting. with Consideration of the Impact on Underground Environmental Safety and Control ' , Proceedings, 5th International Mine Ventilation Congress, Johannesburg, South Africa, 1992, pp 11- 19.
- [58] ' Colliery Ventilation Officers Handbook ' , British Coal, p53.
- [59] McPherson M. J. ' Ventilation Network Analysis ' . In ' Mine Ventilation and Air Conditioning. ' , Mine Ventilation Soc. of South Africa, 1989, p211 - 239.

- [60] Atkinson J.J. ' On the theory of the ventilation of mines ', Trans. of the North of England Instn. of Mining Engineers, Vol. 3, p. 118.
- [61] McPherson M. J. ' Friction Factor Tables ', Department of Mining Engineering, University of Nottingham.
- [62] Minieka E. ' Optimization Algorithms for Networks and Graphs ', Marcel Dekker, New York, 1978, pp 19-24.
- [63] Christofides N. ' Graph Theory : An Algorithmic Approach ', Academic Press. New York, 1975, pp 197-199.
- [64] Cross H. ' Analysis of Flow in Networks of Conduits or Conductors ', University of Illinois, Engineering Experiment Station, Bulletin 286, 1936.
- [65] Kim J. H. , Mutmanský J. M. , Wang Y. J. ' Generation of random networks for evaluation of mine ventilation network methods ' Proceedings, 5th U.S. Mine Ventilation Symposium , University of West Virginia, Morgantown, WV, U.S.A., 1991, pp 419-426.
- [66] Tominaga Y. , Matsukura H. , Higuchi K. ' Algorithm for fast simulation of mine ventilation using dual microcomputers ' Proceedings, 2nd U.S. Mine Ventilation Symposium, University of Nevada, Reno, NV, U.S.A. , 1985, pp 499 - 505.
- [67] Jeppson R.W. ' Analysis of Flows in Pipe Networks ', Ann Arbor Science, Ann Arbor, Michigan, 1976.
- [68] Scott D.R. , Hinsley F.B. ' Ventilation Network Theory - Parts I - IV ', Colliery Engineering, vol. 28, 1951, pp 67-71 , 159-166 , 229-235 , 497-500.
- [69] Wang Y.J. , Li S. 'The Newton Method of Calculating the Ventilation Network' Proceedings, 2nd Conference on the Use of Computers in the Coal Industry, AIME, New York, 1985, pp 388-392.

- [70] Wang Y.J. , Saperstein L.W. ' Computer-Aided Solution of Complex Ventilation Networks ', Transactions of the Society of Mining Engineers, AIME, vol. 247, Sep. 1970, pp 238-250.
- ✓ [71] Epp R. , Fowler A.G. ' Efficient Code for Steady-State Flows in Networks ', Journal of the Hydraulics Division, ASCE, vol. 96, no. HY1, January 1970, pp 43-56.
- ✓ [72] Wood D.J. , Rayes A.G. ' Reliability of Algorithms for Pipe Network Analysis ', Journal of the Hydraulics Division, ASCE, vol. 107, no. HY10, October 1981, pp 1145 - 1161.
- [73] Wood D.J. , Charles C.O.A. ' Hydraulic Network Analysis Using Linear Theory ', Journal of the Hydraulics Division, ASCE, vol. 98, no. HY7, July 1972, pp 1157-1170.
- [74] Martin D.W. , Peters G. ' The Application of Newton's Method of Network Analysis by Digital Computer ', Journal of the Institute of Water Engineers, vol. 17, pp 115-129.
- ✓ [75] Yevdokimov A.G. ' A theory of the solution of steady-state network problems with special reference to mine ventilation networks ', International Journal of Numerical Methods in Engineering, vol. 1, 1969, pp 279-299.
- [76] Duff I.S. ' Data Structure, Algorithms and Software for Sparse Matrices ', Sparsity and its Applications, Cambridge University Press, London, pp 1-29.
- [77] Kim J.H. , Mutmanský J.M. ' A summary of experimental findings on solution methods for mine ventilation networks ', Proceedings, 5th U.S. Mine Ventilation Symposium, University of West Virginia, Morgantown, WV, U.S.A., 1991, pp 361-371.
- [78] Isaacs L.T. , Mills K.G. ' Linear Theory Methods for Pipe Network Analysis ', Journal of the Hydraulics Division, ASCE, vol. 106, no. HY7, July 1980, pp 1191 - 1201.

- [79] Bhamidipati S. , Procarione J.A. ' Linear analysis for the solution of flow distribution problems in mine ventilation networks ', Proceedings, 2nd U.S. Mine Ventilation Symposium, University of Nevada, Reno, NV, U.S.A., 1985, pp 645-654.
- [80] Ueng T.H. , Wang Y.J. ' Analysis of mine ventilation networks using nonlinear programming techniques ', International Journal of Mining Engineering, vol. 2, 1984, pp 245-252.
- [81] Wang Y.J. ' A Non-linear Programming formulation for Mine Venilation Networks with Natural Splitting ', International Journal of Rock Mechanics, Mining Science and Geomechanics, vol. 21, no. 1, 1984, pp 43-45.
- [82] Wang Y.J. , Pana M.T. ' Solution of ventilation network problems by linear programming ', SME Preprint no. 71-AU-132, AIME Annual meeting, New York, 1971.
- [83] Barnes R.J. , Johnson T.B. ' The Out-of-Kilter Algorithm and its Application in Mining engineering ', SME Preprint no. 83-102, AIME Annual meeting, Atlanta, Georgia, 1983.
- [84] Johnson T.B. , Barnes R.J. , King R.H. ' The Optimal Controlled Flow Mine Ventilation Problem : An Operations Research Approach ', SME Preprint no. 82-353, AIME Fall meeting, Honolulu, Hawaii, 1982.
- [85] Wang Y.J. , Hartman H.L. , Mutmanský J.M. ' Recent Developments in mine ventilation network theory and analysis ', Proceedings, 2nd U.S. Mine Ventilation Symposium, University of Nevada, Reno, NV, U.S.A., 1985, pp 667-675.
- [86] Wang Y.J. ' A Critical Path Approach to Mine Ventilation Networks with Controlled Flow ', SME Preprint no. 81-23, AIME Annual meeting, Chicago, Illinois, 1981.
- [87] Wang Y.J. , Mutmanský J.M. ' Application of CPM procedures in mine ventilation ', Proceedings, 1st U.S. Mine Ventilation Symposium, University of Alabama, Tuscaloosa, AL, U.S.A., 1982, pp 159-168.

- [88] Price W.L. ' Graphs and Networks ', Butterworths, London, 1971, pp 87-95.
- [89] Fulkerson D.R. ' Expected Critical Path Lengths in PERT Networks ', Operations Research, vol. 10, no. 6, 1962.
- [90] Wang Y.J. ' Ventilation Network Theory ', in Mine Ventilation and Air Conditioning, Wiley, New York, 1982, pp 483-516.
- [91] Hu W. , Longson I. ' A computer method for the generalized controlled flow problem in ventilation networks ', Mining Science and Technology, vol. 8, 1989, pp 153-167.
- [92] Wang Y.J. ' Minimizing Power Consumption in Multiple-Fan Networks by Equalizing Fan Pressure ', International Journal of Rock Mechanics, Mining Science and Geomechanics, vol. 20, no. 4, 1983, pp 171-179.
- [93] Le Roux W.L. ' Energy Economics of Fans in Remotely Parallel Operation ', Journal of the Mine Ventilation Society of South Africa, vol. 34, October 1981, pp 184-185.
- [94] Wang Z. , Yao E.Y. ' Optimum method of regulating a ventilation network ' Proceedings, 3rd International Mine Ventilation Congress, Harrogate, England, 1988, pp 53-55.
- [95] Wu X. , Topuz E. ' The determination of booster fan locations in underground mines ' Proceedings, 3rd U.S. Mine Ventilation Symposium, Pennsylvania State University, Pennsylvania, U.S.A., 1987, pp 401-407.
- [96] Hu W. , Longson I. ' The optimization of airflow distribution in ventilation networks using a nonlinear programming method ', Mining Science and Technology, vol. 10, 1990, pp 209-219.

- [97] Calizaya F. , McPherson M.J. , Mousset-Jones P. ' An algorithm for selecting the optimum combination of main and booster fans in underground mines ' , Proceedings, 3rd U.S. Mine Ventilation Symposium, Pennsylvania State University, Pennsylvania, U.S.A., 1987, pp 408-417.
- [98] Calizaya F. , McPherson M.J. , Mousset-Jones P. ' A computer program for selecting the optimum combination of fans and regulators in underground mines ' , Proceedings, 4th International Mine Ventilation Congress, Brisbane, Queensland, Australia, 1988, pp 141-150.

APPENDICES

Appendix 1

The Pipe Network Simulation Program

A1.1 Introduction

The pipe network simulation program, based on the mathematical model developed in Chapter 3, predicts the flow rates, pressure drops and purities for a methane/air mixture flowing in a drainage range.

The program, a listing of which can be found in this appendix, was written in Fortran77 and developed on personal computers for personal computer use. With the use of FORTRAN subroutines the computer code has been kept as modular as possible thus reducing duplicated code, program size and allowing for easy maintenance and alteration

A1.2 Coding Specifications

A1.2.1 Parameter Statements and Common Blocks

The parameter statement is used to give names to specified constants which may then be used within the program subroutine. The names used by parameter statements are not names of variables and may not have their values changed by the program. The parameter statement is a non-executable statement and must therefore occur before any executable statement.

Common blocks provide means of making the values of variables and arrays in one program routine available to other program routines. Like parameter statements, common blocks are non-executable statements and must again occur before any executable statement.

In the pipe network program parameter statements are written in a file 'NUMBERS' and hold details of the maximum number of junctions and pipes in the network. This file is then 'included' in each subroutine. If the maximum of junctions or pipes is exceeded it is then a simple matter of updating these values in the 'NUMBERS' file and recompiling the program. Use of these values will keep array sizes to an optimum and speed execution of the program.

Common blocks are written in the file 'GEOM.CMN' and hold details of the number of junctions and pipes in the network, junction and pipe characteristics, mass flows, gas constants and extended pipe lengths due to losses across fittings. Details of junctions attached to elements are also held along with file names for the current program. All these variables will be written to the common block during validation of the data.

```

INTEGER MAXPIP, MAXNOD
REAL TEMP, G
PARAMETER ( MAXPIP=50, MAXNOD=50 )
PARAMETER ( TEMP=313.0, G=9.81 )

```

Figure A1.1, Parameter statement file 'NUMBERS'

```

C-----THIS COMMON BLOCK MUST ALWAYS BE INCLUDED JOINTLY
C-----WITH THE PARAMETER STATEMENT 'NUMBERS'.
      REAL      RNODE( MAXNOD, 4 ), RPIPE( MAXPIP, 5 ),
+             MASSFL( MAXPIP ), R( MAXPIP ), ELENT( MAXPIP )
      INTEGER  NODPIP( MAXNOD*3 + MAXPIP*2 )
      INTEGER  NNODES, NPIPES
      CHARACTER*18  CDATA, CBOUND, CRESUL
      COMMON / GEOM / NNODES, NPIPES, NODPIP, RNODE, RPIPE,
+             MASSFL, R, CDATA, CBOUND, CRESUL, ELENT

```

Figure A1.2. Common block file 'GEOM.CMN'

A1.2.2 Subroutine Format

All subroutines have been written to a template shown in Figure A1.3. The header will contain details of supplied and returned variables, a description of the routine and, if necessary, the structure of any arrays used in the subroutine.

A1.2.3 Function Tests

Each subroutine creating internal data arrays or structures will print these structures if requested by the user. This is done by simply setting the logical flag 'LFTEST' and recompiling the appropriate subroutine. i.e.

```

SUBROUTINE XXXXXX( SUP1, SUP2, RET1, RET2, NSTAT )
C-----C
C
C   ONE LINE DESCRIPTION OF FUNCTION OF SUBROUTINE.
C
C   DATE      -   DD-MM-YY
C   AUTHOR    -   A.T.J. MOLL
C   PROJECT   -   PIPE NETWORKS
C
C   SUPPLIED - SUP1   - DESCRIPTION OF SUP1
C
C               SUP2   - DESCRIPTION OF SUP2
C
C   RETURNED - RET1   - DESCRIPTION OF RET1
C
C               RET2   - DESCRIPTION OF RET2
C
C               NSTAT  - STATUS ON EXIT
C
C                       0 - NO ERRORS OR WARNINGS ENCOUNTERED
C
C   EXTERNAL - ANY EXTERNAL SUBROUTINES ETC CALLED.
C
C   MODIFIED - LIST ANY SUPPLIED PARAMETERS OR COMMON BLOCKS THAT
C               ARE MODIFIED IN THE ROUTINE.
C
C   ALGORITHM- DEFINE ANY ALGORITHMS USED IN THE ROUTINE
C
C   STRUCTURE- DEFINE ANY DATA STRUCTURES CREATED.
C
C   DESCRIPTION - A DETAILED DESCRIPTION OF THE PURPOSE OF THE
C               SUBROUTINE.
C-----C
INCLUDE 'PARAMETER FILES'
INCLUDE 'COMMON BLOCKS'
    LOGICAL DECLARATIONS
    INTEGER DECLARATIONS
    REAL DECLARATIONS
    DOUBLE PRECISION DECLARATIONS
    CHARACTER DECLARATIONS
    EXTERNAL DECLARATIONS
C$$$$$FIRST-EXECUTABLE-STATEMENT-MARKER
C-----INITIALISE STATUS ON EXIT
    NSTAT = 0
C$$$$$LAST-EXECUTABLE-STATEMENT-MARKER
    RETURN
    FORMAT
    END

```

Each of the type declarations mentioned will be ordered as follows;
Taking INTEGER as an example

```

INTEGER supplied and returned array variables
INTEGER supplied and returned variables
INTEGER functions
INTEGER local array variables
INTEGER local variables

```

Figure A1.3 Subroutine structure

```

LFTEST = .TRUE.
IF( LFTEST ) THEN
    print data array.
ENDIF

```

The results will be printed in a file named 'FTESTS'.

These function tests allow easy diagnostic checking of the program in the event of any problems arising or after any alterations to the program have been made.

A1.2.4 Status On Exit Flag

Each subroutine will have 'NSTAT' as one of the returned variables. Although not used in the majority of cases this does allow the future monitoring and diagnosis of variables within the routine, and the status of these variables on exit from the subroutine.

A1.3 Structure of the Program

The basic structure of the pipe network program (MESH.EXE) is shown in Figures A1.4 and A1.5. The program can be divided into five basic parts ;

- (i) Data Input
- (ii) Data Validation
- (iii) Calculation of suction and mass flows
- (iv) Calculation of all other results.
- (v) Output of Results

(iii) and (iv) form the main iterative loop of the solution process.

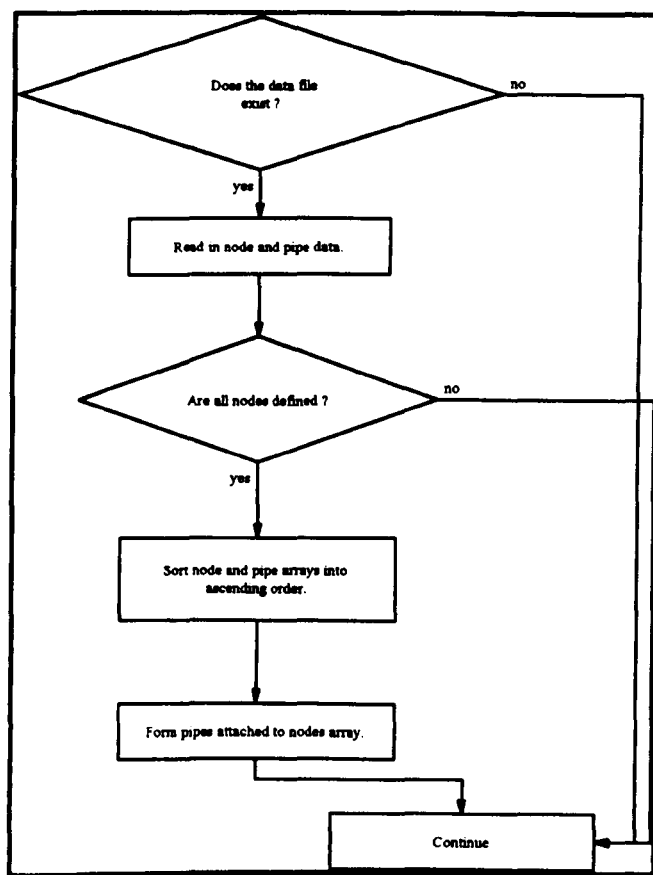


Figure A1.4a. Flowchart for the validation of data.

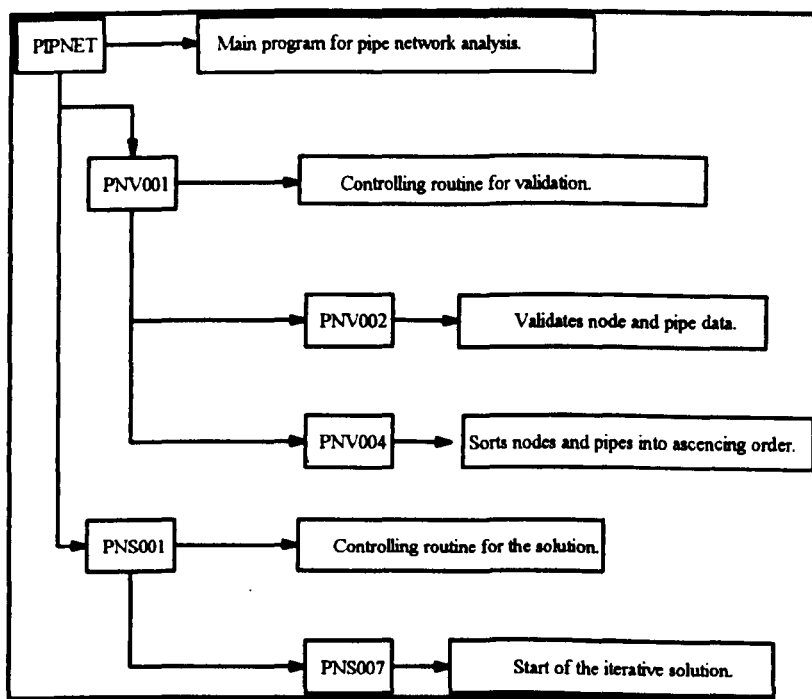


Figure A1.4b. Subroutine structure for the validation of data

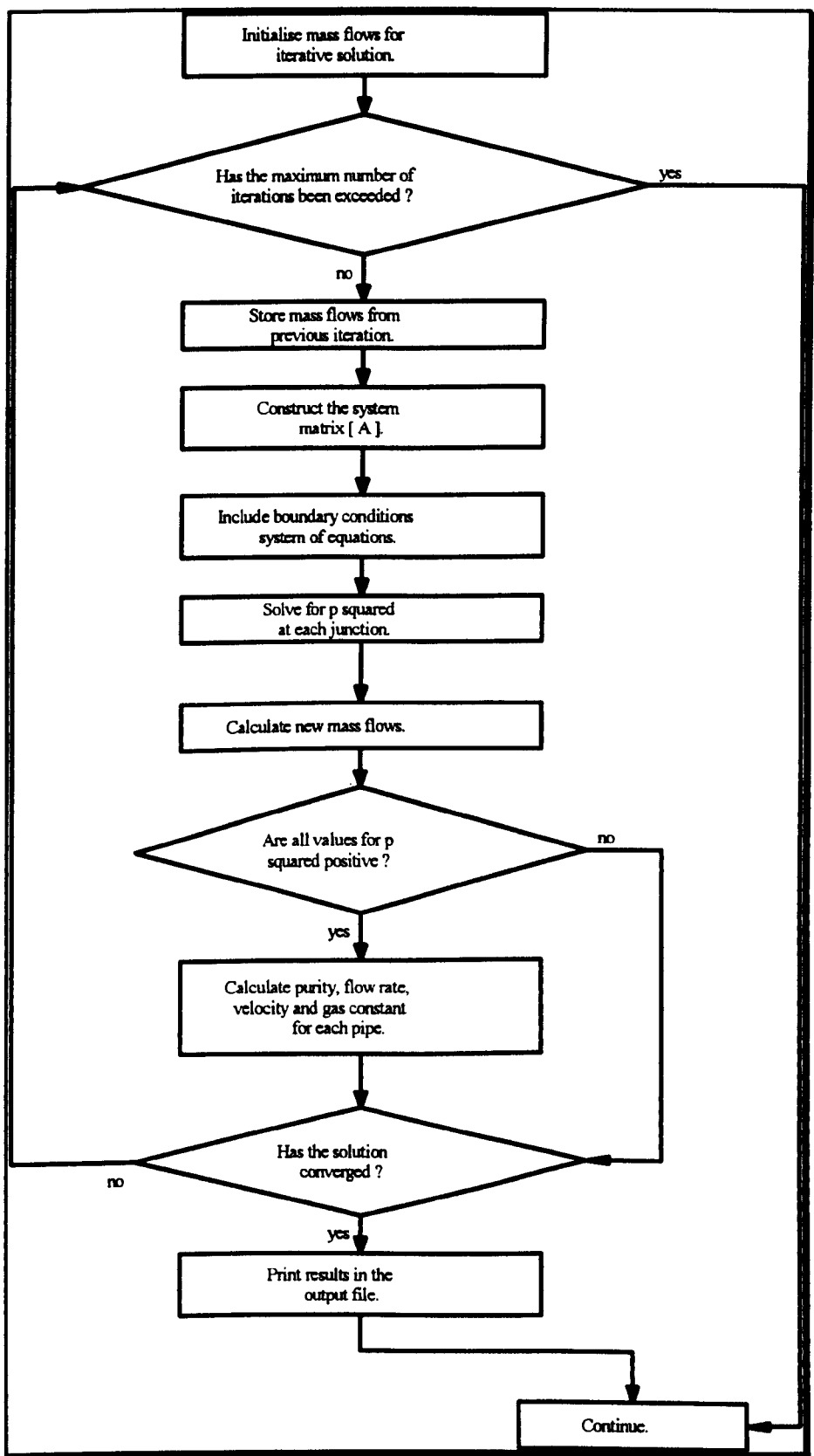


Figure A1.5a. Flowchart for the iterative solution program loop.

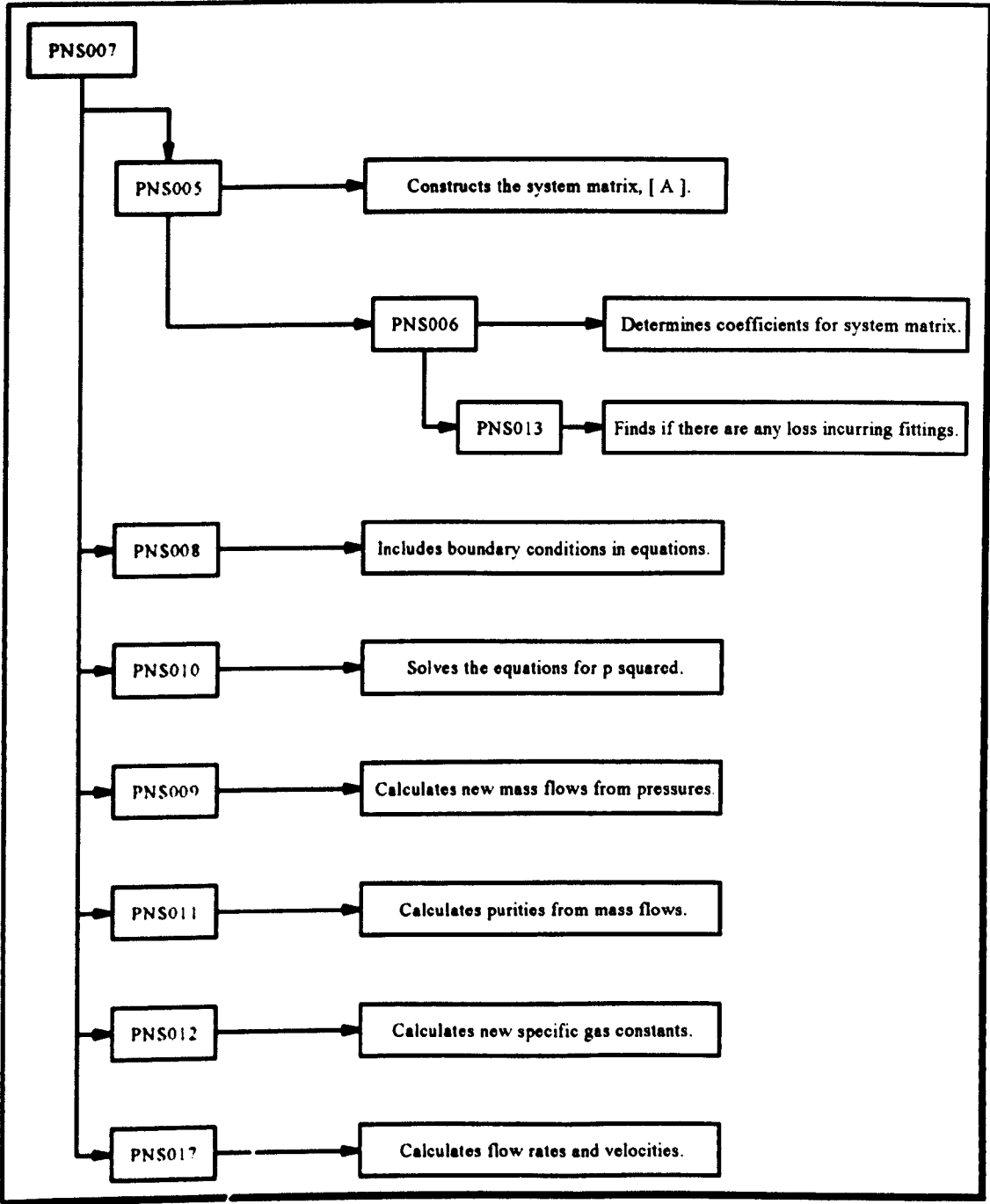


Figure A1.5b. Subroutine structure of the main program loop.

A1.3.1 Data Input

Data required for program execution is read from two text files containing details of the network topology and the boundary conditions. These files are 'DATAXXXX' and 'BOUNXXXX' where 'XXXX' is the four character jobname requested on program initialisation.

A1.3.1.1 DATAXXXX

This will hold details of the junction co-ordinates and pipe characteristics. It is structured as shown in Figure A1.6.

| | | | | |
|------------------------------------|-----------|-----------|----------|-----------------|
| number of junctions in the network | | | | |
| junction 1 | 0.0 | 0.0 | 0.0 | |
| junction 2 | x | y | z | |
| .. | .. | .. | .. | |
| .. | .. | .. | .. | |
| junction n | x | y | z | |
| number of pipes in the network | | | | |
| pipe1 | junction1 | junction2 | diameter | friction factor |
| .. | .. | .. | .. | .. |
| .. | .. | .. | .. | .. |
| pipen | junction1 | junction2 | diameter | friction factor |

Figure A1.6. Structure of the network data file.

The exhausting junction will always be numbered 1 and have co-ordinates (0.0, 0.0, 0.0) i.e. be the origin of the axis set. The axis direction is shown in Figure A1.7. All junction co-ordinates are in metres. Flow along the pipe is assumed from junction1 towards junction2. Again the pipe diameter will be in metres and the friction factor dimensionless. Apart from the node at the origin, junction and pipe numbering need not be sequential and the numbering can be carried out as the user wishes.

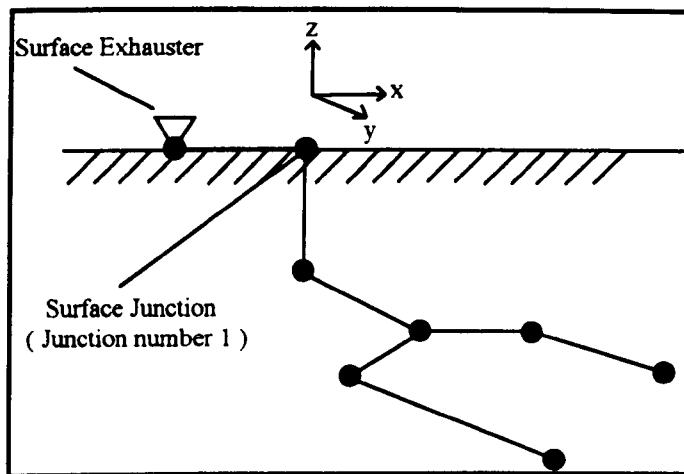


Figure A1.7. The axis set of the methane drainage network.

A1.3.1.2 BOUNXXXXX

This file will hold details of the boundary conditions in the network plus the position of any loss incurring fittings. It is structured as shown in Figure A1.7.

| | | | |
|------------------------------|----------------------|---------|--------|
| Number of boundary junctions | | | |
| junction 1 | flow | suction | purity |
| .. | .. | .. | .. |
| .. | .. | .. | .. |
| junction n | flow | suction | purity |
| Number of pipe fittings | | | |
| pipe number | friction coefficient | | |
| .. | .. | | |
| .. | .. | | |

Figure A1.8. Structure of the boundary condition data file

As explained in the previous chapter the program requires details of the flows entering the network plus one boundary suction pressure. In this case only the first suction input (i.e. that for junction 1 in the file) will be used in the solution. The suctions specified will be converted to pressures to be used in the solution process.

If the suction should be specified at the origin (i.e. the exhausting junction) then the flow, in this case, will not be used by the program but calculated as the output from all the flows which enter the network.

Flow will be specified in m^3/s , pressure in Pascals and purity as a fraction between 0 and 1. The friction coefficients will be calculated using equation (3.54).

A1.3.2 Data Validation

This section of the program validates the junction and pipe data and sets up the arrays needed by the main program loop. Checks are made that all junction numbers used in defining pipes have been declared and that diameter and friction factor values are positive.

A1.3.3 Calculation of Suction and Mass Flow

The calculation of suctions at each junction and mass flows in each pipe is carried out in the main iterative loop of the program. An initial arbitrary estimate of mass flows is made and a system of equations constructed. This system is then solved for the pressure squared and new mass flows calculated. The iterative procedure is continued until the mass flows have converged to an acceptable limit. At present the solution is assumed to have converged if the sum of the differences in mass flow from one iteration to the next, for all pipes in the network, is less than 0.01 times the number of pipes in the network.

A1.3.4 Calculation of Flow Rate, Velocity and Purity

The initial stages of the iterative solution may produce negative results for the pressure squared at some junctions. This is obviously incorrect and is dependent on the initial estimates for the mass flow in each pipe. As the solution converges all pressures will eventually become positive.

Purity is measured on a volumetric basis, hence knowledge of the fluid density is required before volume flows or purities can be calculated for each pipe. The density

is found using pressure results at each junction and the equation of state, $\frac{P}{\rho} = RT$. The calculation of volume flow and purity can therefore only take place once all pressure results have become positive. The changes in density occurring along each pipe, due to the compressible nature of the flow, will affect the flow rate and velocity. The values calculated for these is therefore at the downstream end of each pipe.

Pressure, mass flow, purity, flow rate, velocity and gas constant are all updated during the iterative process. Mass flow and gas constant will affect construction of the system matrix [A] .

A1.3.5 Results Output

Results are printed in a file 'RESLXXXX' where 'XXXX' is again the 4 figure jobname. The file will hold details of the pressure at each junction and the mass flow, volume flow, velocity and purity in each pipe.

| | | | |
|--|-------------------------------|------------------|--------|
| ITERATION NUMBER .. | | | |
| ===== | | | |
| JUNCTION | SUCTION (kPa) | | |
| ===== | ===== | | |
| .. | .. | | |
| .. | .. | | |
| Calculated volume flows have been corrected to a volume flow at an atmospheric pressure of 101.325 KPa. | | | |
| PIPE | CORRECTED VOLUME FLOW (L/s) | VELOCITY (m/s) | PURITY |
| ===== | ===== | ===== | ===== |
| .. | .. | .. | .. |
| .. | .. | .. | .. |
| CONVERGENCE CHECK - RESIDUAL = .. | | | |
| ----- | | | |

Figure A1.9. Example of results output.

A1.4 Program Execution

A number of small additional programs have been written to complement the pipe network prediction model, MESH.EXE.

These are ;

- (i) a network drawing program, NETDRW.EXE.
- (ii) programs creating the data files required by the prediction program, CRNODE.EXE , CRPIPE.EXE , CRBOUN.EXE.
- (iii) Simple programs for quick, single pipe, pressure/flow analyses, PLOSS.EXE , PDIAM.EXE.

Executing the program will bring the following menu on the screen ;

| |
|---------------------------------|
| Network Calculations |
| Single Pipe Calculations |
| Quit |

Figure A1.10. The top level menu

A1.4.1 Single Pipe Calculations

Selecting the **Single Pipe Calculations** option from the top level menu displays the sub-menu shown below ;

| |
|-----------------------------|
| Single Pipe Losses |
| Diameter Comparisons |
| Quit |

Figure A1.11. The single pipe calculations menu

The **Single Pipe Losses** option will calculate the inbye suction, given the outbye suction, using equations 3.22 and 3.23. The **Diameter Comparisons** option will take the supplied input pressure and pressure drop for a specified diameter pipe and calculate the pressure drop for an alternative diameter pipe. The option will also calculate the pressure drop for a number of alternative pipes in parallel. The option was developed from equation 3.61.

These two simple, single pipe options allow the user to quickly ascertain the effect changing parameters will have on a single pipe. The pipe characteristics, flow results and inlet pressure could be taken from results of a network simulation and the effects of changes ascertained before this change is made to the full network and the simulation re-run.

A1.4.2 Network Calculations

Selecting the **Network Calculations** option from the top level menu will bring up the following menu ;

| |
|----------------------------|
| Create Nodes |
| Create Pipes |
| Create Data File |
| Boundary Conditions |
| View Network |
| Execute Job |
| View Results |
| Edit File |
| Quit |

Figure A1.12. The network calculations menu.

A1.4.2.1 Create Nodes

This option allows the input of the co-ordinates of all the junctions in the network. The vertical co-ordinate is the z direction. Once all the junctions have been input the data can be saved. This will hold the data in a temporary file, 'NODEXXXX' where 'XXXX' is the jobname.

A1.4.2.2 Create Pipes

This option allows the specification of pipe data to be used in the program. The first and second nodes will be required to define the position of the pipe and the diameter and friction factor to define the pipe characteristics. The direction of flow along the pipe is assumed from node 1 towards node 2. If the value of the friction factor is unknown then the fully developed turbulent flow model (equation 3.54) can be used to estimate one.

As with the 'Create Nodes' option the pipe data can be stored in a temporary file 'PIPEXXXX'.

A1.4.2.3 Create Data File

This option creates the data file 'DATAXXXX' to be used by the program. It requires that both the temporary files 'NODEXXXX' and 'PIPEXXXX', created in the previous options, exist. These temporary files will be deleted once the data file has been constructed.

A1.4.2.4 Boundary Conditions

This option creates the file 'BOUNXXXX' holding the boundary condition data to be used by the program. The program determines which nodes are boundary nodes. It then requests the node at which the pressure boundary condition is to be specified followed by the gas flow rate and purity. The gas flowrate and purity will then be requested for all the other nodes the program has validated as boundary nodes.

A1.4.2.5 View Network

The network can be viewed in either the xz, yz, or xy planes. The user can specify upper and lower limits on co-ordinates and whether node or pipe numbers will be displayed.

A1.4.2.6 Execute Job

This option executes the job specified by the 4 character jobname. All data and subsequent result files will be stored in the top level \NETWORKS directory.

A1.4.2.7 View Results

The pressure at each junction and the mass flow, volume flow and purity are written to a results file 'RESLXXXX'. This option allows the results file to be viewed. When finished, F3 followed by Q <ret> will return control back to the main menu.

A1.4.2.8 Edit File

Either the boundary condition or data file can be edited by supplying the appropriate jobname. When editing of a file is complete F3 followed by E <ret> will return control back to the main menu.

A1.5 List of Program Subroutines

| Routine Name | Description |
|--|---|
| PIPNET | Main program for methane drainage pipe network simulation |
| Validation Routines | |
| PNV001 | Controlling subroutine for data input |
| PNV002 | Validation of junction and pipe data |
| PNV004 | Sorts the junction and pipe arrays into ascending order |
| Utility Routines | |
| PNU001 | Creates array of pipes attached to nodes |
| PNU002 | Finds maximum and minimum x, y, z co-ordinates |
| PNU003 | Returns co-ordinates of the supplied junction |
| PNU004 | Calculates how many and numbers of pipes attached to supplied junction. |
| PNU005 | Calculates two junctions at either end of supplied pipe. |
| IPNU01 | Finds position in the sorted junction array of supplied junction. |
| IPNU02 | Finds position in the sorted pipes array of supplied pipe. |
| IPNU03 | Given one junction, retrieves junction at other end of supplied pipe. |
| Solution Routines | |
| PNS001 | Main routine controlling the solution. |
| PNS005 | Forms the system matrix, [A]. |
| PNS006 | Determines coefficients to be included in the system matrix. |
| PNS007 | Subroutine controlling iterative loop of the solution. |
| PNS008 | Includes boundary conditions into the system of equations. |
| PNS009 | Updates system and rhs matrices to take account of specified pressure. |
| PNS010 | Solves the system of equations using triangular decomposition. |
| Solution Routines (continued) | |
| PNS011 | Calculates the purities in each pipe in the network. |
| PNS012 | Calculates new specific gas constants. |
| PNS013 | Includes losses arising from fittings into equations. |
| PNS017 | Calculates flow rates and velocities. |
| LUDCMP | Decomposes the System Matrix into lower and upper triangular matrices. |
| LUBKSB | Solves the lower and upper triangular matrices with back substitution. |

| Network Drawing Routines | |
|--|---|
| NETDRW | Controlling routine for drawing network on the screen. |
| NETXZ | Routine drawing the XZ elevation of the pipe network. |
| NETXY | Routine drawing the XY elevation of the pipe network. |
| NETYZ | Routine drawing the YZ elevation of the pipe network. |
| LEGEND | Adds the legend to the drawing of the pipe range. |
| Routines Creating Data Files | |
| CRNODE | Routine creating junction co-ordinates for the network. |
| CRPIPE | Routine creating pipe data for the network. |
| PNF001 | Creates pipe data array when friction factors are known. |
| PNF002 | Creates pipe data array when friction factors are unknown. |
| CRBOUN | Creates boundary conditions file for the network. |
| Routines for Single Pipe Calculations. | |
| PLOSS | Given inlet pressure, pipe characteristics and flow data calculates the pressure drop along a single pipe. |
| PDIAM | Given inlet and outlet pressure for a single pipe, calculates the outlet pressure for combinations of alternative diameter pipes. |

Appendix 2

The Mine Ventilation Simulation Programs

A2.1 Introduction

A suite of computer programs have been written to calculate airflows in mine ventilation networks. Each program will calculate flows in the complete network, according to the fixed flows placed on selected airways, using differing methods discussed previously.

The network will be either ;

- (i) Natural splitting where the flows assign themselves according to the resistance of the airways and pressure supplied by fans within the network.
- (ii) Controlled flow where all flows in the network are constrained and the problem is one of finding the position of regulators to achieve those flows.
- (iii) Semi-controlled flow where some flows will be prescribed and some will assign themselves according to the resistance of the airways.

The programs, listings of which can be found in this appendix, have been written in FORTRAN77 and developed for use on personal computers. With the use of FORTRAN subroutines the computer code has been kept as modular as possible thus reducing duplicated code, program size and allowing for easy maintenance.

A2.2 Coding Specifications

The coding specifications are identical to those used in the methane drainage simulation model. Parameter statements are stored in a file 'SIZES' and hold details of the maximum number of nodes, branches and meshes in the network.


```
integer mxnode, mxbrch, mxmesh
parameter( mxnode=200, mxbrch=200, mxmesh=100 )
```

Figure A2.1. Parameter statements included in the mine ventilation simulation models.

The common block is stored in the file 'NETWRK.CMN' and hold details of the number of junctions, branches and fans in the network. It will also hold the junction-branch and mesh-branch incidence matrices and details of the topology and resistance of each branch in an array 'RBRNCH'.

```
c-----This common block should always be included with the file
c-----'sizes' holding the parameter statements about the size of
c-----the network.
      character*8 cfile
      real rbrnch( mxbrch, 6 ), rfan( 5, 4 )
      integer ia( mxnode, mxbrch ), ib( mxmesh, mxbrch ),
             itype( mxbrch )
      integer nnodes, nbrnch, nfan
      common / netwrk / nnodes, nbrnch, rbrnch, ia, ib, nfan, rfan,
+
             cfile
```

Figure A2.2. Common block included in the mine ventilation simulation models.

A2.3 Directory Structure

All program executables and the appropriate data files are held in directories below the directory \VENTOPTM ;

- \NATSPLIT contains the natural splitting program,
- \CONTRFLW contains the controlled flow program,
- \SEMICONT contains the semi-controlled flow program and
- \FANS contains the program calculating fan performance characteristics.
- \CREATE contains the program to analyse the current data file.

A2.4 Compiling and Linking Executables

All source code required for the executables is stored in the directory \SOURCE below the appropriate directory. This is compiled using the batch file 'COMPILE' in the same directory. All object files will be copied to another directory \OBJECT. The program can then be linked from the top level directory, to produce the executable, using the file 'LINK'. The \FANS and \CREATE directories, due to the small amount of code, have both source and object files in the top level directory.

A2.5 Program Execution

Executing the main program from the \MENU directory will display the following menu on the screen ;

| |
|-----------------------------|
| Problem Type |
| Natural Splitting |
| Controlled Flow |
| Semi Controlled Flow |
| Fan Characteristics |
| Quit |

Figure A2.3. Menu for the mine ventilation network analysis programs.

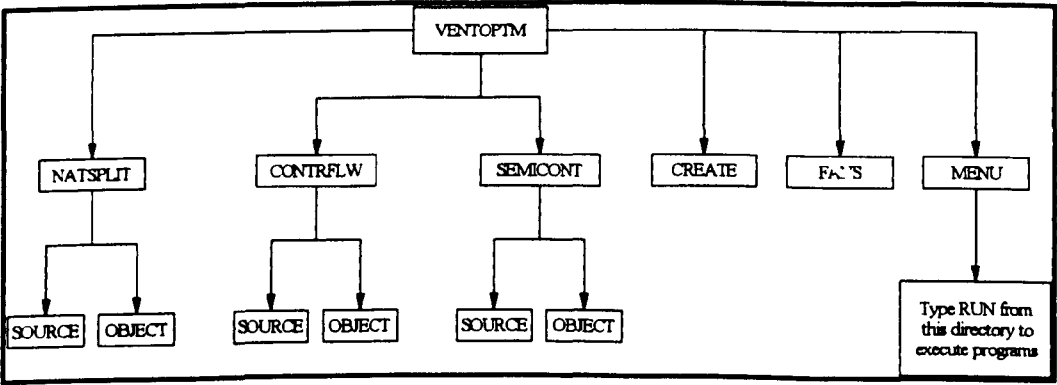


Figure A2.4. Directory structure for the ventilation optimisation programs.

A2.5.1 Problem Type

This program will analyse the current data file 'XXXX.DAT', where 'XXXX' is the 4 character jobname, and specify into which class of network the current problem falls. The data file will then be copied from the directory \VENTOPTM\CREATE, in which the file was created, to the appropriate directory for airflow distribution analysis.

A2.5.1.1 Data File Structure

All data files are constructed in the same way. This file will hold details of the branch connections and resistances plus the characteristics of all the fans in the network. Branch numbering need not be sequential, however no branch number must be omitted in the complete data file. i.e. if there were 4 branches in the network then the branch numbers must be 1,2,3,4 in any order. Similarly the junctions must be numbered 1 to n in any order, where n is the number of junctions in the network.

Flow is assumed from junction 1 to junction 2. If the reverse is true then the quantity calculated by the program will simply be a negative value.

All resistance values are calculated in Gauls (Ns^2m^{-8}). The fixed flow flag can be set to 0 or 1 to indicate whether the current branch has a fixed air flow.

| | | | | | |
|------------------------------------|------------|------------|------------|-----------------|-------------|
| Number of Branches in the Network | | | | | |
| Branch 1 | Junction 1 | Junction 2 | Resistance | Fixed flow flag | Branch type |
| airflow (if fixed flow flag = 1) | | | | | |
| . | . | . | . | . | . |
| . | . | . | . | . | . |
| Number of fans in the network | | | | | |
| Branch number | a | b | c | | |
| . | . | . | . | . | . |
| . | . | . | . | . | . |

Figure A2.5. Structure of a typical data file.

The branch type will be as follows ;

- 1 - Intake branch
- 2 - Face branch
- 3 - Return branch

4 - Leakage branch

The characteristics of a fan situated in the specified branch is assumed to be of the form ;

$$P = aQ^2 + bQ + c$$

where P is the pressure generated by the fan,
 Q the flow rate in the branch,
and a, b, c are fan constants described in the data file.

The fan coefficients may be determined from a series of duty points using polynomial regression on these points. The program developed for this is discussed in section A2.5.6

A2.5.2 Natural Splitting

Executing the natural splitting option will bring the following menu to the screen.

| |
|---------------------|
| Run Job |
| View Results |
| Quit |

Figure A2.6. The natural splitting menu options.

A2.5.2.1 Data Input

The data required for program execution is read from a text file 'XXXX.DAT' where 'XXXX' is the 4 character jobname.

For the natural splitting problem the fixed flow flag will be zero for each branch.

A2.5.2.2 Program Structure

The basic structure of the natural splitting program (NATSPLIT.EXE) is shown in Figures A2.7a and A2.7b. The program can be split into 5 basic parts ;

- (i) Data Input.
- (ii) Find the chords of the network.
- (iii) Find the junction-branch and mesh-branch incidence matrices.
- (iv) Calculation of network airflows.
- (v) Calculation of other results.

Part (iv) forms the main iterative loop of the solution process.

A2.5.2.3 Results Output

Results are printed in a file 'XXXX.RES' where 'XXXX' is the 4 character jobname. The file will hold details of the airflow in each branch of the network and the associated pressure losses.

| Branch | Type | Quantity (m^3/s) | Press. Drop (Pa) |
|---|-------|--------------------|--------------------|
| ===== | ===== | ===== | ===== |
| . | . | . | . |
| . | . | . | . |
| Total leakage in this network is m3/s. | | | |
| Total Air Power = kW. | | | |

Figur : A2.7. Results output for the natural splitting problem.

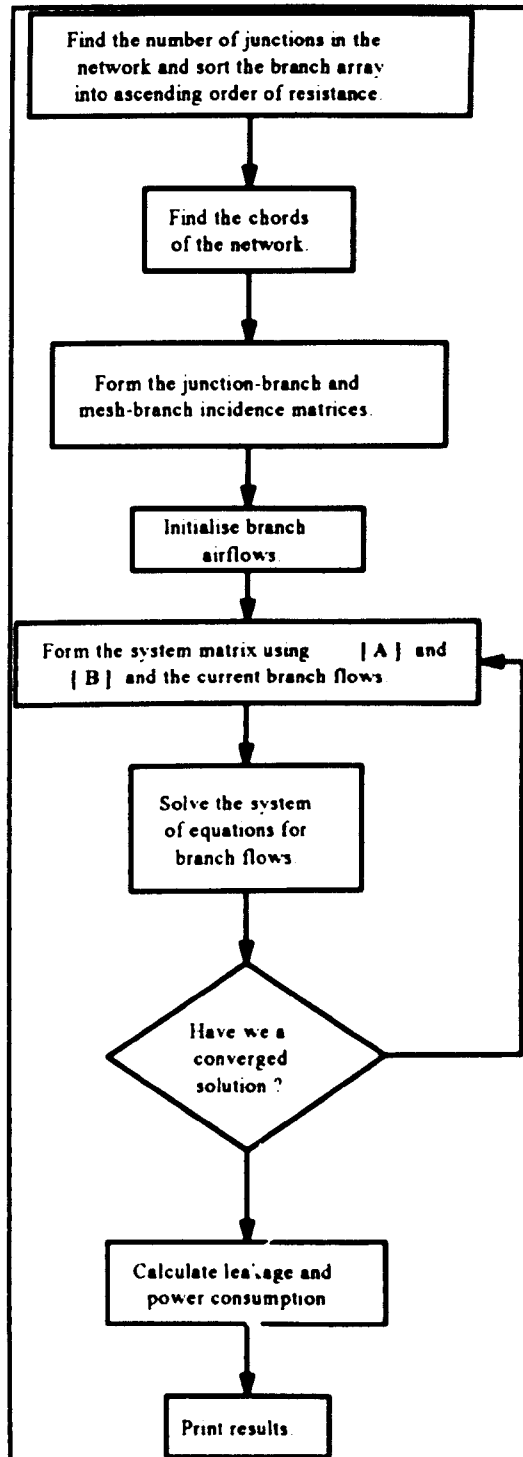


Figure A2.8a. Flowchart for the natural splitting program

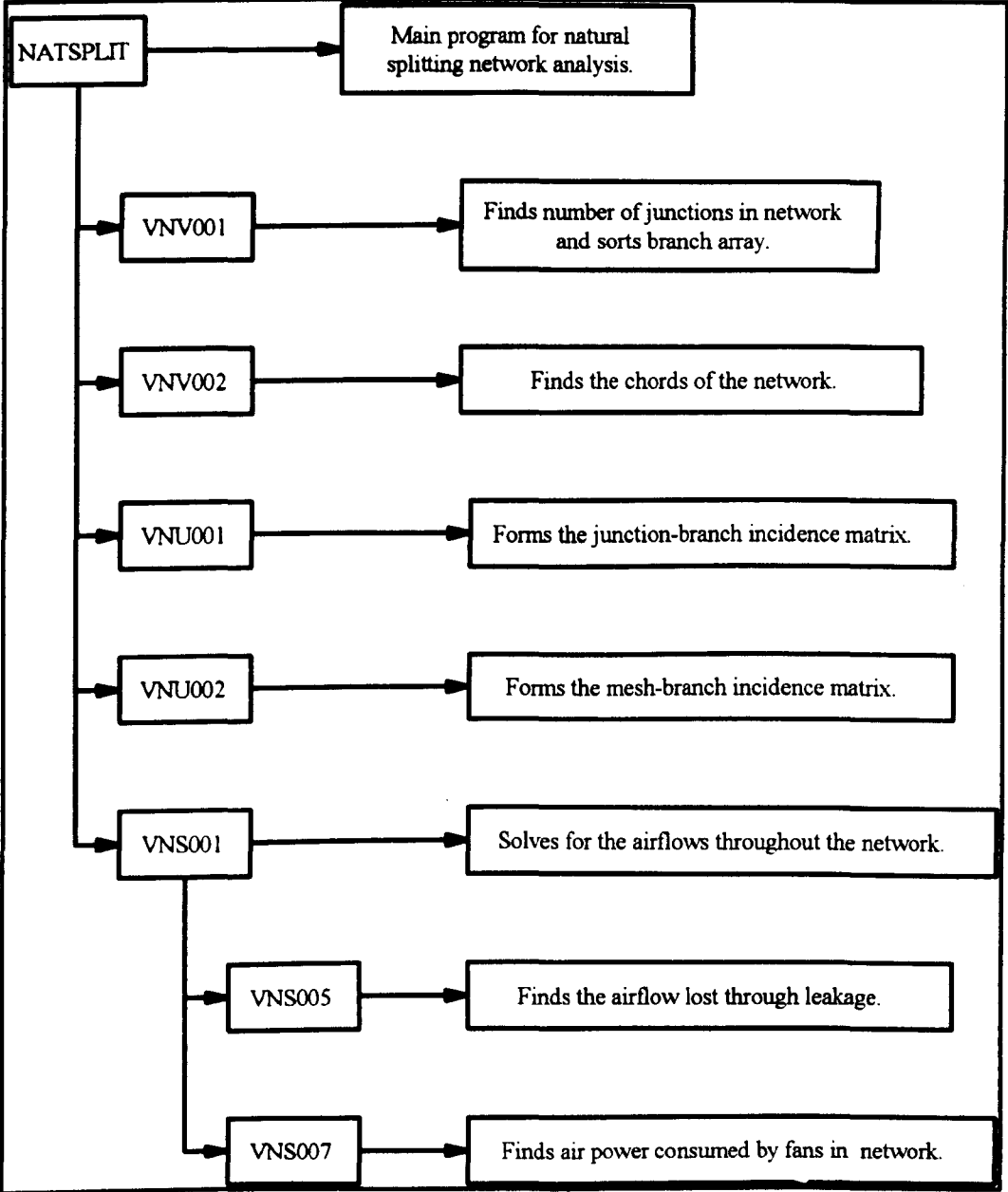


Figure A2.8b. Subroutine flowchart for the natural splitting problem.

A2.5.3 Controlled Flow

Selecting the controlled flow option will display the following menu on the screen ;

| |
|----------------------------------|
| Run Job with Regulators |
| View Regulator Results |
| Run Job with Booster Fans |
| View Booster Fan Results |
| Quit |

Figure A2.9 The controlled flow menu options.

With all flows in the network prescribed, selecting the first option will calculate the position and amount of regulation required by the network to maintain these flows. Selecting the job with booster fans will then calculate the position of booster fans to reduce the power consumed by fans in the network.

A2.5.3.1 Data Input

The data required for program execution is read from a text file 'XXXX.DAT' where 'XXXX' is the 4 character jobname. The structure of the file is shown in Figure A2.5. In this case however there is no need to declare fans in the network. The program will calculate the fan pressure required to overcome the pressure loss along the critical path through the network. To facilitate calculation of the critical path, junction 2 in the branch topology must be numbered greater than junction 1 and the initial and final junctions in the network must be numbered 1 and n respectively where n is the number of junctions in the network.

A2.5.3.2 Program Structure

Using the defined airflows the program will calculate the remainder of the airflows in the network, and hence the highest pressure loss (critical) path from the initial to final junction. This is the pressure that must be supplied by the fan to be able to obtain the airflow quantities. The program will then find the position and amount of regulation in the non-critical path branches to obtain the prescribed airflows. Any regulation placed in the critical path will merely serve to increase the pressure needed to be supplied by the fan.

A2.5.3.3 Results Output

Results are printed in a file 'XXXX.RES' where 'XXXX' is the 4 character jobname. This file will hold details of the airflow in each branch, the pressure drop along the critical path, the amount of regulation required in the remaining branches and a list of branches in the critical path.

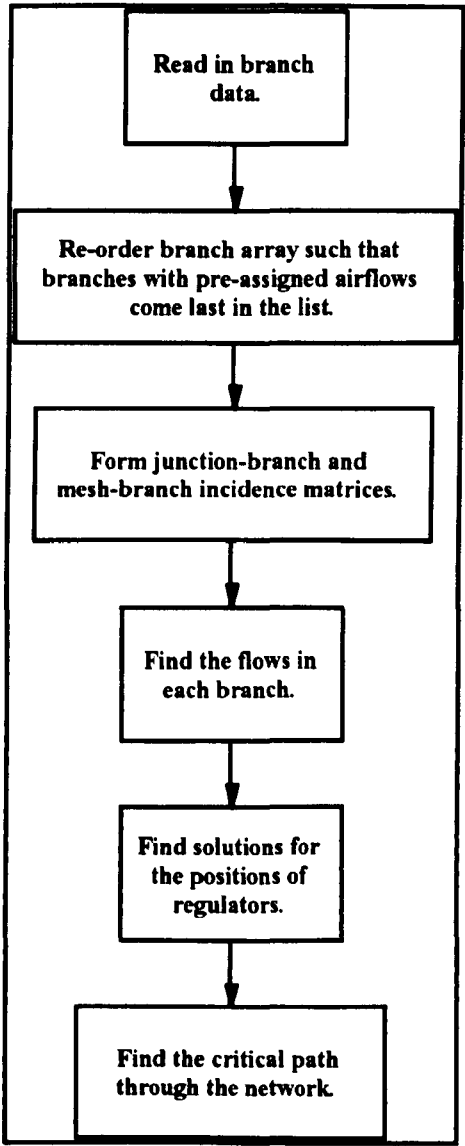


Figure A2.10a. Flow chart for the controlled flow program.

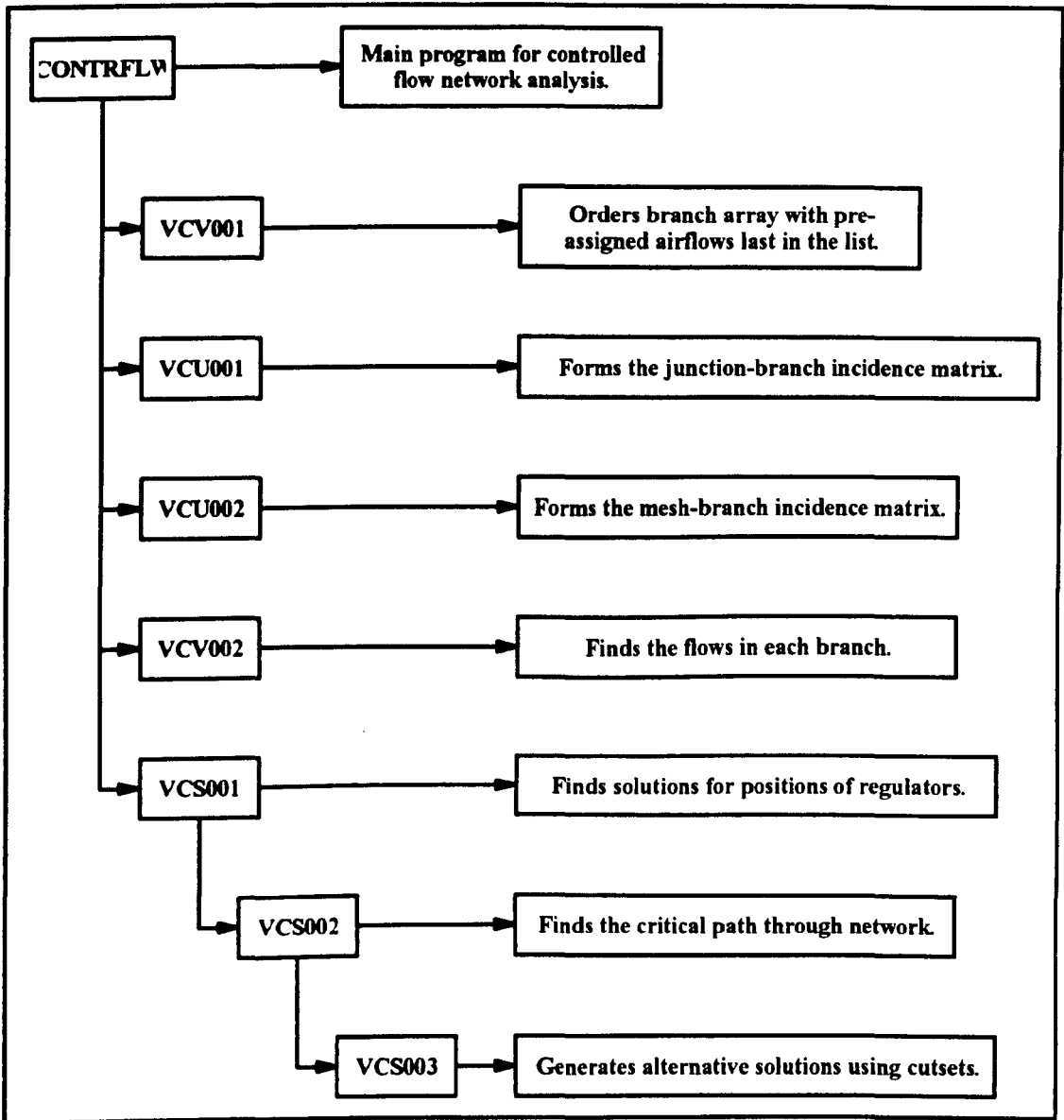


Figure A2.10b. Subroutine flowchart for the controlled flow problem.

| Branch | Type | Quantity(m3/s) | Press. Drop(Pa) |
|--------|------|------------------|-----------------|
|--------|------|------------------|-----------------|

Solution generated from forward pass procedure.

The fan pressure required is pascals.

Regulation required to satisfy pre-defined flow rates

| | | | |
|---------------|-----|------------|----------------|
| Branch number | ... | Regulation | pascals. |
|---------------|-----|------------|----------------|

Alternative solution generated by backward pass.

The fan pressure required is pascals.

Regulation required to satisfy pre-defined flow rates

| | | | |
|---------------|-----|------------|----------------|
| Branch number | ... | Regulation | pascals. |
|---------------|-----|------------|----------------|

Solutions Generated From Cutset Operations.

Cutset number, 1

| | | | |
|---------------|-----|------------|----------------|
| Branch Number | ... | regulation | pascals. |
|---------------|-----|------------|----------------|

List of branches in the critical patn.

Figure A2.11. Results output for the controlled flow program

A2.5.4 Inclusion of Additional Booster Fans

An additional program has been written to analyse the position and optimum duty of additional booster fans placed in the network. If booster fans are used to reduce the duty of the main fan and hence the power consumption of the network they will need to be placed in the largest pressure loss path. Once the position of duty of the fan(s) have been found the problem of finding regulator positions to achieve the design airflows can be re-analysed.

The data required for program execution is identical to that required for the controlled flow problem with regulators discussed above. The data is again stored in a text file 'XXXX.DAT' where 'XXXX' is the 4 character jobname. The program will request the number and location of additional booster fans placed in the network. After the inclusion of each fan an optimum duty and new critical path is found.

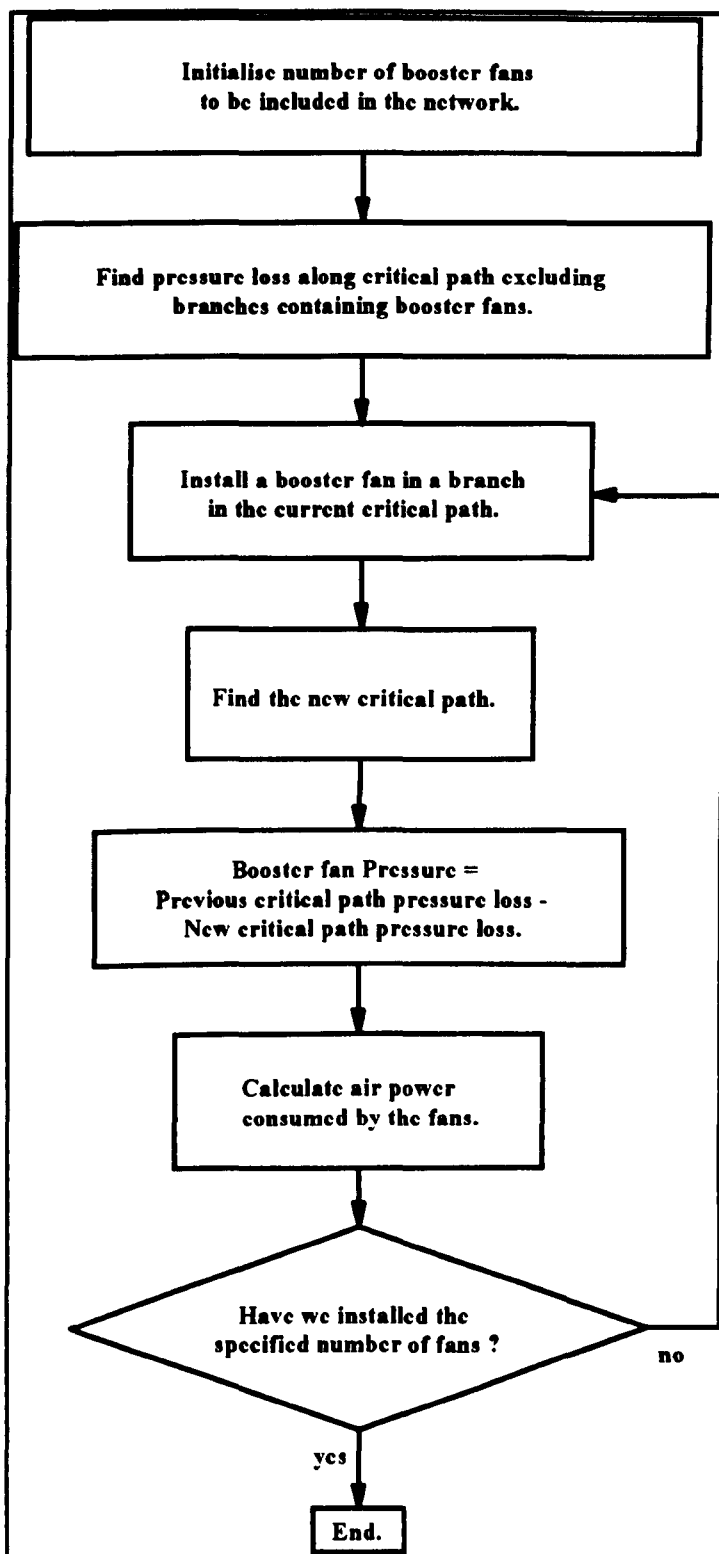


Figure A2.12. Algorithm for installing additional booster fans in the controlled flow network.

A2.5.4.1 Results Output.

Results output will include the flows in each branch of the network plus a copy of that displayed on the screen during program execution indicating the position and duty of booster fans in the network.

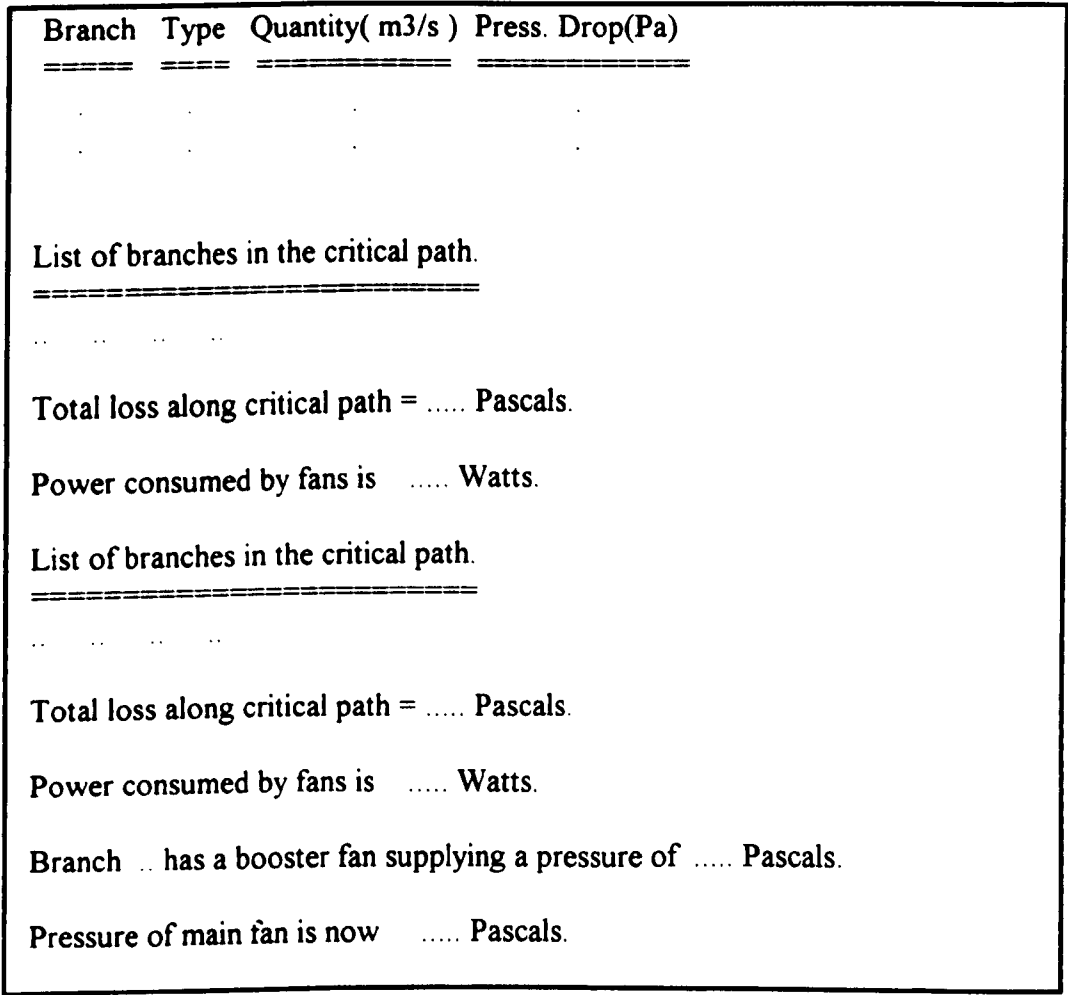


Figure A2.13. Results output for the inclusion of additional booster fans.

A2.5.5 Semi Controlled Flow

Executing the Controlled Flow option will bring the following menu to the screen.

| |
|---------------------|
| Run Job |
| View Results |
| Quit |

Figure A2.14 The semi-controlled flow menu options

In the case of semi controlled flow there is not a unique airflow distribution, as with controlled flow, but one which depends on the siting of booster fans and regulators. However these must be such the prescribed airflow quantities that are imposed on the network are maintained.

A2.5.5.1 Data Input

The data required for program execution will be stored in a file 'XXXX.DAT' where 'XXXX' is the 4 character jobname. The program will find a solution with resistance rather than flow being considered unknown on the fixed flow faces. The resistance, therefore, needed to maintain the fixed flow is the difference between the natural resistance and the calculated resistance. This will be known as the added resistance, AR. This procedure is carried out for a series (at least equal to the number of fixed flow faces in the network) of fan pressure combinations. Results are stored in a file 'XXXX.LIN'.

| |
|--|
| Number of fans we are optimising between (1 or 2) |
| Number of fixed flow faces in the network |
| Number of solutions obtained for regression analysis |
| First fan pressure |
| Second fan pressure |
| Added resistance of face 1 |
| .. |
| .. |
| Added resistance of face n |
| First fan pressure |
| Second fan pressure |
| Added resistance of face 1 |
| .. |
| .. |
| Added resistance of face n |

Figure A2.15. Structure of data held in file required for linear regression analysis

A2.5.5.2 Program Structure

The program will use the data detailed in Figure A2.12 to perform regression analyses producing relationships, for each fixed flow face, of the form ;

$$P_m = a P_b + b AR + c \text{ for the two fan system}$$

or
$$P_m = b AR + c \text{ for the one fan system,}$$

- where P_m is the first or main fan pressure,
- P_b is the second or booster fan pressure,
- AR is the added resistance on the face,
- a is the rate of change of booster fan pressure with main fan pressure,
 - b is the rate of change of added resistance with main fan pressure and
 - c is the intercept.

The program is able to deal with any number of fans in the network but can only optimise between two with all others remaining constant throughout. The two selected selected for optimisation will always be the first two declared in the data file.

The optimisation, for instance, could be between 2 underground fans with the surface fan remaining fixed.

Lines of fan pressure versus added resistance can be plotted to the screen. The two fan system will require the fixing of the second fan pressure.

Lines of zero added resistance can also be plotted and the program will analyse the intersection of these lines to find the optimum combination of the two fans in the network. This will indicate the optimum fan pressures and the amount of regulation required on other faces to achieve the fixed flows.

A2.5.5.3 Results Output

Results are printed in the file 'XXXX.RES' where 'XXXX' is the 4 character jobname. If the linear regression file was created during the current program execution then airflow results for each of the fan pressure settings will be printed in the file. This will be followed by the linear regression results and booster fan position suggestions for a one fan system and optimisation analysis results for the two fan system.

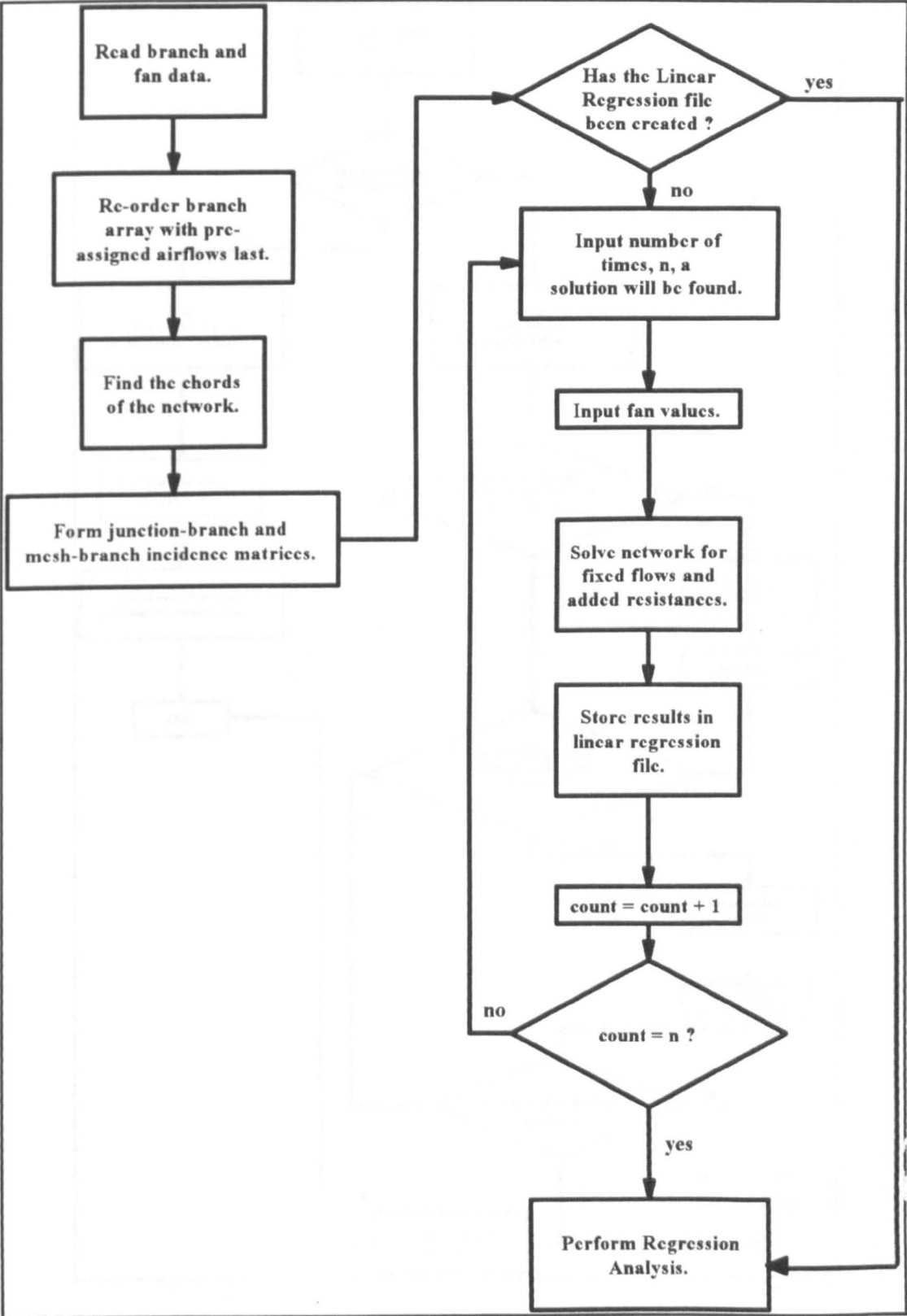


Figure A2.16a. Flowchart of the semi controlled flow program.

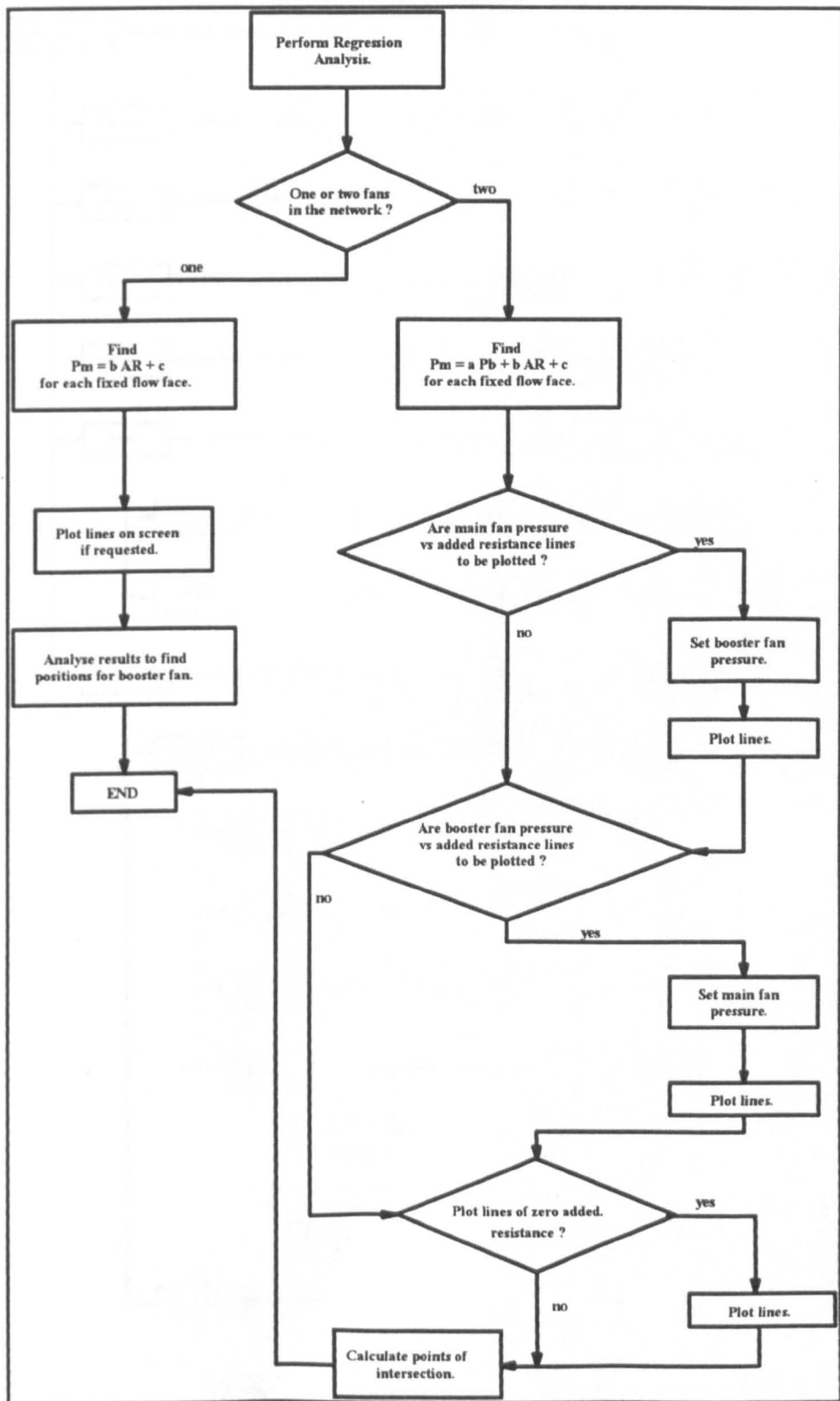


Figure A2.16b. Flowchart of the semi controlled flow program.

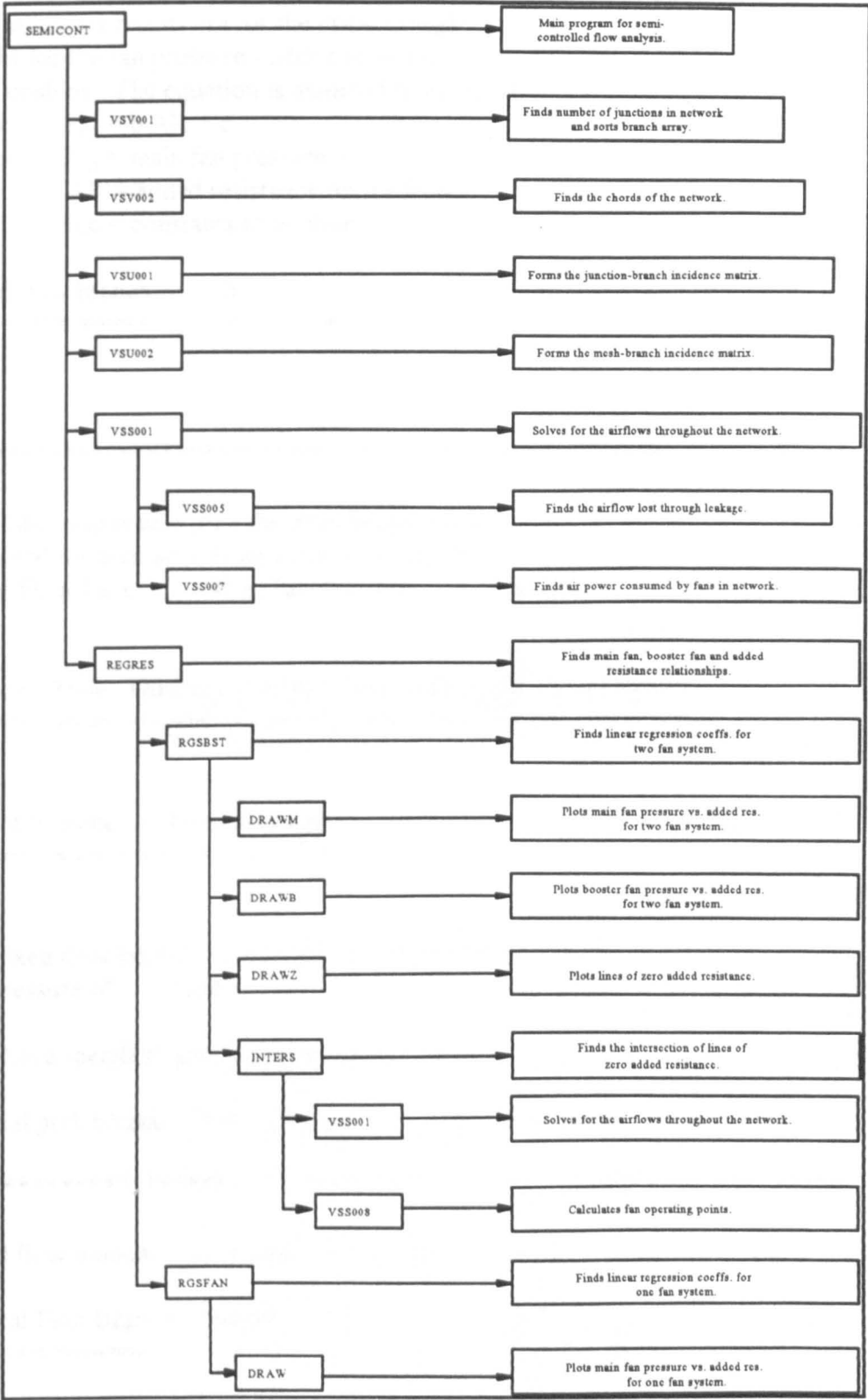


Figure A2.17. Subroutine flowchart for the semi-controlled flow program

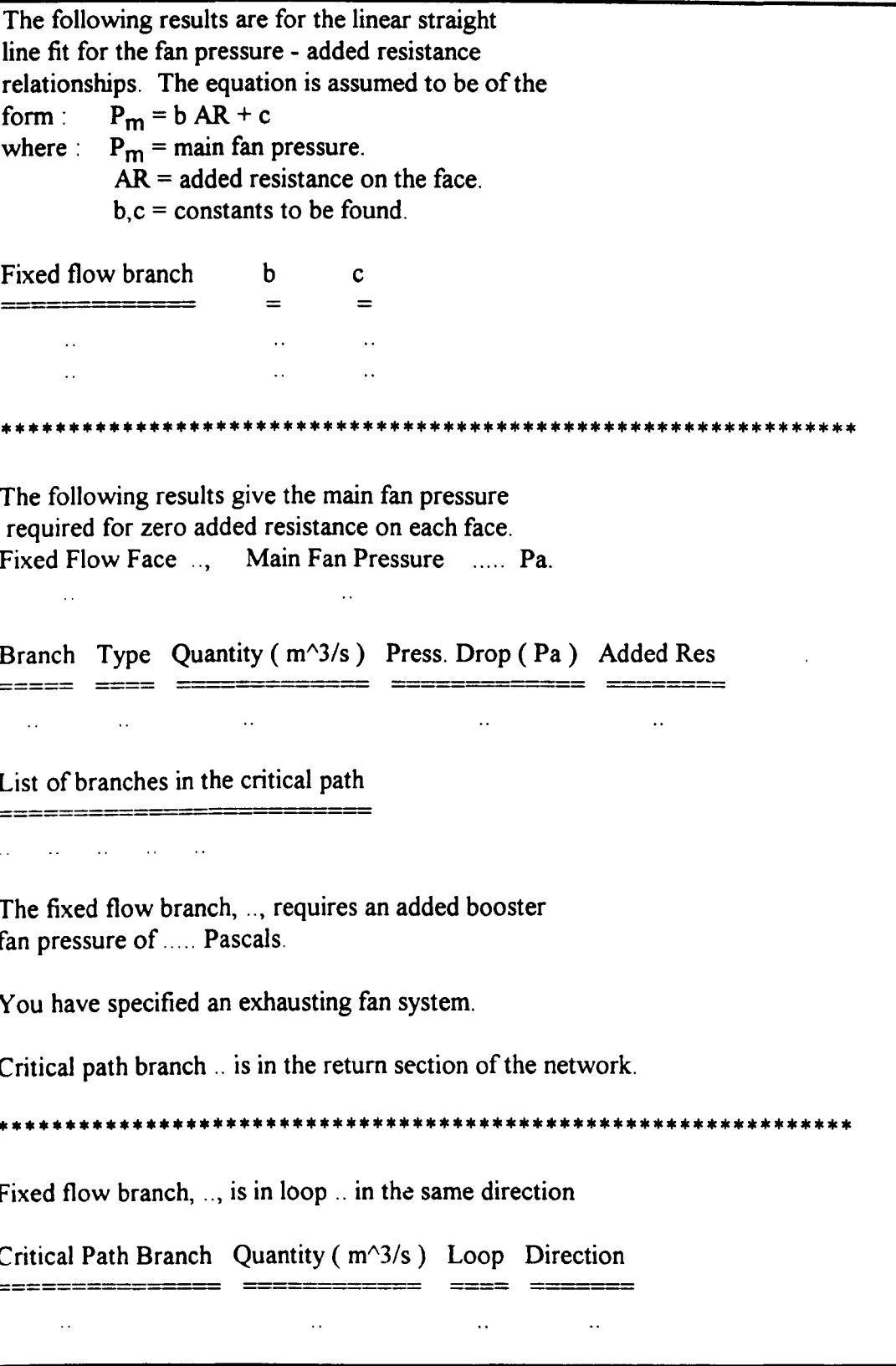


Figure A2.18. Results output for the one fan system

The following results are for the linear straight line fit for the for the fan pressure - added resistance relationships. The equation is assumed to be of the form :

$$P_m = a P_h + b AR + c$$

where :
 P_m = main fan pressure.
 P_h = booster fan pressure.
AR = added resistance on the face.
a,b,c = constants to be found.

| Fixed flow branch | a | b | c |
|-------------------|----|----|----|
| ===== | = | = | = |
| .. | .. | .. | .. |

The following results give the main fan pressure required for zero added resistance on each face at the booster fan setting given.

Booster Fan Pressure Pa.

Fixed Flow Face .., Main Fan Pressure Pa.

The following results give the booster fan pressure required for zero added resistance on each face at the main fan setting given.

Main Fan Pressure Pa.

Fixed Flow Face .., Booster Fan Pressure Pa.

Figure A2.19a. Results output for the two fan system. (continued overleaf)

The following gives the point of intersection of each pair of zero added resistance lines. Using the main and booster fan pressures found, the added resistances on the other fixed flow faces are calculated.

No results are calculated or printed if ;

- (1) the lines do not intersect.
- (2) the main or booster fan values are negative.
- (3) any added resistance value for the other faces is negative, indicating another fan would have to be used.

Intersection of fixed flow branch .. and ..

=====

Main fan pressure - Pa.
Booster fan pressure - Pa.

| Branch | Type | Quantity (m^3/s) | Press. Drop (Pa) | Added Res |
|--------|-------|--------------------|--------------------|-----------|
| ===== | ===== | ===== | ===== | ===== |
| .. | .. | .. | .. | .. |

Fixed Flow Face .., added resistance Ns2m8

Figure A2.19b. Results output for the two fan system.

A2.5.6 Fan Characteristics

Fan characteristics are assumed to be of the form ;

$$P = a Q^2 + b Q + c$$

where a b and c are the coefficients required by the ventilation programs.
This menu option will take a series of data points and perform a regression analysis to calculate the required coefficients. Data is input from a file 'XXXX.FAN' where 'XXXX' is the 4 character jobname.

Number of fans in data file

Number of points for first fan

Pressure Quantity

.. ..

.. ..

Number of points for second fan

Pressure Quantity

.. ..

.. ..

Figure A2.20. Data input for the fan characteristics option

Results are printed to the screen and display the a, b and c coefficients required.

The fan characteristic assumed is of the form

aq^2 + bq + c

a,b and c are the coefficients required by the

network programs. The results are listed below.

| fan no. | no. of points | a | b | c |
|---------|---------------|----|----|----|
| ----- | ----- | - | - | - |
| .. | .. | .. | .. | .. |

Figure A2.21. Results output for the fan characteristics option.

A2.6 List of Program Subroutines

| Natural Splitting Program | |
|---------------------------|---|
| Routine | Description |
| NATSPLIT | Program to solve the natural splitting ventilation problem. |
| Validation Routines | |
| VNV001 | Finds number of nodes in network and sorts the branches array into ascending order of resistance. |
| VNV002 | Finds the chords of the tree and resorts the branch array such that chords come last in the array. |
| VNV003 | Sorts the branches array such that the chords come last in list. |
| Utility Routines | |
| VNU001 | Forms junction-branch incidence matrix. |
| VNU002 | Forms the mesh-branch incidence matrix. |
| VNU003 | Finds branches having supplied node as final or initial node. |
| VNU004 | Finds attributes of supplied branch. |
| IVNU01 | Finds the column of the sorted branch-node and branch-mesh incidence matrices corresponding to supplied branch. |
| IVNU02 | Finds which branch has node1 and node2 as start and finish nodes. |
| CRBTCH | Creates batch file allowing user to view results of current job. |
| Solution Routines | |
| VNS001 | Forms the system matrix and solves the system of equations. |
| VNS005 | Analyses results for recirculation and leakage. |
| VNS007 | Calculates operating cost of fans in the network. |
| GAUSSJ | Solves a system of equations using Gauss Jordan elimination. |
| LUDCMP | Decomposes the System Matrix into lower and upper triangular matrices. |
| LUBKSB | Solves the lower and upper triangular matrices with back substitution. |

| Controlled Flow Program (using Regulators) | |
|--|---|
| Routine | Description |
| CONTRFLW | Program to solve the controlled flow ventilation problem. |
| Validation Routines | |
| VCV001 | Sorts the branches array such that branches with pre-assigned airflows come last in the list. |
| VCV002 | Finds the quantities in each branch of the network. |
| Utility Routines | |
| VCU001 | Finds number of nodes and forms branch-node incidence matrix. |
| VCU002 | Forms the mesh-branch incidence matrix. |
| VCU003 | Finds branches having supplied node as final or initial node. |
| VCU004 | Finds attributes of supplied branch. |
| IVCU01 | Finds which branch has node1 and node2 as start and finish nodes. |
| IVCU02 | Finds the column of the sorted branch-node and branch-mesh incidence matrices corresponding to supplied branch. |
| CRBTCH | Creates batch file allowing user to view results of current job. |
| Solution Routines | |
| VCS001 | Finds two solutions for the position of regulators using forward and backward pass procedure. |
| VCS002 | Finds the critical (longest) path through the network. |
| VCS003 | Finds alternative solutions using cutsets. |
| GAUSSJ | Solves a system of eqautions using Gauss Jordan elimination. |

| Controlled Flow Program (using Booster fans) | |
|--|---|
| Routine | Description |
| CRITPATH | Program to analyse Mine Ventilation Networks given pre-assigned airflows throughout the network and allowing the inclusion of booster fans. |
| Validation Routines | |
| VCV001 | Sorts the branches array such that branches with pre-assigned airflows come last in the list. |
| VCV002 | Finds the quantities in each branch of the network. |
| Utility Routines | |
| VCU001 | Finds number of nodes and forms branch-node incidence matrix. |
| VCU002 | Forms the mesh-branch incidence matrix. |
| VSU003 | Finds branches having supplied node as final or initial node. |
| VSU004 | Finds attributes of supplied branch. |
| IVNU01 | Finds the column of the sorted branch-node and branch-mesh incidence matrices corresponding to supplied branch. |
| IVSU02 | Finds which branch has node1 and node2 as start and finish nodes. |
| CRBTCH | Creates batch file allowing user to view results of current job. |
| Solution Routines | |
| VSS002 | Finds the critical (longest) path through the network and pressure supplied by included booster fans. |
| VSS010 | Finds if current branch has a booster fan in. |
| VSS011 | Finds if new critical path has a booster fan branch in it. |
| GAUSSJ | Solves a system of eqautions using Gauss Jordan elimination. |

| Semi Controlled Flow Program | |
|------------------------------|---|
| Routine | Description |
| SEMICON | Program to analyse Mine Ventilation Networks with some pre-assigned airflows and some natural splitting. |
| Validation Routines | |
| VSV001 | Sorts the branches array such that branches with pre-assigned airflows come last in the list. |
| VSV002 | Finds the chords of the tree and resorts the branch array such that chords come last in the array. |
| VSV003 | Sorts the branches array such that the chords come last in list. |
| Utility Routines | |
| VSU001 | Finds number of nodes and forms branch-node incidence matrix. |
| VSU002 | Forms the mesh-branch incidence matrix. |
| VSU003 | Finds branches having supplied node as final or initial node. |
| VSU004 | Finds attributes of supplied branch. |
| IVSU01 | Finds the column of the sorted branch-node and branch-mesh incidence matrices corresponding to supplied branch. |
| IVSU02 | Finds which branch has node1 and node2 as start and finish nodes. |
| CRBTCH | Creates batch file allowing user to view results of current job. |
| SORT | Sort the fan pressure array values into descending order. |
| DESCRP | Prints description of solution method to screen. |
| Solution Routines | |
| VSS001 | Forms the system matrix and solves the system of equations. |
| VSS002 | Finds the critical (longest) path through the network. |
| VSS004 | Finds a solution for the head loss at each node w.r.t. the first node |
| VSS005 | Analyses results for recirculation and leakage. |
| VSS006 | Analyses results for preferred position of booster fan. |
| VSS007 | Calculates operating cost of fans in the network. |
| VSS008 | Calculates fan operating points |
| VSS009 | Forms the system matrix and solves the system of equations but does not print results. |
| LUDCMP | Decomposes the System Matrix into lower and upper triangular matrices. |
| LUBKSB | Solves the lower and upper triangular matrices with back substitution. |

| | |
|-------------------------|--|
| GAUSSJ | Solves a system of equations using Gauss Jordan elimination (integer) |
| GAUSSR | Solves a system of equations using Gauss Jordan elimination (real) |
| REGRES | Performs the regression analysis on calculated data. |
| RGSBST | Finds the relationship between main fan pressure, booster fan pressure and added resistance on a face. |
| RGSFAN | Finds the relationship between main fan pressure and added resistance on a face. |
| INTERS | Finds the intersection of the lines of zero added resistance. |
| Drawing Routines | |
| DRAW | Plots main fan pressure vs added res. for a one fan system |
| DRAWB | Plots booster fan pressure vs added res. for each fixed flow branch. |
| DRAWM | Plots main fan pressure vs added res. for each fixed flow branch. |
| DRAWZ | Plots main vs booster fan pressure for zero added resistance. |

| Fan Characteristics Program | |
|-----------------------------|--|
| Routine | Description |
| FANDATA | Program to find fan characteristics, given the data points. |
| GAUSSJ | Solves the system of equations using Gauss-Jordan elimination. |
| LEGEND | Subroutine to draw the legend at the bottom of graphs. |
| SORT | Sorts the array values into descending quantity order. |
| DRAW | Plots data points and calculated characterisitic |